Theoretical and Numerical Analysis of Operator Splitting Methods for American Style Option Pricing Problems

Thesis submitted in partial fulfilment

for the Award of Degree

Doctor of Philosophy

by

DEEPAK KUMAR YADAV

DEPARTMENT OF MATHEMATICAL SCIENCES

RAJIV GANDHI INSTITUTE OF PETROLEUM TECHNOLOGY

JAIS - 229304

Roll No: 20BS0006

2025

CERTIFICATE

It is certified that the work contained in the thesis titled ***"Theoretical and Numerical Analysis of Operator Splitting Methods for American Style Option Pricing Problems"*** by ***"Deepak Kumar Yadav"*** has been carried out under our supervision and that this work has not been submitted elsewhere for a degree.

It is further certified that the student has fulfilled all the requirements of Comprehensive, Candidacy and SOTA.

(Dr. Gobinda Rakshit)
Supervisor

(Dr. Alpesh Kumar)
Co-Supervisor

DECLARATION BY THE CANDIDATE

I, ***"Deepak Kumar Yadav"***, certify that the work embodied in this thesis is my own bona fide work and carried out by me under the supervision of ***"Dr. Gobinda Rakshit"*** and the co-supervision of ***"Dr. Alpesh Kumar"*** from ***"August 2020"*** to ***"May 2025"*** at Rajiv Gandhi Institute of Petroleum Technology, Jais (India). The matter embodied in this thesis has not been submitted for the award of any other degree. I declare that I have faithfully acknowledged and given credits to the research workers wherever their works have been cited in my work in this thesis. I further declare that I have not willfully copied any other's work, paragraphs, text, data, results, etc., reported in journals, books, magazines, reports, dissertations, theses, etc., or available at websites and have not included them in this thesis and have not cited as my own work.

Date:
Place:

(DEEPAK KUMAR YADAV)
Roll No: 20BS0006

CERTIFICATE BY THE SUPERVISOR

It is certified that the above statement made by the student is correct to the best of our knowledge.

(Dr. Gobinda Rakshit)	(Dr. Alpesh Kumar)	(Head of Department)
Supervisor	**Co-Supervisor**	**Mathematical Sciences**

CERTIFICATE

CERTIFIED that the work contained in the thesis titled **"Theoretical and Numerical Analysis of Operator Splitting Methods for American Style Option Pricing Problems"** by **Mr. Deepak Kumar Yadav** has been carried out under my supervision. It is also certified that he fulfilled the mandatory requirement of two quality publications arose out of his thesis work.

It is further certified that the two publications (copies enclosed) of the aforesaid **Mr. Deepak Kumar Yadav** have been published in the Journals indexed by –

(a) SCI

(b) SCI Extended

(c) SCOPUS

(d) Non-indexed journal

(Dr. Gobinda Rakshit)	(Dr. Alpesh Kumar)	(Dr. Sudeep Kundu)
Supervisor	**Co-Supervisor**	**Convener, DPGC**

COPYRIGHT TRANSFER CERTIFICATE

Title of the Thesis : Theoretical and Numerical Analysis of Operator Splitting Methods for American Style Option Pricing Problems

Name of the Student : Deepak Kumar Yadav

Copyright Transfer

The undersigned hereby assigns to the Rajiv Gandhi Institute of Petroleum Technology, Jais all rights under copyright that may exist in and for the above thesis submitted for the award of the "*DOCTOR OF PHILOSOPHY*".

\- -

Date: ***(DEEPAK KUMAR YADAV)***

Place: Roll No: 20BS0006

Note: However, the author may reproduce or authorize others to reproduce material extracted verbatim from the thesis or derivative of the thesis for author's personal use provided that the source and the Institute's copyright notice are indicated.

Acknowledgements

This acknowledgment is not merely a note of thanks but a sincere expression of my deep respect and gratitude to all those whose invaluable contributions have played an essential role throughout my Ph.D. journey.

First and foremost, I would like to express my profound gratitude to my research supervisors, Dr. Gobinda Rakshit and Dr. Alpesh Kumar, for instilling confidence in me and enriching my research with their invaluable comments, guidance, and constructive criticism throughout my academic journey. Their constant support has been immensely helpful. Apart from being my mentor, Dr. Alpesh Kumar has also been a guardian and a source of personal strength. I will always remain indebted to you, Sir, for the familiarity, kindness, moral support and guidance you have provided throughout my thesis work.

I would also like to express my sincere gratitude to Dr. Lok Pati Tripathi, Department of Mathematics, IIT Goa, India, for his valuable suggestions, insightful discussions, and constructive feedback on the research papers that form part of this thesis. My heartfelt thanks also go to Prof. Chanchal Kundu and Dr. Rohit Bansal, members of my Research Progress Evaluation Committee, for their valuable comments and suggestions, which have significantly improved the quality of my research and are reflected in this dissertation. Additionally, I am deeply grateful to all the faculty members who taught me during my coursework, an essential part of my Ph.D. journey, as their teachings have directly or indirectly contributed to my research. I also wish to express my sincere appreciation to all the faculty members of the Department of Mathematical Sciences, including Dr. Manoj Rajpoot, Dr. Sudeep Kundu, Dr. Pradeep Das, Dr. Soniya Dhama, and Dr. Dhrubasish Bhattacharyya, for their valuable guidance and constant encouragement throughout my doctoral studies. Their insights and advice have greatly enriched my learning experience.

Next, I wish to convey my deepest gratitude to those for whom words can hardly suffice, my family. Though I may not have expressed it often, I truly recognize the immense role they have played in my Ph.D. journey and in my life. Whatever I have achieved to date, I owe to their unwavering love and support. I am profoundly thankful to Maa and Baba (my grandparents) for their blessings; to Mummy and Papa (my parents) for their boundless love, moral and financial support, and for giving me the freedom to pursue my research; and to Raju (my younger brother) for motivating me to study mathematics, encouraging

me to pursue higher education, and inspiring me to strive for more throughout my research journey. I am equally grateful to my Chachi and Chacha (Aunty and Uncle), Surjeet Bhaiya, and my cousins Jairam, Manoj, Piyush, Nikhil, Pankaj, Vishal, Amit, and Kamal for their blessings, motivation, and constant encouragement to pursue higher education. Your belief in me has inspired me to strive for more throughout my journey. I am deeply thankful for your love, guidance, and unwavering support, it has meant more to me than words can express.

Furthermore, I would like to express my sincere appreciation to my senior labmate, Dr. Akanksha Bhardwaj, for her valuable guidance and encouragement. I am also deeply grateful to my dear close ones Poulami, Rajesh, and Puja, who have been like family to me, for their unwavering support, understanding, and companionship throughout my academic journey. I also feel deeply obliged to express my heartfelt appreciation to my companion on this journey, Jyoti, for her unwavering faith in me, even during the most challenging phases of this endeavor. Your belief in me has been a source of strength and inspiration.

I would like to extend my sincere gratitude to my seniors, Belal Haider, Praveen Maurya, Arijit Patra, Satish Shukla, Satish Gupta, Athar Ullah, Vivek Singh Yadav, Shivangi Singh, Ankit Singh for their guidance, support, and for being part of some of the most memorable moments of my graduate journey. I am equally thankful to my labmates Angana, Shashank, Sishupal, Heera, Vidit, Aman and Mritunjay for their cooperation, encouragement, and for creating a pleasant and motivating research environment.

It is often said that friends do not require thanks, yet I cannot help but express my heartfelt gratitude to my fellow Ph.D. colleagues and friends Neeraj, Suvadeep, Amit, Sujeet, Sidharth, Arvind, Aash, Rohit, Ajeet, and Aamir who have helped create some of the most unforgettable memories of my graduate life. They became my family here, standing by me through every challenge and success. Together, we shared both joy and hardship, building a treasure trove of memories that I will cherish forever.

At various stages of this journey, I have received help and support from many individuals, and it is difficult to name each one of them. I am also sincerely grateful to the teaching and non-teaching staff (especially T. P. Joshi Sir and Ankit Pachouri Sir) of RGIPT, for their kind assistance, guidance, and cooperation throughout my work. I would also like to extend my sincere thanks to the University Grants Commission (UGC) for providing financial support, which played a crucial role in enabling me to complete my Ph.D. research.

Finally, I offer my humble prayers to Mother Nature for her grace, strength, and inspiration throughout this journey.

RGIPT, Jais **Deepak Kumar Yadav**

Dedicated

To

My Parents

Smt. Santosh Devi & Shri Bhoop Singh Yadav

&

Grand Parents

Lt. Sanjya Devi & Shri Bhagirath

Contents

List of Figures

List of Tables

Abstract

The operator splitting approach takes advantage of the auxiliary variable to increase the accuracy and reduce the computational cost in comparison to other methods. Despite these advantages of the operator splitting method, in literature, there is a lack of stability and error estimates of the operator splitting method for American option pricing problems. The first novel contribution in this direction have been made by Feng Chen and Jie Shen [24]. They established the stability results for the first-order backward difference operator splitting method (BDF1-OS) and second-order backward difference operator splitting method (BDF2-OS) along with error analysis of the first-order backward difference method. We make some advancements in this direction by providing stability and error analysis of the operator splitting method for pricing the American option. This is done by precluding the use of the derivative of the payoff function. Therefore, the primary goal of this work is to present the BDF1-OS and BDF2-OS time semidiscretization methods for pricing American options in a Black-Scholes framework and provide the stability and error estimates for these schemes. It is observed that the accuracy of the BDF2-OS is between 1.5 and 2, and the accuracy of the BDF1-OS is almost first-order. The suggested approaches effortlessly approximate the option value as well as some of its significant "Greeks" (Delta & Gamma). By condensing mesh close to the singularity, these techniques efficiently handle the singularity of the non-smooth pay-off function. We need not employ iterations at each time step. Our discretization results in a tridiagonal system at each time step that can be solved quickly and directly. Since the choice of spatial discretization is unrelated to the choice of temporal discretization, one may also use alternative approaches for spatial discretization, such as meshless methods (RBFs), finite elements, spectral methods, etc. The use of a non-uniform grid in spatial discretization is also permitted.

The thesis comprises of six chapters followed by an exhaustive bibliography.

In **Chapter 1**, we have provided the brief introduction of financial markets. Some basic properties and basic definitions of options are also introduced. A review of the literature is also included, which contains current knowledge as well as theoretical and methodological contributions related to our present research work. Moreover the basic feature of implicit explicit backward difference operator splitting method is

also included. On the top of this an overview of the computational problem related to operator splitting method is added.

In **Chapter 2**, we proposed the stability and error analysis for the backward difference operator splitting methods to solve the linear complementarity problem (LCP) for pricing the American option under the Black-Scholes framework. The OS schemes have been successfully applied to a variety of Black-Scholes models. It is easy to apply on LCP because the complementarity conditions and the differential equation are segregated and examined separately. We provided an error estimate for these methods and the priori stability estimates for operator splitting strategies based on the BDF1 and BDF2 approaches. We performed numerical experiments and illustrated the order and efficiency of the BDF1 and BDF2 approaches for the test problems to emphasize the convergence behavior of the proposed methods. We have also verified the numerical results with the existing methods in the literature. Part of the work done in this chapter has been published in *Computational Economics*.

In **Chapter 3**, the operator splitting method has been effectively applied to jump-diffusion models, and it is also easy to implement because the differential and complementarity restrictions are decoupled and solved separately. Despite their ubiquity, these operator-splitting approaches for jump-diffusion models have no stability and error analysis works. In this direction, we performed a priori stability analysis for the implicit-explicit backward difference operator splitting techniques (IMEX-BDF-OS). After the stability analysis, we established the error estimates for IMEX-BDF1-OS and IMEX-BDF2-OS techniques. To validate the theoretical results, numerical evidence of the pricing of American options under Kou's and Merton's jump-diffusion models has been shown. Part of the work done in this chapter has been published in *Computational and Applied Mathematics*.

In **Chapter 4**, we present the stability and error analysis for the IMEX-BDF-OS techniques, which aim to solve the linear complementarity problem for pricing American options in a Markovian regime-switching jump-diffusion (RSJD) economy. Multiple regime-switching models have been fitted with the OS schemes with favourable outcomes. The complementarity requirements and the differential equation are separated and studied independently, making it easier to apply to LCP. Nevertheless, no stability or error analysis is provided for the American option under the RSJD model by these operator-splitting procedures despite their popularity. Based on the IMEX-BDF1 and IMEX-BDF2 approaches, we estimated the error for these techniques and furthermore offered a priori stability estimates for operator splitting strategies. We numerically tested the operator splitting techniques and showed how IMEX-BDF1 and IMEX-BDF2 worked for the test issues, highlighting how well they converged. One manuscript based on this chapter has been *communicated*.

In **Chapter 5**, we presented two efficient and accurate implicit-explicit finite difference (FD) techniques to solve the system of semi-linear PDEs and the system of semilinear complementarity problems arising in

option pricing under liquidity switching model. For the time semi-discretization, we present two numerical techniques: Backward difference formulas of order one and two. The stability of temporal semi-discretized systems is also shown. The computational techniques used for the European option are expanded to include the American alternative. We amalgamate the IMEX-BDF1 and IMEX-BDF2 methods with an operator splitting method for solving the semi-linear system of complementarity problems that determines the price of an American option. Numerical data for European and American call options are presented in order to demonstrate the effectiveness and precision of the proposed techniques. The option value, Gamma, Delta, and computational errors were plotted with different parameters for sensitivity analysis of the proposed option pricing model. One manuscript based on this chapter has been *communicated*.

Finally, in **Chapter 6**, we summarize the key findings of the current study as well as potential future research opportunities, followed by a list of related references. It is to be mentioned here that a list of papers published/communicated based on the thesis is also provided at the end.

Keywords and Phrases: American option pricing, Operator splitting method, Implicit-explicit finite difference scheme, Stability analysis, Convergence analysis.

CHAPTER 1

Introduction and Mathematical Preliminaries

1.1 Introduction

An option is a financial instrument that relies on the value of an underlying asset. Mathematical models are often employed to evaluate the option price. In many circumstances, numerical approaches are necessary to solve option pricing problems since analytical solution formulas do not exist. Options with complicated structures as well as huge sizes of the options trade in general, drive the development of efficient numerical algorithms for option pricing and risk management. Nowadays, numerical approaches are frequently employed in the pricing of many types of financial option contracts, and there are several references to this issue, including [3, 74, 141, 156, 171].

In this thesis, we discuss numerical approaches for pricing American options. We use parabolic partial differential equation (PDE) models based on the Black-Scholes theory, which was first published in [14] and further improved in subsequent studies. Early exercise of American options requires solving a time-dependent linear complementarity problem during pricing. To solve these LCPs, numerical approaches are necessary because of their complexity. The articles [18, 21, 55, 57, 121] discuss pricing methods for option contracts, as do the sources provided above.

The goal of this study is to provide efficient numerical solutions for American option pricing models. In the pricing, we use four different conventional one-dimensional option pricing models. The finite difference

approach is used to discretize PDEs, and operator-splitting strategies are suggested for solving LCPs. This study concentrates on theoretical and numerical analysis of the solution techniques, hence many key problems linked to option pricing.

All financial investments include some level of risk. Risk management is a specialized area that requires analysts to continually identify, measure, and manage the risks associated with investments. Purchasing insurance is an effective strategy to reduce risk. This is the foundation upon which derivatives were developed that provide some protection against financial loss.

1.1.1 Introduction to Financial Options

An option is a financial contract between two parties, with the value based on the underlying asset. The option allows the holder to purchase or sell a certain quantity of the underlying asset at a fixed price and time in the future. The other party in the option contract is known as the writer, who is required to sell or purchase anytime the holder chooses to exercise the option. The option is referred to as a call option if it grants the right to purchase the underlying asset, and a put option if it provides the right to sell the underlying asset. The underlying asset of an option contract might include stocks, foreign currencies, commodities, or other derivative instruments such as future contracts [74].

As previously stated, options can be distinguished as European or American. European options can be exercised only on the expiration date, whereas American options may be exercised at any time before or on the expiry. This early exercise potential is the discriminating factor between the European and American possibilities. The exercise feature of the American option is the most important component in determining the shape of option pricing models. The European option is a straightforward option contract, therefore we begin with a section on European options.

1.1.2 European Options

A European call option is a financial contract that allows the holder to purchase the underlying asset for a strike price K at the expiration date T. The option contract between the holder and writer is formed at time $t = 0$, and the exercise decision is taken at time $t = T$. When a call option is exercised, the holder agrees to purchase the underlying asset at the specified price (K). If the option holder chooses to exercise it, the writer must sell the underlying asset if necessary. Exercising an option is only sensible if the value of the underlying asset S exceeds the exercise price K at time T. Otherwise, the asset may be purchased on the market without the option contract. The payoff function Φ determines the value of the call option at time $t = T$. It is expressed as:

$$\Phi(S) = \max(S - K, 0)$$

The call option is worth $S - K$ if the asset value exceeds the exercise price, and is worthless otherwise. A European put option is another kind of basic option contract. The holder has the right to sell the underlying asset for the exercise price K at time T. The European put option has the following reward function:

$$\Phi(S) = \max(K - S, 0)$$

The European put option is worth $K - S$ if the exercise price exceeds the asset value, else it is worthless. To get the right to purchase or sell the underlying asset at a price of K, the holder is required to pay the option writer. The payoff should be sufficient for both the holder and the writer of the option contract. The holder should consider the payoff worth exercising the option, while the writer should ensure that it covers the risk of selling or buying the underlying asset if necessary. This payment represents the price of the option contract at time $t = 0$.

1.1.2.1 Payoff Function

At time $t = T$, the holder of a European call option will verify the underlying asset's current price, $S = S_T$. The holder has two options for acquiring the underlying asset: purchasing it on the spot market price (costs S) or exercising the call option (costs K). The choice is simple: keep the expenses to a minimum. The holder will only execute the call if S is greater than K. The holder may instantly sell the asset for the spot price S, resulting in a gain of $S - K$ per share. In this case, the option value is $V = S - K$. (This rationale disregards transaction expenses.) If the holder does not exercise, the asset may be acquired on the market for a lower price ($S < K$). In this scenario, the choice is of no use ($V = 0$).

1.1.3 American Options

An American option is a contract that may be exercised at any moment throughout its lifetime. The early exercise potential distinguishes the American option contract from the European option, which only permits exercise at time t = T. American options may be characterized as call or put options. A payoff function determines the value of the American option when exercised. For the American put option, the payoff function is as follows:

$$\Phi(S) = \max(S - K, 0),$$

where $t \in [0, T]$ and S represents the value of the underlying asset at time t. The European option requires a straightforward choice to exercise since it is accessible only at $t = T$. The American option allows for early exercise, making it difficult to choose the best time to exercise. Like European call-and-put options, American options might expire worthless, making exercise unnecessary. At $t = 0$, the holder shall pay the writer's American option price. Since the American option may be exercised immediately upon purchase, its price should exceed the value of the payoff function. If this weren't the case, there would be a clear

arbitrage opportunity. Buying and quickly exercising an American option may result in a risk-free profit. The early exercise feature increases the value of the American option above the European option and complicates option pricing.

1.2 Uses of Option Derivatives

There is much literature on options and financial derivatives due to their widespread usage (see [74] and its references therein). Options may be utilized to mitigate the risk that an investor faces [74]. Next, we provide two instances of using option contracts. The first instance is known as hedging. Investors who buy stocks suffer risks associated with their investments. Purchasing put options decreases the risk of an unexpected fall in stock price. The risk is mitigated by paying the price of the put option. This may be a kind of insurance against declining stock prices. If a corporation plans to make future payments in foreign currency, it may suffer currency risk. Currency options may be used to hedge this risk by purchasing call or put options in the underlying asset, which might be the selected foreign currency. Choosing between call and put options relies on the expected movement of the foreign currency's exchange rate. Options may also be employed for speculative purposes. Options trading allows investors to benefit from stock price swings [74, 172]. When a stock price is projected to climb, investors might purchase and hold the stock until it reaches the forecasted level. After selling these equities, investors earn from the difference between the purchase and selling prices. Losses may occur if the stock price decreases. Buying call options represents an alternate strategy for generating returns. The investor purchases call options on the selected stock. The option premium is typically much lower than the stock's market price, enabling investors to speculate on upward price movements without committing the full capital outlay. By trading stock options, investors can capture gains from rising prices while limiting their investment to the cost of the option itself. The profit from a call option is determined by the difference between the underlying stock's market price and the strike price. Potential losses are limited to the initial premium, as the option confers the right, but not the obligation, to exercise. Thus, option contracts offer the potential for substantial returns while capping downside risk at the original investment.

1.3 Other Types of Option Contracts

This section concludes with a quick overview of other available financial possibilities. The goal is to demonstrate that there are alternatives to call and put options, including European and American exercise possibilities. These European and American selections are considered fundamental, sometimes known as plain vanilla or conventional options. Over time, the range of financial possibilities has grown progressively more complex and sophisticated. The European put option has a predetermined exercise date and a payment function based on the positive difference between the underlying assets and exercise prices.

Changing the reward function allows for many variations of fundamental choices. Exotic options are defined as those with complicated payoff functions or nonstandard exercise [75, 74, 137]. Now, we explain the distinction between barrier options and Asian options.

An example of an exotic option is the barrier option [156, 172, 189]. We shall provide a brief introduction to the fundamental barrier option topologies. The up-and-in barrier option expires worthless if the underlying asset price does not reach the barrier value by the expiration date. The term "up" refers to a barrier level set above the initial price of the underlying asset. If the asset's price reaches this barrier, it must approach it from below. Another related example is the up-and-out barrier option. If the underlying asset price exceeds the barrier value before the expiration date, the option becomes worthless. Barrier options include both down-and-in and down-and-out. The term "down" indicates that the barrier level is set below the initial price of the underlying asset. A down-and-out option generates a payoff only if the barrier is not breached, whereas a down-and-in option becomes active once the asset price falls below the barrier level. Barrier options can take the form of either call or put and may follow European or American exercise styles. For a detailed discussion of barrier options, see references [4, 13, 16, 27, 67, 136]. In addition, there exist double barrier options [148, 171], where both upper and lower barriers are specified. A double barrier option incorporates two thresholds, one set above and the other below the initial price of the underlying asset. In a double-out barrier option, the contract expires worthless if either barrier is breached. Conversely, a double-in barrier option is available, much like the basic barrier choices. This becomes useless if the underlying asset's price fluctuates between the barrier levels. Investors may also benefit from cost savings by purchasing an up-and-out-barrier call instead of a standard call option. In this case, if the asset price rises but does not surpass the upper barrier, the investor can still achieve the desired payoff with a lower initial premium [171].

Another kind of option is known as Asian option [74, 156, 171]. The payoff functions for these options are based on the average asset price. This option, a path-dependence exotic option, is based on asset value history. In earlier sections, we discussed the payoff function for call options. The payoff function is based on the asset value and exercise price. A payoff function may substitute an average of underlying asset values for the exercise price. This provides a payment function for the average strike call option. The payoff function is the difference between the asset price at expiration and the average asset price. By replacing the asset value in the primary call option payoff function with its average value, we get a payoff function for an average rate call option. Asian options might include either European or American-style fitness features. Recent studies, such as [46], have focused on American Asian options. Asian options are established based on the average of underlying asset prices. The arithmetic and geometric averages may be employed here. The average value is affected by the size of the data set used for computation. Average values may be sampled either continuously or selectively. Asian options may be used for commodity trading, with the

underlying asset being a commodity. Asian option contracts may use a foreign currency's exchange rate as the underlying asset. Several publications, including [9, 11, 87, 106, 122, 188], discuss pricing methods for Asian options.

In addition to barrier and Asian options, many other types of option contracts are traded nowadays (refer to [74, 171] for detailed information). Here are a few examples to provide an overview of available possibilities. Investors may buy both call and put options on the same asset simultaneously. These are sometimes referred to as combination or option tactics. A straddle strategy involves purchasing call-and-put options with the same exercise price and expiry time [74]. Basket options refer to option contracts with many underlying assets, ranging from a few to a several hundred. Options and derivatives mitigate various risks. [6] discusses a pricing mechanism for weather derivatives, whereas [88] explores power choices. Option theory may also be used for investment planning using actual options.

1.4 Option Pricing Models

This section describes the American option pricing models studied in this thesis. The key difference between American and European options lies in the early exercise feature. Various methods exist for pricing American options. In the extant models, the price of the American option is determined by solving a time-dependent linear complementarity problem. In this thesis, we employ option pricing models based on parabolic partial differential equations. Here, we analyze models based on the Black and Scholes analysis and its expansions. In option pricing, jumps can occur at any time, and the log-normal distribution characteristic of the stock price cannot capture these jumps in the classical Black-Scholes model. This thesis contains four different option pricing models which vary in their approach to modeling underlying asset price fluctuations. The first option pricing model relies on a basic asset price model, which is based on a one-dimensional PDE. In the second model, we consider the jump-diffusion model for pricing the American option. To evaluate the price of the American option under the jump-diffusion process, the solution of a linear complementarity problem having a non-local integral operator is required. In the third model, we consider the regime-switching jump-diffusion model. Using regime-switching approaches, one may record stochastic volatility and therefore, fat tails in a straightforward manner without having to adhere to the standard lognormality assumption of constant volatility. Some of the empirical biases reported by the traditional lognormal model are explained in further detail when a jump component is added to the regime-switching context. The conventional theory of option pricing is predicated on the fundamental assumption that markets are always liquid and that agents are free to trade anytime they want. However, this is often not the case in actual financial markets. Regarding the availability of liquidity within financial markets or institutions, liquidity shocks are rapid interruptions or variations in the availability of liquidity. In the fourth model, we consider the liquidity shocks in financial markets.

Next, we explain how the Black-Scholes equation is derived and present a pricing model for American options.

1.4.1 The Black-Scholes Model

The efficient market theory suggests that asset prices fluctuate randomly. This theory assumes that the current price reflects previous events and that markets react quickly to fresh information about an item.

Modelling asset prices involves predicting the impact of new information on price movements. Unanticipated fluctuations in asset prices are modelled as a Markov process using the two assumptions mentioned above.

The return on an asset is calculated by dividing the price change by the initial value and is expressed as $\frac{dS}{S}$. The relative measure of a change is a more accurate estimate of its magnitude than absolute inaccuracy. We assume that at every moment t, the asset price is S. Now, if we consider a small time period dt where S changes to $S + dS$, then it raises the question of how to appropriately model the return on assets expressed as $\frac{dS}{S}$, over this interval.

The most typical model divides the return into two components. One kind of return is predictable, similar to that of a risk-free bank investment. It contributes μdt to the return dS, where μ is the average rate of asset price increase, commonly known as drift. In basic models, μ is assumed to be constant. In more complex models, such as exchange rates, μ may be a function of S and t.

The second contribution to $\frac{dS}{S}$ models the random change in asset price due to external factors, such as unexpected news. A random sample from a normal distribution with mean zero is used to calculate σdX, which is then added to dS. σ represents the volatility, which indicates the standard deviation of returns. The amount dX represents the sample from a normal distribution. Combining these contributions yields the stochastic differential equation

$$\frac{dS}{S} = \sigma dX + \mu dt, \tag{1.4.1}$$

a mathematical version of the basic formula for predicting asset prices.

1.4.2 Itô's Lemma

Asset prices are cited at discrete intervals of time in real life. Therefore, there is a practical lower constraint for the fundamental time step dt of the random walk (1.4.1). If we implement this time step in the context of value options, we would encounter an insurmountable volume of data. Rather, we establish our mathematical models within the continuous time limit $dt \to 0$. The resulting differential equations are solved more efficiently than the random walk and is directly simulated on the practical timescale. Itô's lemma is the most critical result regarding the manipulation of random variables in order to accomplish this.

First, we need the result $dX^2 \to dt$ as $dt \to 0$, with probability 1. Consequently, the greater the reduction in dt, the more likely it is that dX^2 will equal to dt. Let us assume that $f(S)$ is a smooth function of S and that we temporarily disregard the stochastic nature of S. If we alter S by a small amount dS, it is evident that f also varies by a small amount, provided we are not in close proximity to the singularities of f. The Taylor series expansion enables us to formulate the following:

$$df = \frac{df}{dS}dS + \frac{1}{2}\frac{d^2f}{dS^2}dS^2 + \cdots \tag{1.4.2}$$

where the dots represent the reminder, which is smaller than any of the terms we have retained. Now, it is important to remember that the value of dS is determined by (1.4.1). By squaring the equation (1.4.1), we determine that

$$\begin{aligned} dS^2 &= (\sigma S dX + \mu S dt)^2 \\ &= \sigma^2 S^2 dX^2 + \mu^2 S^2 dt^2 + 2\sigma\mu S^2 dX dt. \end{aligned} \tag{1.4.3}$$

We shall now analyze the order of magnitude of each term in (1.4.3). Given that

$$dS = O(\sqrt{dt}), \tag{1.4.4}$$

the first term is the biggest for very small dt and outperforms the other two terms. Thus, leading order.

$$dS^2 = \sigma^2 S^2 dX^2 + \cdots . \tag{1.4.5}$$

Since $dX^2 \to dt$, we get

$$dS^2 \to \sigma^2 S^2 dt. \tag{1.4.6}$$

We replace the result of (1.4.6) into (1.4.2) and only keep phrases that are at least as big as $O(dt)$. Using the definition of dS from (1.4.1), we find that

$$\begin{aligned} df &= \frac{df}{dS}(\sigma S dX + \mu S dt) + \frac{1}{2}\frac{d^2f}{dS^2}(\sigma^2 S^2 dt) \\ &= \sigma S \frac{df}{dS}dX + \left(\mu S \frac{df}{dS} + \frac{1}{2}\sigma^2 S^2 \frac{d^2f}{dS^2}\right) dt. \end{aligned} \tag{1.4.7}$$

The Itô's lemma states that a slight change in a random variable's function equals a minor change in the variable itself. To generalise the result (1.4.7), take $f(S,t)$, which is a function of the random variable S and t. To account for the presence of two independent variables, S and t, partial derivatives are necessary. Expanding $f(S + dS, t + dt)$ into a Taylor series about (S,t) yields:

$$df = \frac{df}{dS}dS + \frac{df}{dt}dt + \frac{1}{2}\frac{d^2f}{dS^2}dS^2 + \cdots . \tag{1.4.8}$$

Using expressions (1.4.1) for dS and $dX^2 \to dt$ as $dt \to 0$ for dX^2, we get the following expression for df:

$$df = \sigma S \frac{df}{dS}dX + \left(\mu S \frac{df}{dS} + \frac{1}{2}\sigma^2 S^2 \frac{d^2f}{dS^2} + \frac{df}{dt}\right) dt. \tag{1.4.9}$$

1.4.3 The Black-Scholes Partial Differential Equations

Let us begin this part by discussing the idea of arbitrage. One of the essential concepts in option pricing theory is the lack of arbitrage possibilities, sometimes known as the no-arbitrage principle. We consider an exemplary case of arbitrage opportunity. Let us assume that the price of a specific stock on markets A and B is posted at \$100 and \$102, respectively. Considering no transaction costs, purchasing at \$100 in exchange A and selling at \$102 in exchange B yields a risk-free profit of \$2 per share. The trader who participated in such a deal is known as an arbitrager. In a well-functioning financial market, traders are aware of the difference in stock prices and quickly compete away any potential arbitrage opportunities. However, if there is a transition cost, which is a typical kind of market friction, the minor price difference may remain. For example, if the transaction fees for purchasing and selling each share on Exchanges A and B are both \$1.50, a total transaction cost of \$3 per share would deter arbitrageurs.

An arbitrage opportunity is a self-financing trading method that requires no initial investment, has a 0% likelihood of losing money upon expiry, and has a chance of making a profit in the end. Before discussing the Black-Scholes analysis that determines the value of an option, we shall make the following assumptions. The asset's price follows a lognormal random walk (1.4.1). Other models exist, and Black-Scholes analysis may provide a differential equation for an option's value. The risk-free interest rate ($r \geq 0$) and asset volatility ($\sigma > 0$) are known across the option's life cycle.

- Hedging portfolios incur no transaction costs.
- The underlying asset does not pay dividends throughout the option's life. This assumption may be deleted if payoffs are known ahead of time. They might be paid at regular intervals or throughout the life of the option.
- There are no arbitrage opportunities. In the absence of arbitrage possibilities, all risk-free portfolios must generate the same return.
- Trading on an underlying asset may occur continually. This is definitely an idealisation, but it is essential in the context of transaction costs.
- Short sales are allowed, and the assets are divisible. According to this premise, we may purchase and sell any component of the underlying asset, even assets we do not own.

Let us assume that we have an option whose value, $V(S,t)$, is solely determined by S and t. At this level, it is not required to indicate whether V is a call or a put since it might represent the value of a portfolio of options. Using Itô's lemma, equation (1.4.9) may be written as

$$dV = \sigma S \frac{dV}{dS} dX + \left(\mu S \frac{dV}{dS} + \frac{1}{2} \sigma^2 S^2 \frac{d^2V}{dS^2} + \frac{dV}{dt} \right) dt. \tag{1.4.10}$$

This produces the random walk, followed by V.

We create a portfolio with one option and a number $-\Delta$ of the underlying asset. As of now, this number remains undetermined. The portfolio's worth is

$$\Pi = V - \Delta S, \tag{1.4.11}$$

The increase in the value of this portfolio over a single time period is

$$d\Pi = V - \Delta dS, \tag{1.4.12}$$

Here Δ is fixed throughout the time step; or else, $d\Pi$ would include terms in $d\Delta$. Combining the results from (1.4.1), (1.4.10), and (1.4.11), we conclude that Π follows a random walk.

$$d\Pi = \sigma S \left(\frac{dV}{dS} - \Delta \right) dX + \left(\mu S \frac{dV}{dS} + \frac{1}{2}\sigma^2 S^2 \frac{d^2V}{dS^2} + \frac{dV}{dt} - \mu \Delta S \right) dt. \tag{1.4.13}$$

To remove the random component in this random walk, we choose

$$\Delta = \frac{dV}{dS}. \tag{1.4.14}$$

This produces a portfolio whose increment is completely predictable, i.e.,

$$d\Pi = \left(\frac{1}{2}\sigma^2 S^2 \frac{d^2V}{dS^2} + \frac{dV}{dt} \right) dt. \tag{1.4.15}$$

We now use the ideas of arbitrage and supply and demand, assuming no transaction costs. Investing in risk-free assets yields a return of $r\Pi dt$ over time dt. If the right-hand side of (1.4.14) exceeds this amount, an arbitrager can make a risk-free profit by borrowing Π to invest in the portfolio. This risk-free method offers a bigger return than borrowing costs. If the right side of (1.4.14) is smaller than $r\Pi dt$, the arbitrager will short the portfolio and invest Π in the bank. In either case, the arbitrager would benefit instantly and without risk. The presence of such an arbitrager with the capacity to trade at a cheap cost assures that the portfolio and riskless account returns are about comparable. Therefore, we have

$$r\Pi dt = \left(\frac{1}{2}\sigma^2 S^2 \frac{d^2V}{dS^2} + \frac{dV}{dt} \right) dt. \tag{1.4.16}$$

Substituting (1.4.11) and (1.4.13) into (1.4.15) and dividing by dt, we get

$$\frac{dV}{dt} + \frac{1}{2}\sigma^2 S^2 \frac{d^2V}{dS^2} + rS\frac{dV}{dS} - rV = 0. \tag{1.4.17}$$

(1.4.17) is the classic Black-Scholes partial differential equation. Deriving the partial differential equation for a quantity, such as an option price, is a huge step towards determining its value. The primary objective of this thesis is to develop novel, stable, and faster approaches for determining this value through the solution of the equation. The value of an option must be unique, otherwise, arbitrage opportunities would

arise. To determine this unique solution, one must define its behavior at specific points within the solution domain, primarily through appropriate initial (or final) and boundary conditions.

Assumptions simplify financial markets, resulting in option pricing that may differ from those seen in actual markets. Despite its oversimplified assumptions, the Black-Scholes equation is widely used in option pricing. To determine the price of a European option using the Black–Scholes framework, one must solve the corresponding final value problem subject to suitable boundary conditions. The European option price may be calculated analytically and is widely used in finance. To calculate the price of European options, one solves a final value problem, which can often be handled either analytically or numerically. In contrast, pricing American options requires solving a linear complementarity problem (LCP). The numerical solution of these models is generally more complex than that of European option pricing. In the following section, we present a brief overview of two methods used for pricing American options.

1.5 American Option Pricing Problems

An American option is like a European option except that the holder may exercise at any time between the start date and the expiry date. An American call option grants the holder the right, but not the obligation, to purchase a specified asset from the writer at a predetermined price at any time from the start date up to the designated expiration date. An American put option grants the holder the right, but not the obligation, to sell a specified asset to the writer at a predetermined price at any time from the start date up to the specified expiration date. The holder of an American option is thus faced with the dilemma of deciding when, if at all, to exercise. If, at time t, the option is out-of-the-money then it is clearly best not to exercise. However, if the option is in-the-money it may be beneficial to wait until a later time where the payoff might be even bigger. American options are more widely traded than their European counterparts. In many exchanges, the early-exercise feature is offered by default. It is thus important to know how much extra value (if any), this flexibility builds in. It is never optimal to exercise an American call option before the expiry date. As usual, let $S(t)$ denote the asset price at time t and let E denote the exercise (strike) price. Suppose the holder wishes to exercise the option at some time $t < T$. This is only worthwhile if $S(t) > E$, and it yields a payoff of $S(t) - E$ at time t. Alternatively, the holder could short-sell the asset at the current market price $S(t)$ and then purchase the asset later at time $t = T$ by doing the most favourable of

- exercising the option at $t = T$, and
- buying at the market price at time T .

With this strategy, the holder receives the amount $S(t) > E$ at time t and makes a payment of at most E at time T . This is clearly better than eceiving only $S(t) - E$ at time t. Therefore, it is never optimal

to exercise an American call option before its expiry date, implying that an American call option has the same value as a European call option.

Black-Scholes formulation for American options:

- Let $P(S,t)$ denote the price of an American option when the underlying asset price is S at time t. The corresponding payoff function is defined as

$$\Phi(S(t)) = \max(E - S(t), 0). \tag{1.5.1}$$

- The first key observation is that the option value must always be at least as large as its immediate exercise value, that is,

$$P(S,t) \geq \Phi(S(t)) \quad \text{for all} \quad 0 \leq t \leq T,\ S \geq 0. \tag{1.5.2}$$

Overall, for an American put option, the no arbitrage principle conclude that PDE changes to the partial differential inequality:

$$\frac{\partial P}{\partial \tau} + \frac{1}{2}\sigma^2 s^2 \frac{\partial P^2}{\partial s^2} + rs\frac{\partial P}{\partial s} - rP \leq 0. \tag{1.5.3}$$

Now, at any point (S,t), it will be optimal to either exercise, or hold on to the option.

At expiry, if the option is still held, its payoff matches the European, so we have the final time condition

$$P(S,T) = \Phi(S(T)),\ \text{for all } S \geq 0. \tag{1.5.4}$$

For $S = 0$, the asset always has price zero, so a payoff of E is assured. In this case it is optimal to exercise immediately. We may interpret this formally as a boundary condition of the form

$$P(S,t) \to E \text{ as } S \to 0,\ \text{for all } 0 \leq t \leq T. \tag{1.5.5}$$

Similarly, if S is large, then the option is extremely unlikely to produce a positive payoff, so we have

$$P(S,t) \to 0 \text{ as } S \to \infty,\ \text{for all } 0 \leq t \leq T. \tag{1.5.6}$$

The American put option allows the holder to sell the underlying asset for the exercise price K at any time prior to expiration. If the option is exercised early, its price must not fall below the payoff function. This condition must therefore be incorporated into the option pricing model.

The payoff function, which determines the final value, is crucial to the problem of option pricing. Option pricing aims to determine the value of an option at the current time ($t = 0$). For an American put option, the price is obtained by solving a LCP.

$$\begin{cases} \frac{\partial V}{\partial \tau} - \frac{1}{2}\sigma^2 S^2 \frac{\partial^2 V}{\partial S^2} - rS\frac{\partial V}{\partial S} + rV & \leq & 0 & (S,\tau) \in [0,\infty) \times [0,T), \\ V(S,\tau) - \Phi(S) & \geq & 0 & (S,\tau) \in [0,\infty) \times [0,T), \\ \left(\frac{\partial V}{\partial \tau} - \frac{1}{2}\sigma^2 S^2 \frac{\partial^2 V}{\partial S^2} - rS\frac{\partial V}{\partial S} + rV\right)(V(S,\tau) - \Phi(S)) & = & 0 & (S,\tau) \in [0,\infty) \times [0,T), \\ V(S,T) & = & \Phi(S) & S \in [0,\infty), \end{cases} \tag{1.5.7}$$

where S denotes the stock price of any asset at a given time τ with fixed volatility σ and interest rate r. The value of the option $V(S,T)$ at the time of maturity T is referred to as the **payoff function**. For instance, in the case of a put option, the payoff is defined by

$$\Phi(S) = \max(K - S, 0), \tag{1.5.8}$$

where K denotes the strike price.

This model (1.5.8) determines the value of an American option based on the payoff function, underlying asset volatility, exercise price, time to expiration, and risk-free interest rate (r). For European option pricing, the exercise date is fixed. After purchasing an option contract, the next step is to determine whether to exercise it at time $t = T$. This is not the case when the American alternative is being considered. The American option faces additional challenges related to optimizing both the exercise timing and associated costs. We use a common method to transform the final value problem into an initial value problem. Furthermore, the unbounded domain $(-\infty, \infty)$ is reduced to a limited interval $[x^L, x^R]$.

Albeit the problem (1.5.7) is backward with respect to time and degenerate, we can convert it into forward in time and a non-degenerate problem, by applying the transformations $x := \ln(\frac{S}{K})$, $t := T - \tau$, and $v(x,t) := V(Ke^x, T - \tau)$, i.e.,

$$\begin{cases} \frac{\partial v}{\partial t} - \mathcal{D}v & \geq & 0 \quad (x,t) \in \mathbb{R} \times J, \\ v(x,t) - \Phi(Ke^x) & \geq & 0 \quad (x,t) \in \mathbb{R} \times J, \\ (\frac{\partial v}{\partial t} - \mathcal{D}v)\,(v(x,t) - \Phi(Ke^x)) & = & 0 \quad (x,t) \in \mathbb{R} \times J, \\ v(x,0) & = & \Phi(Ke^x) \quad x \in \mathbb{R}, \end{cases} \tag{1.5.9}$$

where $J = (0,T]$ and the spatial differential operator can be defined as

$$\mathcal{D}v(x,t) = \frac{1}{2}\sigma^2 \frac{\partial^2 v}{\partial x^2} + (r - \frac{1}{2}\sigma^2)\frac{\partial v}{\partial x} - rv. \tag{1.5.10}$$

For computational purposes, the problem (1.5.7) has to be localized on a bounded domain $\Omega := (x^L, x^R)$, with x^L, and $x^R \in \mathbb{R}$. Now considering $u(x,t)$ as a solution of the following localized problem(1.5.11):

$$\begin{cases} \frac{\partial u}{\partial t} - \mathcal{D}u & \geq & 0 \quad (x,t) \in \Omega \times J, \\ u(x,t) - \Phi(Ke^x) & \geq & 0 \quad (x,t) \in \Omega \times J, \\ (\frac{\partial u}{\partial t} - \mathcal{D}u)\,(u(x,t) - \Phi(Ke^x)) & = & 0 \quad (x,t) \in \Omega \times J \\ u(x,0) & = & \Phi(Ke^x) \quad x \in \Omega. \end{cases} \tag{1.5.11}$$

Under certain assumptions related to the coefficients of the differential operator $\mathcal{D}$, the problems (1.5.7) and (1.5.11) are said to have unique solutions. Furthermore, within the interior of the domain, the localization error due to the domain truncation is shown to decrease exponentially with respect to the domain size.

Selecting whether to exercise an option at any given moment is essential. The decision to exercise an option depends on the value of the underlying asset, which determines whether the resulting asset

valuation is favorable or not. The problem of pricing an American option is a free-boundary problem, as it separates the range of asset values into two regions. Exercising the choice is sensible in one part but not in the other. Since the boundary between these regions is unknown in advance, it must be determined by solving the free-boundary problem. Importantly, this boundary is not fixed but evolves over time.

1.6 Hedging and Greeks

Hedging is a fundamental concept in finance that involves the practice of reducing a portfolio's sensitivity to the movements of an underlying asset or market factor by taking offsetting positions in different financial instruments. When we derived the Black-Scholes equation, we chose the Delta to be $\frac{\partial V}{\partial S}$, so that the portfolio Π became risk-free. This gives an important example on how hedging is applied. Let us see another example of hedging that is similar to what we have used in deriving the Black-Scholes equation. If Π denotes the price of option, then the slope is

$$\Delta = \frac{\partial \Pi}{\partial S}.$$

If the movement of the price is not very small, then it might be necessary to use the value of the second derivative of the portfolio with respect to S in order to eliminate most of the risk. The second derivative is known as gamma

$$\Gamma = \frac{\partial^2 \Pi}{\partial S^2}.$$

In practical hedging, it is often necessary to consider additional sensitivities, such as $\frac{\partial \Pi}{\partial t}$, $\frac{\partial \Pi}{\partial \sigma}$, $\frac{\partial \Pi}{\partial r}$, $\frac{\partial \Pi}{\partial D_0}$, which capture the portfolio's exposure to changes in time, volatility, interest rates, and dividends, respectively. Usually, $\frac{\partial \Pi}{\partial t}$, $\frac{\partial \Pi}{\partial \sigma}$, and $\frac{\partial \Pi}{\partial r}$ are referred to as **theta**, **vega**, and **rho**, respectively; that is, the following notation is used:

$$\Theta = \frac{\partial \Pi}{\partial t}, \quad \nu = \frac{\partial \Pi}{\partial \sigma}, \text{ and } \rho = \frac{\partial \Pi}{\partial r}.$$

In currency options, D_0 represents the interest rate in the foreign country. Thus, $\frac{\partial \Pi}{\partial D_0}$ is also known as rho. In order to distinguish between $\frac{\partial \Pi}{\partial r}$ and $\frac{\partial \Pi}{\partial D_0}$, here we define

$$\rho_d = \frac{\partial \Pi}{\partial D_0}.$$

These quantities are usually referred to as Greeks.

1.7 Pricing Models For Both American and European Options

This section provides a brief overview of pricing models for both American and European options. Both fundamental models can be extended in various ways. Although such extensions are not the primary focus

of this thesis, we highlight some notable examples. The Black–Scholes equation was originally derived under the assumption that the underlying asset does not pay dividends. However, dividend payments affect the price of the corresponding option, and several dividend payout schemes exist. For instance, [171] discusses both a constant dividend yield and discrete dividend payments. Further extensions of the model can be made by allowing for time-varying interest rates and volatility, yielding additional results [171]. The incorporation of jump processes in financial modeling is explored in [154].

This thesis uses American option pricing models based on parabolic partial differential equations, as discussed in the preceding section. Since these models cannot be solved analytically, numerical approaches must be used. The finite difference technique provides a straightforward numerical approach for approximating model solutions. The finite difference approach approximates derivatives in PDEs and PIDEs, creating discrete linear complementarity issues.

This section briefly discusses space and temporal discretizations. These concepts are discussed in the context of an initial value problem without an obstacle constraint. The American option may be used to accomplish finite difference discretization in the same manner as with an obstacle constraint. This section provides an overview of subjects related to the discretization of PDEs utilized in American option pricing. This section concludes with a set of linear equations that may be used to price European options. The following part discusses a solution to discrete linear complementarity problems related to American option pricing. In model (1.5.7), the PDE has one space variable, and derivatives have non-constant coefficients.

Since finite difference techniques have been used for decades in scientific computing and have several important applications, we employ these techniques in the articles of this thesis. The finite difference approach replaces partial derivatives with approximations and are ideal for rectangular computational domains [114, 116, 134, 149, 162]. These estimates are based on Taylor series expansions at certain places. The finite discretization scheme's form is determined by the order of the partial differential derivative and the precision of the finite difference approximation.

Other discretization approaches for the aforementioned PDEs include the finite element and finite volume methods. The finite element approach is more adaptable than the finite difference method, making it more straightforward to apply in situations where the computational domain's geometry is more complicated than rectangular. Finite element techniques are also used in the option pricing issue. Some examples can be found in [127, 141].

Finite volume methods are also employed to address option pricing problems (see [128, 187, 186]). Finite difference approximations can be constructed in several ways (e.g., [112]). Forward and backward finite difference schemes are the simplest approaches, providing first-order accurate estimates of the first derivative based on the grid step size. For the second derivative, a symmetric central-difference scheme can be used, achieving second-order accuracy. More sophisticated approximation methods are also available

for higher precision or stability requirements.

In [151], higher-order compact discretization algorithms are used to solve convective diffusion problems with time-dependent conditions. Option pricing follows a similar higher-order structure as described in [76]. There are several finite difference systems available, including those discussed in [156] for option pricing.

Finite difference methods are most straightforward to implement on grids with uniform step sizes, although more advanced, nonuniform grids can also be employed. Accurate approximations can be particularly important in certain regions of the computational domain. To achieve this, nonuniform grids are often used, with the finest discretization concentrated in specific areas of interest. In option pricing, for example, the grid is typically densest around the exercise price. The finite difference discretization then leads to a semi-discrete equation:

$$u_t + Au = 0 \tag{1.7.1}$$

The matrix A's structure is determined by the finite difference approximation. When the one-dimensional Black-Scholes equation is discretized using central finite difference techniques, the resulting matrix is tridiagonal. However, discretizing the two-dimensional PDE results in a sparse block tridiagonal matrix A.

The parabolic LCP (1.5.11) has a first-order time derivative, which also exists in the semi-discrete form (1.7.1). Euler methods, either explicit or implicit, are often used to estimate temporal derivatives.

The Backward difference approach of order two (BDF2) is a more accurate and widely used methodology. This procedure results in a series of linear equations.

$$(3I + 2\Delta tA)u^{n+1} = 4u^n - u^{n-1}, \tag{1.7.2}$$

where $n = 0, ..., N-1$, and Δt is the length of the time step, N is total number of temporal points. For further information on discretizing initial value problems, refer to [114] and [135].

In option pricing, the initial value is determined by the option contract's payoff function. The payoff function for call and put options is not smooth since the first derivative is discontinuous. The Crank–Nicolson method is also widely used in option pricing; however, it can lead to numerical oscillations [60, 77, 99, 128, 189]. This issue arises because the Crank–Nicolson scheme is not fully stable. Alternative time-stepping methods, such as the Runge–Kutta scheme and the Backward Difference Formula (BDF2), are both second-order accurate in time and L-stable [22, 169, 121]. This property is particularly useful in option pricing, as it prevents oscillations caused by non-smooth initial conditions.

A simple and effective approach is the Rannacher time-stepping technique [132], which combines the implicit Euler method with the Crank–Nicolson scheme. To address the oscillation problem, the implicit

Euler method is applied for the first few time steps, followed by the Crank–Nicolson method for the remaining steps. Rannacher time-stepping has been successfully applied in option pricing, for example, in [128]. To simplify the implementation of Rannacher time stepping, one may use implicit Euler steps with a step length half of Crank-Nicolson's step length. This option results in a single coefficient matrix from the Crank-Nicolson discretization, despite using two temporal discretizations.

1.8 Numerical Solution of Discretized Problems

This part briefly discusses numerical solutions for linear equations and discrete linear complementarity problems. These problems occur when partial differential equation models are discretized using finite difference or finite element methods. This section focuses on fundamental techniques for solving linear equations and LCPs, rather than providing a thorough discussion. Furthermore, this part concentrates largely on computational option pricing.

1.8.1 Numerical Solution of a System of Linear Equations

This thesis focuses on numerical solutions for American option pricing, but first introduces several concepts related to European option pricing. This also applies to numerical solutions for discrete option pricing issues. Some American option pricing techniques include solving a system of linear equations. European option pricing issues need linear equation solutions due to their discretization into systems. Direct and iterative solvers can solve linear equations.

The simplest technique to solve a system of linear equations is to utilize a LU decomposition. This is an effective solution strategy, particularly for tridiagonal matrices. However, when modelling produces a big and sparse matrix, the fundamental direct solution approach may be wasteful.

Iterative methods are often more efficient for solving linear systems arising from the discretization of PDEs in multiple dimensions. These methods generate approximate solutions starting from an initial guess and iteratively refine them until the desired accuracy is achieved. The efficiency of an iterative method is determined by the rate of convergence. Some of the most basic and widely used iterative techniques include the Jacobi, Gauss–Seidel, and successive over-relaxation (SOR) methods [58].

Multigrid techniques may solve a system of linear equations more effectively. These approaches aim to minimize low-frequency error using coarser grids, whereas high-frequency error may be reduced using a traditional iterative method on narrow grids. A multigrid approach restricts the solution or residue to a coarser grid. The answer or correction is transferred to a finer grid using interpolation (prolongation). Several papers, including [20, 63, 161, 170], discuss multigrid approaches.

At this point, it's important to discuss splitting approaches for solving linear equation systems. The Peaceman-Rachford formula and Douglas-Rachford approach are described in [125, 47]. These techniques

are known as alternating direction implicit (ADI) procedures. Numerous splitting strategies are discussed, including [59, 105, 109, 110], and references therein. Splitting approaches break complex operators into simpler structures. After dividing, the task remains to solve a series of linear equations. Proper splitting makes the leftover systems simpler to solve than the original.

Strang's suggested symmetry in [152] may improve splitting techniques' accuracy. The ADI approach is used in the context of option pricing [32]. The pricing problem is transformed into a typical diffusion equation without the cross-derivative element, allowing for easy application of the ADI approach.

Books [156] and [171] briefly describe the application of the ADI technique for options pricing issues. In [48], the two-dimensional option pricing problem is changed to a diffusion form, followed by the use of ADI approach. In [90], the splitting approach is used to price European-style options using stochastic volatility assumptions.

1.8.2 Numerical Solution of Linear Complementarity Problem

The finite difference discretization of the time-dependent problem (1.5.7) leads to a discrete LCP. LCPs are used in a variety of fields beyond option pricing, with applications in engineering and economics, as discussed in [54]. LCPs have been widely explored in [38].

This article demonstrates that LCPs are applicable beyond financial option pricing. The article describes several pivoting strategies for solving LCPs, which rely on specific assumptions about the underlying matrix. Pivoting methods are effective for solving smaller problems, whereas iterative methods offer a more flexible approach for tackling larger or more complex LCPs.

The projected SOR (PSOR) method [40] is a widely used iterative approach that applies the SOR technique to solve systems of linear equations. Efficient domain decomposition strategies for obstacle problems using an M-matrix are discussed in [155]. The works [21] and [57] provide comprehensive overviews of numerical methods employed in financial derivative pricing. Brennan and Schwartz [18] present a simple numerical approach for pricing American options by solving an LCP that models the option price implicitly. A detailed analysis of this approach is given in [80]. This method is also employed in this thesis to price American options under stochastic volatility assumptions. Using a component-wise splitting technique allows direct application of the Brennan and Schwartz method to solve subproblems. McCartin [108] also proposes a straightforward approach for American option pricing. Huang [70] studies American option pricing from the perspective of LCPs, while Dempster and Hong [45] use a linear programming approach to solve one-dimensional PDE-based American option pricing problems.

Multigrid techniques have been applied to LCPs in several studies. Brandt [17] develops a projected full approximation scheme (PFAS) to solve LCPs, which is also applicable to American-style options. Clarke [30, 31] employs fast multigrid iteration combined with coordinate transformations for pricing

American options under stochastic volatility. Oosterlee [121] examines multigrid methods with multiple smoothers, and Reisinger [133] applies multigrid techniques to high-dimensional European and American option pricing problems.

The ADI method is another approach used in American option pricing. Villeneuve [163] applies an ADI-type scheme to price an option on two underlying stocks, where the pricing equation is a two-dimensional parabolic PDE. Prior to using the ADI approach, the convection-diffusion equation is transformed into the standard heat equation, and the direct Brennan and Schwartz method is employed to handle the early exercise constraint.

This article examines American option pricing models based on PDEs and finite difference techniques. The necessary conditions for numerical method, convergence, and stability are taken into account. The pivoting technique is used to solve an American option pricing model with transaction costs.

1.9 Motivation of The Work

The operator splitting approach leverages an auxiliary variable to improve accuracy and reduce computational cost compared to other methods. Despite its advantages, the literature lacks comprehensive stability and error analyses of the operator splitting method for American option pricing problems. A pioneering contribution in this area was made by Feng Chen and Jie Shen [24], who established stability results for the first-order and second-order backward difference operator splitting methods, along with an error analysis for the first-order method. In this work, we extend these efforts by providing stability and error analyses for the operator splitting method applied to American option pricing without requiring derivatives of the payoff function. The primary objective is to present the BDF1-OS and BDF2-OS time semi-discretization schemes for pricing American options within the Black–Scholes framework, along with stability and error estimates for these schemes. The BDF2-OS method achieves an accuracy between 1.5 and 2, while the fully discrete BDF1-OS scheme is asymptotically first-order accurate. These methods efficiently approximate both the option value and key "Greeks" such as Delta and Gamma. By refining the mesh near the singularity, the schemes effectively handle the non-smooth payoff function. Iterations at each time step are unnecessary, as the discretization results in a tridiagonal system that can be solved directly and efficiently. Moreover, since the choice of spatial discretization is independent of the temporal discretization, alternative spatial methods such as meshless radial basis functions (RBFs), finite elements, or spectral methods can also be employed. The use of non-uniform grids in spatial discretization is fully compatible with these approaches.

1.10 A Brief Discussion on The Main Results

This thesis is organized into six chapters of which **Chapter 1** is introductory that contains a brief review of the literature concerned with the topic and motivation of the study. In this section of introductory chapter, a concise summary of the contribution for each of the remaining chapters is highlighted.

In **Chapter 2**, we present the stability and error analysis of backward difference operator splitting methods for solving the linear complementarity problem for pricing the American options under the Black-Scholes framework. The OS schemes are effectively applied to a variety of Black-Scholes models since they allow the complementarity conditions and the differential equation to be treated separately. We derive error estimates for these methods and a priori stability results for operator splitting strategies based on the BDF1 and BDF2 approaches. We perform numerical experiments to illustrate the order and efficiency of the BDF1 and BDF2 approaches for the test problems, thereby emphasizing the convergence behavior of the proposed methods. We also verify the numerical results with the existing methods in the literature. Part of the work done in this chapter has been published in *Computational Economics*.

In **Chapter 3**, the operator splitting method is effectively applied to jump-diffusion models, which can be efficiently implemented because the differential and complementarity conditions are decoupled and hence can be solved separately. Despite their ubiquity, these operator-splitting approaches for jump-diffusion models lack stability and error analyses. In this context, we perform a priori stability analysis for the implicit-explicit backward difference operator splitting techniques. Following the stability analysis, we establish the error estimates for IMEX-BDF1-OS and IMEX-BDF2-OS techniques. To validate the theoretical results, numerical experiments on the pricing of American options under Kou's and Merton's jump-diffusion models are presented. Part of this work done in this chapter has been published in *Computational and Applied Mathematics*.

In **Chapter 4**, we present the stability and error analysis for the IMEX-BDF-OS techniques, which aim to solve the linear complementarity problem for pricing American options in a Markovian RSJD economy. Multiple regime-switching models are fitted with the OS schemes which yields favorable outcomes. The complementarity conditions and the differential equation are separated and studied independently, making them efficient to apply to the LCP. Despite their popularity, no stability or error analysis has previously been provided for the American option under the RSJD model using these operator-splitting procedures. Based on the IMEX-BDF1 and IMEX-BDF2 approaches, we estimate the error for these techniques and furthermore offer a priori stability estimates for operator splitting strategies. We numerically test the operator splitting techniques and demonstrate the performance of IMEX-BDF1 and IMEX-BDF2 worked for the test problems, highlighting their convergence behaviour. One manuscript based on the work of this chapter has been *communicated*.

In **Chapter 5**, we present two efficient and accurate implicit-explicit finite difference techniques to solve the system of semi-linear PDEs and the system of semi-linear complementarity problems arising in option pricing under the liquidity switching model. For the time semi-discretization, we employ two numerical techniques, namely, BDF1 and BDF2. The stability of temporal semi-discretized systems is also established. The computational techniques developed for the European options are extended to include the American option. We integrate the IMEX-BDF1 and IMEX-BDF2 methods with an operator splitting method to solve the semi-linear system of complementarity problems that determines the price of an American option. Numerical results for European and American call options are also presented to demonstrate the effectiveness and precision of the proposed techniques. The option value, Gamma, Delta, and computational errors are plotted with different parameters to perform sensitivity analysis of the proposed option pricing model. One manuscript based on this chapter has been *communicated*.

Finally, in **Chapter 6**, we summarize the key findings of the current study as well as potential future research opportunities, followed by a list of related references. A list of papers published/communicated based on the thesis is also provided at the end.

To make each chapter as independent as possible, some definitions and key results are repeated in the upcoming chapters.

CHAPTER 2

Operator Splitting Method to Solve the Linear Complementarity Problem for Pricing American Option: An Approximation of Error[1]

.

2.1 Introduction

An option is considered one of the most important financial derivatives in the financial sector. To meet the objective of computing the price of European options, there exist numerous analytical solutions. However, many intriguing concerns have been raised regarding the analytic form of the exact solution of the American option. Since American options can be exercised at any point during their lifespan, they offer greater flexibility, which generally increases their value compared to other option types. Due to this flexibility, the American option possesses an added limitation for the price of the option, owing to which they result in free boundary value problems. We can thus infer that the numerical estimation for the American option is very

[1]The results discussed in this chapter have been published in *Computational Economics*, 64, 3353-3379 (2024), https://doi.org/10.1007/s10614-024-10564-x

different from those of the European option due to the limitations and moving boundaries. Hence, when we are dealing with the American option, much more practical significance can be derived from numerical methods, currently regarded as a topic of increased interest in the financial market. Throughout this paper, we primarily concentrate on numerical estimations of the American options and undergo careful investigation of the related numerical techniques.

Various methods have been proposed in the literature to help in solving the discretized linear complementarity problem arising in American option pricing. Wu et al. [173] presented the front-fixing method for solving the American option pricing problems. Nielsen et al. [119] presented the front-fixing method and penalty methods to handle the LCP for pricing American options. Front-fixing methods apply a non-linear transformation to fix the boundary and solve the resulting non-linear problem. Penalty methods, on the other hand, eliminate the free boundary by adding a non-linear penalty term to the PDE. Further, Nielsen et al. [120] presented the penalty method for multi-asset American option pricing problems. Tangman et al. [153] proposed a high-order compact finite difference algorithm for pricing American options. Wang et al. [165, 166] proposed the power penalty method for linear complementarity problems arising in American option pricing. Yong Hoon Kwon and Younhee Lee [97] used the tridiagonal method to solve the American option pricing problem. Kumar et al. [96] present a highly accurate wavelet-based approximation technique to explore the sensitivities and value of American options diagnosed by linear complementarity problems. Many authors employed the finite element approach to calculate the American option value. For pricing the Multi-Asset American Options, Kovalov et al. [94] used a Finite Element Method-of-Lines with Smooth Penalty. Holmes and Yang [68] proposed a front-fixing finite element approach for valuing American options on stocks and demonstrated its stability and nonnegativity under some reasonable assumptions. Zhang et al. [184] presented a finite element method for pricing American multi-asset put options. Under the Heston model, Zhang et al. [182] employed the semi-implicit finite element approach to the valuation of American put options. Bani Asadi and Rivaz [10] introduced the Tau approach for pricing American options under complex financial models. Some other works on the solution of the American option can be found in [33, 55, 65, 89, 185] and reference therein.

In recent works, Kadalbajoo et al. [82, 83, 81] examined the efficiency of the meshfree method to deal with option pricing problems based on the local radial basis function for numerically solving the multi-dimensional option pricing problem. Bhuruth et al. [138] brought forward a differential quadrature rule based on RBF for spatial discretization along with integration with respect to exponential time to work upon the jump-diffusion model. In the near past, [158] devised a compact-RBF scheme that helps to achieve an accuracy of higher order when used with a local mesh refinement scheme. Dehghan et al. [43] presented a new class of radial basis function and explored its efficiency in option pricing problems. Some other meshfree methods for option pricing problems can be found in [113, 115, 130, 177] and references

therein.

The method of operator splitting was introduced by Ikonen and Toivanen [78] to solve the LCPs for American option pricing problems. Later on, the operator splitting method was widely used for the pricing of American options under the two-asset Merton model by Boen and Hout [15]. Ikonen and Toivanen [79] used the operator splitting methods for pricing American option under stochastic volatility. V Shcherbakov [142] employed the Operator splitting approach in the Black-Scholes model to price the multi-asset American put option. Xu et al. [174] proposed a new efficient operator splitting method for option pricing problem under the Heston model. In recent research, Chen et al. [26] proposed a new operator splitting method for American options under time-fractional Black-Scholes models. One can see other works on operator splitting techniques that have been applied effectively to solve the LCPs in [103, 184]. The operator splitting approach, on the other hand, takes advantage of the auxiliary variable to increase the accuracy and reduce the computational cost in comparison to other methods. Despite these advantages of the operator splitting method, in literature, there is a lack of stability and error estimates of the operator splitting method for American option pricing problems. The first novel contribution in this direction have been made by Feng Chen and Jie Shen [24]. They established the stability results for the first-order backward difference operator splitting method and second-order backward difference operator splitting method along with error analysis of the first-order backward difference method. In the analysis of [24], the authors used the derivative of the payoff function in equation (4.13), as we know the payoff function for the American option is not smooth at the exercise price.

In this chapter, we make efforts to provide stability and error analysis of the operator splitting method for pricing the American option by precluding the use of the derivative of the payoff function. The objective of this work is to present the BDF1-OS and BDF2-OS time semi-discretization methods for pricing American options in a Black-Scholes framework and provide the stability and error estimates for these schemes. Additionally, the accuracy of the BDF2-OS is between 1.5 and 2, and the BDF1-OS is first-order accurate. The suggested approaches effortlessly approximate the option value as well as some of its significant "Greeks". By condensing mesh close to the singularity, these techniques effectively handle the singularity of the non-smooth pay-off function. We don't need to employ iterations at each time step. Our discretization results in a tridiagonal system at each time step that can be solved quickly and directly. Since the choice of spatial discretization is unrelated to the choice of temporal discretization, one may also use alternative approaches for spatial discretization, such as meshless methods (RBFs), finite elements, spectral methods, etc. The use of a non-uniform grid in spatial discretization is also permitted. The rest of the chapter is structured as follows. We start by describing the linear complementarity problem and its associated characteristics, basic notations, symbols, and assumptions used throughout this chapter and introduced the operator splitting methods. In Sect. 2.4, we verify the stability analysis of operator splitting

methods, and in Section 2.5, we present the error estimates for BDF1-OS and BDF2-OS methods. In Section 2.6, we present some numerical outcomes to verify our theoretical findings and related discussions.

2.2 Linear Complementarity Problem

We can formulate the LCP for pricing American option (for more details see [3]) as (2.2.1):

$$\begin{cases} \frac{\partial V}{\partial \tau} + \mathcal{D}V & \leq & 0 & (S,\tau) \in [0,\infty) \times [0,T), \\ V(S,\tau) - \Phi(S) & \geq & 0 & (S,\tau) \in [0,\infty) \times [0,T), \\ (\frac{\partial V}{\partial \tau} + \mathcal{D}V)\,(V(S,\tau) - \Phi(S)) & = & 0 & (S,\tau) \in [0,\infty) \times [0,T), \\ V(S,T) & = & \Phi(S) & S \in [0,\infty), \end{cases} \tag{2.2.1}$$

where S denotes the stock price of any asset at a given time τ with fixed volatility σ and interest rate r. The spatial differential operator can be defined as:

$$\mathcal{D}V(S,\tau) = \frac{1}{2}\sigma^2 S^2 \frac{\partial^2 V}{\partial S^2} + rS\frac{\partial V}{\partial S} - rV. \tag{2.2.2}$$

The price of the option $V(S,T)$ at the time of maturity T is termed as a payoff function; for example, the put option is governed by the payoff function:

$$\Phi(S) = \max(K - S, 0), \tag{2.2.3}$$

with a strike price of K.

Albeit the problem (2.2.1) is backward in time and degenerate, we can convert it into forward in time and a non-degenerate problem by applying the transformations $x := \ln(\frac{S}{K})$, $t := T - \tau$, and $v(x,t) := V(Ke^x, T-\tau)$, i.e.,

$$\begin{cases} \frac{\partial v}{\partial t} - \mathcal{D}v & \geq & 0 & (x,t) \in \mathbb{R} \times J, \\ v(x,t) - \Phi(Ke^x) & \geq & 0 & (x,t) \in \mathbb{R} \times J, \\ (\frac{\partial v}{\partial t} - \mathcal{D}v)\,(v(x,t) - \Phi(Ke^x)) & = & 0 & (x,t) \in \mathbb{R} \times J, \\ v(x,0) & = & \Phi(Ke^x) & x \in \mathbb{R}, \end{cases} \tag{2.2.4}$$

where $J = (0,T]$ and the spatial differential operator can be defined as

$$\mathcal{D}v(x,t) = \frac{1}{2}\sigma^2 \frac{\partial^2 v}{\partial x^2} + (r - \frac{1}{2}\sigma^2)\frac{\partial v}{\partial x} - rv. \tag{2.2.5}$$

For evaluational purposes, the problem (2.2.4) has to be localized on a bounded domain $\Omega := (x^L, x^R)$, with x^L, and $x^R \in \mathbb{R}$. Now considering $u(x,t)$ as a solution of the following localized problem (2.2.6):

$$\begin{cases} \frac{\partial u}{\partial t} - \mathcal{D}u & \geq & 0 & (x,t) \in \Omega \times J, \\ u(x,t) - \Phi(Ke^x) & \geq & 0 & (x,t) \in \Omega \times J, \\ (\frac{\partial u}{\partial t} - \mathcal{D}u)\,(u(x,t) - \Phi(Ke^x)) & = & 0 & (x,t) \in \Omega \times J \\ u(x,0) & = & \Phi(Ke^x) & x \in \Omega. \end{cases} \tag{2.2.6}$$

Under certain assumptions related to the coefficients of the differential operator $\mathcal{D}$, the problems (2.2.4) and (2.2.6) are said to have unique solutions. Furthermore, within the interior of the domain, the localization error due to the domain truncation is shown to decrease exponentially with respect to the domain size.

2.3 Operator Splitting Method

To solve the linear complementarity problem (2.2.6), we propose the time discretization schemes based on operator splitting. These techniques are generally used in computational fluid dynamics (for more details, see [2, 59]) and references therein. Firstly, the method of operator splitting was proposed by Ikonen and Toivanen [78] for fulfilling the motive of evaluating the American put option. The basic idea is to decouple problematic operators into separate fractional time steps in the discretization. In our case, we decouple the Black-Scholes operator and the constraint for the value of the option. This splitting leads to the solution of a linear problem and to a simple correction step at each time step. Thus, the arising subproblems can be solved much more easily and efficiently than the original problem. The primary idea behind the introduction of the operator splitting method is to derive an expression with the help of an additional variable ψ such that $\psi = u_t - \mathcal{D}u$.

We can reformulate LCP (2.2.6) as

$$\begin{cases} \frac{\partial u}{\partial t} - \mathcal{D}u &= \psi, \\ (u(x,t) - \Phi(Ke^x)) \cdot \psi &= 0, \\ u(x,t) - \Phi(Ke^x) &\geq 0, \\ \psi &\geq 0, \end{cases} \tag{2.3.1}$$

in the region $\Omega \times J$.

Let the system (2.3.1) be initially discretized in time with uniform grid $t_n = nk$, $n = 0, 1, 2, \ldots, N$ and uniform temporal mesh length k, where $u(x, t_n)$ is abbreviated as u_n. Now, we have a brief discussion about BDF1 and BDF2 operator splitting methods for the temporal discretization of LCP (2.3.1).

2.3.1 BDF1-OS Method

It is a first-order implicit backward difference method commonly used for time-stepping in stiff differential equations. For the temporal semi-discretization of the system (2.3.1), let us split the governing equation $u_t - \mathcal{D}u = \psi$ on the $(n+1)^{th}$ time level into two discrete equations as

$$\left(\frac{\tilde{u}_{n+1} - u_n}{k}\right) - \mathcal{D}\tilde{u}_{n+1} = \psi_n, \tag{2.3.2}$$

$$\left(\frac{u_{n+1} - u_n}{k}\right) - \mathcal{D}\tilde{u}_{n+1} = \psi_{n+1}. \tag{2.3.3}$$

Now, the discrete problem for LCP (2.3.1) is to search for the pair (u_{n+1}, ψ_{n+1}), which satisfies both the discrete equations (2.3.2) and(2.3.3) as well as the constraints

$$\begin{cases} u_{n+1} & \geq & \Phi, \\ \psi_{n+1} & \geq & 0, \\ \psi_{n+1}(u_{n+1} - \Phi) & = & 0. \end{cases} \tag{2.3.4}$$

The first step is to find out the intermediate approximation $\tilde{u}_{n+1}$ by solving the equations (2.3.2) with known auxiliary term ψ_n under boundary conditions:

$$\tilde{u}_{n+1}(x^L) = K, \qquad \tilde{u}_{n+1}(x^R) = 0.$$

The second step of the operator splitting method is to establish a connection in (2.3.3) between u_{n+1} and ψ_{n+1} under the constrain (2.3.4). In order to secure this, we need to re-express the equation (2.3.3) using results from equation (2.3.2) along with the constraints in (2.3.4) as a problem to search for the pair (u_{n+1}, ψ_{n+1}), such that

$$\begin{cases} \frac{u_{n+1} - \tilde{u}_{n+1}}{k} & = & \psi_{n+1} - \psi_n, \\ \psi_{n+1}(u_{n+1} - \Phi) & = & 0, \end{cases} \tag{2.3.5}$$

with the constraints

$$u_{n+1} \quad \geq \quad \Phi \quad \text{and} \quad \psi_{n+1} \quad \geq \quad 0. \tag{2.3.6}$$

Again, by solving the problems (2.3.5)-(2.3.6) in (u_{n+1}, ψ_{n+1}) plane, we get

$$(u_{n+1}, \psi_{n+1}) = \begin{cases} (\Phi, \psi_n + \frac{\Phi - \tilde{u}_{n+1}}{k}) & \text{if } \tilde{u}_{n+1} - k\psi_n \leq \Phi, \\ (\tilde{u}_{n+1} - k\psi_n, 0) & \text{otherwise.} \end{cases} \tag{2.3.7}$$

Therefore, one can perform the second step by working out a discrete equation (2.3.2) with the updated formula (2.3.7). The pair (u_0, ψ_0) at zeroth time level can be found with the aid of the given initial condition, followed by assigning the value $\psi_0 = 0$.

Algorithm to evaluate an American option

Below, we present the algorithm to solve the LCP (2.3.1) numerically using BDF1-OS method.

`for` $n = 0 : N - 1$

$\frac{\tilde{U}^m_{n+1} - U^m_n}{k} - \mathcal{D}\tilde{U}^m_{n+1} = \Psi^m_n$

$U^m_{n+1} = \max(\tilde{U}^m_{n+1} - k\Psi^m_n, \Phi(x_m))$

$\Psi^m_{n+1} = \Psi^m_n + \frac{U^m_{n+1} - \tilde{U}^m_{n+1}}{k}$

`end`

2.3.2 BDF2-OS Method

The BDF2 technique, which is often initiated with the first-order backward-difference approach, necessitates solutions at two prior time steps. Usually, the first-time step is taken relatively small to reduce the impact of the first-order error. The accuracy of the BDF2 is higher than the BDF1 method. Now for semi-discretization of LCP (2.3.1), let us assume that the values $\{u_n, \psi_n\}$ and $\{u_{n-1}, \psi_{n-1}\}$ are apriory known at the points t_n and t_{n-1}. Now, we perform two sub-steps at discrete point t_{n+1}; in first step, we compute an intermediate value $\tilde{u}_{n+1}$ using the following BVP

$$\begin{cases} \frac{1}{k}\left(\frac{3}{2}\tilde{u}_{n+1} - 2u_n + \frac{1}{2}u_{n-1}\right) - \mathcal{D}\tilde{u}_{n+1} &= \psi_n, \\ \tilde{u}_{n+1}(x^L) = K, \qquad \tilde{u}_{n+1}(x^R) = 0. \end{cases} \tag{2.3.8}$$

Here, the second step of the operator splitting method proceeds with projecting the $\tilde{u}_{n+1}$ on constraint space to obtain u_{n+1} with the following correction terms

$$\begin{cases} \frac{3}{2}\frac{u_{n+1}-\tilde{u}_{n+1}}{k} &= \psi_{n+1} - \psi_n, \\ u_{n+1} &\geq \Phi, \\ \psi_{n+1} &\geq 0, \\ \psi_{n+1}(u_{n+1} - \Phi) &= 0. \end{cases} \tag{2.3.9}$$

By solving the problems (2.3.9) in (u_{n+1}, ψ_{n+1}) plane, we get

$$(u_{n+1}, \psi_{n+1}) = \begin{cases} (\Phi, \psi_n + \frac{3}{2}\frac{\Phi - \tilde{u}_{n+1}}{k}) & \text{if } \tilde{u}_{n+1} - \frac{2k}{3}\psi_n \leq \Phi, \\ (\tilde{u}_{n+1} - \frac{2k}{3}\psi_n, 0) & \text{otherwise.} \end{cases} \tag{2.3.10}$$

Hence, one can perform the first step by solving a discrete equation (2.3.8) and the second step with the help of the revised formula (2.3.10). The aforementioned implicit method with three levels of time needs the values obtained from the earlier two time levels. The pair (u_0, ψ_0) at the zeroth time level can be acquired by making use of the initial condition and assigning the value given by $\psi_0 = 0$. To get the pair (u_1, ψ_1) at the next level succeeding the zeroth time level, we can use the BDF1-OS method.

Algorithm to evaluate an American option

Similar to BDF1-OS method, we present the algorithm to solve the LCP (2.3.1) numerically using BDF2-OS method.

```
for n = 0 : N − 1
  if n ≤ 1
    (Ũ^m_{n+1} − U^m_n)/k − D Ũ^m_{n+1} = Ψ^m_n
    U^m_{n+1} = max(Ũ^m_{n+1} − kΨ^m_n, Φ(x_m))
    Ψ^m_{n+1} = Ψ^m_n + (U^m_{n+1} − Ũ^m_{n+1})/k
  else
```

$\frac{1}{k}\left(\frac{3}{2}\tilde{U}^m_{n+1} - 2U^m_n + \frac{1}{2}U^m_{n-1}\right) - \mathcal{D}\tilde{U}^m_{n+1} = \Psi^m_n$

$U^m_{n+1} = \max(\tilde{U}^m_{n+1} - \frac{2k}{3}\Psi^m_n, \Phi(x_m))$

$\Psi^m_{n+1} = \Psi^m_n + \frac{3}{2}\frac{U^m_{n+1} - \tilde{U}^m_{n+1}}{k}$

end

end

2.4 Stability Analysis

For theoretical convenience, let us transform the problem (2.3.1) into a problem with homogeneous boundary condition, i.e.,

$$\begin{cases} \frac{\partial w}{\partial t} - \mathcal{D}w &= \psi + f, \quad (x,t) \in \Omega \times J, \\ (w(x,t) - w_0(x)) \cdot \psi &= 0, \quad (x,t) \in \Omega \times J, \\ w(x,t) - w_0(x) &\geq 0, \quad (x,t) \in \Omega \times J, \\ \psi &\geq 0, \quad (x,t) \in \Omega \times J, \\ w(x,0) &= w_0(x), \quad x \in \Omega \\ w(x,t) &= 0, \quad (x,t) \in \partial\Omega \times \bar{J}, \end{cases} \tag{2.4.1}$$

where $w_0(x) := \Phi(Ke^x) - \phi(x)$, $w(x,t) = u(x,t) - \phi(x)$ and $f = \mathcal{D}\phi$, $x \in \mathbb{R}$, and

$$\phi(x) = \frac{x^R - x}{x^R - x^L}\Phi(Ke^{x^L}) + \frac{x - x^L}{x^R - x^L}\Phi(Ke^{x^R}) : x \in \overline{\Omega}.$$

In order to check the stability of the time semi-discretizations, we will need the following Lemma 2.4.1.

Lemma 2.4.1. *(Discrete Gronwall's Lemma) Let us suppose that α_n is a non-negative sequence, and that the sequence β_n satisfies*

$$\begin{cases} \beta_0 \leq \delta_0, \\ \beta_n \leq \delta_0 + \sum_{k=0}^{n-1}\gamma_k + \sum_{k=0}^{n-1}\alpha_k\beta_k \quad n \geq 1, \end{cases}$$

then β_n satisfies

$$\begin{cases} \beta_1 \leq \delta_0(1+\alpha_0) + \gamma_0, \\ \beta_n \leq \delta_0\prod_{k=0}^{n-1}(1+\alpha_k) + \sum_{k=0}^{n-2}\gamma_k\prod_{s=k+1}^{n-1}(1+\alpha_s) + \gamma_{n-1} \quad n \geq 2. \end{cases}$$

Moreover, if $\delta_0 \geq 0$ and $\gamma_n \geq 0$ for $n \geq 0$, it follows

$$\beta_n \leq \left(\delta_0 + \sum_{k=0}^{n-1}\gamma_k\right)\exp(\sum_{k=0}^{n-1}\alpha_k), \ n \geq 1.$$

Proof. For more details, see Lemma (1.4.1) in [129]. □

2.4.1 Identities and Inequalities

We will frequently use the following results throughout the stability and error analysis:

$$\begin{aligned}(\mathcal{D}U, U) &= \frac{1}{2}\sigma^2(U_{xx}, U) + (r - \frac{1}{2}\sigma^2)(U_x, U) - r(U, U)\\ &= -\frac{\sigma^2}{2}\left(\|U_x - \frac{(r-\frac{\sigma^2}{2})}{\sigma^2}U\|^2\right) + \frac{(r-\frac{\sigma^2}{2})^2 - 2r\sigma^2}{2\sigma^2}\|U\|^2\\ &\leq \frac{\left(r-\frac{\sigma^2}{2}\right)^2 - \left(2r\sigma^2\right)}{2\sigma^2}\|U\|^2\\ &\leq \alpha\|U\|^2, \end{aligned} \tag{2.4.2}$$

where $\alpha = \left|\frac{\left(r-\frac{\sigma^2}{2}\right)^2 - \left(2r\sigma^2\right)}{2\sigma^2}\right|$.

We will frequently use the Young's inequality for all $a, b \in \mathbb{R}$ with ϵ (valid for every $\epsilon > 0$), i.e,

$$(a, b) \leq \epsilon a^2 + \frac{1}{4\epsilon}b^2. \tag{2.4.3}$$

We will also use the following algebraic identities in our analysis:

$$2\,(a-b, a) = a^2 - b^2 + (a-b)^2; \tag{2.4.4}$$

$$2\,(3a - 4b + c, a) = a^2 + (2a-b)^2 - b^2 - (2b-c)^2 + (a - 2b + c)^2. \tag{2.4.5}$$

Throughout the paper, the term C refers to a general constant that can rely on the data and the regularity of the precise solution but is independent of the temporal mesh length, k.

2.4.2 Stability Analysis for BDF1-OS

Theorem 2.4.2. *The scheme* (2.3.2) *and* (2.3.5) *is stable under the assumption* $k < \frac{1}{2(4\alpha+1)}$, *in the following sense:*

$$\|w_m\|^2 + \frac{1}{2}\sum_{n=0}^{m-1}\|\tilde{w}_{n+1} - w_n\|^2 + k^2\|\psi_m\|^2 \leq C\left(\|w_0\|^2 + k\|\psi_0\|^2 + k\sum_{n=0}^{m-1}\|f\|^2 + k\sum_{n=0}^{m-1}\|\psi_n\|^2\right),$$

$\forall\ 1 \leq m \leq \frac{T}{k}$, *where* C *is a constant that depends on the parameters* r, σ, *and* T, *but may not be the same at each occurrence.*

Proof. Consider the equation (2.3.2) for the transformed problem (2.4.1), we have

$$\frac{\tilde{w}_{n+1} - w_n}{k} = \mathcal{D}\tilde{w}_{n+1} + f + \psi_n. \tag{2.4.6}$$

Taking the inner product of (2.4.6) with $4k\tilde{w}_{n+1}$ to have

$$2\|\tilde{w}_{n+1}\|^2 - 2\|w_n\|^2 + 2\|\tilde{w}_{n+1} - w_n\|^2 \leq 4k\alpha\|\tilde{w}_{n+1}\|^2 + 4k(f, \tilde{w}_{n+1}) + 4k(\psi_n, \tilde{w}_{n+1}). \tag{2.4.7}$$

Next, we rewrite the equation (2.3.5) as

$$w_{n+1} - w_0 - k\psi_{n+1} = \tilde{w}_{n+1} - w_0 - k\psi_n. \tag{2.4.8}$$

Taking inner product of both sides of (2.4.8) with itself, we have

$$\begin{aligned} \|w_{n+1}\|^2 + \|w_0\|^2 \quad &- \quad 2\|w_{n+1}\|\|w_0\| + k^2\|\psi_{n+1}\|^2 - 2k(w_{n+1} - w_0, \psi_{n+1}) \\ &\leq 2\|\tilde{w}_{n+1}\|^2 + 2\|w_0\|^2 + k^2\|\psi_n\|^2 - 2k(\tilde{w}_{n+1}, \psi_n) + 2k(w_0, \psi_n). \end{aligned}$$

After some sort of calculations, we get

$$\begin{aligned} \|w_{n+1}\|^2 \quad &+ \quad \|w_0\|^2 - \frac{1}{2}\|w_{n+1}\|^2 - 2\|w_0\|^2 + k^2\|\psi_{n+1}\|^2 - 2k(w_{n+1} - w_0, \psi_{n+1}) \\ &\leq 2\|\tilde{w}_{n+1}\|^2 + 2\|w_0\|^2 + k^2\|\psi_n\|^2 - 2k(\tilde{w}_{n+1}, \psi_n) + 2k(w_0, \psi_n). \end{aligned} \tag{2.4.9}$$

Combining the inequalities (2.4.7) and (2.4.9) and taking account of $(w_{n+1} - w_0, \psi_{n+1}) = 0$, we get

$$\begin{aligned} \frac{1}{2}\|w_{n+1}\|^2 - 2\|w_n\|^2 \quad &+ \quad 2\|\tilde{w}_{n+1} - w_n\|^2 + k^2(\|\psi_{n+1}\|^2 - \|\psi_n\|^2) \\ &\leq \quad 3\|w_0\|^2 + 4k\alpha\|\tilde{w}_{n+1}\|^2 + 4k(f, \tilde{w}_{n+1}) + 2k(\tilde{w}_{n+1}, \psi_n) + 2k(w_0, \psi_n). \end{aligned}$$

Furthermore, we have

$$\begin{aligned} \frac{1}{2}\|w_{n+1}\|^2 \quad &- \quad 2\|w_n\|^2 + 2\|\tilde{w}_{n+1} - w_n\|^2 + k^2(\|\psi_{n+1}\|^2 - \|\psi_n\|^2) \\ &\leq \quad 3\|w_0\|^2 + 4k\alpha\|\tilde{w}_{n+1}\|^2 + 8k\|f\|^2 + \frac{1}{2}k\|\tilde{w}_{n+1}\|^2 + 3k\|\psi_n\|^2 + \frac{1}{2}k\|\tilde{w}_{n+1}\|^2 + k\|w_0\|^2 \\ &\leq \quad 3\|w_0\|^2 + k(4\alpha+1)\|\tilde{w}_{n+1} - w_n + w_n\|^2 + 8k\|f\|^2 + 3k\|\psi_n\|^2 + k\|w_0\|^2 \\ &\leq \quad (3+k)\|w_0\|^2 + 2k(4\alpha+1)\|\tilde{w}_{n+1} - w_n\|^2 + 2k(4\alpha+1)\|w_n\|^2 + 8k\|f\|^2 + 3k\|\psi_n\|^2. \end{aligned}$$

After small calculations, we obtain

$$\begin{aligned} &\frac{1}{2}\|w_{n+1}\|^2 - \frac{1}{2}\|w_n\|^2 + \frac{3}{2}\|\tilde{w}_{n+1} - w_n\|^2 + k^2(\|\psi_{n+1}\|^2 - \|\psi_n\|^2) \\ &\leq (3+k)\|w_0\|^2 + 2k(4\alpha+1)\|\tilde{w}_{n+1} - w_n\|^2 + (2k(4\alpha+1) + \frac{3}{2})\|w_n\|^2 + 8k\|f\|^2 + 3k\|\psi_n\|^2. \end{aligned}$$

Now let us imagine that the k is tiny enough such that $k < \frac{1}{2(4\alpha+1)}$, then above inequality implies,

$$\begin{aligned} \frac{1}{2}\|w_{n+1}\|^2 \quad &- \quad \frac{1}{2}\|w_n\|^2 + \frac{1}{2}\|\tilde{w}_{n+1} - w_n\|^2 + k^2(\|\psi_{n+1}\|^2 - \|\psi_n\|^2) \\ &\leq \quad (3+k)\|w_0\|^2 + (2k(4\alpha+1) + \frac{3}{2})\|w_n\|^2 + 8k\|f\|^2 + 3k\|\psi_n\|^2. \end{aligned} \tag{2.4.10}$$

To maintain the generality, let us suppose that m is an integer. Then, after summing up the inequality (2.4.10) for $n = 0$ to $n = m - 1$

$$\|w_m\|^2 \quad + \quad \sum_{n=0}^{m-1} \|\tilde{w}_{n+1} - w_n\|^2 + 2k^2\|\psi_m\|^2$$

$$\leq \|w_0\|^2 + 2k^2\|\psi_0\|^2 + (6+2k)\sum_{n=0}^{m-1}\|w_0\|^2 + \left(4k(4\alpha+1)+\frac{3}{2}\right)\sum_{n=0}^{m-1}\|w_n\|^2$$
$$+16k\sum_{n=0}^{m-1}\|f\|^2 + 6k\sum_{n=0}^{m-1}\|\psi_n\|^2.$$

After applying the discrete Gronwall's Lemma 2.4.1, we get

$$\|w_m\|^2 \quad + \quad \sum_{n=0}^{m-1}\|\tilde{w}_{n+1}-w_n\|^2 + 2k^2\|\psi_m\|^2$$
$$\leq C\left(\|w_0\|^2 + 2k^2\|\psi_0\|^2 + (6+2k)\sum_{n=0}^{m-1}\|w_0\|^2 + 16k\sum_{n=0}^{m-1}\|f\|^2 + 6k\sum_{n=0}^{m-1}\|\psi_n\|^2\right).$$

Further simplifying the above inequality, we obtain the desired result,

$$\|w_m\|^2 + \frac{1}{2}\sum_{n=0}^{m-1}\|\tilde{w}_{n+1}-w_n\|^2 + k^2\|\psi_m\|^2 \leq C\left(\|w_0\|^2 + k\|\psi_0\|^2 + k\sum_{n=0}^{m-1}\|f\|^2 + k\sum_{n=0}^{m-1}\|\psi_n\|^2\right).$$

□

2.4.3 Stability Analysis for BDF2-OS

Next, let us consider the BDF2-based operator splitting technique (2.3.8)-(2.3.9).

Theorem 2.4.3. *The scheme* (2.3.8) *and* (2.3.9) *is stable under the assumption* $k < \frac{1}{2(4\alpha+1)}$, *in the following sense:*

$$\|w_m\|^2 + \|w_{m-1}\|^2 \quad + \quad \frac{1}{2}\sum_{n=1}^{m-1}\|\tilde{w}_{n+1}\|^2 + \frac{8}{9}k^2\|\psi_m\|^2$$
$$\leq C\left(\|w_0\|^2 + \|w_1\|^2 + k\sum_{n=1}^{m-1}\|f\|^2 + k\sum_{n=1}^{m-1}\|\psi_n\|^2 + k^2\|\psi_1\|^2\right),$$

$\forall\ 2 \leq m \leq \frac{T}{k}$, *where* C *is a constant that depends on the parameters* r, σ, *and* T.

Proof. As in previous case, consider equation (2.3.8), for the transformed problem (2.4.1)

$$\frac{3\tilde{w}_{n+1} - 4w_n + w_{n-1}}{2k} = \mathcal{D}\tilde{w}_{n+1} + f + \psi_n. \tag{2.4.11}$$

Taking the inner product of (2.4.11) with $4k\tilde{w}_{n+1}$ to have

$$\|\tilde{w}_{n+1}\|^2 - \|w_n\|^2 \quad + \quad \|2\tilde{w}_{n+1} - w_n\|^2 - \|2w_n - w_{n-1}\|^2 + \|\tilde{w}_{n+1} - 2w_n + w_{n-1}\|^2$$
$$\leq \quad 4k\alpha\|\tilde{w}_{n+1}\|^2 + 4k(f, \tilde{w}_{n+1}) + 4k(\psi_n, \tilde{w}_{n+1}) \tag{2.4.12}$$

Now considering the equation (2.3.9) as

$$w_{n+1} - w_0 - \frac{2}{3}k\psi_{n+1} = \tilde{w}_{n+1} - w_0 - \frac{2}{3}k\psi_n. \tag{2.4.13}$$

Taking inner product of (2.4.13) from both sides with itself, we have

$$\|w_{n+1}-w_0\|^2+\frac{4}{9}k^2\|\psi_{n+1}\|^2-\frac{4}{3}k(w_{n+1}-w_0,\psi_{n+1})=\|\tilde{w}_{n+1}-w_0\|^2+\frac{4}{9}k^2\|\psi_n\|^2-\frac{4}{3}k(\tilde{w}_{n+1}-w_0,\psi_n),$$

$$\begin{aligned}\|w_{n+1}\|^2+\|w_0\|^2-2\|w_{n+1}\|\|w_0\| &+ \frac{4}{9}k^2\|\psi_{n+1}\|^2-\frac{4}{3}k(w_{n+1}-w_0,\psi_{n+1})\\ &\leq 2\|\tilde{w}_{n+1}\|^2+2\|w_0\|^2+\frac{4}{9}k^2\|\psi_n\|^2-\frac{4}{3}k(\tilde{w}_{n+1},\psi_n)+\frac{4}{3}k(w_0,\psi_n).\end{aligned}$$

After simplifying the above inequality, we get

$$\begin{aligned}\|w_{n+1}\|^2+\|w_0\|^2 &- \frac{1}{2}\|w_{n+1}\|^2-2\|w_0\|^2+\frac{4}{9}k^2\|\psi_{n+1}\|^2-\frac{4}{3}k(w_{n+1}-w_0,\psi_{n+1})\\ &\leq 2\|\tilde{w}_{n+1}\|^2+2\|w_0\|^2+\frac{4}{9}k^2\|\psi_n\|^2-\frac{4}{3}k(\tilde{w}_{n+1},\psi_n)+\frac{4}{3}k(w_0,\psi_n). \quad (2.4.14)\end{aligned}$$

Now, multiplying the inequality (2.4.12) by 2 and adding with inequality (2.4.14) with the consideration of $(w_{n+1}-w_0,\psi_{n+1})=0$, we get

$$\begin{aligned}&\frac{1}{2}\|w_{n+1}\|^2-2\|w_n\|^2+2\|2\tilde{w}_{n+1}-w_n\|^2-2\|2w_n-w_{n-1}\|^2+2\|\tilde{w}_{n+1}-2w_n+w_{n-1}\|^2+\frac{4}{9}k^2\|\psi_{n+1}\|^2\\ &\leq 8k\alpha\|\tilde{w}_{n+1}\|^2+8k(f,\tilde{w}_{n+1})+3\|w_0\|^2+\frac{4}{9}k^2\|\psi_n\|^2+\frac{20}{3}k(\tilde{w}_{n+1},\psi_n)+\frac{4}{3}k(w_0,\psi_n). \quad (2.4.15)\end{aligned}$$

After some small calculations, we have

$$\begin{aligned}&\|w_{n+1}\|^2-\|w_n\|^2+16\|\tilde{w}_{n+1}\|^2+8\left(\|w_n\|^2-\|w_{n-1}\|^2\right)+\frac{8}{9}k^2\left(\|\psi_{n+1}\|^2-\|\psi_n\|^2\right)\\ &\leq 39\|w_n\|^2+16(\tilde{w}_{n+1},w_n)+16k\alpha\|\tilde{w}_{n+1}\|^2+16k(f,\tilde{w}_{n+1})+6\|w_0\|^2+\frac{40}{3}k(\tilde{w}_{n+1},\psi_n)+\frac{8}{3}k(w_0,\psi_n),\\ &\leq 39\|w_n\|^2+\frac{64}{13}\|w_n\|^2+13\|\tilde{w}_{n+1}\|^2+16k\alpha\|\tilde{w}_{n+1}\|^2+32k\|f\|^2+2k\|\tilde{w}_{n+1}\|^2+6\|w_0\|^2\\ &+\frac{200}{9}k\|\psi_n\|^2+2k\|\tilde{w}_{n+1}\|^2+\frac{4}{3}k(\|w_0\|^2+\|\psi_n\|^2).\end{aligned}$$

Further simplifying the above inequality, we have

$$\begin{aligned}&\|w_{n+1}\|^2-\|w_n\|^2+3\|\tilde{w}_{n+1}\|^2+8\left(\|w_n\|^2-\|w_{n-1}\|^2\right)+\frac{8}{9}k^2\left(\|\psi_{n+1}\|^2-\|\psi_n\|^2\right)\\ \leq\ &\frac{571}{13}\|w_n\|^2+16k\alpha\|\tilde{w}_{n+1}\|^2+32k\|f\|^2+2k\|\tilde{w}_{n+1}\|^2+6\|w_0\|^2+\frac{200}{9}k\|\psi_n\|^2\\ &+2k\|\tilde{w}_{n+1}\|^2+\frac{4}{3}k(\|w_0\|^2+\|\psi_n\|^2)\\ \leq\ &\frac{571}{13}\|w_n\|^2+4k(4\alpha+1)\|\tilde{w}_{n+1}\|^2+32k\|f\|^2+\frac{212}{9}k\|\psi_n\|^2+\frac{(4k+18)}{3}k\|w_0\|^2.\end{aligned}$$

Now, if we imagine that the k is tiny enough such that $k<\frac{1}{2(4\alpha+1)}$, then above inequality implies:

$$\begin{aligned}\|w_{n+1}\|^2-\|w_n\|^2+\|\tilde{w}_{n+1}\|^2 &+ 8\left(\|w_n\|^2-\|w_{n-1}\|^2\right)+\frac{8}{9}k^2\left(\|\psi_{n+1}\|^2-\|\psi_n\|^2\right)\\ &\leq \frac{571}{13}\|w_n\|^2+32k\|f\|^2+\frac{212}{9}k\|\psi_n\|^2+\frac{(4k+18)}{3}\|w_0\|^2.\end{aligned}$$

To maintain the generality, let us suppose that m is an integer. Then, after summing up the above inequality for $n = 1$ to $n = m - 1$, we obtain

$$\begin{aligned} & \|w_m\|^2 + \sum_{n=1}^{m-1} \|\tilde{w}_{n+1}\|^2 + 8\|w_{m-1}\|^2 + \frac{8}{9}k^2\|\psi_m\|^2 \\ \leq & \left(\frac{4k+18}{3} + 8\right) \sum_{n=1}^{m-1} \|w_0\|^2 + \|w_1\|^2 + \frac{8}{9}k^2\|\psi_1\|^2 + \frac{571}{13}\sum_{n=1}^{m-1}\|w_n\|^2 + 32k\sum_{n=1}^{m-1}\|f\|^2 + \frac{212k}{9}\sum_{n=1}^{m-1}\|\psi_n)\|^2. \end{aligned}$$

After applying the discrete Gronwall's Lemma 2.4.1, we get

$$\begin{aligned} & \|w_m\|^2 + 8\|w_{m-1}\|^2 + \sum_{n=1}^{m-1} \|\tilde{w}_{n+1}\|^2 + \frac{8}{9}k^2\|\psi_m\|^2 \\ & \leq C\left(2\|w_0\|^2 + \|w_1\|^2 + \frac{8}{9}k^2\|\psi_1\|^2 + 32k\sum_{n=1}^{m-1}\|f\|^2 + \left(\frac{4k+18}{3}\right)\sum_{n=1}^{m-1}\|w_0\|^2 + \frac{212k}{9}\sum_{n=1}^{m-1}\|\psi_n\|^2\right). \end{aligned}$$

Further simplifying the equation, we obtain the desired result

$$\begin{aligned} \|w_m\|^2 + \|w_{m-1}\|^2 \quad + \quad & \frac{1}{2}\sum_{n=1}^{m-1}\|\tilde{w}_{n+1}\|^2 + \frac{8}{9}k^2\|\psi_m\|^2 \\ \leq \quad & C\left(\|w_0\|^2 + \|w_1\|^2 + k\sum_{n=1}^{m-1}\|f\|^2 + k\sum_{n=1}^{m-1}\|\psi_n\|^2 + k^2\|\psi_1\|^2\right). \end{aligned}$$

□

2.5 Error Analysis

In the previous section, we established the stability results, and now we discuss the associated error estimates by assuming the exact solution is sufficiently regular. We establish the error estimates for the BDF-OS approaches. First, we will describe the error function and error equation. We have denoted the analytic solution at t_n by $w(\cdot, t_n)$ and similar for other related variables.

2.5.1 Error analysis for BDF1-OS

We define $e_n = w(\cdot, t_n) - w_n$, $\tilde{e}_n = w(\cdot, t_n) - \tilde{w}_n$, $h_n = \psi(\cdot, t_n) - \psi_n$ and $\psi(\cdot, t_{n+1}) - \psi(\cdot, t_n) \leq Ck$, where C is a generic constant and independent of n. From the continuous system (2.4.1), we have

$$\frac{w(\cdot, t_{n+1}) - w(\cdot, t_n)}{k} = \mathcal{D}w(\cdot, t_{n+1}) + \mathcal{D}\phi + \psi(\cdot, t_{n+1}) + R_{n+1} \tag{2.5.1}$$

where, R_{n+1} is truncation error for given method. Now, considering the equation (2.4.6), we get

$$\frac{\tilde{w}_{n+1} - w_n}{k} = \mathcal{D}\tilde{w}_{n+1} + \psi_n + \mathcal{D}\phi. \tag{2.5.2}$$

The first error equation for the BDF1-OS method is defined as

$$\frac{\tilde{e}_{n+1} - e_n}{k} = \mathcal{D}\tilde{e}_{n+1} + g_n + R_{n+1}, \tag{2.5.3}$$

where $g_n = \psi(\cdot, t_{n+1}) - \psi_n$. We can obtain another error equation from (2.3.5), as follows:

$$\frac{e_{n+1} - \tilde{e}_{n+1}}{k} = h_{n+1} - g_n, \tag{2.5.4}$$

with $g_n = h_n + \psi(\cdot, t_{n+1}) - \psi(\cdot, t_n)$ and let ψ is adequately smooth such that $\|g_n\| \leq \|h_n\| + Ck$.

Theorem 2.5.1. *Under the assumption $k < \frac{1}{2(4\alpha+1)}$, and that the solution (w, ψ) is sufficiently smooth, we have the following error estimates for the method* (2.3.2) *and* (2.3.5)*:*

$$\|e_m\|^2 + \frac{1}{2}\sum_{n=0}^{m-1} \|\tilde{e}_{n+1}\|^2 \leq Ck^2, \qquad \forall \;\; 1 \leq m \leq \frac{T}{k}.$$

Proof. Taking the inner product of (2.5.3) both sides with $2k\tilde{e}_{n+1}$ to have

$$\|\tilde{e}_{n+1}\|^2 - \|e_n\|^2 + \|\tilde{e}_{n+1} - e_n\|^2 \leq 2k\alpha\|\tilde{e}_{n+1}\|^2 + 2k(g_n, \tilde{e}_{n+1}) + 2k(R_{n+1}, \tilde{e}_{n+1}). \tag{2.5.5}$$

Taking inner product of (2.5.4) from both sides, with itself, we have

$$\|e_{n+1} - e_0\|^2 + k^2\|h_{n+1}\|^2 - 2k(e_{n+1} - e_0, h_{n+1}) = \|\tilde{e}_{n+1} - e_0\|^2 + k^2\|g_n\|^2 - 2k(\tilde{e}_{n+1} - e_0, g_n). \tag{2.5.6}$$

Now combining (2.5.5) and (2.5.6) to get

$$\|e_{n+1}\|^2 - \|e_n\|^2 + \|\tilde{e}_{n+1} - e_n\|^2 - 2k(e_{n+1}, h_{n+1}) + k^2(\|h_{n+1}\|^2 - \|f_n\|^2) \leq 2k\alpha\|\tilde{e}_{n+1}\|^2 + 2k(R_{n+1}, \tilde{e}_{n+1}).$$

The above inequality, along with the fact $2k(e_{n+1}, h_{n+1}) \leq 0$, reduces to

$$\|e_{n+1}\|^2 - \|e_n\|^2 + \|\tilde{e}_{n+1} - e_n\|^2 + k^2(\|h_{n+1}\|^2 - \|g_n\|^2) \leq k(4\alpha+1)\|\tilde{e}_{n+1} - e_n\|^2 + k(4\alpha+1)\|e_n\|^2 + 4k\|R_{n+1}\|^2.$$

If we assume that $k < \frac{1}{2(4\alpha+1)}$, then the above inequality implies

$$\|e_{n+1}\|^2 - \|e_n\|^2 + \frac{1}{2}\|\tilde{e}_{n+1} - e_n\|^2 + k^2(\|h_{n+1}\|^2 - \|g_n\|^2) \leq k(4\alpha+1)\|e_n\|^2 + 4k\|R_{n+1}\|^2.$$

To maintain the generality, let us suppose that m is an integer. Then, after summing up the above inequality, for $n = 0$ to $n = m - 1$

$$\big(\|e_m\|^2 - \|e_0\|^2\big) + \frac{1}{2}\sum_{n=0}^{m-1} \|\tilde{e}_{n+1} - e_n\|^2 + k^2 \sum_{n=0}^{m-1} (\|h_{n+1}\|^2 - \|g_n\|^2) \leq k(4\alpha+1) \sum_{n=0}^{m-1} \|e_n\|^2 + 4k \sum_{n=0}^{m-1} \|R_{n+1}\|^2.$$

Now, using $\|g_n\|^2 \leq (\|h_n\| + ck)^2 \leq 2\|h_n\|^2 + ck^2$,

$$\begin{aligned} \|e_m\|^2 - \|e_0\|^2 \quad + \quad & \frac{1}{2}\sum_{n=0}^{m-1} \|\tilde{e}_{n+1} - e_n\|^2 + k^2(\|h_m\|^2 - \|h_0\|^2) \\ & \leq 2k(2\alpha+1) \sum_{n=0}^{m-1} \|e_n\|^2 + k^2 \sum_{n=0}^{m-1} (ck + \|h_n\|^2) + k \sum_{n=0}^{m-1} \|R_{n+1}\|^2. \end{aligned}$$

After applying the discrete Gronwall's Lemma 2.4.1, we obtain the desired result:

$$\|e_m\|^2 + \frac{1}{2}\sum_{n=0}^{m-1} \|\tilde{e}_{n+1} - e_n\|^2 \leq Ck^2.$$

□

2.5.2 Error Analysis for BDF2-OS

Following the same procedure as in the previous cases of the BDF1-OS method, the error equations for the BDF2-OS (2.3.8)-(2.3.9) method are given by

$$\frac{3\tilde{e}_{n+1} - 4e_n + e_{n-1}}{2k} = \mathcal{D}\tilde{e}_{n+1} + g_n + R_{n+1}, \tag{2.5.7}$$

$$\frac{3(e_{n+1} - \tilde{e}_{n+1})}{2k} = h_{n+1} - g_n. \tag{2.5.8}$$

Theorem 2.5.2. *Under the assumption $k < \frac{1}{2(4\alpha+1)}$, and that the solution (w, ψ) is sufficiently smooth, we have the following error estimates for the method* (2.3.8) *and* (2.3.9)*.*

$$\|e_m\|^2 + 2\|e_{m-1}\|^2 + \frac{1}{2}\sum_{n=1}^{m-1} \|2\tilde{e}_{n+1} - e_n\|^2 \leq Ck^3, \qquad \forall \;\; 2 \leq m \leq \frac{T}{k}.$$

Proof. Taking the inner product of (2.5.7) with $4k\tilde{e}_{n+1}$ both side to have

$$\begin{aligned} \|\tilde{e}_{n+1}\|^2 - \|e_n\|^2 + \|2\tilde{e}_{n+1} \;\; - \;\; & e_n\|^2 - \|2e_n - e_{n-1}\|^2 + \|\tilde{e}_{n+1} - 2e_n + e_{n-1}\|^2 \\ & \leq 4k\alpha\|\tilde{e}_{n+1}\|^2 + 4k(g_n, \tilde{e}_{n+1}) + 4k(R_{n+1}, \tilde{e}_{n+1}). \end{aligned} \tag{2.5.9}$$

Taking inner product of (2.5.8) from both sides with itself and multiplying by 3

$$3\|e_{n+1}\|^2 + \frac{4}{3}k^2\|h_{n+1}\|^2 - 4k(e_{n+1}, h_{n+1}) = 3\|\tilde{e}_{n+1}\|^2 + \frac{4}{3}k^2\|g_n\|^2 - 4k(\tilde{e}_{n+1}, g_n). \tag{2.5.10}$$

Combining (2.5.9) and (2.5.10), and considering that $(e_{n+1}, h_{n+1}) \leq 0$ and $\|\tilde{e}_{n+1} - 2e_n + e_{n-1}\|^2 \geq 0$ we get

$$\begin{aligned} 3\|e_{n+1}\|^2 - \|e_n\|^2 + \|2\tilde{e}_{n+1} - e_n\|^2 \;\; - \;\; & \|2e_n - e_{n-1}\|^2 + \frac{4}{3}k^2\|h_{n+1}\|^2 - \frac{4}{3}k^2\|g_n\|^2 \\ & \leq 2\|\tilde{e}_{n+1}\|^2 + 4k\alpha\|\tilde{e}_{n+1}\|^2 + 4k(R_{n+1}, \tilde{e}_{n+1}), \end{aligned}$$

$$\begin{aligned} 3\|e_{n+1}\|^2 - \|e_n\|^2 \;\; + \;\; & 4\|\tilde{e}_{n+1}\|^2 + \|e_n\|^2 + \frac{4}{3}k^2\left(\|h_{n+1}\|^2 - \|g_n\|^2\right) \\ & \leq 2\|\tilde{e}_{n+1}\|^2 + 4k\alpha\|\tilde{e}_{n+1}\|^2 + 4k(R_{n+1}, \tilde{e}_{n+1}) + \|2e_n - e_{n-1}\|^2 + 4(e_n, \tilde{e}_{n+1}). \end{aligned}$$

Now, after small calculations

$$\begin{aligned} \|e_{n+1}\|^2 - \|e_n\|^2 + \|\tilde{e}_{n+1}\|^2 \;\; + \;\; & \frac{4}{3}k^2\left(\|h_{n+1}\|^2 - \|g_n\|^2\right) + 2\left[\|e_n\|^2 - \|e_{n-1}\|^2\right] \\ & \leq 13\|e_n\|^2 + (4\alpha+1)k\|\tilde{e}_{n+1}\|^2 + 4k\|R_{n+1}\|^2. \end{aligned}$$

Let us assume that, $k < \frac{1}{2(4\alpha+1)}$. Then the above inequality implies

$$\|e_{n+1}\|^2 - \|e_n\|^2 + \frac{1}{2}\|\tilde{e}_{n+1}\|^2 + \frac{4}{3}k^2\left(\|h_{n+1}\|^2 - \|g_n\|^2\right) + 2\left[\|e_n\|^2 - \|e_{n-1}\|^2\right] \leq 13\|e_n\|^2 + 4k\|R_{n+1}\|^2.$$

To maintain the generality, let us suppose that m is an integer. Then, after summing up the above inequality for $n = 1$ to $n = m - 1$, and using the condition $\|g_n\|^2 \leq \|h_n\|^2 + ck^2 + ck\|h_n\|$, we get

$$\begin{aligned}\|e_m\|^2 \quad + \quad & 2\|e_{m-1}\|^2 + \frac{1}{2}\sum_{n=1}^{m-1}\|\tilde{e}_{n+1}\|^2 + \frac{4}{3}k^2\|h_m\|^2 \\ & \leq \|e_1\|^2 + 2\|e_0\|^2 + \frac{4}{3}k^2\|h_1\|^2 + 13\sum_{n=0}^{m-1}\|e_n\|^2 + 4k\sum_{n=1}^{m-1}\|R_{n+1}\|^2 + \frac{4}{3}k^2\sum_{n=1}^{m-1}(ck^2 + ck\|h_n\|).\end{aligned}$$

After applying the discrete Gronwall's Lemma 2.4.1, we obtain the desired results

$$\|e_m\|^2 + 2\|e_{m-1}\|^2 + \frac{1}{2}\sum_{n=1}^{m-1}\|\tilde{e}_{n+1}\|^2 \leq Ck^3.$$

□

It is important to note that the restrictions on k in the preceding theorems are only sufficient for stability. These restrictions are not optimized in any way, and they can be slightly modified with a refined analysis.

2.6 Numerical Results and Discussions

Now, to verify the analysis of proposed methods, we present numerical results and discuss the convergence behavior of both the BDF1-OS and BDF2-OS numerical schemes for pricing the American options. We approximated the time derivative by the BDF1-OS and BDF2-OS methods, and the spatial derivative at each grid point is approximated by the central difference formulas:

$$\begin{aligned}u_x(x_i) \quad &\approx \quad \frac{u_{i+1} - u_{i-1}}{2h}, \\ u_{xx}(x_i) \quad &\approx \quad \frac{u_{i+1} - 2u_i + u_{i-1}}{h^2},\end{aligned}$$

with spatial mesh length h in computational domain Ω of the log price. In all the computational investigations for BDF2-OS, the first step is calculated by the BDF1-OS method. We used MATLAB R2022b on a PC with Processor Intel(R) Core(TM) i5-10500 CPU @ 3.10GHz, 3096 Mhz, 6 Core(s), 12 Logical Processor(s) and 16.00GB RAM.

Throughout all of the tests, we computed the point-wise error at different stock prices $S = 90,\ 100,\ 110$, with N temporal discretization points. We used a well enough fine mesh h with $M = 2^{10} + 1$ spatial discretization points so that time discretization dominates the errors.

We computed the rate of convergence using the following formula:

$$\text{Rate} = \log_2 \frac{\|u(k,h) - u(\frac{k}{2},\frac{h}{2})\|}{\|u(\frac{k}{2},\frac{h}{2}) - u(\frac{k}{4},\frac{h}{4})\|},$$

where $u(k,h)$ is the computed price of the American put option with temporal meth length k and spatial mesh length h. To estimate the value of the American put option at stock prices that do not coincide with the predefined grid points, we used the piecewise cubic Hermite interpolation method. This approach ensures smooth and accurate estimation between the known data points. For the purpose of conducting numerical simulations related to American option pricing, we considered the following illustrative examples.

Example 2.6.1. *Pricing American put option with the parameters,* $\sigma = 0.2, \quad r = 0.01, \quad T = 1, \quad K = 100, \quad \Omega := [-1.5, 1.5]$.

First, we performed the numerical simulation for the BDF1 type operator splitting method, and the option value, along with the pointwise error and rate of convergence at different asset prices, are reported in Table 2.1.

The numerical results in Table 2.1 demonstrate that the pointwise errors are reducing with the ratio of two and that they show the first-order convergence rate for the BDF1-OS method, which is entirely in agreement with the theoretical outcomes. We can observe that the convergence rate reached its asymptotic order when the temporal mesh are sufficiently small. The optimal exercise boundary and graphical information of options are then provided for a better understanding of the American option pricing problem. So we presented the American put option values and optimal early exercise boundary at $N = 2048$ for the BDF1-OS method in Figure 2.1, and the graphs demonstrate that the option values are quite stable, with no erroneous oscillation at or near the strike price. It is crucial to estimate the Delta and Gamma for hedging reasons [73]. In Figure 2.2, we presented the graphs of Gamma and Delta using BDF1-OS at $N = 2048$, and the graphs are quite stable, with no erroneous oscillation at or near the strike price. We have verified the Delta & Gamma for American option by [55], and the suggested approaches effortlessly

Table 2.1: Numerical results of BDF1-OS scheme for American put options with specified parameters at various stock prices.

	N	64	128	264	512	1024	2048
S=90	Value	13.019361	13.026411	13.030080	13.031980	13.032959	13.033462
	Error	7.0505e-03	3.6684e-03	1.8999e-03	9.7937e-04	5.0298e-04	2.5823e-04
	Rate	-	0.94	0.95	0.96	0.96	0.96
S=100	Value	7.493290	7.502989	7.507975	7.510530	7.511837	7.512503
	Error	9.6992e-03	4.9855e-03	2.5557e-03	1.3065e-03	6.6605e-04	3.3897e-04
	Rate	-	0.96	0.96	0.97	0.97	0.97
S=110	Value	3.967126	3.974111	3.977718	3.979574	3.980526	3.981012
	Error	6.9850e-03	3.6078e-03	1.8560e-03	9.5153e-04	4.8616e-04	2.4762e-04
	Rate	-	0.95	0.96	0.96	0.97	0.97

Gamma for hedging reasons [73]. In Figure 2.2, we presented the graphs of Gamma and Delta using BDF1-OS at $N = 2048$, and the graphs are quite stable, with no erroneous oscillation at or near the strike price. We have verified the Delta & Gamma for American option by [55], and the suggested approaches effortlessly

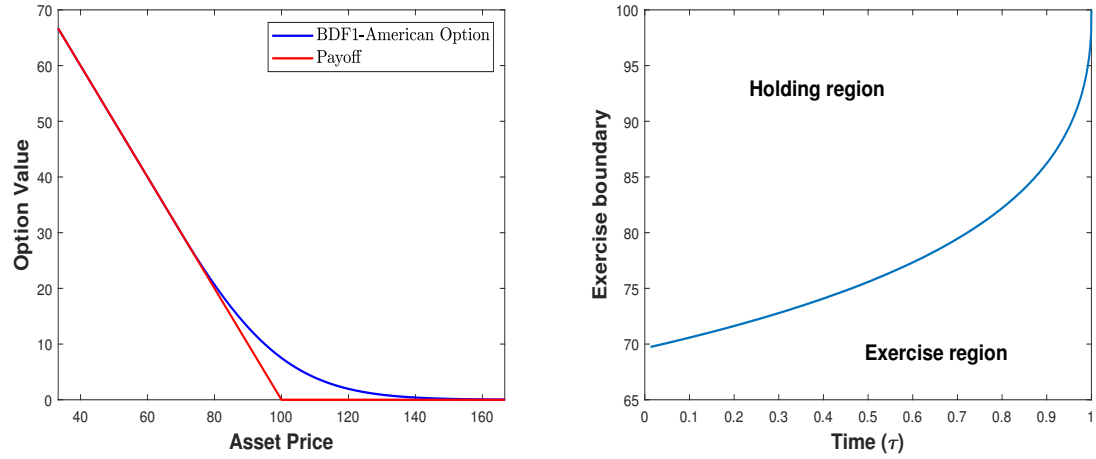

Figure 2.1: American put option value, and optimal early exercise boundary for BDF1-OS method with parameters as provided in Example 2.6.1.

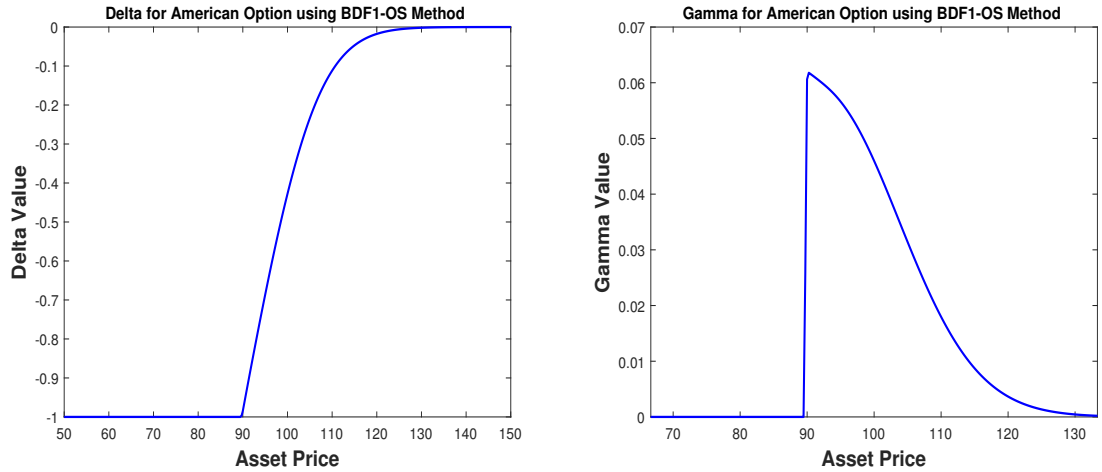

Figure 2.2: Delta and Gamma values for pricing American put option for BDF1-OS method with parameters $\sigma = 0.2, \quad r = 0.1, \quad T = 0.25, \quad K = 100, \quad N = 1024.$

approximate the option value as well as some of its significant "Greeks" without any extra effort. In the same line-up, we executed the numerical simulation for the BDF2-OS method with the parameters as provided in Example 2.6.1, and the results are reported in Table 2.2. We observed that the pointwise errors are reducing with a ratio of nearly three. Thus, the temporal discretization scheme BDF2-OS is convergent with the rate of 1.5, as shown in Table 2.2. For a better visualization of the BDF2-OS method, the American put option values and optimal early exercise boundary are presented in Figure 2.3, and the graphs demonstrate that the option values are quite stable with no erroneous oscillation at or near the

Table 2.2: Numerical results of BDF2-OS scheme for American put options with specified parameters at various stock prices.

	N	64	128	264	512	1024	2048
S=90	Value	13.032463	13.033493	13.033829	13.033937	13.033971	13.033982
	Error	1.0300e-03	3.3575e-04	1.0798e-04	3.4048e-05	1.0593e-05	4.0245e-06
	Rate	-	1.62	1.64	1.67	1.68	1.40
S=100	Value	7.511214	7.512469	7.512927	7.513095	7.513156	7.513178
	Error	1.2548e-03	4.5875e-04	1.6757e-04	6.1051e-05	2.1779e-05	7.9711e-06
	Rate	-	1.45	1.45	1.46	1.49	1.45
S=110	Value	3.979828	3.980857	3.981260	3.981417	3.981478	3.981501
	Error	1.0290e-03	4.0245e-04	1.5725e-04	6.1110e-05	2.3108e-05	8.5802e-06
	Rate	-	1.35	1.36	1.36	1.40	1.43

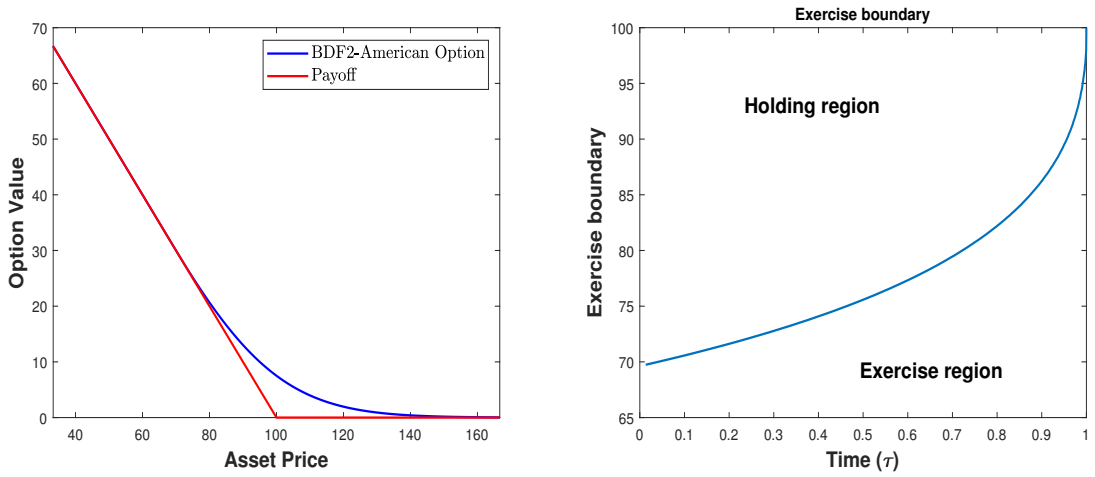

Figure 2.3: American put option value, and optimal early exercise boundary for BDF2-OS method with parameters as provided in Example 2.6.1.

strike price. In Figure 2.4, we presented the graphs of Gamma and Delta using BDF2-OS, and the graphs are quite stable, with no erroneous oscillation at or near the strike price.

Example 2.6.2. *Pricing American put option with the parameters,* $\sigma = 0.25, \quad r = 0.01, \quad T = 0.25, \quad K = 100, \quad \Omega := [-4, 4]$.

In Example 2.6.2, we have taken different values of parameters and the results are reported in Table 2.3 and 2.4. We can observe from both tables that both of the proposed methods are quite stable when we take the big domain $\Omega := [-4, 4]$ for underlying asset prices.

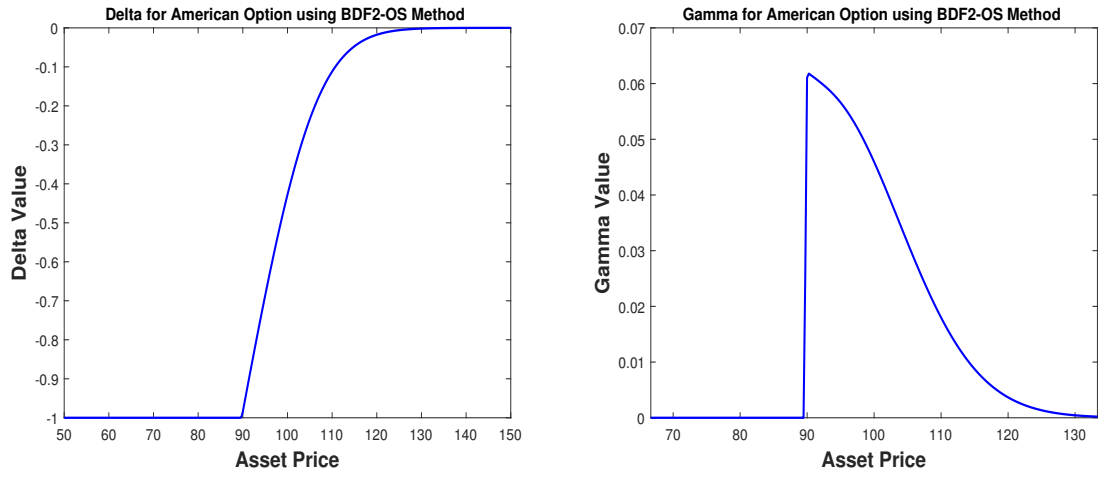

Figure 2.4: Delta and Gamma values for pricing American put option for BDF2-OS method with parameters $\sigma = 0.2, \quad r = 0.1, \quad T = 0.25, \quad K = 100, \quad N = 1024.$

Table 2.3: Numerical results of BDF1-OS scheme for American put options with specified parameters provided in Example 2.6.2 at various stock prices.

	$S = 90$			$S = 100$			$S = 110$		
N	Value	Error	Rate	Value	Error	Rate	Value	Error	Rate
64	11.159156	-	-	4.854197	-	-	1.619302	-	-
128	11.161157	2.000516e-03	-	4.859739	5.541615e-03	-	1.621211	1.909022e-03	-
256	11.162210	1.052773e-03	0.92	4.862556	2.816650e-03	0.97	1.622198	9.863779e-04	0.95
512	11.162764	5.547037e-04	0.92	4.863988	1.432220e-03	0.97	1.622706	5.083506e-04	0.95
1024	11.163054	2.900423e-04	0.93	4.864713	7.254953e-04	0.98	1.622965	2.592931e-04	0.97
2048	11.163205	1.504963e-04	0.94	4.865081	3.675492e-04	0.98	1.623098	1.323414e-04	0.97

Table 2.4: Numerical results of BDF2-OS scheme for American put options with specified parameters provided in Example 2.6.2 at various stock prices.

	$S = 90$			$S = 100$			$S = 110$		
N	Value	Error	Rate	Value	Error	Rate	Value	Error	Rate
64	11.162665	-	-	4.864550	-	-	1.622733	-	-
128	11.163138	4.729171e-04	-	4.865132	5.816924e-04	-	1.623040	3.069125e-04	-
256	11.163283	1.454414e-04	1.70	4.865336	2.047809e-04	1.50	1.623158	1.178559e-04	1.38
512	11.163333	4.959376e-05	1.55	4.865412	7.551695e-05	1.43	1.623205	4.726685e-05	1.31
1024	11.163350	1.699748e-05	1.54	4.865438	2.619019e-05	1.52	1.623223	1.717505e-05	1.46
2048	11.163357	6.550697e-06	1.37	4.865448	9.920660e-06	1.40	1.623229	6.714163e-06	1.35

To solve LCP for pricing American option, Shi et al. [143] presented a fixed point (FP) iterative approach, and the outcomes were contrasted with the Projected Successive Over Relaxation (PSOR) technique. We have verified the option value, error, and CPU time (seconds) with [143], and data are reported in Table 2.5 and 2.6. We note that the proposed method is significantly faster than the projected SOR and fixed point methods. Although the computing time of the new algorithm increases with the number of time steps N, the savings in CPU time are quite substantial in all cases. In particular, a greater improvement over the PSOR and FP is observed when the option time to maturity or the volatility has varied.

Table 2.5: Comparison of Numerical results of BDF2-OS scheme for American put option with specified parameters $\sigma = 0.2, \quad r = 0.05, \quad T = 0.5, \quad K = 100$, $\Omega := [-1.5, 1.5]$ at stock price $S = 100$.

		FP [143]			PSOR [143]			BDF2-OS		
M	N	Value	Error	CPU (s)	Value	Error	CPU (s)	Value	Error	CPU (s)
600	400	4.654667	8.93e-4	1.30	4.653713	1.84e-3	1.40	4.655250	5.209999e-04	0.014544
800	600	4.655110	4.50e-4	2.48	4.653845	1.71e-3	2.54	4.655437	1.870000e-04	0.028176
800	800	4.655116	4.44e-4	3.16	4.653955	1.60e-3	3.21	4.655444	7.000000e-06	0.030004
1000	1000	4.655318	2.42e-4	5.18	4.653714	1.84e-3	5.31	4.655527	8.300000e-05	0.043782

Table 2.6: Comparison of Numerical results of BDF2-OS scheme for American put option with specified parameters $\sigma = 0.3, \quad r = 0.05, \quad T = 0.25, \quad K = 100$, $\Omega := [-3, 3]$ at stock price $S = 100$.

		FP [143]			PSOR [143]			BDF2-OS		
M	N	Value	Error	CPU (s)	Value	Error	CPU (s)	Value	Error	CPU (s)
1600	800	5.441780	3.69e-4	6.16	5.440519	1.63e-3	6.19	5.442154	4.420000e-04	0.054934
2000	1000	5.441972	1.77e-4	9.60	5.440161	1.98e-3	9.81	5.442212	5.799999e-05	0.081046
2400	1500	5.442081	6.81e-5	17.29	5.439489	2.66e-3	17.69	5.442250	3.799999e-05	0.131646
3000	2500	5.442161	1.13e-5	35.60	5.437334	4.81e-3	36.58	5.442280	3.000000e-05	0.307972

2.7 Conclusion

In this chapter, we presented the stability and error analysis of two operator splitting methods for linear complementarity problems describing the American option under the Black-Scholes model. We give an error estimate for the BDF1 and BDF2 types of operator splitting methods and show that the order of convergence in time for BDF1-OS and BDF2-OS methods are 1 and 1.5, respectively. To verify our theoretical error estimates, we presented the numerical results to demonstrate the convergence behavior

of each operating splitting method. We presented the results for the American put option and showed the plots for the American option value, Gamma, Delta, and exercise region. This work can be extended in the future by enhancing the stability condition through a more refined analysis.

CHAPTER 3

Errors in the IMEX-BDF-OS Methods for Pricing American Style Options under the Jump-Diffusion Model[1]

3.1 Introduction

One of the most extensively used models in option pricing is the Black-Scholes (BS). The stock price in the classical Black-Scholes model is a standard Wiener process that is continuous in time. Jumps can occur at any time, and the log-normal distribution characteristic of the stock price cannot capture these jumps in the classical Black-Scholes model. Several models have been developed in the literature to overcome the above problem. Merton's [111] and Kou's [93] jump-diffusion models are the most frequently applied models among them. For the jump-amplitudes, Merton recommended a log-normally distributed process, whereas Kou proposed a log-double-exponentially distributed process.

To evaluate the price of the American option under the jump-diffusion process, the solution of a linear

[1]The results discussed in this chapter have been published in *Computational and Applied Mathematics*, 43, 6 (2024). https://doi.org/10.1007/s40314-023-02510-8

complementarity problem having a non-local integral operator is required. Many methods have been proposed in the literature to solve the discretized linear complementarity problem arising in American option pricing.

For these types of problems, Lee et al. [98] proposed a three-time levels implicit numerical method combined with an operator splitting technique to approximate the value of American options where the underlying asset acts in accordance with a jump-diffusion model. Huang et al. [71] proposed the finite difference technique under the jump-diffusion model on a piecewise uniform grid with the help of a penalty approach for pricing the American put options. Huang et al. [72] analyzed a number of techniques with penalty approach for pricing American options under a regime switching stochastic process. In [139, 140], Salmi and Toivanen proposed an iterative method and a family of implicit-explicit time discretization techniques for option pricing problems. To handle the different boundary conditions and non-smooth initial conditions for numerous underlying claims, Chen et al. [25] presented a spectral element method, Pindza et al. [126] established a robust spectral technique, Company et al. [34] proposed a front-fixing exponential time differencing (FF-ETD) technique, Kumar et al. [96] provided a wavelet-based approximation approach for examining the sensitivity and value of American options determined by LCPs. In [167], Wang et al. show the stability and error estimations of the variable step-size IMEX BDF2 approach applied to the abstract partial integro-differential equation with nonsmooth initial data, which demonstrates the jump-diffusion option pricing model in finance. They gave the stability analysis and derived the consistency error and the global error bounds for the variable step-size IMEX BDF2 method up to the second order for the European style option and explored the possibilities for the American style option.
In recent works, Kadalbajoo et al. [84, 83, 81] examined the efficiency of the meshfree method to deal with option pricing problems based on the local radial basis function for numerically solving the multi-dimensional option pricing problem and solved the PIDE that occurs when the underlying asset act in accordance with the jump-diffusion process using an RBF-based approach. Saib et al. [138] came up with a differential quadrature rule based on RBF for spatial discretization along with integration with respect to exponential time to work under the jump-diffusion model, Yousuf et al. [181] solved the complex PIDE systems and Thakoor et al. [158] devised a compact-RBF scheme with the use of local mesh refinement scheme which helps to achieve the higher order accuracy. Dehgahn et al. [43] presented a new class of radial basis function and explored its efficiency in option pricing problems. Haghi et al. [64] introduced a new combination of an RBF-based finite difference method, and Bastani et al. [12] presented an RBF-based collocation method for pricing American options. Some other mesh free works for option pricing problems can be found in [115, 130] and references therein.

Further, Akbari et al. [5] used a compact finite difference scheme to evaluate the option value under the exponential jump-diffusion models, Patel and Mehra [124] presented a fourth-order compact method

to evaluate the option value under the Kou's and Merton's jump-diffusion models. Several other authors also used the compact finite difference schemes for option pricing models [26, 49, 157]. To solve parabolic PIDEs with non-smooth pay-off function, Wang et al. [168] developed an IMEX midpoint formula with variable spatial step sizes and variable time steps. In [44], the authors show the effects of jump-diffusion models for the house price evolution in the pricing of fixed-rate mortgages with prepayment and default options. Tour et al. [159] introduced a spectral element method to evaluate the price of the option. The mesh-free moving least-squares approximation is used in [144] to evaluate the price of multi-asset options under the jump-diffusion processes.

To mitigate the iterative procedure, we employ the Backward difference IMEX methodology with the association of the operator splitting approach to evaluate the price of an American option. Operator splitting technique has been used proficiently for several Black-Scholes models [24, 28, 79, 86, 102, 123, 174]. In recent research, Chen et al. [26] developed a new OS technique for pricing the value of American options under the time-fractional Black-Scholes models, Boen and In 't Hout [15] presented the operator splitting strategies for two-asset Merton jump-diffusion model. OS techniques are robust to apply since the differential equation and complementarity conditions are decoupled and can be solved independently. Nevertheless, beyond their omnipresence, these operator-splitting approaches still lack some mathematical support. In this chapter, we primarily focus on the stability and error analysis of the operator splitting method for the jump-diffusion model and carry out a careful investigation of the related numerical techniques. We present the stability and error estimates for IMEX-BDF1-OS and IMEX-BDF2-OS techniques to solve LCPs arising in the American option pricing under the jump-diffusion model.

The rest of the chapter is structured in the following manner. We begin with introducing the jump-diffusion model, describing the basic notations, symbols, and assumptions used throughout this paper and the construction of the LCP and its associated characteristics. In Section 3.3, we present the operator splitting methods, and in Section 3.4, we verify their stability analysis. In Section 3.5, we show the error estimates for IMEX-BDF1-OS and IMEX-BDF2-OS methods. In Section 3.6, we provide some numerical outcomes to verify our theoretical results and associated discussions.

3.2 The Jump-Diffusion Model

Consider an asset with price S and the stochastic differential equation (SDE) that represents the fluctuation of the stock price.

$$\frac{dS}{S} = (\nu - \kappa\lambda)d\tau + \sigma dZ + (\eta - 1)dq, \tag{3.2.1}$$

where, τ is the time to maturity, dZ is an enhancement of standard Gauss-Wiener process, ν is drift rate, σ is nonzero constant volatility and λ is taken as the intensity of the independent Poisson process dq, where

$$dq = \begin{cases} 0 & \text{if probability is } 1 - \lambda d\tau \ , \\ 1 & \text{if probability is } \lambda d\tau \ . \end{cases}$$

κ is expected relative jump size expressed as $\kappa = \mathbb{E}(\eta - 1)$, where $\mathbb{E}[\cdot]$ represent the expectation operator and $\eta - 1$ is an impulse function producing jump from S to S_η. To put it in another way, the arrival of a jump is stochastic, and this is a feature of the stochastic differential equation for S. As a result, there are two sources of uncertainty. To begin with, the term dZ denotes typical Brownian motion, and the term dq denotes exceptional and infrequent events. Geometric Brownian motion and pure jump-diffusion are two particular examples of equation (3.2.1). If the Poisson event does not occur ($dq = 0$), then equation (3.2.1) is equivalent to the usual stochastic process of geometric Brownian motion assumed in the Black-Scholes model.

If, on the other hand, the Poisson event occurs, then equation (3.2.1) can be written as

$$\frac{dS}{S} \simeq \eta - 1.$$

In this situation, most of the time, the path of S is continuous, but finite positive or negative jumps may appear at discrete points in time. We assume that the jumps and Brownian motion are independent.

Let $V(S, \tau)$ represent the value of the American option, which depends on the asset price S with current time τ. As we can exercise the American option at any time up to the life of the option, and we can formulate it as the linear complementarity problem (LCP) based on the stochastic differential equation (3.2.1)

$$\begin{cases} \frac{\partial V}{\partial \tau} + \mathcal{L}V & \leq & 0, & (S,\tau) \in [0,\infty) \times [0,T) \\ V(S,\tau) - \Phi(S) & \geq & 0, & (S,\tau) \in [0,\infty) \times [0,T) \\ (\frac{\partial V}{\partial \tau} + \mathcal{L}V)\,(V(S,\tau) - \Phi(S)) & = & 0 & (S,\tau) \in [0,\infty) \times [0,T) \\ V(S,T) & = & \Phi(S) & S \in [0,\infty). \end{cases} \tag{3.2.2}$$

The spatial operator $\mathcal{L}$ can be defined as:

$$\mathcal{L}V(S,\tau) = \frac{1}{2}\sigma^2 S^2 \frac{\partial^2 V}{\partial S^2} + (r - \lambda\kappa) S \frac{\partial V}{\partial S} - (r + \lambda)V + \lambda \int_0^\infty V(S\eta) g(\eta) d\eta, \tag{3.2.3}$$

where S is the stock price of any asset at time τ with constant volatility $\sigma \neq 0$ and interest rate r, and the probability density function of the jump with amplitude η is given by $g(\eta)$. Here $g(\eta)$ follow the given properties: $g(\eta) \geq 0$, $\forall\ \eta$ and $\int_0^\infty g(\eta) d\eta = 1$.

The option value $V(S, T)$ at the time of maturity T is termed as pay-off function. For the put option, the pay-off function is given by:

$$\Phi(S) = \max(K - S, 0) \tag{3.2.4}$$

with the strike price K.

For the Merton's jump-diffusion model, $g(\eta)$ represent the log-normal density

$$g(\eta) := \frac{1}{\sqrt{2\pi}\sigma_J \eta} \exp - \frac{(\ln \eta - \mu_J)^2}{2\sigma_J^2},$$

where $\kappa := \mathbb{E}(\eta - 1) = \exp\left(\mu_J + \frac{\sigma_J^2}{2}\right) - 1$, and μ_J and σ_J^2 are the mean and the variance of jump in return respectively.

Under the Kou's model, $g(\eta)$ follows the log-double-exponential density, represented as:

$$g(\eta) := \frac{1}{\eta}\left(p\eta_1 e^{-\eta_1 \ln(\eta)}\mathcal{H}(\ln(\eta)) + q\eta_2 e^{-\eta_2 \ln(\eta)}\mathcal{H}(-\ln(\eta))\right),$$

where $\mathcal{H}(\cdot)$ represents a Heaviside function with $p > 0$, $q = 1 - p$,$\eta_1 > 1$, $\eta_2 > 0$ and κ is given by $\kappa := \frac{p\eta_1}{\eta_1 - 1} + \frac{q\eta_2}{\eta_1 + 1} - 1$.

Moreover, since the problem (3.2.2) is degenerate and backward in time so we can transform it into a non-degenerate and forward in time problem by using the transformations $x = \ln(\frac{S}{K})$, $y = \ln(\eta)$, $t = T - \tau$ and $v(x,t) := V(Ke^x, T - \tau)$, i.e.

$$\begin{cases} \frac{\partial v}{\partial t} - \mathcal{L}v & \geq & 0 & (x,t) \in \mathbb{R} \times J, \\ v(x,t) - \Phi(Ke^x) & \geq & 0 & (x,t) \in \mathbb{R} \times J, \\ \left(\frac{\partial v}{\partial t} - \mathcal{L}v\right)(v(x,t) - \Phi(Ke^x)) & = & 0 & (x,t) \in \mathbb{R} \times J, \\ v(x,0) & = & \Phi(Ke^x) & x \in \mathbb{R}, \end{cases} \tag{3.2.5}$$

where $J = (0, T]$ and the spatial operator can be defined as:

$$\mathcal{L}v(x,t) = \frac{1}{2}\sigma^2 \frac{\partial^2 v}{\partial x^2} + \left(r - \frac{\sigma^2}{2} - d - \lambda\kappa\right)\frac{\partial v}{\partial x} - (r + \lambda)v + \lambda \int_{-\infty}^{\infty} v(y,t) f(y - x) dy. \tag{3.2.6}$$

We have, $\mathcal{L} = \mathcal{D} + \mathcal{I}$, where $\mathcal{D}$ represents the differential operator and $\mathcal{I}$ is used as an integral operator, such that

$$\mathcal{D}v(x,t) = \frac{1}{2}\sigma^2 \frac{\partial^2 v}{\partial x^2} + \left(r - \frac{\sigma^2}{2} - d - \lambda\kappa\right)\frac{\partial v}{\partial x} - (r + \lambda)v, \tag{3.2.7}$$

$$\mathcal{I}v(x,t) = \lambda \int_{-\infty}^{\infty} v(y,t) f(y - x) dy. \tag{3.2.8}$$

After applying the given transformation, we can write the function $f(y)$ as:

$$f(y) := \begin{cases} \frac{1}{\sqrt{2\pi}\sigma_J} \exp(-\frac{(y - \mu_J)^2}{2\sigma_J^2}) & \text{Merton's model,} \\ p\eta_1 e^{-\eta_1 y}\mathcal{H}(y) + q\eta_2 e^{-\eta_2 y}\mathcal{H}(-y) & \text{Kou's model.} \end{cases}$$

To approximate the integral term on truncated domain Ω, we used the composite trapezoidal rule.

For evaluational purposes, we localized the problem (3.2.5) on a bounded domain $\Omega := (x^L, x^R)$ with x^L and $x^R \in \mathbb{R}$. Now, considering $u(x,t)$ as a solution of the following localized problem (3.2.9)

$$\begin{cases} \frac{\partial u}{\partial t} - \mathcal{L}u & \geq & 0 \ (x,t) \in \Omega \times J, \\ u(x,t) - \Phi(Ke^x) & \geq & 0 \ (x,t) \in \Omega \times J, \\ (\frac{\partial u}{\partial t} - \mathcal{L}u)\,(u(x,t) - \Phi(Ke^x)) & = & 0 \ (x,t) \in \Omega \times J, \\ u(x,0) & = & \Phi(Ke^x) \quad x \in \Omega, \end{cases} \tag{3.2.9}$$

with

$$u(x,t) = B(x,t), \quad (x,t) \in \Omega^c \times \bar{J},$$

and

$$B(x,t) = \begin{cases} \Phi(Ke^x) & : & (x,t) \in \partial\Omega \times \bar{J}, \\ \Phi(Ke^x) & : & (x,t) \in \left(\overline{\Omega}^c \cap \overline{\Omega}_{Big}\right) \times \bar{J}, \Omega \subseteq \Omega_{Big}, \\ 0 & : & (x,t) \in \overline{\Omega}^c_{Big} \times \bar{J}. \end{cases}$$

Here, $\partial\Omega$ represents the boundary of Ω, $\Omega^c = \mathbb{R} \setminus \Omega$, $\bar{J} = [0,T]$ and Ω_{Big} is an open connected and bounded subset of $\mathbb{R}$ (See, for example, [82]).

The problems (3.2.2) and (3.2.9) are stated to have unique solutions under specific assumptions relating to the coefficients of the spatial operator $\mathcal{L}$. Moreover, within the interior of the domain, the localization error due to the domain truncation decreases exponentially with respect to the domain size (see, for example, [36, 56, 107]).

3.3 Operator Splitting Methods

Ikonen and Toivanen [78] introduced the operator splitting approach for pricing the value of the American put option. The primary idea behind introducing the operator splitting technique is to derive an expression with the help of an additional variable ψ such that $\psi = u_t - \mathcal{L}u$.

We can reformulate LCP (3.2.9) as

$$\begin{cases} \frac{\partial u}{\partial t} - \mathcal{L}u & = & \psi, \\ (u(x,t) - \Phi(Ke^x)) \cdot \psi & = & 0, \\ u(x,t) - \Phi(Ke^x) & \geq & 0, \\ \psi & \geq & 0, \end{cases} \tag{3.3.1}$$

in the region $\Omega \times J$.

Let the system (3.3.1) be initially discretized in time with uniform grid $t_n = nk$, $n = 0, 1, 2, \ldots, N$ with temporal mesh length k and $N+1$ to be the total numbers of temporal mesh points, where $u(x, t_n)$ abbreviated as u_n.

Now, we briefly discuss the IMEX-BDF-OS methods for the temporal discretization of LCP (3.3.1).

3.3.1 IMEX-BDF1-OS Method

Let us split the governing equation $u_t - \mathcal{L}u = \psi$ into two discrete equations on the $(n+1)^{th}$ time level as

$$\left(\frac{\tilde{u}_{n+1} - u_n}{k}\right) - \mathcal{D}\tilde{u}_{n+1} - \lambda\mathcal{I}(u_n) = \psi_n, \tag{3.3.2}$$

$$\left(\frac{u_{n+1} - u_n}{k}\right) - \mathcal{D}\tilde{u}_{n+1} - \lambda\mathcal{I}(u_n) = \psi_{n+1}. \tag{3.3.3}$$

Here the discrete problem for LCP (3.3.1) is to find the pair (u_{n+1}, ψ_{n+1}) that satisfy the discrete equations (3.3.2) and (3.3.3) as well as the constraints:

$$\begin{cases} u_{n+1} \geq \Phi, \\ \psi_{n+1} \geq 0, \\ \psi_{n+1}(u_{n+1} - \Phi) = 0. \end{cases} \tag{3.3.4}$$

We will compute the solution of (3.3.1) using the IMEX-BDF1-OS techniques in two steps. First, we determine the intermediate approximation $\tilde{u}_{n+1}$ with the help of equation (3.3.2) under given boundary conditions

$$\tilde{u}_{n+1}(x^L) = K, \qquad \tilde{u}_{n+1}(x^R) = 0,$$

and the known auxiliary term ψ_n.

Second, we develop a relationship between u_{n+1} and ψ_{n+1} in (3.3.3). To do so, we restate the equation (3.3.3) as a problem, combining equation (3.3.2) and the restrictions in (3.3.4) in order to determine the pair (u_{n+1}, ψ_{n+1}), such that

$$\begin{cases} \frac{u_{n+1} - \tilde{u}_{n+1}}{k} = \psi_{n+1} - \psi_n, \\ \psi_{n+1}(u_{n+1} - \Phi) = 0, \end{cases} \tag{3.3.5}$$

with the constraints:

$$u_{n+1} \geq \Phi \quad \text{and} \quad \psi_{n+1} \geq 0. \tag{3.3.6}$$

Again, by solving the problems (3.3.5)-(3.3.6) in (u_{n+1}, ψ_{n+1}) plane, we get

$$(u_{n+1}, \psi_{n+1}) = \begin{cases} (\Phi, \psi_n + \frac{\Phi - \tilde{u}_{n+1}}{k}) & \text{if } \tilde{u}_{n+1} - k\psi_n \leq \Phi, \\ (\tilde{u}_{n+1} - k\psi_n, 0) & \text{otherwise.} \end{cases} \tag{3.3.7}$$

As a result, the second step can be completed by solving the discrete equation (3.3.2) using the modified formula (3.3.7). Using initial condition and assigning value $\psi_0 = 0$ on the zeroth time level, the pair (u_0, ψ_0) may be achieved. One can use the algorithm discussed in [97].

3.3.2 IMEX-BDF2-OS Method

Let us assume that the values $\{u_n, \psi_n\}$ and $\{u_{n-1}, \psi_{n-1}\}$ are a priori, known at the points t_n and t_{n-1}. We perform two sub-steps at discrete point t_{n+1}. In first step, we compute an intermediate value $\tilde{u}_{n+1}$

using the following BVP (3.3.8)

$$\begin{cases} \frac{1}{k}\left(\frac{3}{2}\tilde{u}_{n+1} - 2u_n + \frac{1}{2}u_{n-1}\right) - \mathcal{D}\tilde{u}_{n+1} - \lambda\mathcal{I}(\mathcal{E}u_n) &= \psi_n, \\ \tilde{u}_{n+1}(x^L) = K, \qquad\qquad \tilde{u}_{n+1}(x^R) = 0, \end{cases} \tag{3.3.8}$$

where $\mathcal{E}u_n = 2u_n - u_{n-1}$.

In the second step of the operator splitting method, we project the $\tilde{u}_{n+1}$ on constraint space to obtain u_{n+1} with the following correction terms

$$\begin{cases} \frac{3(u_{n+1}-\tilde{u}_{n+1})}{2k} &= \psi_{n+1} - \psi_n, \\ u^{n+1} &\geq \Phi, \\ \psi_{n+1} &\geq 0, \\ \psi_{n+1}(u_{n+1} - \Phi) &= 0. \end{cases} \tag{3.3.9}$$

Now, by solving the problems (3.3.8)-(3.3.9) in (u_{n+1}, ψ_{n+1}) plane, we get

$$(u_{n+1}, \psi_{n+1}) = \begin{cases} (\Phi, \psi_n + \frac{3}{2}\frac{\Phi - \tilde{u}_{n+1}}{k}) & \text{if } \tilde{u}_{n+1} - \frac{2k}{3}\psi_n \leq \Phi, \\ (\tilde{u}_{n+1} - \frac{2k}{3}\psi_n, 0) & \text{otherwise.} \end{cases} \tag{3.3.10}$$

Thus, the first step may be accomplished by solving a discrete equation (3.3.8), and the second step can be performed by using the updating formula (3.3.10). The value on the previous two-time levels is required by the implicit technique with three-time levels, as described above. Using starting condition and assigning value $\psi_0 = 0$, the pair (u_0, ψ_0) on the zeroth time level may be achieved. We shall use the IMEX-BDF1-OS method to find the pair (u_1, ψ_1) at first level.

3.4 Stability Analysis

For theoretical convenience, let us transform the problem (3.3.1) into a problem with homogeneous boundary conditions without loss of generality, i.e.,

$$\begin{cases} \frac{\partial w}{\partial t} - \mathcal{L}w &= \psi + f, & (x,t) \in \Omega \times J, \\ (w(x,t) - w_0(x)) \cdot \psi &= 0, & (x,t) \in \Omega \times J, \\ w(x,t) - w_0(x) &\geq 0, & (x,t) \in \Omega \times J, \\ \psi &\geq 0, & (x,t) \in \Omega \times J, \\ w(x,0) &= w_0(x), & x \in \Omega \\ w(x,t) &= 0, & (x,t) \in \partial\Omega \times \bar{J}, \end{cases} \tag{3.4.1}$$

where $w_0(x) := \Phi(Ke^x) - \phi(x)$, $w(x,t) = u(x,t) - \phi(x)$ and $f = \mathcal{L}\phi$, $x \in \mathbb{R}$, and

$$\phi(x) = \begin{cases} \frac{x^R - x}{x^R - x^L}\Phi(Ke^{x^L}) + \frac{x - x^L}{x^R - x^L}\Phi(Ke^{x^R}) & : \quad x \in \overline{\Omega}, \\ \Phi(Ke^x) & : \quad x \in \overline{\Omega}^c \cap \overline{\Omega}_{Big}, \\ 0 & : \quad x \in \overline{\Omega}^c_{Big}. \end{cases}$$

Alternatively, one can also find this algorithm in [81].

Lemma 3.4.1. *(Discrete Gronwall's Lemma) Suppose that α_n is a non negative sequence, and that the sequence β_n satisfies*

$$\begin{cases} \beta_0 \leq \delta_0, \\ \beta_n \leq \delta_0 + \sum_{k=0}^{n-1} \gamma_k + \sum_{k=0}^{n-1} \alpha_k \beta_k \quad n \geq 1, \end{cases}$$

then β_n satisfies

$$\begin{cases} \beta_1 \leq \delta_0(1+\alpha_0) + \gamma_0, \\ \beta_n \leq \delta_0 \prod_{k=0}^{n-1}(1+\alpha_k) + \sum_{k=0}^{n-2} \gamma_k \prod_{s=k+1}^{n-1}(1+\alpha_s) + \gamma_{n-1} \quad n \geq 2. \end{cases}$$

Moreover, if $\delta_0 \geq 0$ and $\gamma_n \geq 0$ for $n \geq 0$, it follows

$$\beta_n \leq \left(\delta_0 + \sum_{k=0}^{n-1} \gamma_k\right) \exp\left(\sum_{k=0}^{n-1} \alpha_k\right), \ n \geq 1.$$

Proof. The proof can be found in [129]. □

3.4.1 Identities and Inequalities

We shall frequently use the following identities and inequalities in the stability and error analysis.

$$(\mathcal{D}w, w) \leq \alpha \|w\|^2, \tag{I1}$$

$$(a,b) \leq \epsilon a^2 + \frac{1}{4\epsilon} b^2, \quad a, b \in \mathbb{R} \ \text{ and } \ \epsilon > 0, \tag{I2}$$

$$2\,(a-b,a) = \|a\|^2 - \|b\|^2 + \|a-b\|^2, \tag{I3}$$

$$2\,(3a-4b+c,a) = a^2 + (2a-b)^2 - b^2 - (2b-c)^2 + (a-2b+c)^2, \tag{I4}$$

where $\alpha = \left| \frac{\left(r - \frac{\sigma^2}{2} - \lambda\kappa\right)^2 - \left(2(r+\lambda)\sigma^2\right)}{2\sigma^2} \right|$, and for the proof of inequality (I1), one can see [83] and reference therein.

We shall use the following result in the analysis, for all $w(\cdot,t) \in L^2(\Omega)$, $t \in (0,T)$ such that

$$\overline{w}(x,t) = \begin{cases} w(x,t) & : \ (x,t) \in \Omega \times [0,T], \\ 0 & : \ (x,t) \in \Omega^c \times [0,T]. \end{cases}$$

The integral operator $\mathcal{I}(w)$ follow the condition $\|\mathcal{I}\overline{w}(\cdot,t)\| \leq \mathcal{C}_I \|w(\cdot,t)\|$, where $\mathcal{C}_I$ is a constant that is independent to t and $\|u\| := \left(\int_\Omega |u(x)|^2 dx\right)^{\frac{1}{2}}$.

3.4.2 Stability Analysis for IMEX-BDF1-OS

Theorem 3.4.2. *Under the assumption $k < \frac{1}{2(4\alpha+1+\lambda\mathcal{C}_I)}$, the scheme is stable, $\forall\ 1 \leq m \leq \frac{T}{k}$ in the following sense:*

$$\|w_m\|^2 + \frac{1}{2}\sum_{n=0}^{m-1} \|\tilde{w}_{n+1} - w_n\|^2 + k^2\|\psi_m\|^2 \leq C\left(\|w_0\|^2 + k\|\psi_0\|^2 + k\sum_{n=0}^{m-1}\|w_0\|^2 + k\sum_{n=0}^{m-1}\|f\|^2 + k\sum_{n=0}^{m-1}\|\psi_n\|^2\right),$$

where C is a constant that depends on the parameters C_I, r, σ, λ and T, but may not be the same at each occurrence.

Proof. Considering the equation (3.4.1), we have

$$\frac{\tilde{w}_{n+1} - w_n}{k} = \mathcal{D}\tilde{w}_{n+1} + \lambda\mathcal{I}(w_n) + f + \psi_n. \tag{3.4.2}$$

After taking the inner product of both sides of (3.4.2) with $4k\tilde{w}_{n+1}$ and using the identities (I3) and (I1), we have

$$\begin{aligned} 2\|\tilde{w}_{n+1}\|^2 - 2\|w_n\|^2 + 2\|\tilde{w}_{n+1} - w_n\|^2 \quad &\leq \quad 4k\alpha\|\tilde{w}_{n+1}\|^2 + 4k\lambda(\mathcal{I}(w_n), \tilde{w}_{n+1}) + 4k(f, \tilde{w}_{n+1}) \\ &\quad +4k(\psi_n, \tilde{w}_{n+1}). \end{aligned} \tag{3.4.3}$$

From equation (3.3.5), we get

$$w_{n+1} - w_0 - k\psi_{n+1} = \tilde{w}_{n+1} - w_0 - k\psi_n. \tag{3.4.4}$$

Taking the inner product of both sides of (3.4.4) with itself and using some inequalities from subsection 3.4.1, we have

$$\begin{aligned} \|w_{n+1}\|^2 + \|w_0\|^2 \quad - \quad &\frac{1}{2}\|w_{n+1}\|^2 - 2\|w_0\|^2 + k^2\|\psi_{n+1}\|^2 - 2k(w_{n+1} - w_0, \psi_{n+1}) \\ &\leq 2\|\tilde{w}_{n+1}\|^2 + 2\|w_0\|^2 + k^2\|\psi_n\|^2 - 2k(\tilde{w}_{n+1}, \psi_n) + 2k(w_0, \psi_n). \end{aligned} \tag{3.4.5}$$

Now, adding up the inequalities (3.4.3) and (3.4.5) with the use of $(w_{n+1} - w_0, \psi_{n+1}) = 0$, we get

$$\begin{aligned} &\frac{1}{2}\|w_{n+1}\|^2 - 2\|w_n\|^2 + 2\|\tilde{w}_{n+1} - w_n\|^2 + k^2(\|\psi_{n+1}\|^2 - \|\psi_n\|^2) \\ &\leq 3\|w_0\|^2 + 4k\alpha\|\tilde{w}_{n+1}\|^2 + 4k\lambda(\mathcal{I}(w_n), \tilde{w}_{n+1}) + 4k(f, \tilde{w}_{n+1}) + 2k(\tilde{w}_{n+1}, \psi_n) + 2k(w_0, \psi_n). \end{aligned}$$

After small calculations

$$\begin{aligned} &\frac{1}{2}\|w_{n+1}\|^2 - \frac{1}{2}\|w_n\|^2 + \frac{3}{2}\|\tilde{w}_{n+1} - w_n\|^2 + k^2(\|\psi_{n+1}\|^2 - \|\psi_n\|^2) \\ &\leq 3\|w_0\|^2 + 2k(4\alpha + 1 + \lambda\mathcal{C}_I)\|\tilde{w}_{n+1} - w_n\|^2 + (2k(4\alpha + 1 + \lambda\mathcal{C}_I) + 4k\lambda\mathcal{C}_I + \frac{3}{2})\|w_n\|^2 \\ &+8k\|f\|^2 + 2k\|\psi_n\|^2 + k\|w_0\|^2 + k\|\psi_n\|^2. \end{aligned}$$

Assuming that $k < \frac{1}{2(4\alpha+1+\lambda\mathcal{C}_I)}$, we get

$$\begin{aligned} &\frac{1}{2}\|w_{n+1}\|^2 - \frac{1}{2}\|w_n\|^2 + \frac{1}{2}\|\tilde{w}_{n+1} - w_n\|^2 + k^2(\|\psi_{n+1}\|^2 - \|\psi_n\|^2) \\ &\leq 3\|w_0\|^2 + \left(2k(4\alpha + 1 + \lambda\mathcal{C}_I) + 4k\lambda\mathcal{C}_I + \frac{3}{2}\right)\|w_n\|^2 + 8k\|f\|^2 + 2k\|\psi_n\|^2 + k\|w_0\|^2 + k\|\psi_n\|^2. \end{aligned}$$

Taking the summation on both sides of the above inequality from $n = 0$ to $m - 1$

$$\|w_m\|^2 + \sum_{n=0}^{m-1}\|\tilde{w}_{n+1} - w_n\|^2 + 2k^2\|\psi_m\|^2$$

$$\leq \|w_0\|^2 + 2k^2\|\psi_0\|^2 + (6+2k)\sum_{n=0}^{m-1}||w_0||^2 + (4k(4\alpha+1+\lambda\mathcal{C}_I)+8k\lambda\mathcal{C}_I+3)\sum_{n=0}^{m-1}||w_n||^2$$
$$+16k\sum_{n=0}^{m-1}\|f\|^2 + 6k\sum_{n=0}^{m-1}\|\psi_n\|^2.$$

Applying the Lemma 3.4.1, we get,

$$\|w_m\|^2 + \sum_{n=0}^{m-1}\|\tilde{w}_{n+1}-w_n\|^2 + 2k^2\|\psi_m\|^2$$
$$\leq C'\left(\|w_0\|^2 + 2k^2\|\psi_0\|^2 + (6+2k)\sum_{n=0}^{m-1}\|w_0\|^2 + 16k\sum_{n=0}^{m-1}\|f\|^2 + 6k\sum_{n=0}^{m-1}\|\psi_n\|^2\right). \quad (3.4.6)$$

Further simplifying the inequality (3.4.6) we obtain the desired result,

$$\|w_m\|^2+\frac{1}{2}\sum_{n=0}^{m-1}\|\tilde{w}_{n+1}-w_n\|^2+k^2\|\psi_m\|^2 \leq C\left(\|w_0\|^2 + k\|\psi_0\|^2 + k\sum_{n=0}^{m-1}\|w_0\|^2 + k\sum_{n=0}^{m-1}\|f\|^2 + k\sum_{n=0}^{m-1}\|\psi_n\|^2\right),$$

where C' and C are the constants depending on the parameters C_I, r, σ, λ and T. □

3.4.3 Stability Analysis for IMEX-BDF2-OS

Theorem 3.4.3. *Under the assumption $k < \frac{1}{2(4\alpha+1+\lambda\mathcal{C}_I)}$ the scheme is stable, for all $2 \leq m \leq \frac{T}{k}$ in the following sense:*

$$\|w_m\|^2 + \|w_{m-1}\|^2 + \frac{1}{2}\sum_{n=1}^{m-1}\|\tilde{w}_{n+1}\|^2 + \frac{8}{9}k^2\|\psi_m\|^2$$
$$\leq C\left(\|w_0\|^2 + \|w_1\|^2 + k\sum_{n=1}^{m-1}\|f\|^2 + k\sum_{n=1}^{m-1}\|w_0\|^2 + k\sum_{n=1}^{m-1}\|\psi_n\|^2 + k^2\|\psi_1\|^2\right),$$

where C is a constant that depends on the parameters C_I, r, σ, λ and T.

Proof. Considering the equation (3.3.8), we obtain

$$\frac{3\tilde{w}_{n+1}-4w_n+w_{n-1}}{2k} = \mathcal{D}\tilde{w}_{n+1} + \lambda\mathcal{I}(\mathcal{E}w_n) + f + \psi_n. \quad (3.4.7)$$

Taking the inner product of both sides of the equation (3.4.7) with $4k\tilde{w}_{n+1}$ and using the identity (I1) and (I4), we have

$$\begin{aligned}\|\tilde{w}_{n+1}\|^2 &- \|w_n\|^2 + \|2\tilde{w}_{n+1}-w_n\|^2 - \|2w_n-w_{n-1}\|^2 + \|\tilde{w}_{n+1}-2w_n+w_{n-1}\|^2\\ &= 4k(\mathcal{D}\tilde{w}_{n+1},\tilde{w}_{n+1}) + 4k\lambda(\mathcal{I}(\mathcal{E}w_n),\tilde{w}_{n+1}) + 4k(f,\tilde{w}_{n+1}) + 4k(\psi_n,\tilde{w}_{n+1}),\\ &\leq 4k\alpha\|\tilde{w}_{n+1}\|^2 + 4k\lambda(\mathcal{I}(\mathcal{E}w_n),\tilde{w}_{n+1}) + 4k(f,\tilde{w}_{n+1}) + 4k(\psi_n,\tilde{w}_{n+1}). \quad (3.4.8)\end{aligned}$$

Now, from equation (3.3.9), we get

$$w_{n+1} - w_0 - \frac{2}{3}k\psi_{n+1} = \tilde{w}_{n+1} - w_0 - \frac{2}{3}k\psi_n. \quad (3.4.9)$$

Taking inner product of (3.4.9) from both sides with itself, we have

$$\|w_{n+1}-w_0\|^2+\frac{4}{9}k^2\|\psi_{n+1}\|^2-\frac{4}{3}k(w_{n+1}-w_0,\psi_{n+1})=\|\tilde{w}_{n+1}-w_0\|^2+\frac{4}{9}k^2\|\psi_n\|^2-\frac{4}{3}k(\tilde{w}_{n+1}-w_0,\psi_n).$$

Using some inequalities from subsection 3.4.1 and some calculations, we have

$$\begin{aligned}\|w_{n+1}\|^2 \quad &+ \quad \|w_0\|^2-\frac{1}{2}\|w_{n+1}\|^2-2\|w_0\|^2+\frac{4}{9}k^2\|\psi_{n+1}\|^2-\frac{4}{3}k(w_{n+1}-w_0,\psi_{n+1})\\ &\le 2\|\tilde{w}_{n+1}\|^2+2\|w_0\|^2+\frac{4}{9}k^2\|\psi_n\|^2-\frac{4}{3}k(\tilde{w}_{n+1},\psi_n)+\frac{4}{3}k(w_0,\psi_n). \qquad (3.4.10)\end{aligned}$$

Now, multiplying the inequality (3.4.8) by 2 and adding with inequality (3.4.10) and using $(w_{n+1}-w_0,\psi_{n+1})=0$, we get

$$\begin{aligned}&\frac{1}{2}\|w_{n+1}\|^2-2\|w_n\|^2+2\|2\tilde{w}_{n+1}-w_n\|^2-2\|2w_n-w_{n-1}\|^2+2\|\tilde{w}_{n+1}-2w_n+w_{n-1}\|^2\\ &+\frac{4}{9}k^2\|\psi_{n+1}\|^2\\ &\le 8k\alpha\|\tilde{w}_{n+1}\|^2+8k\lambda(\mathcal{I}(\mathcal{E}w_n),\tilde{w}_{n+1})+8k(f,\tilde{w}_{n+1})+3\|w_0\|^2+\frac{4}{9}k^2\|\psi_n\|^2\\ &+\frac{20}{3}k(\tilde{w}_{n+1},\psi_n)+\frac{4}{3}k(w_0,\psi_n).\end{aligned}$$

After some calculation with the help of some inequalities from subsection 3.4.1, we have

$$\begin{aligned}&\|w_{n+1}\|^2-\|w_n\|^2+3\|\tilde{w}_{n+1}\|^2+8\left(\|w_n\|^2-\|w_{n-1}\|^2\right)+\frac{8}{9}k^2\left(\|\psi_{n+1}\|^2-\|\psi_n\|^2\right)\\ &\le\frac{571}{13}\|w_n\|^2+32k\lambda\mathcal{C}_I\|w_n\|^2+8k\lambda\mathcal{C}_I\|w_{n-1}\|^2+4k(4\alpha+1+\lambda\mathcal{C}_I)\|\tilde{w}_{n+1}\|^2\\ &+32k\|f\|^2+\frac{212}{9}k\|\psi_n\|^2+\frac{(4k+18)}{3}\|w_0\|^2. \qquad (3.4.11)\end{aligned}$$

Assuming that $k<\frac{1}{2(4\alpha+1+\lambda\mathcal{C}_I)}$, then from (3.4.11), we have

$$\begin{aligned}\|w_{n+1}\|^2-\|w_n\|^2 \quad &+ \quad \|\tilde{w}_{n+1}\|^2+8\left(\|w_n\|^2-\|w_{n-1}\|^2\right)+\frac{8}{9}k^2\left(\|\psi_{n+1}\|^2-\|\psi_n\|^2\right)\\ &\le \quad \frac{571}{13}\|w_n\|^2+32k\lambda\mathcal{C}_I\|w_n\|^2+8k\lambda\mathcal{C}_I\|w_{n-1}\|^2+32k\|f\|^2\\ &\quad +\frac{212}{9}k\|\psi_n\|^2+\frac{(4k+18)}{3}\|w_0\|^2. \qquad (3.4.12)\end{aligned}$$

Adding the equation (3.4.12) from $n=1$ to $m-1$

$$\begin{aligned}\|w_m\|^2-\|w_1\|^2 \quad &+ \quad \sum_{n=1}^{m-1}\|\tilde{w}_{n+1}\|^2+8\|w_{m-1}\|^2-8\|w_0\|^2+\frac{8}{9}k^2\|\psi_m\|^2-\frac{8}{9}k^2\|\psi_1\|^2\\ &\le \quad \left(\frac{571}{13}+32k\lambda\mathcal{C}_I\right)\sum_{n=1}^{m-1}\|w_n\|^2+8k\lambda\mathcal{C}_I\sum_{n=1}^{m-1}\|w_{n-1}\|^2+32k\sum_{n=1}^{m-1}\|f\|^2\\ &\quad +\left(\frac{4k+18}{3}\right)\sum_{n=1}^{m-1}\|w_0\|^2+\frac{212}{9}k\sum_{n=1}^{m-1}\|\psi_n)\|^2. \qquad (3.4.13)\end{aligned}$$

$$\begin{aligned}\|w_m\|^2 &+ \sum_{n=1}^{m-1}\|\tilde{w}_{n+1}\|^2 + 8\|w_{m-1}\|^2 + \frac{8}{9}k^2\|\psi_m\|^2 \\ &\leq 8\|w_0\|^2 + \|w_1\|^2 + \frac{8}{9}k^2\|\psi_1\|^2 + \left(\frac{571}{13} + 40k\lambda\mathcal{C}_I\right)\sum_{n=0}^{m-1}\|w_n\|^2 \\ &\quad +32k\sum_{n=1}^{m-1}\|f\|^2 + \left(\frac{4k+18}{3}\right)\sum_{n=1}^{m-1}\|w_0\|^2 + \frac{212k}{9}\sum_{n=1}^{m-1}\|\psi_n)\|^2. \end{aligned} \tag{3.4.14}$$

Applying the Lemma 3.4.1 on (3.4.14), we have

$$\begin{aligned}&\|w_m\|^2 + \|w_{m-1}\|^2 + \frac{1}{2}\sum_{n=1}^{m-1}\|\tilde{w}_{n+1}\|^2 + \frac{8}{9}k^2\|\psi_m\|^2 \\ &\leq C\left(\|w_0\|^2 + \|w_1\|^2 + k\sum_{n=1}^{m-1}\|f\|^2 + k\sum_{n=1}^{m-1}\|w_0\|^2 + k\sum_{n=1}^{m-1}\|\psi_n)\|^2 + k^2\|\psi_1\|^2\right). \end{aligned} \tag{3.4.15}$$

□

3.5 Error Analysis

In the last section, we have established the stability results. Now, we derive the corresponding error estimates for IMEX-BDF1-OS and IMEX-BDF2-OS techniques by assuming the exact solution is adequately regular. First, we establish the error function and error equation. Denoting the analytic solution at t_n by $w(\cdot, t_n)$ and similar for other related variables.

3.5.1 Error Analysis for IMEX-BDF1-OS

We define e_n= $w(\cdot, t_n)$- w_n, $\tilde{e}_n$= $w(\cdot, t_n) - \tilde{w}_n$, $h_n = \psi(\cdot, t_n)$- ψ_n and $\psi(\cdot, t_{n+1}) - \psi(\cdot, t_n) \leq ck$, where c is a generic constant and independent of n.

From the continuous system (3.4.1), we have

$$\frac{w(\cdot, t_{n+1}) - w(\cdot, t_n)}{k} = \mathcal{D}w(\cdot, t_{n+1}) + \lambda\mathcal{I}(w(t_n)) + f + \psi(\cdot, t_{n+1}) + R_{n+1}, \tag{3.5.1}$$

where, R_{n+1} is truncation error for given method.

Now, we consider the equation for IMEX-BDF1-OS,

$$\frac{\tilde{w}_{n+1} - w_n}{k} = \mathcal{D}(\tilde{w}_{n+1}) + \lambda\mathcal{I}(w_n) + \psi_n + f. \tag{3.5.2}$$

To get the error equation, we subtract (3.5.2) from (3.5.1) and get

$$\frac{\tilde{e}_{n+1} - e_n}{k} = \mathcal{D}(\tilde{e}_{n+1}) + \lambda\mathcal{I}(e_n) + g_n + R_{n+1}, \tag{3.5.3}$$

where $g_n = \psi(\cdot, t_{n+1}) - \psi_n$, we can obtain another error equation from (3.3.5), as follows:

$$\frac{e_{n+1} - \tilde{e}_{n+1}}{k} = h_{n+1} - g_n + \psi(t_{n+1}) - \psi(t_n), \tag{3.5.4}$$

or

$$\frac{e_{n+1}-\tilde{e}_{n+1}}{k} = h_{n+1} - g_n, \tag{3.5.5}$$

where $g_n = h_n + \psi(\cdot, t_{n+1}) - \psi(\cdot, t_n)$ and let ψ is adequately smooth such that $\|g_n\| \leq \|h_n\| + ck$.

Theorem 3.5.1. *Under the assumption $k < \frac{1}{2(4\alpha+1+\lambda\mathcal{C}_I)}$, we have the following error estimates for the given method.*

$$\|e_m\|^2 + \frac{1}{2}\sum_{n=0}^{m-1}\|\tilde{e}_{n+1}\|^2 \leq Ck^2, \quad \forall\ 1 \leq m \leq \frac{T}{k},$$

where C is a constant that depends on the parameters C_I, r, σ, λ and T.

Proof. Considering the equation (3.5.3), we obtain

$$\frac{\tilde{e}_{n+1}-e_n}{k} = \mathcal{D}(\tilde{e}_{n+1}) + \lambda\mathcal{I}(e_n) + g_n + R_{n+1}. \tag{3.5.6}$$

Taking the inner product from both sides of (3.5.6) with $2k(\tilde{e}_{n+1})$ and using the identities (I1) and (I3), we have

$$\|\tilde{e}_{n+1}\|^2 - \|e_n\|^2 + \|\tilde{e}_{n+1}-e_n\|^2 \leq 2k\alpha\|\tilde{e}_{n+1}\|^2 + 2k\lambda\mathcal{C}_I\|e_n\|\|\tilde{e}_{n+1}\| + 2k(g_n, \tilde{e}_{n+1}) + 2k(R_{n+1}, \tilde{e}_{n+1}). \tag{3.5.7}$$

Cosidering the equation (3.5.5), we get

$$e_{n+1} - kh_{n+1} = \tilde{e}_{n+1} - kg_n. \tag{3.5.8}$$

Taking inner product of (3.5.8) from both sides, with itself:

$$\|e_{n+1}\|^2 + k^2\|h_{n+1}\|^2 - 2k(e_{n+1}, h_{n+1}) = \|\tilde{e}_{n+1}\|^2 + k^2\|f_n\|^2 - 2k(\tilde{e}_{n+1}, g_n). \tag{3.5.9}$$

Now, adding up the equations (3.5.7) and (3.5.9), and using $2k(e_{n+1}, h_{n+1}) \leq 0$ along with some inequalities from Subsection 3.4.1, we have

$$\begin{aligned}&\|e_{n+1}\|^2 - \|e_n\|^2 + \|\tilde{e}_{n+1}-e_n\|^2 + k^2(\|h_{n+1}\|^2 - \|g_n\|^2)\\ &\leq k(4\alpha+1+\lambda\mathcal{C}_I)\|\tilde{e}_{n+1}-e_n\|^2 + k(4\alpha+3\lambda\mathcal{C}_I+1)\|e_n\|^2 + 4k\|R_{n+1}\|^2.\end{aligned} \tag{3.5.10}$$

Assuming that $k < \frac{1}{2(4\alpha+1+\lambda\mathcal{C}_I)}$, we have from (3.5.10)

$$\|e_{n+1}\|^2 - \|e_n\|^2 + \frac{1}{2}\|\tilde{e}_{n+1}-e_n\|^2 + k^2(\|h_{n+1}\|^2 - \|g_n\|^2) \leq k(4\alpha+3\lambda\mathcal{C}_I+1)\|e_n\|^2 + 4k\|R_{n+1}\|^2.$$

Adding the above equation from $n = 0$ to $m-1$ and using the result $\|g_n\|^2 \leq 2\|h_n\|^2 + 2ck^2$ with some calculations, we have

$$\|e_m\|^2 - \|e_0\|^2 \quad + \quad \frac{1}{2}\sum_{n=0}^{m-1}\|\tilde{e}_{n+1}-e_n\|^2 + k^2(\|h_m\|^2 - \|h_0\|^2)$$

$$\leq k(4\alpha + 3\lambda\mathcal{C}_I + 1)\sum_{n=0}^{m-1}\|e_n\|^2 + k^2\sum_{n=0}^{m-1}(\|h_n\|^2 + ck^2) + k\sum_{n=0}^{m-1}\|R_{n+1}\|^2.$$

Applying the Lemma 3.4.1, we get the desired result

$$\|e_m\|^2 + \frac{1}{2}\sum_{n=0}^{m-1}\|\tilde{e}_{n+1} - e_n\|^2 \leq Ck^2.$$

□

3.5.2 Error Analysis for IMEX-BDF2-OS

Similarly, for IMEX-BDF2-OS, the error equations are as follows:

$$\frac{3\tilde{e}_{n+1} - 4e_n + e_{n-1}}{2k} = \mathcal{D}(\tilde{e}_{n+1}) + \lambda\mathcal{I}(\mathcal{E}e_n) + g_n + R_{n+1}, \tag{3.5.11}$$

and

$$\frac{3(e_{n+1} - \tilde{e}_{n+1})}{2k} = h_{n+1} - g_n. \tag{3.5.12}$$

Theorem 3.5.2. *Under the assumption $k < \frac{1}{2(4\alpha+1+\lambda\mathcal{C}_I)}$, we have following error estimates for the given method:*

$$\|e_m\|^2 + 2\|e_{m-1}\|^2 + \frac{1}{2}\sum_{n=1}^{m-1}\|2\tilde{e}_{n+1} - e_n\|^2 \leq Ck^3, \quad \forall\ 2 \leq m \leq \frac{T}{k},$$

where C is a constant that depends on the parameters C_I, r, σ, λ and T.

Proof. Considering the equation (3.5.11), we have

$$\frac{3\tilde{e}_{n+1} - 4e_n + e_{n-1}}{2k} = \mathcal{D}\tilde{e}_{n+1} + \mathcal{I}(\mathcal{E}e_n) + g_n + R_{n+1}. \tag{3.5.13}$$

Taking the inner product from both sides of the equation (3.5.13) with $4k\tilde{e}_{n+1}$ and using the identity (I1) and (I4) , we have

$$\begin{aligned}\|\tilde{e}_{n+1}\|^2 \quad - \quad & \|e_n\|^2 + \|2\tilde{e}_{n+1} - e_n\|^2 - \|2e_n - e_{n-1}\|^2 + \|\tilde{e}_{n+1} - 2e_n + e_{n-1}\|^2 \\ & \leq 4k\alpha\|\tilde{e}_{n+1}\|^2 + 4k\lambda\mathcal{C}_I\|\mathcal{E}e_n\|\|\tilde{e}_{n+1}\| + 4k(g_n, \tilde{e}_{n+1}) + 4k(R_{n+1}, \tilde{e}_{n+1}).\end{aligned} \tag{3.5.14}$$

From the equation (3.5.12), we get

$$e_{n+1} - \frac{2}{3}kh_{n+1} = \tilde{e}_{n+1} - \frac{2}{3}kg_n. \tag{3.5.15}$$

Taking the inner product of (3.5.15) from both sides with itself and multiplying by three, we obtain

$$3\|e_{n+1}\|^2 + \frac{4}{3}k^2\|h_{n+1}\|^2 - 4k(e_{n+1}, h_{n+1}) = 3\|\tilde{e}_{n+1}\|^2 + \frac{4}{3}k^2\|g_n\|^2 - 4k(\tilde{e}_{n+1}, g_n). \tag{3.5.16}$$

Adding up the equations (3.5.14) and (3.5.16), and noting $(e_{n+1}, h_{n+1}) \leq 0$ and $\|\tilde{e}_{n+1} - 2e_n + e_{n-1}\|^2 \geq 0$, along with some calculations using some inequalities from subsection 3.4.1, we get

$$\begin{aligned} \|e_{n+1}\|^2 &- \|e_n\|^2 + \|\tilde{e}_{n+1}\|^2 + \frac{4}{3}k^2\left(\|h_{n+1}\|^2 - \|g_n\|^2\right) + 2\left[\|e_n\|^2 - \|e_{n-1}\|^2\right] \\ &\leq 13\|e_n\|^2 + (4\alpha + \lambda\mathcal{C}_I + 1)k\|\tilde{e}_{n+1}\|^2 + 32k\lambda\mathcal{C}_I\|e_n\|^2 + 8k\lambda\mathcal{C}_I\|e_{n-1}\|^2 + 4k\|R_{n+1}\|^2. \end{aligned}$$

Furthermore, sssuming that $k < \frac{1}{2(4\alpha+\lambda\mathcal{C}_I+1)}$, with some basic calculations, we obtain

$$\begin{aligned} \|e_{n+1}\|^2 - \|e_n\|^2 &+ \frac{1}{2}\|\tilde{e}_{n+1}\|^2 + \frac{4}{3}k^2\left(\|h_{n+1}\|^2 - \|g_n\|^2\right) + 2\left[\|e_n\|^2 - \|e_{n-1}\|^2\right] \\ &\leq 13\|e_n\|^2 + 32k\lambda\mathcal{C}_I\|e_n\|^2 + 8k\lambda\mathcal{C}_I\|e_{n-1}\|^2 + 4k\|R_{n+1}\|^2. \end{aligned} \tag{3.5.17}$$

Summing up both sides of the equation (3.5.17) from $n = 1$ to $m - 1$ and performing some mathematical calculations, we get

$$\begin{aligned} &\|e_m\|^2 + 2\|e_{m-1}\|^2 + \frac{1}{2}\sum_{n=1}^{m-1}\|\tilde{e}_{n+1}\|^2 + \frac{4}{3}k^2\|h_m\|^2 \\ &\leq \|e_1\|^2 + 2\|e_0\|^2 + \frac{4}{3}k^2\|h_1\|^2 + (40k\lambda\mathcal{C}_I + 13)\sum_{n=0}^{m-1}\|e_n\|^2 + 4k\sum_{n=1}^{m-1}\|R_{n+1}\|^2 + \frac{4}{3}k^2\sum_{n=1}^{m-1}(ck^2 + ck\|h_n\|^2). \end{aligned}$$

Applying Lemma 3.4.1, we get

$$\begin{aligned} \|e_m\|^2 &+ 2\|e_{m-1}\|^2 + \frac{1}{2}\sum_{n=1}^{m-1}\|\tilde{e}_{n+1}\|^2 + \frac{4}{3}k^2\|h_m\|^2 \\ &\leq C\left(\|e_1\|^2 + 2\|e_0\|^2 + \frac{4}{3}k^2\|h_1\|^2 + 4k\sum_{n=1}^{m-1}\|R_{n+1}\|^2 + \frac{4}{3}k^2\sum_{n=1}^{m-1}(ck^2 + ck\|h_n\|^2)\right). \end{aligned}$$

Further simplifying the equation, we get the desired result

$$\|e_m\|^2 + 2\|e_{m-1}\|^2 + \frac{1}{2}\sum_{n=1}^{m-1}\|\tilde{e}_{n+1}\|^2 \leq Ck^3.$$

□

It is important to keep in mind that the limitations on k in the aforementioned theorems are only adequate for stability. These limitations can be marginally altered with more accurate analysis.

3.6 Numerical Discussion

In this section, we provide some numerical examples to reinforce our theoretical study. In order to determine the price of the American option under Kou's and Merton's jump-diffusion models, we explored the convergence behavior of both the IMEX-BDF1-OS and IMEX-BDF2-OS numerical techniques. To tackle the inequality constraints in the LCP for the American option, we used the implicit-explicit backward

difference approaches in conjunction with the operator splitting method. For spatial discretization, we employ the second-order central finite difference schemes

$$\begin{aligned} u_x(x_i) &\approx \frac{u_{i+1} - u_{i-1}}{2h}, \\ u_{xx}(x_i) &\approx \frac{u_{i+1} - 2u_i + u_{i-1}}{h^2}, \end{aligned}$$

with uniform spatial mesh length h in the computational domain $\Omega := [-1.5, 1.5]$.

Since for the American option pricing problem, the analytical form of solution is not available so we computed the point-wise errors at different asset prices, $S = 90,\ 100,\ 110$, using the difference between successive option prices.

To determine the rate of convergence (Rate) of given methods at different asset prices, we used the double mesh principle. The rate of convergence is computed by the formula,

$$\text{Rate} = \log_2 \frac{\|u(k,h) - u(\frac{k}{2}, \frac{h}{2})\|}{\|u(\frac{k}{2}, \frac{h}{2}) - u(\frac{k}{4}, \frac{h}{4})\|},$$

where $u(k,h)$ is the computed price of the American put option with temporal meth length k and spatial mesh length h.

We used the piecewise cubic Hermite interpolation to analyze the pricing of the American put option at the non-mesh points of stock prices.

Throughout all of the tests, we calculated the point-wise errors at different stock prices S with $M = 2^{10} + 1$ spatial discretization points and N temporal discretization points.

To perform numerical simulation, the following set of examples are taken.

Example 3.6.1. *The Merton's jump-diffusion model for the American put option along with the parameters:* $\sigma = 0.15$, $r = 0.04$, $T = 0.5$, $K = 100$, $\sigma_J = 0.45$, $\mu_J = -0.90$, $\lambda = 0.10$.

In the first numerical simulation, we presented the numerical results for the IMEX-BDF1-OS method under Merton's model. The option values along with point-wise errors and convergence rates at different asset prices are reported in Table 3.1. We can observe that the convergence rate reached its asymptotic order when the temporal mesh is sufficiently small.

In the same lineup, we executed the same numerical simulation for the IMEX-BDF2-OS method for Merton's model, and the results are reported in Table 3.2. We observe that IMEX-BDF1-OS is linearly convergent, and the rate of convergence for the IMEX-BDF2-OS method is near 1.5, which is consistent with the error estimate shown in Section 3.5. The American put option values for IMEX-BDF1-OS and IMEX-BDF2-OS under Merton's jump-diffusion model are presented in Figure 3.1. The graphs demonstrate that the option values are quite stable with no erroneous oscillation at or near the strike price.

Table 3.1: Numerical results of IMEX-BDF1-OS method under Merton's jump-diffusion model for American put options with specified parameters at various stock prices as given in Example 3.6.1.

	$S = 90$			$S = 100$			$S = 110$		
N	Value	Error	Rate	Value	Error	Rate	Value	Error	Rate
64	10.454172	-	-	4.901017	-	-	2.878383	-	-
128	10.454664	4.92e-04	-	4.906693	5.68e-03	-	2.881250	2.87e-03	-
256	10.455038	3.74e-04	0.40	4.909613	2.92e-03	0.96	2.882723	1.47e-03	0.96
512	10.455287	2.48e-04	0.60	4.911114	1.50e-03	0.96	2.883477	7.54e-04	0.97
1024	10.455451	1.64e-04	0.60	4.911884	7.71e-04	0.96	2.883861	3.84e-04	0.97

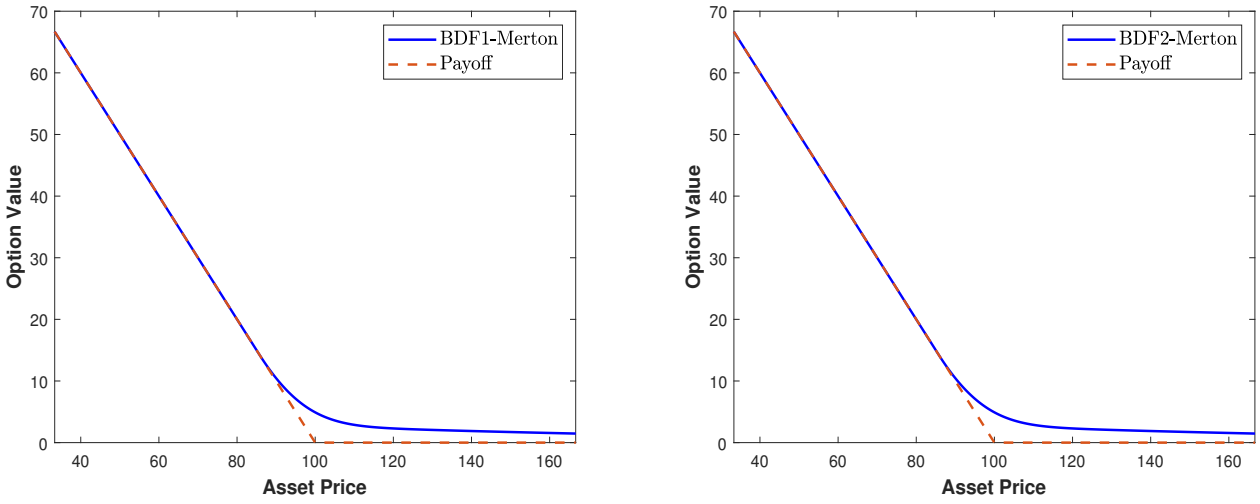

Figure 3.1: American put option value for IMEX-BDF1-OS (left) and IMEX-BDF2-OS (right) under the Merton's jump-diffusion model with parameters as provided in the Example 3.6.1.

Example 3.6.2. *The Kou's jump-diffusion model for American put option along with the parameters:* $\sigma = 0.15$, $r = 0.04$, $T = 0.5$, $K = 100$, $\eta_1 = 3.0465$, $\eta_2 = 3.0775$, $p = 0.3445$, $\lambda = 0.10$.

Next, we execute a similar simulation for IMEX-BDF1-OS and IMEX-BDF2-OS method for Kou's model. The obtained numerical results are reported in Table 3.3 and 3.4 respectively. We can observe that IMEX-BDF1-OS is linearly convergent and for IMEX-BDF2-OS method the error is reducing with ratio nearly three thus the discretization scheme is convergent with rate 1.5, as shown in the Table 3.4 which agree with our error estimate. The option values for IMEX-BDF1-OS and IMEX-BDF2-OS under Kou's jump-diffusion model for American put options are presented in Figure 3.2. The graphs demonstrate that the option values are quite stable with no erroneous oscillation at or near the strike price. From both

Table 3.2: Numerical results of IMEX-BDF2-OS method under Merton's jump-diffusion model for American put options with specified parameters at various stock prices as given in Example 3.6.1.

	$S = 90$			$S = 100$			$S = 110$		
N	Value	Error	Rate	Value	Error	Rate	Value	Error	Rate
64	10.456521	-	-	4.911746	-	-	2.883627	-	-
128	10.456092	4.29e-04	-	4.912395	6.49e-04	-	2.884030	4.03e-04	-
256	10.455851	2.41e-04	0.84	4.912602	2.07e-04	1.64	2.884177	1.47e-04	1.46
512	10.455737	1.15e-04	1.06	4.912666	6.39e-05	1.69	2.884230	5.37e-05	1.45
1024	10.455696	4.07e-05	1.49	4.912685	1.90e-05	1.74	2.884249	1.84e-05	1.54

Table 3.3: Numerical results of IMEX-BDF1-OS method under Kou's jump-diffusion model for American put options with specified parameters at various stock prices as given in Example 3.6.2.

	$S = 90$			$S = 100$			$S = 110$		
N	Value	Error	Rate	Value	Error	Rate	Value	Error	Rate
64	10.332776	-	-	4.008922	-	-	1.353754	-	-
128	10.333855	1.08e-03	-	4.014711	5.79e-03	-	1.355915	2.16e-03	-
256	10.334494	6.39e-04	0.76	4.017678	2.97e-03	0.96	1.357037	1.12e-03	0.95
512	10.334865	3.71e-04	0.79	4.019205	1.53e-03	0.96	1.357620	5.83e-04	0.94
1024	10.335081	2.16e-04	0.78	4.019989	7.84e-04	0.96	1.357921	3.01e-04	0.95

Table 3.4: Numerical results of IMEX-BDF2-OS method under Kou's jump-diffusion model for American put options with specified parameters at various stock prices as given in Example 3.6.2.

	$S = 90$			$S = 100$			$S = 110$		
N	Value	Error	Rate	Value	Error	Rate	Value	Error	Rate
64	10.335902	-	-	4.019887	-	-	1.357578	-	-
128	10.335621	2.81e-04	-	4.020513	6.26e-04	-	1.357990	4.12e-04	-
256	10.335455	1.66e-04	0.77	4.020711	1.97e-04	1.66	1.358144	1.53e-04	1.43
512	10.335378	7.67e-05	1.11	4.020775	6.40e-05	1.62	1.358202	5.86e-05	1.39
1024	10.335354	2.48e-05	1.62	4.020798	2.35e-05	1.44	1.358225	2.30e-05	1.35

examples, we have shown that the pointwise errors have a convergence rate of 1.5 for IMEX-BDF2-OS and 1 for IMEX-BDF1-OS, although the order of convergence at the early exercise border is less precise for both Merton's and Kou's models.

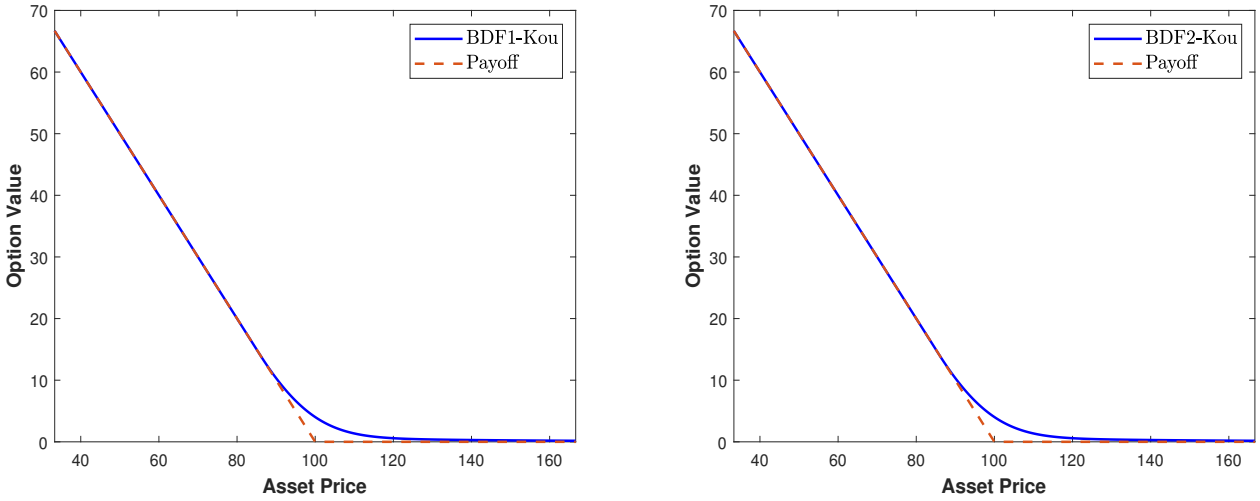

Figure 3.2: American put option value for IMEX-BDF1-OS (left) and IMEX-BDF2-OS (right) under the Kou's jump-diffusion model with parameters as provided in the Example 3.6.2.

3.7 Conclusion

In this work, we established the stability and error estimates for the operator splitting method combined with implicit-explicit backward difference techniques for American option pricing problems under jump-diffusion models. The solution of the linear complementarity problem (3.2.2) is the value of the American put option under the jump-diffusion model. We have approximated the integral operator by a numerical quadrature rule. In contrast, the differential operator is computed with the help of the finite difference operator analogous to the implicit-explicit backward difference techniques. To validate our theoretical results and demonstrate the convergence behaviors of operating splitting methods, we performed the numerical computations for the American put option under both Kou's and Merton's jump-diffusion models and presented the plots for the values of American put options. In our future work, we are interested in refining the rigorous error analysis of the IMEX-BDF2-OS method up to the second order using the variable step-size IMEX-BDF approach, as suggested in [167], and explore the rigorous analysis for other classes of problems.

CHAPTER 4

Implicit-Explicit BDF-OS Schemes for Pricing American Style Options in Markovian Regime-Switching Economy with Jumps: An Approximation of Error [1]

In this chapter, we present the stability and error analysis for the implicit-explicit backward difference formula combined with operator splitting (IMEX-BDF-OS) techniques, which aim to solve the linear complementarity problem (LCP) for pricing American options in a Markovian regime-switching jump-diffusion (RSJD) economy. Multiple regime-switching models have been fitted with the OS schemes with favourable outcomes. The complementarity requirements and the differential equation are separated and studied independently, making it easier to apply to LCP. Nevertheless, no stability or error analysis has been provided for the American option under the RSJD model by these operator-splitting procedures despite their popularity. Based on the IMEX-BDF1 and IMEX-BDF2 approaches, we estimate the error for

[1] The results discussed in this chapter are *communicated*

these techniques and offer a priori stability estimates for operator splitting (OS) strategies. We numerically test the operator splitting techniques to demonstrate the effectiveness of IMEX-BDF1 and IMEX-BDF2 methods in test problems, highlighting their efficiency in converging.

4.1 Introduction

The Black-Scholes (BS) model's ease of use and analytical adaptability have made it a popular choice for option pricing problems. On the other hand, statistical data indicates that when unrealistic assumptions of continuous volatility or interest rate are adopted, the Black-Scholes model does not effectively explain the behaviour of the financial market. The Black-Scholes model does not account for other defects, such as fluctuations in the price of the underlying asset. As a result, tremendous effort has been devoted to developing improved models in order to overcome these restricting assumptions. Alternative models include dynamics [36], jump-diffusion models [93], and stochastic volatility models (Merton model [111]).

The most popular technique for discretizing the differential operators in the context of option pricing is the use of finite difference approaches, which have been extensively studied in the pricing of options under jump models (see, for example, Achdou and Pironneau [3] and Tavella and Randall [156]). For representing the impact of jumps in option pricing, a number of alternative numerical techniques have been devised. A quadratic spline collocation approach for pricing options under the jump-diffusion models was introduced by Christara and Leung [29]. The MLS approach for pricing the multi-asset jump-diffusion model was introduced by Shirzadi et al. [144]. A novel kind of radial basis function was presented, and its applicability to option pricing problems was assessed by Dehghan et al. [43]. European and American options were priced by Rad et al. [131] using radial basis point interpolation. A reduced-order model for option pricing based on integrated radial basis functions and the partition of unity technique was suggested by A. Ebrahimijahan et al. [50] in jump-diffusion models. Using a reduced-order model based on the cubic B-spline basis function and the SSP-RK algorithm, M. Abbaszadeh et al. [1] examined option pricing under jump-diffusion models. Our work [177] presented several IMEX techniques based on RBF-FD for pricing options in the context of the local volatility jump-diffusion model. The finite point technique, commonly known as the moving least-squares (MLS) mesh-free point collocation approach, was employed by Shirzadi et al. [145] to solve second-order elliptic partial integro-differential equations (PIDEs). Further applications of mesh-free approaches in option pricing problems are provided by Kadalbajoo et al. [82, 83].

Requirements for assessing the cost of an option have also changed recently, with regime-switching drawing a lot of interest. Using regime-switching approaches, one may record stochastic volatility and, therefore, fat tails in a straightforward manner without adhering to the standard lognormality assumption of constant volatility. Some of the empirical biases reported by the traditional lognormal model are explained in further details when a jump component is added to the regime-switching context. Regime-

switching processes have applications in a wide range of fields, including insurance, power markets, natural gas, optimal forestry management, trading methods, stock loan valuation, convertible bond pricing, and interest rate dynamics [8, 25, 35, 41, 66, 85, 164, 183]. Regime-switching models, as opposed to stochastic volatility jump-diffusion models, are more understandable and computationally efficient. Shirzadi et al. [147] employed mesh-free moving least-squares collocation to handle jump-diffusion regime-switching processes in American option pricing. Several approaches have been proposed to handle American options in regime-switching frameworks (e.g., [33, 72, 101, 181]).

Bastani et al. [12] proposed a collocation technique based on RBF strategy for pricing the American option when the underlying asset is put through to the RSJD model. Tour et al. [159] presented a spectral element technique, while Costabile et al. [37] suggested an explicit formula and a multinomial technique. Much study has been conducted on numerical techniques based on radial basis functions (RBFs) to address American option difficulties, including both single-asset and multi-asset scenarios. Kumar et al. [95] introduced the radial basis function approach, Mollapourasl et al. [115], Rad and Parand [130], Tour et al. [160] and Chen et al. [26] employed compact finite difference approach. In their study, Egorova et al. [51] proposed a unique numerical approach that offers enhanced efficiency in pricing the American option inside the regime-switching paradigm. Lee et al. [100] considered the regime-switching jump-diffusion model for pricing real options on the finite horizon. They employed the BDF2 and operator splitting methods to solve the LCPs for value functions and under the RSJD model numerically. A comprehensive literature on the regime-switching framework is available in the references [23, 42, 160, 69, 180, 53].

We investigated the operator splitting strategies such as those in [78] to solve the LCPs in American option pricing under the RSJD model. To address the issue of iterative procedures, we employ the backward difference IMEX technique in conjunction with the OS strategy to assess the valuation of an American option. The OS methods are effectively applied in various financial models [24, 79, 86, 176, 175]. Shirzadi et al. [147] introduced a mesh-free technique using moving least-squares approximation for pricing American options in regime-switching jump-diffusion models with finite activity. The suggested approach is used with the operator splitting method to address the linear complementary issue caused by American option constraints. This technique is considered robust for application due to its ability to separate and solve the differential equation and complementarity conditions independently. However, in addition to their widespread use, these operator-splitting methods lack stability and error analysis capabilities for the jump-diffusion regime-switching model. In order to value American options within an RSJD framework, this research aims to present time-dependent semi-discretization approaches known as IMEX-BDF1-OS and IMEX-BDF2-OS. Additionally, this research aims to show the stability and error estimates associated with these approaches. The proposed temporal semi-discrete methods for the LCP demonstrate stability and convergence. Furthermore, the IMEX-BDF2-OS exhibits an accuracy ranging from 1.5 to 2, whereas the

IMEX-BDF1-OS, which is a wholly discrete approach, demonstrates first-order accuracy asymptotically. The proposed methodologies effectively estimate the value of the option, together with its notable "Greeks" (Delta & Gamma). By compressing the mesh close to the singularity, these techniques effectively handle the singularity of the non-smooth pay-off function.

There is no need to utilize iterations at every time step. At each time step, our method of discretization yields a tridiagonal system that can be efficiently and quickly solved. Due to the lack of correlation between the selection of spatial discretization and temporal discretization, various techniques for spatial discretization, such as finite elements methods, spectral techniques, meshless approaches (for example, RBFs), and others, may be used. Spatial discretization allows for the use of a non-uniform grid.

The subsequent section of this chapter is structured in the following manner. Firstly, we establish the RSJD model, along with providing a concise explanation of the fundamental abbreviations, symbols, and premises that will be used in this study. Additionally, we will elucidate the development of the LCP and its related characteristics. The operator splitting techniques for IMEX-BDF-OS schemes are proposed in Section 4.3. In Section 4.4, we conduct a stability analysis validate their findings. In Section 4.5, the error estimates for the proposed schemes are presented. Section 4.6 presents computational results to confirm the theoretical conclusions.

4.2 Regime-Switching Jump-Diffusion Models

We consider the regime-switching jump-diffusion model as a stochastic process of an underlying asset for option pricing. These models describe the various phases of an economy as well as the consequences of jumps in the underlying asset. A continuous Markov chain process $(\mathcal{X}_\tau)_{\tau\geq 0}$, is defined on a probability space $(\Omega,\mathcal{F},\mathbf{P})$, to take a value in a finite state space $\mathcal{H} = \{\mathfrak{e}^1, \mathfrak{e}^2, \cdots, \mathfrak{e}^Q\}$ with the following property,

$$\mathbf{P}(\mathcal{X}_{\tau+\delta\tau} = \mathfrak{e}^i | \mathcal{X}_\tau = \mathfrak{e}^j) = \begin{cases} q_{ij}\delta\tau + O(\delta\tau) & \text{for} \quad i \neq j, \\ 1 + q_{ij}\delta\tau + O(\delta\tau) & \text{for} \quad i = j, \end{cases} \tag{4.2.1}$$

for a Q-dimensional vector $\mathfrak{e}^j := \mathfrak{e}^i_j$, such that

$$\mathfrak{e}^i_j = \begin{cases} 0 & for \quad i \neq j, \\ 1 & for \quad i = j. \end{cases} \tag{4.2.2}$$

We postulated that the economy switches from one state to another state regulated by the finite state continuous time Markov chain $\mathcal{X}_\tau$ with the state space $\{1, \cdots, Q\}$.

A Markov chain process can be written as $d\mathcal{X}_\tau = d\mathcal{M}_\tau + \mathcal{A}\mathcal{X}_{\tau-}d\tau$, where $\mathcal{A} = [q_{ij}]_{Q\times Q}$ is the generator of the Markov chain $\mathcal{X}_\tau$, and $\mathcal{M}_\tau$ is a martingale.

The entry element q_{ij} satisfies the condition, if $i \neq j$, $q_{ij} \geq 0$ and $q_{jj} = -\sum_{i\neq j} q_{ij}$ for $i = 1, 2, \cdots, Q$.

The volatility σ_τ and risk free interest rate r_τ are given as $\sigma_\tau = \langle \sigma, \mathcal{X}_\tau \rangle$ and $r_\tau = \langle r, \mathcal{X}_\tau \rangle$, where $\sigma := (\sigma^1, \sigma^2, \cdots, \sigma^Q)^T$ and $r := (r^1, r^2, \cdots, r^Q)^T$ are Q dimensional vectors with $\sigma^j \geq 0$ and $r^j \geq 0$ for all $1 \leq j \leq Q$. Here, $(\cdots)^T$ reflects the matrix's transposition, and $\langle \cdot, \cdot \rangle$ specifies the dot product in $\mathbb{R}^Q$.

Suppose the underlying asset S_τ behaves according to RSJD, then

$$\frac{dS_\tau}{S_{\tau-}} = (r_\tau - \lambda_\tau \kappa_\tau)d\tau + \eta_\tau dN_\tau + \sigma_\tau dW_\tau, \tag{4.2.3}$$

where $N_\tau := \langle \mathcal{N}_\tau \ , \ \mathcal{X}_\tau \rangle$ is a Poisson process with $\mathcal{N}_\tau := (N_\tau^1, N_\tau^2, N_\tau^3, \cdots, N_\tau^Q)^T$ and the intensity λ_τ of the Poisson process is defined as $\lambda_\tau := \langle \lambda \ , \ \mathcal{X}_\tau \rangle$ with $\lambda := (\lambda^1, \lambda^2, \lambda^3, \cdots, \lambda^Q)^T$, W_τ is a Wiener process, $\eta_\tau := \langle \eta \ , \ \mathcal{X}_\tau \rangle$ with $\eta := (\eta^1, \eta^2, \eta^3, \cdots, \eta^Q)^T$ is a random variable to generate jump size from $S_{\tau-}$ to S_τ and $\kappa_\tau := \langle \kappa \ , \ \mathcal{X}_\tau \rangle$ with $\kappa := (\kappa^1, \kappa^2, \kappa^3, \cdots, \kappa^Q)^T$ with $\kappa^j = \mathbb{E}[\eta^j]$ for $1 \leq j \leq Q$.

The values of the American option $v(z, \tau, \mathfrak{e}^j)$ under the RSJD model address the following linear complementarity problem (LCP):

$$\begin{cases} \frac{\partial v}{\partial \tau}(z, \tau, \mathfrak{e}^j) - \mathcal{L}v(z, \tau, \mathfrak{e}^j) \geq 0, & (z, \tau, \mathfrak{e}^j) \in \mathbb{R} \times J \times \mathcal{H}, \\ v(z, \tau, \mathfrak{e}^j) - \Phi^j(Ke^z) \geq 0, & (z, \tau, \mathfrak{e}^j) \in \mathbb{R} \times J \times \mathcal{H}, \\ \left(\frac{\partial v}{\partial \tau}(z, \tau, \mathfrak{e}^j) - \mathcal{L}v(z, \tau, \mathfrak{e}^j)\right)\left(v(z, \tau, \mathfrak{e}^j) - \Phi^j(Ke^z)\right) = 0, & (z, \tau, \mathfrak{e}^j) \in \mathbb{R} \times J \times \mathcal{H}, \\ v_0^j(z) = \Phi^j(Ke^z), & x \in \mathbb{R}, \end{cases} \tag{4.2.4}$$

where $J = (0, T]$ and the spatial differential operator can be defined as

$$\begin{aligned} \mathcal{L}v(z, \tau, \mathfrak{e}^j) = & \frac{1}{2}(\sigma^j)^2 \frac{\partial^2 v}{\partial z^2}(z, \tau, \mathfrak{e}^j) + \left(r^j - \frac{(\sigma^j)^2}{2} - \lambda^j \kappa^j\right) \frac{\partial v}{\partial z}(z, \tau, \mathfrak{e}^j) - (r^j + \lambda^j) v(z, \tau, \mathfrak{e}^j) \\ & + \lambda^j \int_{-\infty}^{\infty} v(z, \tau, \mathfrak{e}^j) f(y - z, \mathfrak{e}^j) dy + \langle \mathbf{v_n} \ , \ \mathcal{A}\mathfrak{e}^j \rangle. \end{aligned} \tag{4.2.5}$$

The option value $v(z, \tau, \mathfrak{e}^j)$ at the time of maturity T is termed as the pay-off function. For the American put option, the pay-off function is given by:

$$v_0^j(z) = \max(K - Ke^z, 0) \tag{4.2.6}$$

with a strike price of K, $z = \ln(\frac{S}{K})$, the log asset price with respect to a strike price K and $\mathcal{L} = \mathcal{D} + \mathcal{I} + \mathcal{E}$, such that

$$\mathcal{D}v(z, \tau, \mathfrak{e}^j) = \frac{1}{2}(\sigma^j)^2 \frac{\partial^2 v}{\partial z^2}(z, \tau, \mathfrak{e}^j) + \left(r^j - \frac{(\sigma^j)^2}{2} - \lambda^j \kappa^j\right) \frac{\partial v}{\partial z}(z, \tau, \mathfrak{e}^j) - (r^j + \lambda^j) v(z, \tau, \mathfrak{e}^j), \tag{4.2.7}$$

$$\mathcal{I}v(z, \tau, \mathfrak{e}^j) = \lambda^j \int_{-\infty}^{\infty} v(z, \tau, \mathfrak{e}^j) f(y - z, \mathfrak{e}^j) dy, \tag{4.2.8}$$

$$\mathcal{E}v(z, \tau, \mathfrak{e}^j) = \langle \mathbf{v_n} \ , \ \mathcal{A}\mathfrak{e}^j \rangle, \tag{4.2.9}$$

where $\langle \mathbf{v_n} \ , \ \mathcal{A}\mathfrak{e}^j \rangle = \sum_{i=1}^{Q} v_n^i q_{i,j}$, $\mathbf{v_n}$ is a Q dimensional vector $\mathbf{v_n} = (v_n^1, v_n^2, v_n^3, \cdots, v_n^Q)^T$ with $v^j(z,\tau) = v(z,\tau,\mathfrak{e}^j)$, $1 \leq j \leq Q$ and the function $f(y,\mathfrak{e}^j)$ can be written as:

$$f(y,\mathfrak{e}^j) = \begin{cases} \frac{1}{\sqrt{2\pi}\sigma_J^j} \exp(-\frac{(y-\mu_J^j)^2}{2(\sigma_J^j)^2}), & \text{Merton model,} \\ p^j \eta_1^j e^{-\eta_1^j y}\mathcal{H}(y) + q^j \eta_2^j e^{-\eta_2^j y}\mathcal{H}(-y), & \text{Kou model.} \end{cases}$$

To numerically approximate the integral operator $\mathcal{I}v(z,\tau,\mathfrak{e}^j)$, we first split the integral into two portions on Ω and Ω^c.

The integral operator may now be divided into two parts:

$$\mathcal{I}v(z,\tau,\mathfrak{e}^j) = \lambda^j \int_{\Omega} v(y,\tau,\mathfrak{e}^j) f(y-z,\mathfrak{e}^j)dy + \mathcal{R}(z,\tau,\mathfrak{e}^j). \tag{4.2.10}$$

By using the asymptotic behaviour of the option, the integral over Ω^c is given by

$$\mathcal{R}(z,\tau,\mathfrak{e}^j) := \lambda^j \int_{\Omega^c} (K - Ke^y) f(y-z,\mathfrak{e}^j)dy. \tag{4.2.11}$$

The above expression may be rewritten as follows in the case of the American put option:

$$\mathcal{R}(z,\tau,\mathfrak{e}^j) := \begin{cases} K\mathcal{N}(\frac{z_{min}-z-\mu_J^j}{\sigma_J^j}) - Ke^{z+\mu_J^j+\frac{(\sigma_J^j)^2}{2}}\mathcal{N}(\frac{z_{min}-z-\mu_J^j-(\sigma_J^j)^2}{\sigma_J^j}) & \text{Merton model,} \\ K(1-p^j)e^{\eta_2^j(z_{min}-z)} - K(1-p^j)\frac{\eta_2^j}{\eta_2^j+1}e^{-\eta_2^j z+(\eta_2^j+1)z_{min}} & \text{Kou model,} \end{cases}$$

where $\mathcal{N}(\cdot)$ is the cumulative normal distribution.

For the computational purposes, the problem (4.2.1) needs to be localized on a bounded domain $\Omega := (z^L, z^R)$, with $z^L \in \mathbb{R}$ and $z^R \in \mathbb{R}$ and considered $u(z,\tau,\mathfrak{e}^j)$ as a solution of the following localized problem (4.2.12):

$$\begin{cases} \frac{\partial u^j}{\partial \tau} - \mathcal{L}u^j \ \geq \ 0 \quad (z,\tau,\mathfrak{e}^j) \in \Omega \times J \times \mathcal{H}, \\ u(z,\tau,\mathfrak{e}^j) - \Phi^j(Ke^z) \ \geq \ 0 \quad (z,\tau,\mathfrak{e}^j) \in \Omega \times J \times \mathcal{H}, \\ (\frac{\partial u^j}{\partial \tau} - \mathcal{L}u^j)\left(u(z,\tau,\mathfrak{e}^j) - \Phi^j(Ke^z)\right) = 0 \quad (z,\tau,\mathfrak{e}^j) \in \Omega \times J \times \mathcal{H}, \\ u_0^j(z) = \Phi^j(Ke^z) \qquad z \in \Omega, \end{cases} \tag{4.2.12}$$

with

$$u(z,\tau,\mathfrak{e}^j) = B(z,\tau,\mathfrak{e}^j), \qquad (z,\tau,\mathfrak{e}^j) \in \Omega^c \times \bar{J} \times \mathcal{H},$$

where

$$B(z,\tau,\mathfrak{e}^j) = \begin{cases} \Phi^j(Ke^z) \ : & (z,\tau,\mathfrak{e}^j) \in \partial\Omega \times \bar{J} \times \mathcal{H}, \\ \Phi^j(Ke^z) \ : & (z,\tau,\mathfrak{e}^j) \in \left(\overline{\Omega}^c \cap \overline{\Omega}_{Big}\right) \times \bar{J} \times \mathcal{H}, \ \ \Omega \subseteq \Omega_{Big}, \\ 0 \ : & (z,\tau,\mathfrak{e}^j) \in \overline{\Omega}_{Big}^c \times \bar{J} \times \mathcal{H}, \end{cases}$$

where $\bar{J} = [0,T]$, $\Omega^c = \mathbb{R} \setminus \Omega$, $\partial\Omega$ represents the boundary of Ω and Ω_{Big} denotes a bounded and open connected subset of $\mathbb{R}$ (see, for example, [81]).

The problems (4.2.4) and (4.2.12) are stated to have unique solutions under specific assumptions relating to the coefficients of the spatial operator $\mathcal{L}$. Furthermore, the localization error due to domain truncation falls exponentially with domain size within the interior of the domain (see, for example, [36, 107]).

4.3 Operator Splitting Methods

Ikonen and Toivanen [78] established the operator splitting approach to evaluate the American put option. The basic concept behind the operator splitting approach is the use of an auxiliary variable ψ^j in the formulation where $\psi^j = u^j_\tau - \mathcal{L}u^j$.

Now, we can reformulate LCP (4.2.12) as

$$\begin{cases} \frac{\partial u^j}{\partial \tau} - \mathcal{L}u^j &= \psi^j, \\ (u(z,\tau,\mathfrak{e}^j) - \Phi^j(Ke^z))\psi^j &= 0, \\ u(z,\tau,\mathfrak{e}^j) - \Phi^j(Ke^z) &\geq 0, \\ \psi^j &\geq 0, \end{cases} \tag{4.3.1}$$

in the region $\Omega \times J \times \mathcal{H}$.

Let the system (4.3.1) be initially discretized in time with uniform grid $\tau_n = nk$, $n = 0, 1, 2, \ldots, N$ with uniform temporal mesh length k. Here, $u(z, \tau_n, \mathfrak{e}^j)$ is abbreviated as u^j_n and $N+1$ is the total number of temporal mesh points. In this section, we briefly discuss the IMEX-BDF-OS methods for the temporal discretization of LCP (4.3.1). We use the IMEX operator splitting technique to decompose the discretized equations into explicit and implicit components. This splitting allows handling different parts of the equations separately, explicitly treating some parts while implicitly treating others. Formally, a discounted expectation determined at the optimal stopping time may be used to demonstrate that the systems (4.3.1) have a unique solution [70]. Additionally, the variational inequality can be utilized to comprehend it precisely [52], and in order to account for jumps and systems of equations, [39] provides appropriate definitions of viscosity solutions for regime-switching model.

4.3.1 IMEX-BDF1-OS Method

Let us split the governing equation $u^j_\tau - \mathcal{L}u^j = \psi^j$ on the $(n+1)^{th}$ time level into two discrete equations as

$$\left(\frac{\tilde{u}^j_{n+1} - u^j_n}{k}\right) - \mathcal{D}\tilde{u}^j_{n+1} - \lambda^j \mathcal{I}(u^j_n) - \mathcal{E}u^j_n = \psi^j_n, \tag{4.3.2}$$

$$\left(\frac{u^j_{n+1} - u^j_n}{k}\right) - \mathcal{D}\tilde{u}^j_{n+1} - \lambda^j \mathcal{I}(u^j_n) - \mathcal{E}u^j_n = \psi^j_{n+1}. \tag{4.3.3}$$

Here, the discrete problem for LCP (4.3.1) is to find the pair $(u^j_{n+1}, \psi^j_{n+1})$, that satisfies the discrete equations (4.3.2) and (4.3.3) along with the constraints

$$\begin{cases} u^j_{n+1} &\geq \Phi^j, \\ \psi^j_{n+1} &\geq 0, \\ \psi^j_{n+1}(u^j_{n+1} - \Phi^j) &= 0. \end{cases} \tag{4.3.4}$$

The first step is to compute the intermediate approximation $\tilde{u}^j_{n+1}$ by solving the equations (4.3.2) with known auxiliary term ψ^j_n, under the boundary conditions:

$$\tilde{u}^j_{n+1}(z^L) = K, \qquad \tilde{u}^j_{n+1}(z^R) = 0.$$

Now, the second step of the operator splitting method is to derive a relationship in (4.3.3) between u^j_{n+1} and ψ^j_{n+1}. To do this, we need to rewrite the equation (4.3.3) using equation (4.3.2), together with the constraints in (4.3.4) as a problem to find the pair $(u^j_{n+1}, \psi^j_{n+1})$ such that

$$\begin{cases} \frac{u^j_{n+1}-\tilde{u}^j_{n+1}}{k} &= \psi^j_{n+1} - \psi^j_n, \\ \psi^j_{n+1}(u^j_{n+1} - \Phi^j) &= 0, \end{cases} \tag{4.3.5}$$

with the constraints

$$u^j_{n+1} \geq \Phi^j \quad \text{and} \quad \psi^j_{n+1} \geq 0. \tag{4.3.6}$$

Again, by solving the problems (4.3.5)-(4.3.6), in $(u^j_{n+1}, \psi^j_{n+1})$ plane, we get

$$(u^j_{n+1}, \psi^j_{n+1}) = \begin{cases} (\Phi^j, \psi^j_n + \frac{\Phi^j - \tilde{u}^j_{n+1}}{k}) & \text{if } \tilde{u}^j_{n+1} - k\psi^j_n \leq \Phi^j, \\ (\tilde{u}^j_{n+1} - k\psi^j_n, 0) & \text{otherwise.} \end{cases} \tag{4.3.7}$$

Thus, one can do the second step by solving the discrete equation (4.3.2) with the updated formula (4.3.7). The pair (u^j_0, ψ^j_0) on zeroth time level can be obtained by using the initial condition and assigning value $\psi^j_0 = 0$. As a result, the second step may be completed by solving the discrete equation (4.3.2) using the modified formula (4.3.7). On the zeroth time level, the pair (u^j_0, ψ^j_0) may be achieved by using initial condition and setting value $\psi^j_0 = 0$.

4.3.2 IMEX-BDF2-OS Method

Let us assume that the values $\{u^j_n, \psi^j_n\}$ and $\{u^j_{n-1}, \psi^j_{n-1}\}$ are a priory known at the points τ_n and τ_{n-1}. Now, we perform the two sub-steps at discrete point τ_{n+1}. In the first step, we compute an intermediate value $\tilde{u}^j_{n+1}$ using the following BVP

$$\begin{cases} \frac{1}{k}\left(\frac{3}{2}\tilde{u}^j_{n+1} - 2u^j_n + \frac{1}{2}u^j_{n-1}\right) - \mathcal{D}\tilde{u}^j_{n+1} - \lambda\mathcal{I}(\mathbf{E}u^j_n) - \mathcal{E}(\mathbf{E}u^j_n) &= \psi^j_n, \\ \tilde{u}^j_{n+1}(z^L) = K, \qquad \tilde{u}^j_{n+1}(z^R) = 0, \end{cases} \tag{4.3.8}$$

where $\mathbf{E}u^j_n = 2u^j_n - u^j_{n-1}$. Now, the operator splitting method's second step is to project the $\tilde{u}^j_{n+1}$ on constraint space to obtain u^j_{n+1} with the following correction terms

$$\begin{cases} \frac{3}{2}\frac{u^j_{n+1}-\tilde{u}^j_{n+1}}{k} &= \psi^j_{n+1} - \psi^j_n, \\ u^j_{n+1} &\geq \Phi^j, \\ \psi^j_{n+1} &\geq 0, \\ \psi^j_{n+1}(u^j_{n+1} - \Phi^j) &= 0. \end{cases} \tag{4.3.9}$$

By solving the problems (4.3.9) in $(u^j_{n+1}, \psi^j_{n+1})$ plane, we get

$$(u^j_{n+1}, \psi^j_{n+1}) = \begin{cases} (\Phi^j, \psi^j_n + \frac{3}{2}\frac{\Phi^j - \tilde{u}^j_{n+1}}{k}) & \text{if } \tilde{u}^j_{n+1} - \frac{2k}{3}\psi^j_n \leq \Phi^j, \\ (\tilde{u}^j_{n+1} - \frac{2k}{3}\psi^j_n, 0) & \text{otherwise.} \end{cases} \tag{4.3.10}$$

Thus, the first step may be completed by solving the discrete equation (4.3.8), and the second step can be performed by using the updating formula (4.3.10). The implicit approach with the three-time levels requires the values from the previous two-time levels, as described above. Using the initial condition and assigning the value $\psi^j_0 = 0$, the pair (u^j_0, ψ^j_0) on the zeroth time level can be obtained. Alternatively, the algorithm described in [97] can be used. We utilize the IMEX-BDF1-OS approach to determine the pair (u^j_1, ψ^j_1) at the first level. In both the proposed discretization, we represent the American option price as a solution for the collection of coupled linear complementarity problems (LCPs) under the regime switching jump diffusion model. We discretize these LCPs and use an explicit approach for the regime coupling terms and the American restrictions. The implicit treatment provides a more detailed representation of regime shifts but typically increases the complexity of the pricing formula. While treating the regime-switching term explicitly in the pricing of American options under the RSJD model can simplify the pricing methodology, but it may come at the cost of accuracy and a less precise representation of the regime-switching behavior.

4.4 Stability Analysis

For theoretical convenience, let us transform the problem (4.3.1) into a problem with homogeneous boundary condition, i.e.

$$\begin{cases} \frac{\partial w}{\partial \tau}(z,\tau,\mathfrak{e}^j) - \mathcal{L}w(z,\tau,\mathfrak{e}^j) &= \psi^j + f^j, & (z,\tau,\mathfrak{e}^j) \in \Omega \times J \times \mathcal{H}, \\ \Big(w(z,\tau,\mathfrak{e}^j) - w^j_0(z)\Big)\psi^j &= 0, & (z,\tau,\mathfrak{e}^j) \in \Omega \times J \times \mathcal{H}, \\ w(z,\tau,\mathfrak{e}^j) - w^j_0(z) &\geq 0, & (z,\tau,\mathfrak{e}^j) \in \Omega \times J \times \mathcal{H}, \\ \psi^j &\geq 0, & (z,\tau,\mathfrak{e}^j) \in \Omega \times J \times \mathcal{H}, \\ w(z,0,\mathfrak{e}^j) &= w^j_0(z), & z \in \Omega, \\ w(z,\tau,\mathfrak{e}^j) &= 0, & (z,\tau,\mathfrak{e}^j) \in \partial\Omega \times \bar{J} \times \mathcal{H}, \end{cases} \tag{4.4.1}$$

where $w^j_0(z) := \Phi^j(Ke^z) - \phi^j(z)$, $w(z,\tau,\mathfrak{e}^j) = u(z,\tau,\mathfrak{e}^j) - \phi^j(z)$, $f^j = \mathcal{L}\phi^j$, $z \in \mathbb{R}$, and

$$\phi(z,\mathfrak{e}_j) = \begin{cases} \frac{z^R - z}{z^R - z^L}\Phi^j(Ke^{z^L}) + \frac{z - z^L}{z^R - z^L}\Phi^j(Ke^{z^R}) & : \quad (z,\mathfrak{e}_j) \in \overline{\Omega} \times \mathcal{H}, \\ \Phi^j(Ke^z) & : \quad (z,\mathfrak{e}_j) \in \overline{\Omega}^c \cap \overline{\Omega}_{Big} \times \mathcal{H}, \\ 0 & : \quad (z,\mathfrak{e}_j) \in \overline{\Omega}^c_{Big} \times \mathcal{H}. \end{cases}$$

Lemma 4.4.1. ***Discrete Gronwall Lemma:*** *Suppose that α_n is a non negative sequence, and that the sequence β_n satisfies*

$$\begin{cases} \beta_0 \leq \delta_0, \\ \beta_n \leq \delta_0 + \sum_{k=0}^{n-1} \gamma_k + \sum_{k=0}^{n-1} \alpha_k \beta_k \quad n \geq 1, \end{cases}$$

then β_n *satisfies*

$$\begin{cases} \beta_1 \leq \delta_0(1+\alpha_0)+\gamma_0, \\ \beta_n \leq \delta_0 \prod_{k=0}^{n-1}(1+\alpha_k) + \sum_{k=0}^{n-2}\gamma_k \prod_{s=k+1}^{n-1}(1+\alpha_s)+\gamma_{n-1} \quad n \geq 2. \end{cases}$$

Moreover, if $\delta_0 \geq 0$ *and* $\gamma_n \geq 0$ *for* $n \geq 0$*, it follows that*

$$\beta_n \leq \left(\delta_0 + \sum_{k=0}^{n-1}\gamma_k\right)\exp(\sum_{k=0}^{n-1}\alpha_k),\ n \geq 1.$$

Proof. One can see more details about this Lemma in [129]. □

4.4.1 Identities and Inequalities

We will frequently use the following identities and inequalities in this section.

$$\left(\mathcal{D}w^j, w^j\right) \leq \alpha^j \|w^j\|^2, \tag{I1}$$

$$(a,b) \leq \epsilon a^2 + \frac{1}{4\epsilon}b^2, \quad \forall a,b \in \mathbb{R} \text{ and } \forall\ \epsilon > 0, \tag{I2}$$

$$2\,(a-b,a) = a^2 - b^2 + (a-b)^2, \tag{I3}$$

$$2\,(3a-4b+c,a) = a^2 + (2a-b)^2 - b^2 - (2b-c)^2 + (a-2b+c)^2, \tag{I4}$$

where $\alpha^j = |\frac{(r^j - \frac{(\sigma^j)^2}{2} - \lambda^j\kappa^j)^2 - \left(2(r^j+\lambda^j)(\sigma^j)^2\right)}{2(\sigma^j)^2}|$ and one can also see [83] for (I1).

In the subsequent analyses, we use the following result: for all $w(\cdot,\tau,\mathfrak{e}^j) \in L^2(\Omega)$, $\tau \in (0,T)$,

$$\overline{w}(z,\tau,\mathfrak{e}^j) = \begin{cases} w(z,\tau,\mathfrak{e}^j) & : \quad (z,\tau,\mathfrak{e}^j) \in \Omega \times [0,T] \times \mathcal{H}, \\ 0 & : \quad (z,\tau,\mathfrak{e}^j) \in \Omega^c \times [0,T] \times \mathcal{H}. \end{cases}$$

The integral operator $\mathcal{I}(w)$ follow the condition $\|\mathcal{I}\overline{w}(\cdot,\tau,\mathfrak{e}^j)\| \leq \mathcal{C}_I\|w(\cdot,\tau,\mathfrak{e}^j)\|$, where $\mathcal{C}_I$ is a constant that is independent to τ and $\|u\| := (\int_\Omega |u(z)|^2 dz)^{\frac{1}{2}}$. We bound the regime-switching term $\langle \mathbf{w_n}\ ,\ \mathcal{A}\mathfrak{e}^j\rangle$ by the inequality

$$|\langle \mathbf{w_n}\ ,\ \mathcal{A}\mathfrak{e}^j\rangle| = \left|\sum_{i=1}^{Q} w_n^i q_{i,j}\right| \leq \sum_{i=1}^{Q} \max_{i=1,2,\ldots,Q}|w_n^i||q_{i,j}|.$$

Let $w_n^{i_n} := \max\limits_{i=1,2,\ldots,Q}|w_n^i|$, then

$$|\langle \mathbf{w_n}\ ,\ \mathcal{A}\mathfrak{e}^j\rangle| \leq \left||w_n^{i_n}|\sum_{i=1}^{Q} q_{i,j}\right| = 2|q_{j,j}||w_n^{i_n}|.$$

Throughout the analysis, C signifies a generic constant that is independent of the time step size, k, but may be affected by the data and the regularity of the analytical solution and may not be the same at each occurrence.

4.4.2 Stability Analysis for IMEX-BDF1-OS

Theorem 4.4.2. *If the uniform temporal step size* $k < \frac{1}{2(4\alpha^j+1+4|q_{j,j}|+\lambda^j\mathcal{C}_I)}$*, then the scheme* (4.3.2) *and* (4.3.5) *is stable for all* $1 \le m \le \frac{T}{k}$ *in the following sense:*

$$\begin{aligned} \|w_m^j\|^2 \quad + \quad & \frac{1}{2}\sum_{n=0}^{m-1}\|\tilde{w}_{n+1}^j - w_n^j\|^2 + k^2\|\psi_m^j\|^2 \\ & \le C\left(\max_{1\le i\le Q}\|w_0^i\|^2 + \max_{1\le i\le Q}\|\psi_0^i\|^2 + \sum_{n=0}^{m-1}\|f^j\|^2 + \sum_{n=0}^{m-1}\|\psi_n^j\|^2\right). \end{aligned} \tag{4.4.2}$$

Proof. By equation (4.3.2), we can write

$$\frac{\tilde{w}_{n+1}^j - w_n^j}{k} = \mathcal{D}\tilde{w}_{n+1}^j + \lambda^j\mathcal{I}(w_n^j) + \mathcal{E}w_n^j + f^j + \psi_n^j \tag{4.4.3}$$

After taking the inner product of both sides of (4.4.3) with $4k\tilde{w}_{n+1}^j$ and using the identities (I3) and (I1), we have

$$\begin{aligned} 2\|\tilde{w}_{n+1}^j\|^2 - 2\|w_n^j\|^2 \quad + \quad & 2\|\tilde{w}_{n+1}^j - w_n^j\|^2 \\ \le \quad & 4k\alpha^j\|\tilde{w}_{n+1}^j\|^2 + 4k\lambda^j(\mathcal{I}(w_n^j), \tilde{w}_{n+1}^j) + 4k(\mathcal{E}w_n^j, \tilde{w}_{n+1}^j) \\ & + 4k(f^j, \tilde{w}_{n+1}^j) + 4k(\psi_n^j, \tilde{w}_{n+1}^j). \end{aligned} \tag{4.4.4}$$

Consider the equation (4.3.5), we have

$$w_{n+1}^j - w_0^j - k\psi_{n+1}^j = \tilde{w}_{n+1}^j - w_0^j - k\psi_n^j. \tag{4.4.5}$$

Taking the inner product of both sides of (4.4.5) with itself and using some inequalities from subsection (3.4.1), we get

$$\begin{aligned} \|w_{n+1}^j\|^2 \quad + \quad & \|w_0^j\|^2 - \frac{1}{2}\|w_{n+1}^j\|^2 - 2\|w_0^j\|^2 + k^2\|\psi_{n+1}^j\|^2 - 2k(w_{n+1}^j - w_0^j, \psi_{n+1}^j) \\ & \le 2\|\tilde{w}_{n+1}^j\|^2 + 2\|w_0^j\|^2 + k^2\|\psi_n^j\|^2 - 2k(\tilde{w}_{n+1}^j, \psi_n^j) + 2k(w_0^j, \psi_n^j). \end{aligned} \tag{4.4.6}$$

Now, adding up the inequalities (4.4.4) and (4.4.6) and using $(w_{n+1}^j - w_0^j, \psi_{n+1}^j) = 0$, we get

$$\begin{aligned} \frac{1}{2}\|w_{n+1}^j\|^2 \quad - \quad & 2\|w_n^j\|^2 + 2\|\tilde{w}_{n+1}^j - w_n^j\|^2 + k^2(\|\psi_{n+1}^j\|^2 - \|\psi_n^j\|^2) \\ \le \quad & 3\|w_0^j\|^2 + 4k\alpha^j\|\tilde{w}_{n+1}^j\|^2 + 4k\lambda^j(\mathcal{I}(w_n^j), \tilde{w}_{n+1}^j) + 4k(\mathcal{E}w_n^j, \tilde{w}_{n+1}^j) \\ & + 4k(f^j, \tilde{w}_{n+1}^j) + 2k(\tilde{w}_{n+1}^j, \psi_n^j) + 2k(w_0^j, \psi_n^j). \end{aligned}$$

After minor calculations, we obtain

$$\begin{aligned} & \frac{1}{2}\|w_{n+1}^j\|^2 - \frac{1}{2}\|w_n^j\|^2 + \frac{3}{2}\|\tilde{w}_{n+1}^j - w_n^j\|^2 + k^2(\|\psi_{n+1}^j\|^2 - \|\psi_n^j\|^2) \\ & \le 2k(4\alpha^j + 1 + 4|q_{j,j}| + \lambda^j\mathcal{C}_I)\|\tilde{w}_{n+1}^j - w_n^j\|^2 + 4k|q_{j,j}|\|w_n^{i_n}\|^2 + 3\|w_0^j\|^2 + 8k\|f^j\|^2 \end{aligned}$$

$$+(2k(4\alpha^j+1+4|q_{j,j}|+\lambda^j\mathcal{C}_I)+4k\lambda^j\mathcal{C}_I+\frac{3}{2})\|w_n^j\|^2+2k\|\psi_n^j\|^2+k\|w_0^j\|^2+k\|\psi_n^j\|^2.$$

Assuming that $k<\frac{1}{2(4\alpha^j+1+4|q_{j,j}|+\lambda^j\mathcal{C}_I)}$, we get

$$\begin{aligned}&\frac{1}{2}\|w_{n+1}^j\|^2-\frac{1}{2}\|w_n^j\|^2+\frac{1}{2}\|\tilde{w}_{n+1}^j-w_n^j\|^2+k^2(\|\psi_{n+1}^j\|^2-\|\psi_n^j\|^2)\\&\leq 3\|w_0^j\|^2+(2k(4\alpha^j+1+4|q_{j,j}|+\lambda^j\mathcal{C}_I)+4k\lambda^j\mathcal{C}_I+\frac{3}{2})\|w_n^j\|^2+4k|q_{j,j}|\|w_n^{i_n}\|^2\\&+8k\|f^j\|^2+2k\|\psi_n^j\|^2+k\|w_0^j\|^2+k\|\psi_n^j\|^2.\end{aligned}$$

If we consider $w_n^{i_n}:=\max_{i=1,2,...,Q}|w_n^i|\neq w_n^j$, then $|w_0^j|<|w_0^i|$ and $w_n^i=\max\{w_1^{i_1},w_2^{i_2},w_3^{i_3},...,w_n^{i_n}\}$. Consequently, we obtain

$$\begin{aligned}\frac{1}{2}\|w_{n+1}^j\|^2-\frac{1}{2}\|w_n^j\|^2 \quad+\quad &\frac{1}{2}\|\tilde{w}_{n+1}^j-w_n^j\|^2+k^2(\|\psi_{n+1}^j\|^2-\|\psi_n^j\|^2)\\&\leq 3\|w_0^j\|^2+(2k(4\alpha^j+1+8k|q_{j,j}|+\lambda^j\mathcal{C}_I)+4k\lambda^j\mathcal{C}_I+\frac{3}{2})\|w_n^i\|^2\\&+8k\|f^j\|^2+2k\|\psi_n^j\|^2+k\|w_0^j\|^2+k\|\psi_n^j\|^2. \qquad (4.4.7)\end{aligned}$$

Taking the summation on both sides of the inequality (4.4.7) from $n=0$ to $m-1$, for $1\leq m\leq N$, and performing some calculations, we obtain

$$\begin{aligned}\|w_m^j\|^2 \quad+\quad &\sum_{n=0}^{m-1}\|\tilde{w}_{n+1}^j-w_n^j\|^2+2k^2\|\psi_m^j\|^2\\\leq\quad &\|w_0^j\|^2+2k^2\|\psi_0^j\|^2+\big(4k(4\alpha^j+1+8k|q_{j,j}|+\lambda^j\mathcal{C}_I)+8k\lambda^j\mathcal{C}_I+3\big)\sum_{n=0}^{m-1}||w_n^i||^2\\&+(6+2k)\sum_{n=0}^{m-1}||w_0^j||^2+16k\sum_{n=0}^{m-1}\|f^j\|^2+6k\sum_{n=0}^{m-1}\|\psi_n^j\|^2.\end{aligned}$$

After simplification, the above inequality leads to

$$\begin{aligned}\|w_m^j\|^2 \quad+\quad &\sum_{n=0}^{m-1}\|\tilde{w}_{n+1}^j-w_n^j\|^2+2k^2\|\psi_m^j\|^2\\&\leq C\left(\|w_0^j\|^2+\|\psi_0^j\|^2+\sum_{n=0}^{m-1}\|f^j\|^2+c_k\sum_{n=0}^{m-1}||w_n^i||^2+\sum_{n=0}^{m-1}\|\psi_n^j\|^2\right),\end{aligned}$$

where $c_k=(4k(4\alpha^j+1+8k|q_{j,j}|+\lambda^j\mathcal{C}_I)+8k\lambda^j\mathcal{C}_I+3)$.

Applying the discrete Gronwall's Lemma 4.4.1, and simplifying the equation, we obtain the desired result 4.4.2. □

4.4.3 Stability Analysis for IMEX-BDF2-OS

Theorem 4.4.3. *If the uniform temporal step size* $k<\frac{1}{2(4\alpha^j+1+2|q_{j,j}|+\lambda^j\mathcal{C}_I)}$, *then the scheme* (4.3.8) *and* (4.3.9) *is stable for all* $2\leq m\leq\frac{T}{k}$ *in the following sense:*

$$\|w_m^j\|^2+\|w_{m-1}^j\|^2 \quad+\quad \frac{1}{2}\sum_{n=1}^{m-1}\|\tilde{w}_{n+1}^j\|^2+\frac{8}{9}k^2\|\psi_m^j\|^2$$

$$\leq C\left(\max_{1\leq i\leq Q}\|w_0^i\|^2+\max_{1\leq i\leq Q}\|w_1^i\|^2+\sum_{n=1}^{m-1}\|f^j\|^2+\sum_{n=1}^{m-1}\|\psi_n^j)\|^2\right). \quad (4.4.8)$$

Proof. Using the equation (4.3.8), we can write

$$\frac{3\tilde{w}_{n+1}^j-4w_n^j+w_{n-1}^j}{2k}=\mathcal{D}\tilde{w}_{n+1}^j+\lambda^j\mathcal{I}(\mathbf{E}w_n^j)+\mathcal{E}(\mathbf{E}w_n^j)+f^j+\psi_n^j. \quad (4.4.9)$$

Taking the inner product of both sides of the equation (4.4.9) with $4k\tilde{w^j}_{n+1}$ and using the identity (I4) and (I1), we have

$$\begin{aligned}
&\|\tilde{w}_{n+1}^j\|^2-\|w_n^j\|^2+\|2\tilde{w}_{n+1}^j-w_n^j\|^2-\|2w_n^j-w_{n-1}^j\|^2+\|\tilde{w}_{n+1}^j-2w_n^j+w_{n-1}^j\|^2\\
=\;&4k(\mathcal{D}\tilde{w}_{n+1}^j,\tilde{w}_{n+1}^j)+4k\lambda^j(\mathcal{I}(\mathbf{E}w_n^j),\tilde{w}_{n+1}^j)+4k(\mathcal{E}(\mathbf{E}w_n^j),\tilde{w}_{n+1})+4k(f^j,\tilde{w}_{n+1}^j)+4k(\psi_n^j,\tilde{w}_{n+1}^j)\\
\leq\;&4k\alpha^j\|\tilde{w}_{n+1}^j\|^2+4k\lambda^j(\mathcal{I}(\mathbf{E}w_n^j),\tilde{w}_{n+1}^j)+4k(\mathcal{E}(\mathbf{E}w_n^j),\tilde{w}_{n+1}^j)\\
&+4k(f^j,\tilde{w}_{n+1}^j)+4k(\psi_n^j,\tilde{w}_{n+1}^j). \quad (4.4.10)
\end{aligned}$$

Now, from equation (4.3.9), we have

$$w_{n+1}^j-w_0^j-\frac{2}{3}k\psi_{n+1}=\tilde{w}_{n+1}^j-w_0^j-\frac{2}{3}k\psi_n^j. \quad (4.4.11)$$

Taking inner product of (4.4.11) from both sides with itself, we get

$$\|w_{n+1}^j-w_0^j\|^2+\frac{4}{9}k^2\|\psi_{n+1}^j\|^2-\frac{4}{3}k(w_{n+1}^j-w_0^j,\psi_{n+1}^j)=\|\tilde{w}_{n+1}^j-w_0^j\|^2+\frac{4}{9}k^2\|\psi_n^j\|^2-\frac{4}{3}k(\tilde{w}_{n+1}^j-w_0^j,\psi_n^j).$$

Using some inequalities from subsection (3.4.1) and some calculations, we have

$$\begin{aligned}
\|w_{n+1}^j\|^2\quad+\quad&\|w_0^j\|^2-\frac{1}{2}\|w_{n+1}^j\|^2-2\|w_0^j\|^2+\frac{4}{9}k^2\|\psi_{n+1}^j\|^2-\frac{4}{3}k(w_{n+1}^j-w_0^j,\psi_{n+1}^j)\\
&\leq 2\|\tilde{w}_{n+1}^j\|^2+2\|w_0^j\|^2+\frac{4}{9}k^2\|\psi_n^j\|^2-\frac{4}{3}k(\tilde{w}_{n+1}^j,\psi_n^j)+\frac{4}{3}k(w_0^j,\psi_n^j). \quad (4.4.12)
\end{aligned}$$

Now, multiplying (4.4.10) by 2 followed by adding with (4.4.12) and using $(w_{n+1}^j-w_0^j,\psi_{n+1}^j)=0$, we obtain

$$\begin{aligned}
&\frac{1}{2}\|w_{n+1}^j\|^2-2\|w_n^j\|^2+2\|2\tilde{w}_{n+1}^j-w_n^j\|^2-2\|2w_n^j-w_{n-1}\|^2+2\|\tilde{w}_{n+1}^j-2w_n^j+w_{n-1}^j\|^2\\
&+\frac{4}{9}k^2\|\psi_{n+1}^j\|^2\\
&\leq 8k\alpha^j\|\tilde{w}_{n+1}^j\|^2+8k\lambda^j(\mathcal{I}(\mathbf{E}w_n^j),\tilde{w}_{n+1}^j)+8k(\mathcal{E}(\mathbf{E}w_n^j),\tilde{w}_{n+1}^j)+8k(f^j,\tilde{w}_{n+1}^j)+3\|w_0^j\|^2\\
&+\frac{4}{9}k^2\|\psi_n^j\|^2+\frac{20}{3}k(\tilde{w}_{n+1}^j,\psi_n^j)+\frac{4}{3}k(w_0^j,\psi_n^j).
\end{aligned}$$

Using the inequalities of subsection (3.4.1), we get

$$\begin{aligned}
&\|w_{n+1}^j\|^2-\|w_n^j\|^2+3\|\tilde{w}_{n+1}^j\|^2+8\left(\|w_n^j\|^2-\|w_{n-1}^j\|^2\right)+\frac{8}{9}k^2\left(\|\psi_{n+1}^j\|^2-\|\psi_n^j\|^2\right)\\
&\leq\frac{571}{13}\|w_n\|^2+32k\lambda^j\mathcal{C}_I\|w_n^j\|^2+8k\lambda^j\mathcal{C}_I\|w_{n-1}^j\|^2+4k(4\alpha^j+1+2|q_{j,j}|+\lambda^j\mathcal{C}_I)\|\tilde{w}_{n+1}^j\|^2
\end{aligned}$$

$$+64k|q_{j,j}|\|w_n^{i_n}\|^2+16k|q_{j,j}|\|w_{n-1}^{i_n}\|^2+32k\|f^j\|^2+\frac{212}{9}k\|\psi_n^j\|^2+\frac{(4k+18)}{3}\|w_0^j\|^2. \tag{4.4.13}$$

Assuming $k<\frac{1}{2(4\alpha+1+2|q_{j,j}|+\lambda\mathcal{C}_I)}$, from (4.4.13), we have

$$\begin{aligned}&\|w_{n+1}^j\|^2-\|w_n^j\|^2+\|\tilde{w}_{n+1}^j\|^2+8\left(\|w_n^j\|^2-\|w_{n-1}^j\|^2\right)+\frac{8}{9}k^2\left(\|\psi_{n+1}^j\|^2-\|\psi_n^j\|^2\right)\\&\leq\frac{571}{13}\|w_n^j\|^2+32k\lambda\mathcal{C}_I\|w_n^j\|^2+8k\lambda^j\mathcal{C}_I\|w_{n-1}^j\|^2+32k\|f^j\|^2+64k|q_{j,j}|\|w_n^{i_n}\|^2\\&+16k|q_{j,j}|\|w_{n-1}^{i_n}\|^2+\frac{212}{9}k\|\psi_n^j\|^2+\frac{(4k+18)}{3}\|w_0^j\|^2.\end{aligned} \tag{4.4.14}$$

Let $w_n^{i_n}:=\max_{i=1,2,...,Q}|w_n^i|\neq w_n^j$, then $|w_0^j|<|w_0^i|$, $|w_1^j|<|w_1^i|$ and $w_n^i=\max\{w_1^{i_1},w_2^{i_2},w_3^{i_3},...,w_n^{i_n}\}$. Thus, we obtain

$$\begin{aligned}&\|w_{n+1}^j\|^2-\|w_n^j\|^2+\|\tilde{w}_{n+1}^j\|^2+8\left(\|w_n^j\|^2-\|w_{n-1}^j\|^2\right)+\frac{8}{9}k^2\left(\|\psi_{n+1}^j\|^2-\|\psi_n^j\|^2\right)\\&\leq\left(\frac{571}{13}+32k\lambda^j\mathcal{C}_I+64k|q_{j,j}|\right)\|w_n^{i_n}\|^2+\left(8k\lambda^j\mathcal{C}_I+16k|q_{j,j}|\right)\|w_{n-1}^{i_n}\|^2+32k\|f^j\|^2\\&+\frac{212}{9}k\|\psi_n^j\|^2+\frac{(4k+18)}{3}\|w_0^j\|^2.\end{aligned} \tag{4.4.15}$$

Adding up the inequality (4.4.15) from $n=1$ to $m-1$, for $2\leq m\leq N$, we get

$$\begin{aligned}\|w_m^j\|^2 \quad+\quad&\sum_{n=1}^{m-1}\|\tilde{w}_{n+1}^j\|^2+8\|w_{m-1}^j\|^2+\frac{8}{9}k^2\|\psi_m^j\|^2\\\leq\quad&8\|w_0^j\|^2+\|w_1^j\|^2+\frac{8}{9}k^2\|\psi_1^j\|^2+\left(\frac{571}{13}+40k\lambda^j\mathcal{C}_I+80k|q_{j,j}|\right)\sum_{n=0}^{m-1}\|w_n^{i_n}\|^2\\&+32k\sum_{n=1}^{m-1}\|f^j\|^2+\left(\frac{4k+18}{3}\right)\sum_{n=1}^{m-1}\|w_0^j\|^2+\frac{212k}{9}\sum_{n=1}^{m-1}\|\psi_n^j)\|^2.\end{aligned}$$

$$\begin{aligned}\|w_m^j\|^2 \quad+\quad&\sum_{n=1}^{m-1}\|\tilde{w}_{n+1}^j\|^2+8\|w_{m-1}^j\|^2+\frac{8}{9}k^2\|\psi_m^j\|^2\\\leq\quad&C(\|w_0^j\|^2+\|w_1^j\|^2+c_k\sum_{n=0}^{m-1}\|w_n^{i_n}\|^2+\sum_{n=1}^{m-1}\|f^j\|^2+\sum_{n=1}^{m-1}\|\psi_n^j)\|^2),\end{aligned} \tag{4.4.16}$$

where $c_k=\frac{571}{13}+40k\lambda^j\mathcal{C}_I+80k|q_{j,j}|$.

Applying the discrete Gronwall's Lemma 4.4.1 on (4.4.16) and simplifying the expression, we obtain the desired result (4.4.8). □

Regarding the viscosity solution of governing option pricing problem, Briani et al. [19] provided an explicit finite difference approach, while Cont et al. [36] suggested an implicit explicit finite difference method for the approximation of viscosity solutions. However, this is not the main focus of this work. We are primarily interested in efficiently solving the discretized system of LCPs and giving a priori stability and error analysis for IMEX-BDF-OS methods.

4.5 Error Analysis

In the previous section, we establish the stability results, and now we discuss the associated error estimates by assuming the exact solution is sufficiently regular. We establish the error estimates for the IMEX-BDF-OS approaches. First, we shall describe the error function and error equation. We have denoted the analytic solution at t_n by $w^j(\cdot, t_n)$ in j^{th} regime and similar for other related variables.

4.5.1 Error Analysis for BDF1-OS

We define $e_n^j = w^j(t_n) - w_n^j$, $\tilde{e}_n^j = w^j(t_n) - \tilde{w}_n^j$, $h_n^j = \psi^j(t_n) - \psi_n^j$ and $\psi^j(t_{n+1}) - \psi^j(t_n) \leq ck$, where c is a generic constant and independent of n.

From the continuous system (4.3.1), we have

$$\frac{w^j(t_{n+1}) - w^j(t_n)}{k} = \mathcal{D}w^j(t_{n+1}) + \lambda^j \mathcal{I}(w^j(t_n)) + \mathcal{E}w^j(t_n) + f^j + \psi^j(t_{n+1}) + R_{n+1}^j, \tag{4.5.1}$$

where R_{n+1} is truncation error for given method.

Now, considering the equation for BDF1-OS,

$$\frac{\tilde{w}_{n+1}^j - w_n^j}{k} = \mathcal{D}(\tilde{w}_{n+1}^j) + \lambda^j \mathcal{I}(w_n^j) + \mathcal{E}w_n^j + \psi_n^j + f^j. \tag{4.5.2}$$

To obtain the error equation, we subtract (4.5.2) from (4.5.1) and get

$$\frac{\tilde{e}_{n+1}^j - e_n^j}{k} = \mathcal{D}(\tilde{e}_{n+1}^j) + \lambda^j \mathcal{I}(e_n^j) + \mathcal{E}e_n^j + g_n^j + R_{n+1}^j, \tag{4.5.3}$$

where $g_n^j = \psi^j(t_{n+1}) - \psi_n^j$.

We can obtain another error equation from (4.3.5), as follows:

$$\frac{e_{n+1}^j - \tilde{e}_{n+1}^j}{k} = h_{n+1}^j - g_n^j + \psi^j(t_{n+1}) - \psi^j(t_n), \tag{4.5.4}$$

or

$$\frac{e_{n+1}^j - \tilde{e}_{n+1}^j}{k} = h_{n+1}^j - g_n^j, \tag{4.5.5}$$

where $g_n^j = h_n^j + \psi^j(., t_{n+1}) - \psi^j(., t_n)$. Let ψ^j is adequately smooth such that $\|g_n^j\| \leq \|h_n^j\| + ck$.

Theorem 4.5.1. *Under the assumption* $k < \frac{1}{2(4\alpha^j + 1 + 4|q_{j,j}| + \lambda^j \mathcal{C}_I)}$ *and that the solution* (w, ψ) *is sufficiently smooth, we have following error estimates for the method* (4.3.2) *and* (4.3.5)*:*

$$\|e_m^j\|^2 + \frac{1}{2}\sum_{n=0}^{m-1} \|\tilde{e}_{n+1}^j\|^2 \leq Ck^2, \quad \forall 1 \leq m \leq \frac{T}{k}. \tag{4.5.6}$$

Proof. Considering the equation (4.5.3), we have

$$\frac{\tilde{e}_{n+1}^j - e_n^j}{k} = \mathcal{D}(\tilde{e}_{n+1}^j) + \lambda^j \mathcal{I}(e_n^j) + \mathcal{E}e_n^j + g_n^j + R_{n+1}^j. \tag{4.5.7}$$

Taking the inner product from both sides of (4.5.7) with $2k(\tilde{e}_{n+1})$ and using the identities (I1) and (I3), we have

$$\begin{aligned}\|\tilde{e}^j_{n+1}\|^2 - \|e^j_n\|^2 &+ \|\tilde{e}^j_{n+1} - e^j_n\|^2 \\ &\leq 2k\alpha\|\tilde{e}^j_{n+1}\|^2 + 2k\lambda^j\mathcal{C}_I\|e^j_n\|\|\tilde{e}^j_{n+1}\| + 2k(\mathcal{E}e^j_n, \tilde{e}^j_{n+1}) \\ &\quad +2k(g^j_n, \tilde{e}^j_{n+1}) + 2k(R^j_{n+1}, \tilde{e}^j_{n+1}). \end{aligned} \tag{4.5.8}$$

Adding to this, (4.5.5) yields

$$e^j_{n+1} - kh^j_{n+1} = \tilde{e}^j_{n+1} - kg^j_n. \tag{4.5.9}$$

Taking inner product of (4.5.9) from both sides with itself :

$$\|e^j_{n+1}\|^2 + k^2\|h^j_{n+1}\|^2 - 2k(e^j_{n+1}, h^j_{n+1}) = \|\tilde{e}^j_{n+1}\|^2 + k^2\|f^j_n\|^2 - 2k(\tilde{e}^j_{n+1}, g^j_n). \tag{4.5.10}$$

Now, adding up (4.5.8) with (4.5.10) and considering that $2k(e^j_{n+1}, h^j_{n+1}) \leq 0$ with the use of inequalities from subsection (3.4.1), we have

$$\begin{aligned}\|e^j_{n+1}\|^2 - \|e^j_n\|^2 &+ \|\tilde{e}^j_{n+1} - e^j_n\|^2 + k^2(\|h^j_{n+1}\|^2 - \|g^j_n\|^2) \\ &\leq k(4\alpha^j + 1 + 4|q_{j,j}| + \lambda^j\mathcal{C}_I)\|\tilde{e}^j_{n+1} - e_n\|^2 + 2k|q_{j,j}|\|e^{i_n}_n\|^2 \\ &\quad +k(4\alpha^j + 3\lambda^j\mathcal{C}_I + 4|q_{j,j}| + 1)\|e^j_n\|^2 + 4k\|R^j_{n+1}\|^2. \end{aligned} \tag{4.5.11}$$

Assuming that $k < \frac{1}{2(4\alpha^j+1+4|q_{j,j}|+\lambda^j\mathcal{C}_I)}$, we have

$$\begin{aligned}\|e^j_{n+1}\|^2 - \|e^j_n\|^2 &+ \frac{1}{2}\|\tilde{e}^j_{n+1} - e^j_n\|^2 + k^2(\|h^j_{n+1}\|^2 - \|g^j_n\|^2) \\ &\leq k(4\alpha^j + 3\lambda^j\mathcal{C}_I + 4|q_{j,j}| + 1)\|e^j_n\|^2 + 2k|q_{j,j}|\|e^{i_n}_n\|^2 + 4k\|R^j_{n+1}\|^2. \end{aligned}$$

Let $e^{i_n}_n := \max_{i=1,2,...,Q} |e^i_n| \neq e^j_n$, then $|e^j_0| < |e^i_0|$ and $e^i_n = \max\{e^{i_1}_1, e^{i_2}_2, e^{i_3}_3, ..., e^{i_n}_n\}$. Consequently, we obtain

$$\|e^j_{n+1}\|^2 - \|e^j_n\|^2 + \frac{1}{2}\|\tilde{e}^j_{n+1} - e^j_n\|^2 + k^2(\|h^j_{n+1}\|^2 - \|g^j_n\|^2) \leq k(4\alpha^j + 3\lambda^j\mathcal{C}_I + 6|q_{j,j}| + 1)\|e^i_n\|^2 + 4k\|R^j_{n+1}\|^2.$$

Adding the above inequality from $n = 0$ to $m - 1$ and using the result $\|g^j_n\|^2 \leq 2\|h^j_n\|^2 + 2ck^2$ with some calculations, we have

$$\begin{aligned}&\|e^j_m\|^2 + \frac{1}{2}\sum_{n=0}^{m-1}\|\tilde{e}^j_{n+1} - e^j_n\|^2 + k^2\|h^j_m\|^2 \\ &\leq \|e^j_0\|^2 + \|h^j_0\|^2 + k(4\alpha^j + 3\lambda^j\mathcal{C}_I + 6|q_{j,j}| + 1)\sum_{n=0}^{m-1}\|e^i_n\|^2 + k^2\sum_{n=0}^{m-1}(\|h^j_n\|^2 + ck^2) \\ &+k\sum_{n=0}^{m-1}\|R^j_{n+1}\|^2. \end{aligned}$$

Applying the discrete Gronwall's Lemma 4.4.1 and simplifying the expression, we obtain the desired result 4.5.6. □

4.5.2 Error Analysis for IMEX-BDF2-OS

Similarly, for BDF2-IMEX-OS, the error equations are as follows:

$$\frac{3\tilde{e}^j_{n+1} - 4e^j_n + e^j_{n-1}}{2k} = D(\tilde{e}^j_{n+1}) + \lambda^j \mathcal{I}(\mathbf{E}e^j_n) + \mathcal{E}(\mathbf{E}e^j_n) + g^j_n + R^j_{n+1} \tag{4.5.12}$$

and

$$\frac{3(e^j_{n+1} - \tilde{e}^j_{n+1})}{2k} = h^j_{n+1} - g^j_n. \tag{4.5.13}$$

Theorem 4.5.2. *Under the assumption* $k < \frac{1}{2(4\alpha^j + \lambda^j \mathcal{C}_I + 2|q_{j,j}|+1)}$ *and that the solution* (w, ψ) *is sufficiently smooth, we have following error estimates for the method* (4.3.8) *and* (4.3.9)

$$||e^j_m||^2 + 2||e^j_{m-1}||^2 + \frac{1}{2}\sum_{n=1}^{m-1} ||2\tilde{e}^j_{n+1} - e^j_n||^2 \leq Ck^3, \quad \textit{for all } 2 \leq m \leq \frac{T}{k}. \tag{4.5.14}$$

Proof. Considering the equation (4.5.12), we can write

$$\frac{3\tilde{e}^j_{n+1} - 4e^j_n + e^j_{n-1}}{2k} = D\tilde{e}^j_{n+1} + \lambda^j \mathcal{I}(\mathbf{E}e^j_n) + g^j_n + \mathcal{E}(\mathbf{E}e^j_n) + R^j_{n+1}. \tag{4.5.15}$$

Taking the inner product from both sides of the equation (4.5.15) with $4k\tilde{e}_{n+1}$ and using the identity (I1) and (I4), we have

$$\begin{aligned} \|\tilde{e}^j_{n+1}\|^2 - \|e^j_n\|^2 \quad + \quad & \|2\tilde{e}^j_{n+1} - e^j_n\|^2 - \|2e^j_n - e^j_{n-1}\|^2 + \|\tilde{e}^j_{n+1} - 2e^j_n + e^j_{n-1}\|^2 \\ & \leq 4k\alpha^j \|\tilde{e}^j_{n+1}\|^2 + 4k\lambda^j \mathcal{C}_I(\mathbf{E}e^j_n, \tilde{e}^j_{n+1}) + 8k|q_{j,j}|\|\mathbf{E}e^{i_n}_n\|\|\tilde{e}^j_{n+1}\| \\ & +4k(g^j_n, \tilde{e}^j_{n+1}) + 4k(R^j_{n+1}, \tilde{e}^j_{n+1}). \end{aligned} \tag{4.5.16}$$

From the equation (4.5.13), we obtain

$$e^j_{n+1} - \frac{2}{3}kh^j_{n+1} = \tilde{e}^j_{n+1} - \frac{2}{3}kg^j_n. \tag{4.5.17}$$

Taking the inner product of (4.5.17) from both sides with itself and multiplying by three, we get

$$3\|e^j_{n+1}\|^2 + \frac{4}{3}k^2\|h^j_{n+1}\|^2 - 4k(e^j_{n+1}, h^j_{n+1}) = 3\|\tilde{e}^j_{n+1}\|^2 + \frac{4}{3}k^2\|g^j_n\|^2 - 4k(\tilde{e}^j_{n+1}, g^j_n). \tag{4.5.18}$$

Adding up (4.5.16) with (4.5.18), and considering $(e^j_{n+1}, h^j_{n+1}) \leq 0$ and $\|\tilde{e}^j_{n+1} - 2e^j_n + e^j_{n-1}\|^2 \geq 0$, with the use of some inequalities from subsection (3.4.1), we get

$$\begin{aligned} & \|e^j_{n+1}\|^2 - \|e^j_n\|^2 + \|\tilde{e}^j_{n+1}\|^2 + \frac{4}{3}k^2\left(\|h^j_{n+1}\|^2 - \|g^j_n\|^2\right) + 2\left[\|e^j_n\|^2 - \|e^j_{n-1}\|^2\right] \\ \leq \quad & 13\|e^j_n\|^2 + k(4\alpha^j + \lambda^j\mathcal{C}_I + 2k|q_{j,j}| + 1)\|\tilde{e}^j_{n+1}\|^2 + 32k\lambda^j\mathcal{C}_I\|e^j_n\|^2 + 8k\lambda^j\mathcal{C}_I\|e^j_{n-1}\|^2 \end{aligned}$$

$$+64k|q_{j,j}|\|e_n^{i_n}\|^2+16k|q_{j,j}|\|e_{n-1}^{i_{n-1}}\|^2+4k\|R_{n+1}^j\|^2.$$

Let $e_n^{i_n}:=\max_{i=1,2,...,Q}|e_n^i|\neq e_n^j$, then $|e_0^j|<|e_0^i|, |e_1^j|<|e_1^i|$ and $e_n^i=\max\{e_1^{i_1},e_2^{i_2},e_3^{i_3},...,e_n^{i_n}\}$. Consequently, we obtain

$$\begin{aligned}\|e_{n+1}^j\|^2 &- \|e_n^j\|^2+\|\tilde{e}_{n+1}^j\|^2+\frac{4}{3}k^2\left(\|h_{n+1}^j\|^2-\|g_n^j\|^2\right)+2\left[\|e_n^j\|^2-\|e_{n-1}^j\|^2\right]\\ &\leq (13+64k|q_{j,j}|+32k\lambda^j\mathcal{C}_I)\|e_n^{i_n}\|^2+k(4\alpha^j+\lambda^j\mathcal{C}_I+2|q_{j,j}|+1)\|\tilde{e}_{n+1}^j\|^2\\ &\quad+(8k\lambda^j\mathcal{C}_I+16k|q_{j,j}|)\|e_{n-1}^i\|^2+4k\|R_{n+1}^j\|^2.\end{aligned}$$

Assuming $k<\frac{1}{2(4\alpha^j+\lambda^j\mathcal{C}_I+2|q_{j,j}|+1)}$, and applying some basic calculations, we get

$$\begin{aligned}\|e_{n+1}^j\|^2-\|e_n^j\|^2 &+ \frac{1}{2}\|\tilde{e}_{n+1}^j\|^2+\frac{4}{3}k^2\left(\|h_{n+1}^j\|^2-\|g_n^j\|^2\right)+2\left[\|e_n^j\|^2-\|e_{n-1}^j\|^2\right]\\ &\leq (13+64k|q_{j,j}|+32k\lambda^j\mathcal{C}_I)\|e_n^{i_n}\|^2+(8k\lambda^j\mathcal{C}_I+16k|q_{j,j}|)\|e_{n-1}^i\|^2\\ &\quad+4k\|R_{n+1}^j\|^2.\end{aligned}\tag{4.5.19}$$

Summing up both sides of the inequality (4.5.19) from $n=1$ to $m-1$ and performing some mathematical calculations, we get

$$\begin{aligned}&\sum_{n=1}^{m-1}(\|e_{n+1}^j\|^2-\|e_n^j\|^2)+\frac{1}{2}\sum_{n=1}^{m-1}\|\tilde{e}_{n+1}^j\|^2+\frac{4}{3}k^2\sum_{n=1}^{m-1}\left(\|h_{n+1}^j\|^2-\|g_n^j\|^2\right)\\ &+2\sum_{n=1}^{m-1}\left[\|e_n^j\|^2-\|e_{n-1}^j\|^2\right]\\ &\leq (13+64k|q_{j,j}|+32k\lambda^j\mathcal{C}_I)\sum_{n=1}^{m-1}\|e_n^{i_n}\|^2+(8k\lambda^j\mathcal{C}_I+64k|q_{j,j}|)\sum_{n=1}^{m-1}\|e_{n-1}^i\|^2\\ &+4k\sum_{n=1}^{m-1}\|R_{n+1}^j\|^2.\end{aligned}\tag{4.5.20}$$

After performing some calculations, we obtain

$$\begin{aligned}\|e_m^j\|^2 &+ 2\|e_{m-1}^j\|^2+\frac{1}{2}\sum_{n=1}^{m-1}\|\tilde{e}_{n+1}^j\|^2+\frac{4}{3}k^2\|h_m^j\|^2\\ &\leq \|e_1^j\|^2+2\|e_0^j\|^2+\frac{4}{3}k^2\|h_1^j\|^2+(13+40k\lambda\mathcal{C}_I+80k|q_{j,j}|)\sum_{n=0}^{m-1}\|e_n^i\|^2\\ &\quad+4k\sum_{n=1}^{m-1}\|R_{n+1}^j\|^2+\frac{4}{3}k^2\sum_{n=1}^{m-1}(ck^2+ck\|h_n^j\|^2).\end{aligned}\tag{4.5.21}$$

Applying discrete Gronwall's Lemma 4.4.1 on (4.5.21) and simplifying the expression, we obtain the desired result 4.5.14. □

It is worth noting that the criteria on uniform temporal step size k in the preceding theorems are only sufficient for stability. These criteria are not optimized in any way, and they can be further relaxed through a deep investigation.

4.6 Numerical Discussion

In this part, we present several numerical examples and investigate the convergence behaviour of the IMEX-BDF-OS techniques for pricing the American option in accordance with the RSJD model proposed by Kou and Merton. We employed the IMEX-BDF-OS techniques in conjunction with the OS method [78] to address the inequality constraints in the LCP. The discretization of the differential operator $\mathcal{D}$ is performed using the following scheme:

$$\begin{aligned} u_z^j(z_i) &\approx \frac{u_{i+1}^j - u_{i-1}^j}{2h}, \\ u_{zz}^j(z_i) &\approx \frac{u_{i+1}^j - 2u_i^j + u_{i-1}^j}{h^2}, \end{aligned}$$

with spatial mesh length h in computational domain $\Omega := [-1.5, 1.5]$. We employed the composite trapezoidal method to discretize the integral term I on the reduced domain Ω. To compute the product of a dense matrix and a column vector via the discrete integral operator, we applied the Fast Fourier Transformation (FFT) technique, as described in [7, 98].

Using the double mesh concept, we managed to calculate the point-wise errors for a variety of alternative asset values 90, 100, and 110. We applied the piecewise cubic Hermite interpolation to investigate the price of the option at points not lying in the spatial mesh. In the computational results, we presented the American option values, the pointwise errors at various asset prices, and the rate of convergence (ROC) of the proposed numerical techniques, where the number of temporal discretization points are denoted by N and the number of spatial discretization points by M. The rate of convergence achieved by the IMEX-BDF-OS approaches is calculated using

$$\text{ROC} = \log_2 \left(\frac{\|u^j(k,h) - u^j(\frac{k}{2}, \frac{h}{2})\|}{\|u^j(\frac{k}{2}, \frac{h}{2}) - u^j(\frac{k}{4}, \frac{h}{4})\|} \right), \tag{4.6.1}$$

where $u^j(k,h)$ is the numerical price of American option in the j^{th} regime with k temporal step size and h spatial step size.

4.6.1 Three States RSJD Model

First, we use the three states RSJD model to conduct the numerical experiment for the IMEX-BDF2-OS method. The following parameter values are utilised in the simulations:

$$r = \begin{bmatrix} 0.05 \\ 0.05 \\ 0.05 \end{bmatrix}, \quad \sigma = \begin{bmatrix} 0.15 \\ 0.15 \\ 0.15 \end{bmatrix}, \quad \mathcal{A} = \begin{bmatrix} -0.8 & 0.6 & 0.2 \\ 0.2 & -1.0 & 0.8 \\ 0.1 & 0.3 & -0.4 \end{bmatrix}, \quad \lambda = \begin{bmatrix} 0.3 \\ 0.5 \\ 0.7 \end{bmatrix}. \tag{4.6.2}$$

For the numerical simulation in the third economic condition, we have selected the following collection of examples:

Example 4.6.1. *The American put option is priced using Merton's three states RSJD model with the following variables:* $T = 0.25$, $E = 100$, $\sigma_J^j = 0.45$, *and* $\mu_J^j = -0.90$.

For pricing American put options under Merton's three states RSJD model, we performed a numerical simulation using the IMEX-BDF2-OS method in Example 4.6.1. The results are shown in Table 4.1, which also includes point-wise errors and the rate of convergence at various asset prices $S = 90, 100, 110$. We found that the IMEX-BDF2-OS method's convergence rate is consistent with our theoretical error estimate, ranging from 1.5 to 2.

Table 4.1: Under Merton's three states RSJD model, the values of the American put option in the third state of the economy, and the rate of convergence of IMEX-BDF2-OS are shown at $S = 90, 100, 110$.

		$S = 90$			$S = 100$			$S = 110$		
M	N	Value	Error	ROC	Value	Error	ROC	Value	Error	ROC
65	25	10.6749	-	-	6.0299	-	-	4.8510	-	-
129	50	10.7201	4.52e-02	-	6.1611	1.31e-01	-	4.8676	1.65e-02	-
257	100	10.7346	1.45e-02	1.64	6.1908	2.97e-02	2.13	4.8726	5.06e-03	1.71
513	200	10.7388	4.18e-03	1.79	6.1983	7.50e-03	1.98	4.8740	1.33e-03	1.91
1025	400	10.7399	1.08e-03	1.94	6.2003	1.91e-03	1.97	4.8743	3.42e-04	1.96

Example 4.6.2. *Under Kou's three states RSJD model, the American put option is priced using the following variables:* $T = 0.25$, $E = 100$, $\eta_1^j = 3$, $\eta_2^j = 2$, $p^j = 0.5$.

To simulate Kou's three-state RSJD model, we applied the same strategy using the parameters given in Example 4.6.2. The computed results for IMEX-BDF2-OS method are listed in Table 4.2, and the American option value, Gamma, Delta, and exercise region under Merton's three states RSJD model are presented in Figure 4.1. The graphs show that there is no incorrect fluctuation at or close to the strike price, indicating that the option values are quite steady. Furthermore, Tables 4.3 and 4.4 list the temporal ROC of the IMEX-BDF1-OS and IMEX-BDF2-OS methods, respectively, for pricing the American put option under the Merton's three states RSJD model. In the spatial domain $\Omega = [-1.5, 1.5]$, we set $M = 10^3 + 1$ and present results for various values of N. From Table 4.4, we can observe that, for BDF2-OS, the error is reduced by a factor of approximately 3 across different values of N, indicating that the temporal order of convergence of BDF2-OS lies between 1.5 and 2. On the other hand, temporal convergence order of BDF1-OS in Table 4.3 is asymptotically 1.

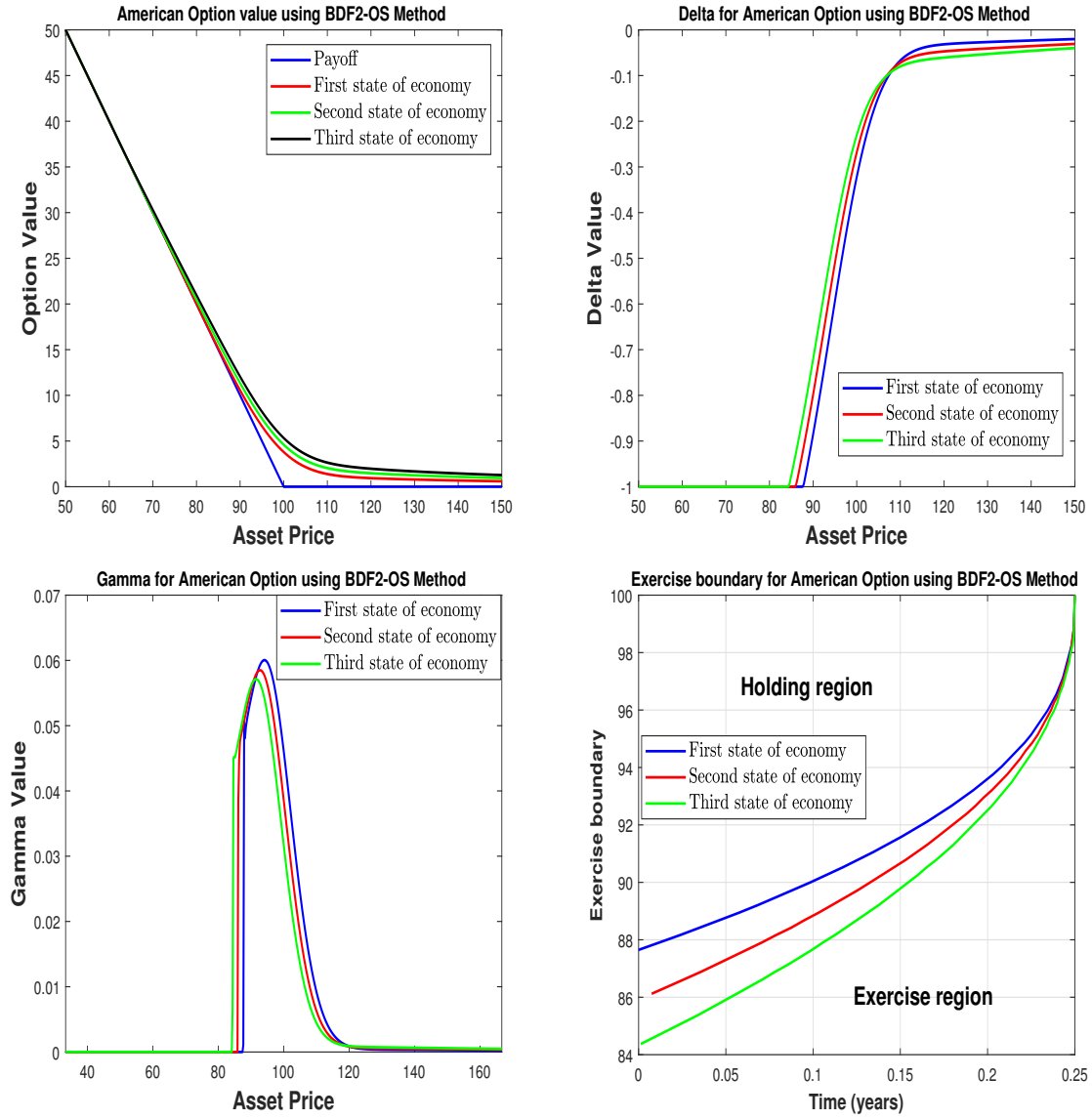

Figure 4.1: Option value, Delta, Gamma, and exercise boundary at $M = 1000$, $N = 400$ for Merton's three states RSJD model, where the parameters are taken from Example 4.6.1.

Table 4.2: Under Kou's three states RSJD model, the values of the American put option in the third state of the economy and the rate of convergence of IMEX-BDF2-OS are shown at $S = 90, 100, 110$.

		$S = 90$			$S = 100$			$S = 110$		
M	N	Value	Error	ROC	Value	Error	ROC	Value	Error	ROC
65	25	12.0357	-	-	5.1958	-	-	2.6159	-	-
129	50	12.0512	1.54e-02	-	5.3019	1.06e-01	-	2.6316	1.56e-02	-
257	100	12.0542	3.06e-03	2.33	5.3259	2.39e-02	2.14	2.6365	4.94e-03	1.66
513	200	12.0550	7.30e-04	2.06	5.3318	5.89e-03	2.02	2.6378	1.30e-03	1.92
1025	400	12.0551	1.85e-04	1.97	5.3332	1.46e-03	2.00	2.6382	3.32e-04	1.96

Table 4.3: Under Merton's three states RSJD model, the values of the American put option in the third state of the economy and the convergence rate.

	$S = 90$			$S = 100$			$S = 110$		
N	Value	Error	ROC	Value	Error	ROC	Value	Error	ROC
25	15.888997	-	-	11.310930	-	-	8.207977	-	-
50	15.918032	2.90e-02	-	11.349152	3.82e-02	-	8.244002	3.60e-02	-
100	15.933071	1.50e-02	0.95	11.368717	1.95e-02	0.96	8.262422	1.84e-02	0.96
200	15.940814	7.74e-03	0.96	11.378696	9.97e-03	0.97	8.271802	9.37e-03	0.97
400	15.944789	3.97e-03	0.97	11.383776	5.07e-03	0.98	8.276567	4.76e-03	0.98

Table 4.4: Under Merton's three states RSJD model, the values of the American put option in the third state of the economy and the convergence rate.

	$S = 90$			$S = 100$			$S = 110$		
N	Value	Error	ROC	Value	Error	ROC	Value	Error	ROC
25	15.9422	-	-	11.3822	-	-	8.2754	-	-
50	15.9468	4.61e-03	-	11.3867	4.43e-03	-	8.2793	3.92e-03	
100	15.9483	1.43e-03	1.68	11.3882	1.51e-03	1.55	8.2807	1.35e-03	1.53
200	15.9487	4.37e-04	1.71	11.3887	5.14e-04	1.55	8.2811	4.77e-04	1.50
400	15.9488	1.30e-04	1.74	11.3889	1.76e-04	1.54	8.2813	1.71e-04	1.48

4.6.2 Five States RSJD Model

Our next computational scenario considers the regime-switching jump-diffusion model with five hidden Markov chain states. We applied the results for the IMEX-BDF2-OS scheme to approximate the price of an American put option under the five-state Kou and Merton RSJD models and presented the results in the fifth state of the economy. The model parameters used in Examples 4.6.3 and 4.6.4 are the same as

those employed in [86, 101], given as

$$r = \begin{bmatrix} 0.05 \\ 0.05 \\ 0.05 \\ 0.05 \\ 0.05 \end{bmatrix}, \quad \sigma = \begin{bmatrix} 0.15 \\ 0.15 \\ 0.15 \\ 0.15 \\ 0.15 \end{bmatrix}, \quad \mathcal{A} = \begin{bmatrix} -1.00 & 0.25 & 0.25 & 0.25 & 0.25 \\ 0.25 & -1.00 & 0.25 & 0.25 & 0.25 \\ 0.25 & 0.25 & -1.00 & 0.25 & 0.25 \\ 0.25 & 0.25 & 0.25 & -1.00 & 0.25 \\ 0.25 & 0.25 & 0.25 & 0.25 & -1.00 \end{bmatrix}, \quad \lambda = \begin{bmatrix} 0.1 \\ 0.3 \\ 0.5 \\ 0.7 \\ 0.9 \end{bmatrix}.$$

Example 4.6.3. *Pricing the American put option under the five states regime-switching Merton's jump-diffusion model with the parameters,* $T = 0.25, \quad K = 100$, $\sigma_J^j = 0.45$, $\mu_J^j = -0.90$.

The numerical results for the IMEX-BDF2-OS method for Merton and Kou models are presented in Table 4.5 and 4.6 respectively. From these results, we can observe that the rate of convergence lies between 1.5 and 2, which is consistent with the theoretical error estimates presented in Section 4.5.

Table 4.5: Under Merton's five states regime-switching jump-diffusion model, the values of the American put option in the fifth state of the economy and the rate of convergence of IMEX-BDF2-OS are shown at $S = 90, 100, 110$.

		$S = 90$			$S = 100$			$S = 110$		
M	N	Value	Error	Rate	Value	Error	Rate	Value	Error	Rate
65	25	16.7006	-	-	12.2343	-	-	9.1370	-	-
129	50	16.7317	3.11e-02	-	12.2671	3.28e-02	-	9.1658	2.88e-02	-
257	100	16.7397	8.01e-03	1.95	12.2758	8.66e-03	1.92	9.1734	7.58e-03	1.92
513	200	16.7418	2.14e-03	1.90	12.2781	2.32e-03	1.89	9.1754	2.04e-03	1.89
1025	400	16.7424	5.67e-04	1.91	12.2787	6.28e-04	1.88	9.1760	5.56e-04	1.87

Example 4.6.4. *Pricing the American put option under the five states regime-switching Kou's jump-diffusion model, with the parameters,* $T = 0.25, \quad K = 100$, $\eta_1^j = 3$, $\eta_2^j = 2$, $p^j = 0.5$.

The American put option value, Delta, Gamma, exercise boundary for IMEX-BDF2-OS method under Merton's five states regime-switching jump-diffusion model are presented in Figure 4.2. The graphs demonstrate that the option values are stable, with no erroneous oscillation at or near the strike price.

4.6.3 Sensitivity of the Parameters

Example 4.6.5. *Pricing the American put option under the three states regime-switching Merton's jump-diffusion model with the parameters,* $T = 1, \quad K = 100$, $\sigma_J^j = 0.45$, $\mu_J^j = -0.90$, $\Omega = [-6, 6]$, *volatility is defined in equations (4.6.3,4.6.4, 4.6.5) and other parameters are as (4.6.2).*

Table 4.6: Under Kou's five states regime-switching jump-diffusion model, the values of the American put option in the fifth state of the economy and the rate of convergence of IMEX-BDF2-OS are shown at $S = 90, 100, 110$.

		$S = 90$			$S = 100$			$S = 110$		
M	N	Value	Error	Rate	Value	Error	Rate	Value	Error	Rate
65	25	17.0065	-	-	11.9502	-	-	8.3031	-	-
129	50	17.0306	2.41e-02	-	11.9795	2.93e-02	-	8.3310	2.79e-02	-
257	100	17.0364	5.79e-03	2.06	11.9868	7.30e-03	2.00	8.3379	6.96e-03	2.00
513	200	17.0378	1.45e-03	2.00	11.9886	1.83e-03	1.99	8.3397	1.75e-03	1.99
1025	400	17.0382	3.61e-04	2.00	11.9891	4.59e-04	1.99	8.3401	4.41e-04	1.98

We selected the parameters based on the literature, where several authors have reported numerical outcomes for pricing American-style options using the operator splitting approach. These parameters satisfy the theoretical constraints, ensuring high accuracy of the methods. Additionally, a different range of parameters may be used for these procedures. Let us consider

$$\sigma_1(x,t) = 0.25 + 0.35(0.5 + 3(T-t))\frac{(\frac{Ke^x}{100} - 1.5)^2}{((\frac{Ke^x}{100})^2 + 1.7)}, \tag{4.6.3}$$

$$\sigma_2(x,t) = 0.15 + 0.15(0.5 + 2(T-t))\frac{(\frac{Ke^x}{100} - 0.5)^2}{((\frac{Ke^x}{100})^2 + 1.44)}, \tag{4.6.4}$$

$$\sigma_3(x,t) = 1.9x^2 - 0.5x + (0.7x - 0.2)(T-t) + 0.35, \tag{4.6.5}$$

Table 4.7: Under Merton's three states regime-switching jump-diffusion model, the values of the American put option in the third state of the economy, and the rate of convergence of IMEX-BDF2-OS are shown at $S = 90, 100, 110$ for Example 4.6.5.

		$S = 90$			$S = 100$			$S = 110$			
M	N	Value	Error	Rate	Value	Error	Rate	Value	Error	Rate	Time (Seconds)
128	64	22.357419	-	-	18.368842	-	-	15.737387	-	-	0.179519
256	128	22.383728	2.63e-02	-	18.409093	4.03e-02	-	8.3310	3.32e-02	-	1.089513
512	256	22.393422	9.69e-03	1.44	18.422194	1.31e-02	1.62	8.3379	1.05e-02	1.67	11.020835
1024	512	22.396550	3.13e-03	1.63	18.425909	3.71e-03	1.82	8.3397	2.97e-03	1.81	92.486743
2048	1024	22.397378	8.28e-04	1.92	18.426884	9.75e-04	1.93	8.3401	7.84e-04	1.92	709.680301

Table 4.7 presents the results for the three chosen continuous volatility functions to demonstrate the sensitivity of the parameters for pricing American options under the three states RSJD model. It also demonstrates that the proposed technique preserves the convergent feature throughout the given range of parameters.

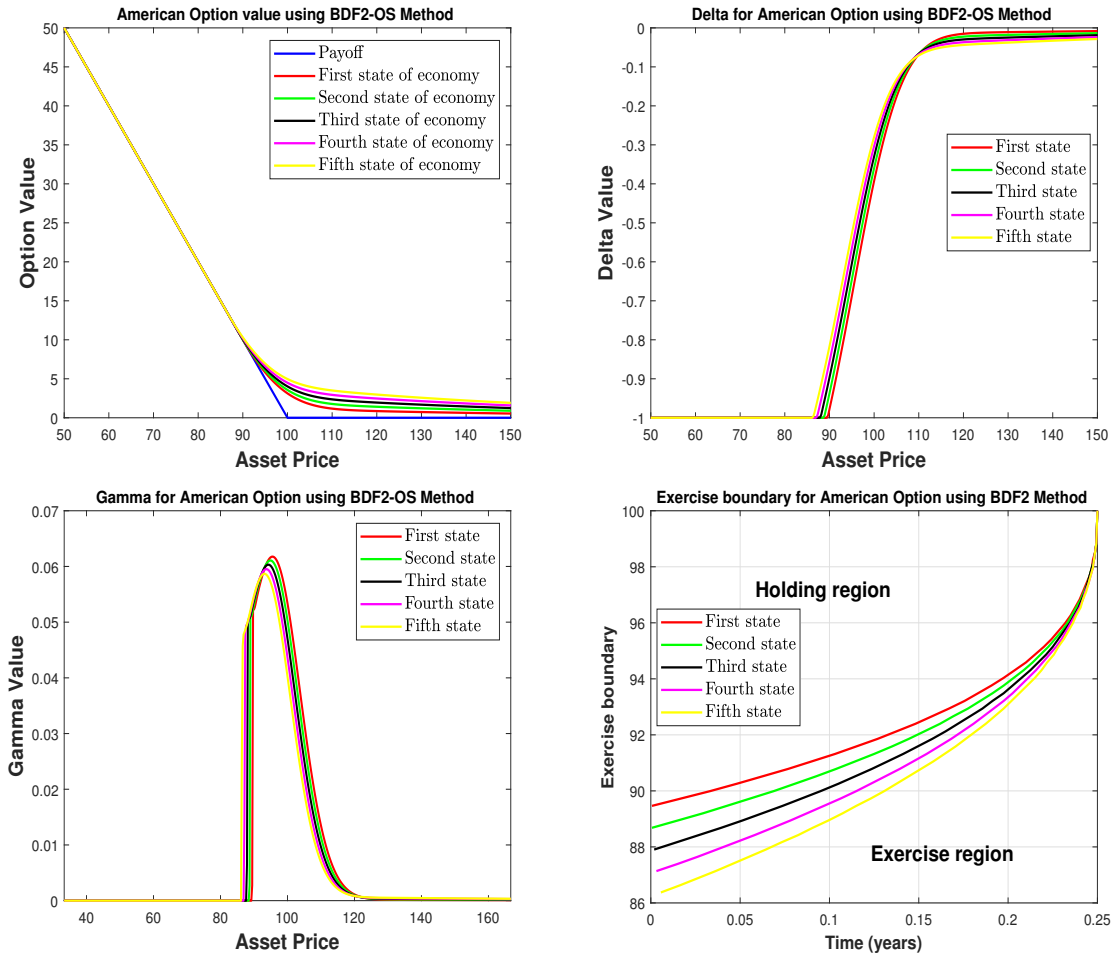

Figure 4.2: Option value, Delta, Gamma, and exercise boundary for Merton's five states regime-switching jump-diffusion model with parameters as provided in the Example 4.6.3.

Example 4.6.6. *Pricing the American put option under the three states regime-switching Merton's jump-diffusion model with the parameters,* $T = 0.5, \quad K = 100$, $\sigma_J^j = 0.45$, $\mu_J^j = -0.90$, $\Omega = [-3, 3]$, *volatility is* $\sigma = 1, 3, 5$ *and other parameters are as (4.6.2).*

Table 4.8 presents the results for the selected high volatilities ($\sigma_1 = 1, \sigma_2 = 3, \sigma_3 = 5$), illustrating the sensitivity of the parameters in pricing American options under the three states RSJD model. It also demonstrates that the proposed technique preserves convergence for these high volatility scenarios.

4.6.4 Validation of the Numerical Results

In section 4.5, we presented the IMEX-BDF-OS method's error estimates; here, we compare our numerical results with existing literature.

Table 4.8: Error behavior of IMEX -BDF1-OS (Upper) differ in practice from IMEX-BDF2-OS (Lower) for high-volatility $\sigma = 1, 3, 5$ scenarios.

		Regime 1 ($\sigma = 1$)			Regime 2 ($\sigma = 3$)			Regime 3 ($\sigma = 5$)			
M	N	Value	Error	Order	Value	Error	Order	Value	Error	Order	Time (Seconds)
64	32	37.631505	-	-	71.570648	-	-	85.443475	-	-	0.10
128	64	37.909432	2.779269e-01	-	71.885085	3.144361e-01	-	85.665833	2.223585e-01	-	0.13
256	128	38.048966	1.395337e-01	0.9940	72.043288	1.582033e-01	0.9909	85.776509	1.106759e-01	1.0065	0.94
512	256	38.118961	6.999473e-02	0.9952	72.122777	7.948898e-02	0.9929	85.831709	5.520016e-02	1.0035	9.67
1024	512	38.154072	3.511186e-02	0.9952	72.162702	3.992476e-02	0.9934	85.859301	2.759224e-02	1.0004	80.25
2048	1024	38.171688	1.761505e-02	0.9951	72.182743	2.004152e-02	0.9942	85.873105	1.380353e-02	0.9992	608
4096	2048	38.180524	8.836260e-03	0.9953	72.192798	1.005511e-02	0.9950	85.880013	6.907769e-03	0.9987	9833
64	32	38.161591	-	-	72.185834	-	-	85.898718	-	-	0.06
128	64	38.180545	1.895450e-02	-	72.197169	1.133532e-02	-	85.889177	9.540928e-03	-	0.16
256	128	38.186404	5.858670e-03	1.69	72.200964	3.795583e-03	1.58	85.887271	1.906028e-03	2.32	1.05
512	256	38.188347	1.943568e-03	1.59	72.202244	1.279222e-03	1.57	85.886938	3.327847e-04	2.51	10
1024	512	38.189026	6.785491e-04	1.51	72.202682	4.381112e-04	1.54	85.886907	3.096252e-05	3.42	90
2048	1024	38.189270	2.445633e-04	1.47	72.202831	1.493397e-04	1.55	85.886917	1.02694e-05	1.59	704
4096	2048	38.189359	8.911244e-05	1.46	72.202881	5.006873e-05	1.57	85.886926	8.617118e-06	0.53	9407

To show the flexibility of the RSJD model, we used the following parameters (4.6.6-4.6.7) (also given in Kazmi [86]):

$$\Omega = [-1.5, 1.5], \quad E = 100, \quad T = 0.5, \tag{4.6.6}$$

$$r = \begin{bmatrix} 0.04 \\ 0.02 \\ 0.07 \end{bmatrix}, \sigma = \begin{bmatrix} 0.13 \\ 0.20 \\ 0.15 \end{bmatrix}, \mathcal{A} = \begin{bmatrix} -0.8 & 0.6 & 0.2 \\ 0.2 & -1.0 & 0.8 \\ 0.1 & 0.3 & -0.4 \end{bmatrix}, \lambda = \begin{bmatrix} 2.0 \\ 0.8 \\ 1.0 \end{bmatrix}, \mu^j = \begin{bmatrix} -0.2 \\ 0 \\ 0.10 \end{bmatrix}, \sigma_J^j = \begin{bmatrix} 0.25 \\ 0.30 \\ 0.35 \end{bmatrix}. \tag{4.6.7}$$

Table 4.9 presents the point-wise errors at different discretization points and compares them with the results reported in Table 4 of Kazmi [86]. We can observe that the errors of the proposed method (IMEX-BDF2-OS) decrease faster than those reported by Kazmi [86]. At $N = 3200$ and $M = 4096$, the error of [86] is $3.6e-05$ and the error of our method is $1.2e-05$, that three times less than [86]. Additionally, in

Table 4.9: Comparison of numerical results with Table 4 of [86] for pricing American put options under the Merton's jump-diffusion model.

		Regime1		Regime2		Regime3	
M	N	Kazmi [86]	Our Method	Kazmi [86]	Our Method	Kazmi [86]	Our Method
128	100	0.038964	0.016453	0.047656	0.001357	0.059015	0.010946
256	200	0.009472	0.003528	0.011661	0.000423	0.014214	0.002710
512	400	0.002368	0.000865	0.002902	0.000109	0.003524	0.000669
1024	800	0.000592	0.000214	0.000723	0.000027	0.000878	0.000166
2048	1600	0.000147	0.000052	0.000180	0.000006	0.000220	0.000041
4096	3200	0.000036	0.000012	0.000045	0.000001	0.000054	0.000010

Table 4.10, we present the errors for various values of M and N by using the parameters of [101]. We also

compare our numerical outcomes with Table 3 of [101]. At $N = 3200$ and $M = 4096$, the error reported in [101] is $5.3e-05$, and the error of our method is $4.6e-05$, which is smaller. Upon examining Table 4.10, it becomes evident that the strategy that we have provided is better compared to Lee [101].

Table 4.10: Comparison of numerical results with Table 3 of [101] for pricing American put options under Merton's jump-diffusion model.

		$S = 90$		$S = 100$		$S = 110$	
M	N	Lee [101]	Our Method	Lee [101]	Our Method	Lee [101]	Our Method
64	50	0.224160	0.137115	0.138456	0.125603	0.045267	0.058200
128	100	0.071107	0.044026	0.044535	0.029501	0.019213	0.013595
256	200	0.016497	0.011919	0.010601	0.007618	0.005057	0.003601
512	400	0.004323	0.003078	0.002733	0.001962	0.001280	0.000935
1024	800	0.001066	0.000777	0.000688	0.000500	0.000325	0.000239
2048	1600	0.000242	0.000191	0.000161	0.000125	0.000078	0.000060
4096	3200	0.000053	0.000046	0.000037	0.000031	0.000018	0.000014

4.6.5 Effects of the restrictions on the order of convergence

In section 4.4, we have shown that the IMEX-BDF-OS method's stability has restrictions on the uniform time step size k. To show the effects of the restrictions on stability numerically, we present the results using the following parameters:

$T = 1, \quad K = 100, \sigma_J^j = 0.45, \mu_J^j = -0.90, \eta_1^j = 3, \eta_2^j = 2, p^j = 0.5.$

$$r = \begin{bmatrix} 0.02 \\ 0.03 \\ 0.04 \end{bmatrix}, \quad \sigma 1 = \begin{bmatrix} 0.01 \\ 0.01 \\ 0.01 \end{bmatrix}, \quad \sigma 2 = \begin{bmatrix} 0.25 \\ 0.25 \\ 0.25 \end{bmatrix}, \quad \mathcal{A} = \begin{bmatrix} -0.8 & 0.6 & 0.2 \\ 0.2 & -1.0 & 0.8 \\ 0.1 & 0.3 & -0.4 \end{bmatrix}, \quad \lambda = \begin{bmatrix} 0.1 \\ 0.1 \\ 0.1 \end{bmatrix}. \tag{4.6.8}$$

We choose a fine enough mesh in space, $h = 1/2^{10}$, in the domain $[-2, 2]$ for the IMEX-BDF-OS approach, so that time discretization dominates the errors. Our stability restrictions depend on the parameters. In our analysis, we have taken $\alpha > 0$. If $\alpha \leq 0$, then the restrictions become $k < \frac{1}{2(1+4|q_{j,j}|+\lambda^j \mathcal{C}_I)}$. To numerically show the restriction's effects on the accuracy of IMEX-OS schemes, we have taken two different values of σ and performed the numerical simulation. We have taken $\sigma 1 = [0.01, 0.01, 0.01]'$ and $\sigma 2 = [0.25, 0.25, 0.25]'$. For $\sigma 1$, we have $\alpha > 0$, and for $\sigma 2$, $\alpha < 0$.

The corresponding numerical results are reported in Tables 4.11, 4.12, 4.13, and 4.14. The order of convergence for the BDF1-OS method (4.3.2 and 4.3.5) with $\alpha < 0$ is shown in Table 4.11. The outcomes are shown in Table 4.13 when $\alpha > 0$ for BDF1-OS. The convergence rate approaches its asymptotic value in both instances when the time step size is small enough. We have shown the order of convergence for the IMEX-BDF2 technique for both the cases, $\alpha < 0$ and $\alpha > 0$, in Tables 4.12 and 4.14 respectively. We

observe that the order of convergence rapidly approaches its asymptotic rate of 2 when $\alpha > 0$. However, for both the values of α, the order of convergence of IMEX-BDF-OS would achieve its asymptotic rate only for somewhat lower time step sizes when $\alpha < 0$. From all these results, we can conclude that our proposed methods are stable and converging with asymptotic rates for both the conditions: $\alpha > 0$ and $\alpha < 0$. However, In both situation, the accuracy depends on temporal uniform step size k.

Table 4.11: Effect of temporal step size k on the convergence order of the IMEX-BDF1-OS for pricing American option under RSJD model, where $\alpha < 0$.

		Regime1		Regime2		Regime3	
	k=$\frac{1}{2^l}$	Error	Order	Error	Order	Error	Order
Merton	l=4	1.049871e-01	-	1.091853e-01	-	1.122400e-01	-
	l=5	5.434548e-02	0.9499	5.622621e-02	0.9574	5.759853e-02	0.9624
	l=6	2.795821e-02	0.9588	2.883990e-02	0.9631	2.949281e-02	0.9656
	l=7	1.434584e-02	0.9626	1.478563e-02	0.9638	1.511164e-02	0.9647
	l=8	7.355775e-03	0.9636	7.586130e-03	0.9627	7.756519e-03	0.9621
	l=9	3.767056e-03	0.9654	3.888213e-03	0.9642	3.976116e-03	0.9640
Kou	l=4	1.028666e-01	-	1.080147e-01	-	1.117484e-01	-
	l=5	5.270648e-02	0.9647	5.538525e-02	0.9636	5.723498e-02	0.9652
	l=6	2.690528e-02	0.9700	2.834298e-02	0.9665	2.929068e-02	0.9664
	l=7	1.369559e-02	0.9741	1.448460e-02	0.9684	1.498515e-02	0.9669
	l=8	6.957533e-03	0.9770	7.393763e-03	0.9701	7.660871e-03	0.9679
	l=9	3.527718e-03	0.9798	3.767714e-03	0.9726	3.909359e-03	0.9705

4.7 Conclusion

We have shown the stability and error estimates for the operator splitting method to solve the linear complementarity problem (4.2.4), and the solution of LCP is the value of the American put option under the regime-switching jump-diffusion model. The approach combines the Backward difference techniques with the operator splitting method. We have approximated the integral operator by composite trapezoidal rule and the FFT algorithm is used to compute the product of a dense matrix and a column vector in the discrete integral operator. In contrast, the differential operator is computed with the help of a finite difference operator analogous to the backward difference implicit-explicit techniques. Our primary focus is to rely on the stability and error estimate for given numerical methods. We performed several numerical computations for IMEX-BDF-OS methods for pricing the American put option under both Kou's and Merton's regime-switching jump-diffusion models to demonstrate the convergence behaviors of

Table 4.12: Effect of temporal step size k on the convergence order of the IMEX-BDF2-OS for pricing American option under RSJD model, where $\alpha < 0$.

		Regime1		Regime2		Regime3	
	k=$\frac{1}{2^l}$	Error	Order	Error	Order	Error	Order
Merton	l=4	2.910457e-02	-	3.053357e-02	-	3.008514e-02	-
	l=5	9.742728e-03	1.5788	9.577994e-03	1.6726	8.974913e-03	1.7450
	l=6	3.206405e-03	1.6033	2.961256e-03	1.6935	2.654498e-03	1.7574
	l=7	1.040039e-03	1.6243	9.005805e-04	1.7172	7.649767e-04	1.7949
	l=8	3.370054e-04	1.6257	2.718466e-04	1.7280	2.164034e-04	1.8216
	l=9	1.050402e-04	1.6818	7.823568e-05	1.7968	5.557656e-05	1.9611
Kou	l=4	2.341261e-02	-	2.631473e-02	-	2.661240e-02	-
	l=5	7.449704e-03	1.6520	8.117189e-03	1.6968	7.873932e-03	1.7569
	l=6	2.330268e-03	1.6766	2.484637e-03	1.7079	2.324897e-03	1.7599
	l=7	7.025778e-04	1.7297	7.490739e-04	1.7298	6.792828e-04	1.7750
	l=8	1.970459e-04	1.8341	2.161012e-04	1.7934	1.869170e-04	1.8616
	l=9	4.705639e-05	2.0660	5.630662e-05	1.9403	4.560990e-05	2.0349

Table 4.13: Effect of temporal step size k on the convergence order of the IMEX-BDF1-OS for pricing American option under RSJD model, where $\alpha > 0$.

		Regime1		Regime2		Regime3	
	k=$\frac{1}{2^l}$	Error	Order	Error	Order	Error	Order
Merton	l=4	1.927725e-02	-	2.128769e-02	-	2.307458e-02	-
	l=5	9.790635e-03	0.9774	1.077072e-02	0.9829	1.168412e-02	0.9817
	l=6	4.917576e-03	0.9934	5.405198e-03	0.9946	5.953264e-03	0.9727
	l=7	2.453429e-03	1.0031	2.718329e-03	0.9916	3.077982e-03	0.9516
	l=8	1.222941e-03	1.0044	1.370890e-03	0.9876	1.594573e-03	0.9488
	l=9	6.100308e-04	1.0034	6.904368e-04	0.9895	8.186111e-04	0.9619
Kou	l=4	6.626579e-03	-	8.558854e-03	-	1.014220e-02	-
	l=5	3.373806e-03	0.9738	4.363160e-03	0.9720	5.117048e-03	0.9869
	l=6	1.694033e-03	0.9939	2.200141e-03	0.9877	2.561057e-03	0.9985
	l=7	8.491653e-04	0.9963	1.104430e-03	0.9943	1.279777e-03	1.0008
	l=8	4.253949e-04	0.9972	5.533287e-04	0.9970	6.394131e-04	1.0010
	l=9	2.130047e-04	0.9979	2.769608e-04	0.9985	3.195821e-04	1.0005

the operating splitting method. We presented the results for the American Put option and showed the plots for American option values, Gamma, Delta, and exercise region.

Table 4.14: Effect of temporal step size k on the convergence order of the IMEX-BDF2-OS for pricing American option under RSJD model, where $\alpha > 0$.

		Regime1		Regime2		Regime3	
	k=$\frac{1}{2^l}$	Error	Order	Error	Order	Error	Order
Merton	l=4	5.760233e-03	-	5.557893e-03	-	5.232251e-03	-
	l=5	1.082830e-03	2.4113	1.355369e-03	2.0358	2.394653e-03	1.1276
	l=6	3.646854e-04	1.5700	6.408508e-04	1.0806	8.418278e-04	1.5082
	l=7	9.791600e-05	1.8970	1.517961e-04	2.0778	1.216734e-04	2.7905
	l=8	2.454780e-05	1.9959	3.528875e-05	2.1048	2.198793e-05	2.4682
	l=9	6.123418e-06	2.0031	8.589291e-06	2.0385	4.783704e-06	2.2005
Kou	l=4	2.216093e-03	-	2.597591e-03	-	2.474387e-03	-
	l=5	5.574075e-04	1.9912	6.361016e-04	2.0298	6.282472e-04	1.9776
	l=6	1.365860e-04	2.0289	1.583256e-04	2.0063	1.595991e-04	1.9768
	l=7	3.346539e-05	2.0290	3.943506e-05	2.0053	4.031457e-05	1.9850
	l=8	8.560724e-06	1.9668	9.886719e-06	1.9959	1.001781e-05	2.0087
	l=9	2.190215e-06	1.9666	2.484622e-06	1.9924	2.524571e-06	1.9884

CHAPTER 5

Computation and Analysis of an Implicit–Explicit Backward Difference Operator Splitting Method for Pricing American Options Under the Liquidity Shocks [1]

This chapter presents an effective and precise implicit-explicit (IMEX) finite difference (FD) method for resolving the semi-linear PDE system and the semi-linear complementarity system that arise in the liquidity switching model of option pricing. We employ backward difference formulae of order two (BDF2) for the temporal semi-discretization and demonstrate the stability of the resulting system. The computational technique developed for the European option are extended for pricing American option by combining an operator splitting (OS) approach with the IMEX-BDF2 method to solve the semi-linear system of complementarity problems (LCPs) that establishes the price of an American option. To illustrate the efficiency and accuracy of the suggested method, numerical data for American and European options are

[1] The results discussed in this chapter are *Communicated*.

presented. We also plot the option values, Gamma, Delta, along with computational errors under varying parameters to analyse the sensitivity of the proposed option pricing model.

5.1 Introduction

Classical option pricing theory fails to accurately represent actual markets because it makes the fundamental assumption that markets are always liquid and that agents may trade anytime they want. Consequently, great effort has been devoted to developing better models as a solution to these limiting assumptions. Jump-diffusion models [93], such as Merton model [111], Lévy dynamics (see, for example, [36]), and stochastic volatility models are some examples of alternative models. In addition, regime switching is considered one of the fastest-growing areas of interest in computing option prices. Regime-switching techniques, as proposed by Yang *et al.*[179], provide a direct method to capture stochastic volatility and, therefore, fat tails. This overcomes the limitation of the usual assumption of constant volatility based on lognormality. The pricing and hedging problems associated with European options in a market vulnerable to liquidity shocks are examined in [104]. The authors use a distinct Markovian liquidity component to create a regime-switching description of market liquidity. The utility indifference method of valuing derivatives is then explained. The primary findings are the development and examination of a semi-linear coupled HJB equation that is fulfilled by the indifference price. European options with liquidity shocks are modelled as a coupled system, where one is a degenerate parabolic equation, and the other has no diffusion factor. Koleva et al. [91] proposed a fourth-order compact scheme for a parabolic-ordinary system of liquidity shocks model for European options pricing. Gyulov et al. [61] applied the interior penalty method for pricing the American option in a liquidity-switching market. In this direction, other research can be found in [62, 92]. We propose two IMEX finite difference schemes that preserve the positivity of the solution to the differential problem. Our focus is on the numerical solution of the associated PDE system for the European option and semi-linear complementarity problem system for the American style options, which satisfied by the indifference prices of the writer and the buyer. More specifically, we construct and analyze a linearized IMEX finite difference scheme for the non-linear parabolic-ordinary systems corresponding to these problems, i.e., system (5.3.8). Numerical approaches for approximating degenerate nonlinear parabolic equations face a challenging burden of simultaneously preserving the maximum principle and achieving high-order spatial accuracy. Numerous finite difference methods have been developed in recent decades to address evolution-related issues. Meshfree methods based on radial basis functions (RBFs) [43, 83] are often used for solving partial differential equations due to their potential for achieving spectral convergence in complex geometries, particularly for smooth solutions. Shirzadi *et al.*[144, 146] proposed the mesh-free moving least-squares approximation and obtained the optimized uniform error limits for the pricing option in jump-diffusion models. Other mesh-free work can be found in

[115, 130, 147, 157, 150, 160, 178] and reference therein.

Various methods have been proposed in the literature to address the discretised linear complementarity issue that emerges in American option pricing, as reported by [25, 72, 139, 140, 175]. Our main focus is on the numerical pricing of options utilising FD-based BDF2 approaches. We also thoroughly examine the numerical techniques associated with the liquidity switching model. We address a class of methods for solving the semi-linear LCPs for the American options, which is considered crucial, namely, the operator splitting technique introduced in [78]. We find that operator splitting provides an efficient way to compute the price of American-style options without directly solving the linear complementarity problem. In addition to being applicable to many Black-Scholes models, it is also relatively easy to implement as the the differential and complementarity criteria are separable and straightforward to solve. However, a notable challenge arises from the splitting when the slack function and its complementarity conditions are considered. Several authors have successfully applied the operator splitting method to solve LCPs in option pricing [26, 79, 175, 176].

The primary aim of this study is to introduce the IMEX-BDF2 temporal semi-discretization technique for valuing European and American options within a liquidity-switching framework. Additionally, this research seeks to provide stability estimations for the proposed schemes. Asymptotically, the BDF2-OS exhibits second-order accuracy. The proposed methodology effectively estimates the value of the option, along with its notable "Greeks" (Delta & Gamma). These strategies successfully handle the singularity of the non-smooth pay-off function by compressing the mesh near the singularity. There is no need for iterations at every time step. The process of differentiation yields a tridiagonal system at each time step, which can be efficiently and directly solved. Given the independence between spatial and temporal discretization, different techniques can be used for spatial discretization, including meshless methods, finite elements, spectral methods, and others. Spatial discretization also allows for the use of a non-uniform grid. The remaining portion of this chapter is organised as follows. We begin by defining the liquidity switching model and to describing the basic abbreviations, symbols, and assumptions used throughout this work, as well as the formation and associated features of the semi-linear PDEs and LCPs. In Section 5.3, we propose the time semi-discretizations and present the stability analysis of the proposed schemes. In Section 5.4, we present the BDF2 operator splitting time semi-discretization for the American option. In Section 5.5, to validate the theoretical results, numerical results for the pricing of the European and American options are presented.

5.2 Liquidity Switching Model

In this section, we present the mathematical framework underlying behind the "liquidity shocks" in options. We discuss the market model in the context of possible liquidity shocks. Let us assume that $\mathbb{P}$ is the actual

probability measure and (Ω, $\mathbb{F}$,$\mathbb{P}$) constitutes the complete probability space. We consider a financial market that is vulnerable to liquidity shocks and consists of a stock and a risk-free asset (cash), with a finite investment time horizon $T < \infty$, corresponding to the expiry date of all securities in this model. To keep things simple, we adopt discounted pricing procedures, which guarantee that the cash value is always one and the interest rate is always zero. To represent the total wealth, the proportion of wealth invested in the stock, and the discounted stock price at time $\tau \in [0, T]$, we define $(X_\tau, \pi_\tau, S_\tau)$ on $\mathbb{R} \times \mathbb{R} \times \mathbb{R}^+$. This market is incomplete due to the presence of liquidity shocks, which is a source of liquidity risk. This section provides an overview of the model developed by Ludkovski and Shen [104]. For a detailed derivation of their results, the reader is referred to [104]. The starting point for the utility-based pricing approach is the value functions $U^i(S, X, \tau)$ for the optimal investment problem in the presence of a contingent claim,

$$U^i(S, X, \tau) = \sup_{\pi_\tau \in \mathbb{A}} \mathbb{E}^{\mathbb{P}}_{S,X,\tau,i}[-e^{-\gamma(X_T + hS_T)}], i = 0,\ 1, \tag{5.2.1}$$

where the state variables in the liquidity state at time $\tau \in [0, T]$ are $(X_\tau, \pi_\tau, S_\tau)$. Here, $\mathbb{A}$ denotes the set of acceptable trading strategies π_τ, T is the expiry date of all assets, and $\mathbb{E}^{\mathbb{P}}$ stands for the expectation under measure $\mathbb{P}$ (the real-world probability). Conventional techniques for stochastic control suggest the following for a holder of a bounded contingent claim paying out $\Phi(S_T)$ at terminal time T, the optimum value functions $U^i(S, X, \tau)$ are given by

$$U^i(S, X, \tau) = e^{-\gamma X - \gamma R^i(S,\tau)},$$

where the prices of the options in the two states are represented by $R^i(S, \tau)$, $i = 0, 1$ and γ is a risk aversion measure. Consequently, the unique viscosity solution of the coupled semi-linear parabolic-ordinary system (5.2.2) unique viscosity solution is represented by the pair (R^0, R^1), which satisfies the following [104]:

$$\begin{cases} R^0_\tau + \frac{1}{2}\sigma^2 S^2 R^0_{SS} - \frac{\nu_{01}}{\gamma} e^{-\gamma(R^1 - R^0)} + \frac{(d_0 + \nu_{01})}{\gamma} = 0, \\ R^1_\tau - \frac{\nu_{10}}{\gamma} e^{-\gamma(R^0 - R^1)} + \frac{\nu_{10}}{\gamma} = 0. \end{cases} \tag{5.2.2}$$

with the terminal conditions

$$R^i(S, T) = \Phi(S). \tag{5.2.3}$$

Here, the underlying price $S \geq 0$ and time satisfies $T \geq \tau \geq 0$, i.e., backward in time. The parameter $\sigma > 0$ represents the volatility of the stock. The constraint ν_{01} is the transition rate from state 0 to 1 and ν_{10} is the transition rate from state 1 to 0 (assuming the market to have two states, namely, liquid-0 and illiquid-1). Furthermore, $d_0 = \frac{\mu}{2\sigma^2}$, where μ is the drift. Under the illiquidity shocks, the value function for the best investment is:

$$V^i(X, \tau) = \sup_{\pi_\tau \in \mathbb{A}} \mathbb{E}^{\mathbb{P}}_{X,\tau,i}[-e^{-\gamma X_T}] = -e^{-\gamma X} F_i(\tau), \quad i = 0,\ 1, \tag{5.2.4}$$

where $F_0(\tau)$ and $F_1(\tau)$ are the solutions of the ODE system $F'(\tau) = (\mathcal{D} - \mathcal{A})F(\tau)$ with

$$\mathcal{D} = \begin{bmatrix} d_0 & 0 \\ 0 & 0 \end{bmatrix}, \quad \mathcal{A} = \begin{bmatrix} -\nu_{01} & \nu_{01} \\ \nu_{10} & -\nu_{10} \end{bmatrix}, \quad F(\tau) \equiv [F_0(\tau), F_1(\tau)], \quad F(T) \equiv [1, 1].$$

Specifically, solutions are given by:

$$F_0(\tau) = c_1 e^{\lambda_1 \tau} + c_2 e^{\lambda_2 \tau}, \quad F_1(\tau) = \frac{1}{\nu_{01}} \{c_1(d_0 + \nu_{01} - \lambda_1) e^{\lambda_1 \tau} + c_1(d_0 + \nu_{01} - \lambda_2) e^{\lambda_2 \tau}\},$$

where

$$c_1 = \frac{\lambda_2 - d_0}{\lambda_2 - \lambda_1} e^{-\lambda_1 T}, \quad c_2 = \frac{\lambda_1 - d_0}{\lambda_1 - \lambda_2} e^{-\lambda_2 T}, \quad \lambda_{1,2} = \frac{d_0 + \nu_{01} + \nu_{10} \pm \sqrt{(d_0 + \nu_{01} + \nu_{10})^2 - 4 d_0 \nu_{10}}}{2}.$$

The indifference prices

$$p = R^0 + \frac{\ln F_0(\tau)}{\gamma}, \quad q = R^1 + \frac{\ln F_1(\tau)}{\gamma},$$

will satisfy the parabolic-ordinary system

$$\begin{cases} p_\tau + \frac{1}{2}\sigma^2 S^2 p_{SS} - \frac{\nu_{01}}{\gamma} e^{-\gamma(q-p)} + \frac{(d_0 + \nu_{01})}{\gamma} - \frac{1}{\gamma} \frac{F_0'}{F_0} = 0, \\ q_\tau - \frac{\nu_{10}}{\gamma} e^{-\gamma(p-q)} + \frac{\nu_{10}}{\gamma} - \frac{1}{\gamma} \frac{F_1'}{F_1} = 0, \end{cases} \tag{5.2.5}$$

with the terminal conditions

$$p(S, T) = q(S, T) = \Phi(S). \tag{5.2.6}$$

Albeit the problem (5.2.5) is backward in time and degenerate, we can convert it into forward in time and a non-degenerate problem by applying the transformations $t = T - \tau$, $u = \gamma R^0$ and $v = \gamma R^1$, i.e.,

$$\begin{cases} u_t = \frac{1}{2}\sigma^2 S^2 u_{SS} - a e^{-(v-u)} + b, \\ v_t = c - c e^{-(u-v)}, \end{cases} \tag{5.2.7}$$

where $a = \nu_{01}$, $b = d_0 + \nu_{01}$ and $c = \nu_{10}$. According to (5.2.6), we consider the initial conditions to be

$$u(S, 0) = v(S, 0) = \Phi(S). \tag{5.2.8}$$

Considering the solutions $u(S, t)$ and $v(S, t)$ of the following localised system of PDE (5.2.9) in the spatial domain $\Omega^* = (S^L, S^R)$:

$$\frac{\partial u}{\partial t} = \mathscr{L} u(S, t), \qquad \frac{\partial v}{\partial t} = \mathscr{L}^* v(S, t), \tag{5.2.9}$$

where

$$\mathscr{L} u(S, t) = \frac{1}{2}\sigma^2 S^2 u_{SS} - a e^{-(v-u)} + b, \quad \mathscr{L}^* v(S, t) = c - c e^{-(u-v)}. \tag{5.2.10}$$

The initial and boundary conditions for a call option can be defined as:

$$\Phi(S) = \max(S - K, 0),$$

$$u(S,t) = v(S,t) = \begin{cases} 0 & : \quad S \to S^L, \\ S-K & : \quad S \to S^R, \end{cases}$$

where K is the strike price.

Given that the American option can be exercised at any time until maturity, it can be reformulated as a non-linear complementarity problem (NLCP) within a liquidity-switching economy,

$$\begin{cases} \frac{\partial u}{\partial t} - \mathscr{L}u(S,t) & \geq & 0 & (S,t) \in \mathbb{R}^+ \times J, \\ \frac{\partial v}{\partial t} - \mathscr{L}^* v(S,t) & \geq & 0 & (S,t) \in \mathbb{R}^+ \times J, \\ u(S,t) - \Phi(S) & \geq & 0 & (S,t) \in \mathbb{R}^+ \times J, \\ v(S,t) - \Phi(S) & \geq & 0 & (S,t) \in \mathbb{R}^+ \times J, \\ \left(\frac{\partial u}{\partial t} - \mathscr{L}u(S,t)\right)\left(u(S,t) - \Phi(S)\right) & = & 0 & (S,t) \in \mathbb{R}^+ \times J, \\ \left(\frac{\partial v}{\partial t} - \mathscr{L}^* v(S,t)\right)\left(v(S,t) - \Phi(S)\right) & = & 0 & (S,t) \in \mathbb{R}^+ \times J, \\ u(S,0) & = & \Phi(S) & S \in \mathbb{R}^+, \\ v(S,0) & = & \Phi(S) & S \in \mathbb{R}^+, \end{cases} \tag{5.2.11}$$

where $J = (0,T]$ and the spatial operator is defined as previously described, and the American option's boundary conditions are

$$u(S,t) = v(S,t) = \begin{cases} 0 & : \quad S \to S^L, \\ S-K & : \quad S \to S^R. \end{cases} \tag{5.2.12}$$

5.3 Discretization

In this section, we discuss the BDF1 and BDF2 temporal discretization techniques for the system of coupled PDEs (5.3.1) on the reduced domain $\Omega^* = (S^L, S^R)$ and let $\phi(S,t) = \frac{1}{2}\sigma^2 S^2$.

$$\begin{cases} \frac{\partial u}{\partial t} = \phi(S,t)u_{SS} - ae^{-(v-u)} + b, \\ \frac{\partial v}{\partial t} = c - ce^{-(u-v)}, \qquad \forall (S,t) \in \Omega^* \times \bar{J}. \end{cases} \tag{5.3.1}$$

We initially discretize the system (5.3.1) in temporal direction with uniform grid $t_n = nk$, $n = 0,1,2,\ldots,N$, and in spatial direction with uniform grid $S^m = mh$, $m = 0,1,2,\ldots,M$, where k is the uniform temporal mesh length and h is the uniform spatial mesh length. Let the solution $u(S^m, t_n)$ be abbreviated as u_n^m.

For the spatial discretization, we introduce the finite difference operators. Denoting $(u_i)_{\bar{S}} \approx \frac{u_i - u_{i-1}}{h}$ and $(u_i)_S \approx \frac{u_{i+1}-u_i}{h}$ as the backward and forward difference operators, respectively, the central difference operators are defined as $(u_i)_{\hat{S}} \approx \frac{u_{i+1}-u_{i-1}}{2h}$, $(u_i)_{S\bar{S}} \approx \frac{u_{i+1}-2u_i+u_{i-1}}{h^2}$. We now briefly discuss the two IMEX discretisation methods to solve the coupled PDEs (5.3.1).

5.3.1 IMEX-BDF1 method

$$\frac{u_{n+1}^m - u_n^m}{k} = \mathscr{L}u_{n+1}^m, \qquad \frac{v_{n+1}^m - v_n^m}{k} = \mathscr{L}^* v_{n+1}^m, \quad n,\ m \geq 0, \tag{5.3.2}$$

$$u_{n+1}^m(S^L) = v_{n+1}^m(S^L) = 0, \qquad u_{n+1}^m(S^R) = v_{n+1}^m(S^R) = S - K, \tag{5.3.3}$$

$$\mathscr{L}u_{n+1}^m = \phi(S^m, t_{n+1})(u_{S\bar{S}})_{n+1}^m - ae^{(u_{n+1}^m - v_{n+1}^m)} + b, \quad \mathscr{L}^* v_{n+1}^m = c - ce^{(v_{n+1}^m - u_{n+1}^m)}. \tag{5.3.4}$$

Using Taylor expansion up to the second order, we can obtain an approximation of the nonlinear implicit term:

$$\begin{aligned} e^{u_{n+1}^m - v_{n+1}^m} &= e^{u_n^m - v_n^m}(1 + v_n^m - u_n^m) + e^{u_n^m - v_n^m}(u_{n+1}^m - v_{n+1}^m), \\ e^{v_{n+1}^m - u_{n+1}^m} &= e^{v_n^m - u_n^m}(1 + u_n^m - v_n^m) + e^{v_n^m - u_n^m}(v_{n+1}^m - u_{n+1}^m). \end{aligned} \tag{5.3.5}$$

Thus, we have the linearised IMEX BDF1 scheme as

$$\begin{aligned} \tfrac{u_{n+1}^m - u_n^m}{k} &= \phi(S^m, t_{n+1})(u_{S\bar{S}})_{n+1}^m - a(e^{u_n^m - v_n^m}(1 + v_n^m - u_n^m) + e^{u_n^m - v_n^m}(u_{n+1}^m - v_{n+1}^m)) + b, \\ \tfrac{v_{n+1}^m - v_n^m}{k} &= c - c(e^{v_n^m - u_n^m}(1 + u_n^m - v_n^m) + e^{v_n^m - u_n^m}(v_{n+1}^m - u_{n+1}^m)), \quad n \geq 0, \end{aligned} \tag{5.3.6}$$

along with the boundary conditions

$$u_{n+1}^m(S^L) = v_{n+1}^m(S^L) = 0, \qquad u_{n+1}^m(S^R) = v_{n+1}^m(S^R) = S - K. \tag{5.3.7}$$

5.3.2 IMEX-BDF2 method

IMEX-BDF2 is a second-order approach that balances accuracy and computing cost. It avoids the complexity of higher-order techniques while offering more accuracy than first-order techniques like backward Euler. The BDF2 formulation is a suitable choice for large-scale simulations as it reduces computational overhead compared to other IMEX techniques with similar stability, including Runge-Kutta IMEX schemes. Due to stability restrictions on the time step, fully explicit methods are not suitable for stiff systems, although they are computationally simpler. In contrast, fully implicit approaches are stable for stiff problems but computationally expensive as they require solving complex nonlinear systems at each time step. When second-order precision is sufficient, IMEX-BDF2 is an appropriate choice as it is simpler to implement and computationally efficient than higher-order IMEX Runge-Kutta techniques.

Similar to MEX-BDF1, we can drive the IMEX-BDF2 scheme as:

$$\begin{aligned} \tfrac{3u_{n+1}^m - 4u_n^m + u_{n-1}^m}{2k} &= \phi(S^m, t_{n+1})(u_{S\bar{S}})_{n+1}^m - a(e^{u_n^m - v_n^m}(1 + v_n^m - u_n^m) + e^{u_n^m - v_n^m}(u_{n+1}^m - v_{n+1}^m)) + b, \\ \tfrac{3v_{n+1}^m - 4v_n^m + v_{n-1}^m}{2k} &= c - c(e^{v_n^m - u_n^m}(1 + u_n^m - v_n^m) + e^{v_n^m - u_n^m}(v_{n+1}^m - u_{n+1}^m)), \quad n \geq 1, \end{aligned} \tag{5.3.8}$$

with the boundary conditions

$$u_{n+1}^m(S^L) = v_{n+1}^m(S^L) = 0, \qquad u_{n+1}^m(S^R) = v_{n+1}^m(S^R) = S - K. \tag{5.3.9}$$

The BDF2 approach requires two initial values at the zeroth and first-time levels. At the zeroth time level, the initial condition yields the value (u_0^m, v_0^m), and the backward difference technique of order one can be used to determine the value (u_1^m, v_1^m).

We now demonstrate the stability of both the time semi-discretization schemes. The Young's inequality will be frequently applied for all $a, b \in \mathbb{R}$ with ϵ^* (valid for every $\epsilon^* > 0$), i.e,

$$(a, b) \leq \epsilon^* a^2 + \frac{1}{4\epsilon^*} b^2. \tag{5.3.10}$$

Considering the solutions u_n, v_n and $\tilde{u}_n, \tilde{v}_n$ of the equation (5.3.6) and the perturbed equation (5.3.11), respectively. Then,

$$\begin{aligned} \tfrac{\tilde{u}^m_{n+1}-\tilde{u}^m_n}{k} &= \phi(S^m, t_{n+1})(\tilde{u}_{S\bar{S}})^m_{n+1} - a(e^{\tilde{u}^m_n - \tilde{v}^m_n}(1 + \tilde{v}^m_n - \tilde{u}^m_n) + e^{\tilde{u}^m_n - \tilde{v}^m_n}(\tilde{u}^m_{n+1} - \tilde{v}^m_{n+1})) + b + \mathcal{T}^m_{n+1}, \\ \tfrac{\tilde{v}^m_{n+1}-\tilde{v}^m_n}{k} &= c - c(e^{\tilde{v}^m_n - \tilde{u}^m_n}(1 + \tilde{u}^m_n - \tilde{v}^m_n) + e^{\tilde{v}^m_n - \tilde{u}^m_n}(\tilde{v}^m_{n+1} - \tilde{u}^m_{n+1})) + \mathcal{R}^m_{n+1}, \quad n \geq 0, \end{aligned} \tag{5.3.11}$$

combined with the conditions at the boundaries,

$$\tilde{u}^m_{n+1}(S^L) = \tilde{v}^m_{n+1}(S^L) = 0, \qquad \tilde{u}^m_{n+1}(S^R) = \tilde{v}^m_{n+1}(S^R) = S - K, \tag{5.3.12}$$

It is easy to check that for BDF1, $\mathcal{T}^m_{n+1}, \mathcal{R}^m_{n+1} \leq Ck$. We examine the effects of the perturbations $\mathcal{T}^m_j, \mathcal{R}^m_j$ on the data at each subsequent time level t_j as time progresses. To prove the stability of time semi-discretization schemes, we show that the error at each time level is bounded by the error at the initial time levels (t^m_0 & t^m_1; for all specified techniques) and is a bounded multiple of the perturbations presented.

The error representation can be precisely defined as

$$\mathcal{P}^m_n := \tilde{u}^m_n - u^m_n, \quad \mathcal{Q}^m_n := \tilde{v}^m_n - v^m_n. \tag{5.3.13}$$

Since the referenced equations $(5.3.6 - 5.3.7)$ and the perturbed equations $(5.3.11 - 5.3.12)$ have the same boundary conditions, $\mathcal{P}^m_n$ and $\mathcal{Q}^m_n$ will therefore have zero values at the boundaries.

The error equation for IMEX-BDF1 scheme is obtained by subtracting $(5.3.11 - 5.3.12)$ from $(5.3.6 - 5.3.7)$, and is given as

$$\begin{aligned} \tfrac{\mathcal{P}^m_{n+1}-\mathcal{P}^m_n}{k} &= \phi(S_m, t_{n+1})(\mathcal{P}_{S\bar{S}})^m_{n+1} + aC_u e^{\mathcal{P}^m_n - \mathcal{Q}^m_n}(\mathcal{P}^m_n - \mathcal{Q}^m_n + \mathcal{Q}^m_{n+1} - \mathcal{P}^m_{n+1}) + \mathcal{T}^m_{n+1}, \\ \tfrac{\mathcal{Q}^m_{n+1}-\mathcal{Q}^m_n}{k} &= cC_v e^{\mathcal{Q}^m_n - \mathcal{P}^m_n}(\mathcal{Q}^m_n - \mathcal{P}^m_n + \mathcal{P}^m_{n+1} - \mathcal{Q}^m_{n+1}) + \mathcal{R}^m_{n+1}, \quad n, m \geq 0, \end{aligned} \tag{5.3.14}$$

combined with the following conditions at the boundaries:

$$\mathcal{P}_{n+1}(S^L) = \mathcal{Q}_{n+1}(S^L) = 0, \qquad \mathcal{P}_{n+1}(S^R) = \mathcal{Q}_{n+1}(S^R) = 0, \tag{5.3.15}$$

where

$$C_u = \max_{0 \leq n \leq N} e^{\tilde{u}_n - \tilde{v}_n} \text{ and } C_v = \max_{0 \leq n \leq N} e^{\tilde{v}_n - \tilde{u}_n}, \text{ and } (S, t) \in \Omega^* \times \bar{J}. \tag{5.3.16}$$

Similarly, we can obtain the error equation for BDF2 scheme, where $\mathcal{T}^m_{n+1}, \mathcal{R}^m_{n+1} \leq Ck^2$. To demonstrate the error estimate, we define the norm as

$$\|u\| = \sqrt{h \sum_{m=1}^{M-1} (u^m)^2}. \tag{5.3.17}$$

Throughout the analysis, C signifies a generic constant that is independent of the time step size, k, but may be affected by the data and the regularity of the analytical solution and may not be the same at each occurrence.

Lemma 5.3.1. *Let the exact solution be sufficiently smooth (at least first-order differentiable in time and second-order differentiable in space), and let $\mathcal{C}$ be a constant. Then the following results hold for $k \leq \mathcal{C}$.*

$$\|\mathcal{P}_n\| \leq 1 \qquad \|\mathcal{Q}_n\| \leq 1 \qquad n = 0, 1, 2, \cdots, N = \frac{T}{k}. \tag{5.3.18}$$

Proof. Considering the system represented by (5.3.14) with boundary condition (5.3.15), we can have

$$\frac{\mathcal{P}^m_{n+1} - \mathcal{P}^m_n}{k} = \phi(S_m, t_{n+1})(\mathcal{P}_{S\bar{S}})^m_{n+1} + aC_u e^{\mathcal{P}^m_n - \mathcal{Q}^m_n}(\mathcal{P}^m_n - \mathcal{Q}^m_n + \mathcal{Q}^m_{n+1} - \mathcal{P}^m_{n+1}) + \mathcal{T}^m_{n+1}, \tag{5.3.19}$$

$$\frac{\mathcal{Q}^m_{n+1} - \mathcal{Q}^m_n}{k} = cC_v e^{\mathcal{Q}^m_n - \mathcal{P}^m_n}(\mathcal{Q}^m_n - \mathcal{P}^m_n + \mathcal{P}^m_{n+1} - \mathcal{Q}^m_{n+1}) + \mathcal{R}^m_{n+1}, \tag{5.3.20}$$

$$\mathcal{P}^m_{n+1}(S^L) = \mathcal{Q}^m_{n+1}(S^L) = 0, \qquad \mathcal{P}^m_{n+1}(S^R) = \mathcal{Q}^m_{n+1}(S^R) = 0. \tag{5.3.21}$$

The conclusion will be established using mathematical induction. It is evident that $\mathcal{P}^m_0 \leq 1$ and $\mathcal{Q}^m_0 \leq 1$. We assume that at time t_n, the numerical error function has a L^2 bound, $\mathcal{P}^m_n \leq 1$ and $\mathcal{Q}^m_n \leq 1$ such that $e^{|\mathcal{P}^m_n - \mathcal{Q}^m_n|} \leq e^{C_{uv}}$. We then show that $\mathcal{P}^m_{n+1} \leq 1$ and $\mathcal{Q}^m_{n+1} \leq 1$ also hold.
Multiplying (5.3.17) by $h(\mathcal{P}^m_{n+1})$, and summing up for $m = 1, 2, \ldots, M-1$, we get

$$\begin{aligned}\frac{\langle \mathcal{P}^m_{n+1} - \mathcal{P}^m_n, h\mathcal{P}^m_{n+1}\rangle}{k} &= h\sum_{m=1}^{M-1} \phi(S^m, t_{n+1})(\mathcal{P}^m_{n+1})_{S\bar{S}}\mathcal{P}^m_{n+1} + C_1 h\sum_{m=1}^{M-1}(\mathcal{P}^m_n - \mathcal{Q}^m_n + \mathcal{Q}^m_{n+1} - \mathcal{P}^m_{n+1})\mathcal{P}^m_{n+1} \\ &+ h\sum_{m=1}^{M-1} \mathcal{T}^m_{n+1}\mathcal{P}^m_{n+1},\end{aligned} \tag{5.3.22}$$

where $\langle \cdot\ ,\ \cdot \rangle$ define the inner product and $C_1 = cC_v e^{C_{uv}}$. Using the identity $2\,(A - B, A) = A^2 - B^2 + (A - B)^2$ in left side of equation (5.3.22), and further simplifying the equation we get

$$\frac{\langle \mathcal{P}^m_{n+1} - \mathcal{P}^m_n, h\mathcal{P}^m_{n+1}\rangle}{k} \geq \frac{1}{2k}(\|\mathcal{P}_{n+1}\|^2 - \|\mathcal{P}_n\|^2 + \|\mathcal{P}_{n+1} - \mathcal{P}_n\|^2) \tag{5.3.23}$$

We now estimate the right-hand side of the equation (5.3.22), term by term. By the use of discrete Green formula (see [117]), we approximate the first term as:

$$\begin{aligned}&h\sum_{m=1}^{M-1} \phi(S^m, t_{n+1})(\mathcal{P}^m_{n+1})_{S\bar{S}}\mathcal{P}^m_{n+1} \\ &= -h\sum_{m=1}^{M} [\phi(S^m, t_{n+1})\mathcal{P}^m_{n+1}]_{\bar{S}}(\mathcal{P}^m_{n+1})_{\bar{S}} - \Phi(S^m, t_{n+1})\mathcal{P}^m_{n+1}(\mathcal{P}^m_{n+1})_S|_{m=0} \\ &+\phi(S^m, t_{n+1})\mathcal{P}^m_{n+1}(\mathcal{P}^m_{n+1})_{\bar{S}}|_{m=M}\end{aligned}$$

$$
\begin{aligned}
&= -h\sum_{m=1}^{M}(\phi(S^m,t_{n+1})\mathcal{P}_{n+1}^m)_{\bar{S}}(\mathcal{P}_{n+1}^m)_{\bar{S}}\\
&= -h\sum_{m=1}^{M}(\mathcal{P}_{n+1}^m)_{\bar{S}}[(\mathcal{P}_{n+1}^m)_{\bar{S}}\phi(S^m,t_{n+1})+(\mathcal{P}_{n+1}^{m-1})(\phi(S^m,t_{n+1}))_{\bar{S}}]\\
&\leq -h\sum_{m=1}^{M}(\mathcal{P}_{n+1}^m)_{\bar{S}}(\mathcal{P}_{n+1}^{m-1})(\phi(S^m,t_{n+1}))_{\bar{S}}. \qquad (5.3.24)
\end{aligned}
$$

Moreover, we obtain that

$$
\begin{aligned}
&h\sum_{m=1}^{M-1}\phi(S^m,t_{n+1})(\mathcal{P}_{n+1}^m)_{S\bar{S}}\mathcal{P}_{n+1}^m\\
&= -h\sum_{m=1}^{M}(\phi(S^m,t_{n+1})\mathcal{P}_{n+1}^m)_{\bar{S}}(\mathcal{P}_{n+1}^m)_{\bar{S}}\\
&= -h\sum_{m=1}^{M}(\mathcal{P}_{n+1}^m)_{\bar{S}}[(\mathcal{P}_{n+1}^m)_{\bar{S}}\phi(S^{m-1},t_{n+1})+(\mathcal{P}_{n+1}^m)(\phi(S^m,t_{n+1}))_{\bar{S}}]\\
&\leq -h\sum_{m=1}^{M}(\mathcal{P}_{n+1}^m)_{\bar{S}}\mathcal{P}_{n+1}^m(\phi(S^m,t_{n+1}))_{\bar{S}}. \qquad (5.3.25)
\end{aligned}
$$

Now, adding up the inequalities (5.3.24) and (5.3.25), we get

$$
\begin{aligned}
h\sum_{m=1}^{M-1}\phi(S^m,t_{n+1})(\mathcal{P}_{n+1}^m)_{S\bar{S}}\mathcal{P}_{n+1}^m &\leq -\frac{1}{2}h\sum_{m=1}^{M}\phi(S^m,t_{n+1})_{\bar{S}}(\mathcal{P}_{n+1}^{m-1}+\mathcal{P}_{n+1}^m)(\mathcal{P}_{n+1}^m)_{\bar{S}}\\
&= -\frac{1}{2}\sum_{m=1}^{M}\phi(S^m,t_{n+1})_{\bar{S}}((\mathcal{P}_{n+1}^m)^2-(\mathcal{P}_{n+1}^{m-1})^2)\\
&= -\frac{1}{2}\sum_{m=1}^{M}\phi(S^m,t_{n+1})_{\bar{S}}(\mathcal{P}_{n+1}^m)^2+\frac{1}{2}\sum_{m=1}^{M}(\phi(S^m,t_{n+1})_{\bar{S}}(\mathcal{P}_{n+1}^{m-1})^2\\
&= -\frac{1}{2}\sum_{m=1}^{M-1}\phi(S^m,t_{n+1})_{\bar{S}}(\mathcal{P}_{n+1}^m)^2+\frac{1}{2}\sum_{m=0}^{M-1}(\phi(S^m,t_{n+1})_{\bar{S}}(\mathcal{P}_{n+1}^m)^2\\
&= -\frac{1}{2}\sum_{m=1}^{M-1}\phi(S^m,t_{n+1})_{\bar{S}}(\mathcal{P}_{n+1}^m)^2+\frac{1}{2}\sum_{m=1}^{M-1}(\phi(S_{i+1},t_{n+1})_{\bar{S}}(\mathcal{P}_{n+1}^m)^2\\
&= \frac{1}{2}\sum_{m=1}^{M-1}(\phi(S^{m+1},t_{n+1})_{\bar{S}}-(\phi(S^m,t_{n+1})_{\bar{S}})(\mathcal{P}_{n+1}^m)^2\\
&= \frac{\sigma^2}{2}h\sum_{m=1}^{M-1}(\mathcal{P}_{n+1}^m)^2\leq C_2\|\mathcal{P}_{n+1}\|^2,\quad C_2=\frac{\sigma^2}{2}. \qquad (5.3.26)
\end{aligned}
$$

Now, we use the cauchy-Schwartz inequality for the other terms as

$$
h\sum_{i=1}^{M-1}U_{n+1}^mV_{n+1}^m\leq\|U_{n+1}\|\|V_{n+1}\|. \qquad (5.3.27)
$$

Further, we estimate the second term of the right-hand side of the equation (5.3.22) as

$$
h\sum_{i=1}^{M-1}(\mathcal{P}_n^m-\mathcal{Q}_n^m+\mathcal{Q}_{n+1}^m-\mathcal{P}_{n+1}^m)\mathcal{P}_{n+1}^m\leq\|\mathcal{P}_n-\mathcal{Q}_n+\mathcal{Q}_{n+1}-\mathcal{P}_{n+1}\|\|\mathcal{P}_{n+1}\|, \qquad (5.3.28)
$$

and we estimate the third term of the right-hand side of the equation (5.3.22) as

$$h\sum_{i=1}^{M-1}\mathcal{T}_{n+1}^{m}\mathcal{P}_{n+1}^{m}\leq\|\mathcal{P}_{n+1}\|\|\mathcal{T}_{n+1}\|. \tag{5.3.29}$$

Combining (5.3.23), (5.3.26), (5.3.28) and (5.3.29), we obtain

$$\begin{aligned}\frac{1}{2k}(\|\mathcal{P}_{n+1}\|^2-\|\mathcal{P}_n\|^2+\|\mathcal{P}_{n+1}-\mathcal{P}_n\|^2) &\leq C_2\|\mathcal{P}_{n+1}\|^2+C_1\|\mathcal{P}_n-\mathcal{Q}_n+\mathcal{Q}_{n+1}-\mathcal{P}_{n+1}\|\|\mathcal{P}_{n+1}\|\\ &\quad+\|\mathcal{P}_{n+1}\|\|\mathcal{T}_{n+1}\|. \end{aligned}\tag{5.3.30}$$

$$\begin{aligned}\|\mathcal{P}_{n+1}\|^2-\|\mathcal{P}_n\|^2 &\leq 2kC_2\|\mathcal{P}_{n+1}\|^2+4kC_1(\|\mathcal{P}_n\|^2+\|\mathcal{Q}_n\|^2+\|\mathcal{Q}_{n+1}\|^2+\|\mathcal{P}_{n+1}\|^2)+kC_1\|\mathcal{P}_{n+1}\|^2\\ &\quad+k\|\mathcal{P}_{n+1}\|^2+k\|\mathcal{T}_{n+1}\|^2. \end{aligned}\tag{5.3.31}$$

$$\begin{aligned}\|\mathcal{P}_{n+1}\|^2-\|\mathcal{P}_n\|^2 &\leq k(2C_2+5C_1+1)\|\mathcal{P}_{n+1}\|^2+4kC_1\|\mathcal{Q}_{n+1}\|^2+4kC_1(\|\mathcal{P}_n\|^2+\|\mathcal{Q}_n\|^2)\\ &\quad+k\|\mathcal{T}_{n+1}\|^2. \end{aligned}\tag{5.3.32}$$

Multiplying (5.3.18) by $h(\mathcal{Q}_{n+1}^m)$, and summing up for $m=1,2,\ldots,M-1$

$$\begin{aligned}\frac{\langle\mathcal{Q}_{n+1}^m-\mathcal{Q}_n^m,h\mathcal{Q}_{n+1}^m\rangle}{k} &= C_3h\sum_{m=1}^{M-1}(\mathcal{Q}_n^m-\mathcal{P}_n^m+\mathcal{P}_{n+1}^m-\mathcal{Q}_{n+1}^m)\mathcal{Q}_{n+1}^m\\ &\quad+h\sum_{m=1}^{M-1}\mathcal{R}_{n+1}^m\mathcal{Q}_{n+1}^m, \end{aligned}\tag{5.3.33}$$

where $C_3=cC_ve^{C_{uv}}$. Simplifying the equation (5.3.24) and using Cauchy-Schwartz inequality, we get

$$\begin{aligned}\frac{1}{2k}(\|\mathcal{Q}_{n+1}\|^2-\|\mathcal{Q}_n\|^2+\|\mathcal{Q}_{n+1}-\mathcal{Q}_n\|^2) &\leq C_3\|\mathcal{Q}_n-\mathcal{P}_n+\mathcal{P}_{n+1}-\mathcal{Q}_{n+1}\|\|\mathcal{Q}_{n+1}\|\\ &\quad+\|\mathcal{Q}_{n+1}\|\|\mathcal{R}_{n+1}\|. \end{aligned}\tag{5.3.34}$$

After simplifying the above inequality, we get

$$\begin{aligned}\|\mathcal{Q}_{n+1}\|^2-\|\mathcal{Q}_n\|^2 &\leq k(5C_3+1)\|\mathcal{Q}_{n+1}\|^2+4kC_3\|\mathcal{P}_{n+1}\|^2+4kC_3(\|\mathcal{P}_n\|^2+\|\mathcal{Q}_n\|^2)\\ &\quad+k\|\mathcal{R}_{n+1}\|^2. \end{aligned}\tag{5.3.35}$$

Adding up the inequalities yields

$$\begin{aligned}\|\mathcal{P}_{n+1}\|^2-\|\mathcal{P}_n\|^2+\|\mathcal{Q}_{n+1}\|^2-\|\mathcal{Q}_n\|^2 &\leq k\mathcal{C}(\|\mathcal{P}_{n+1}\|^2+\|\mathcal{Q}_{n+1}\|^2)+k\mathcal{C}(\|\mathcal{P}_n\|^2+\|\mathcal{Q}_n\|^2)\\ &\quad+k(\|\mathcal{T}_{n+1}\|^2+\|\mathcal{R}_{n+1}\|^2), \end{aligned}\tag{5.3.36}$$

where $\mathcal{C}* = \max(C_1, C_2, C_3)$ and $\mathcal{C} = (7\mathcal{C}*+1)$. To maintain the generality, let us suppose that $0 \leq \mathcal{M} \leq N$ is an integer. Then, after summing up the inequality (5.3.36) from $n = 0$ to $n = \mathcal{M}$, we get

$$\begin{aligned}\|\mathcal{P}_{\mathcal{M}+1}\|^2 - \|\mathcal{P}_0\|^2 + \|\mathcal{Q}_{\mathcal{M}+1}\|^2 - \|\mathcal{Q}_0\|^2 \quad &\leq \quad \mathcal{C}k(\|\mathcal{P}_{\mathcal{M}+1}\|^2 + \|\mathcal{Q}_{\mathcal{M}+1}\|^2) + \mathcal{C}k\sum_{n=1}^{\mathcal{M}}(\|\mathcal{P}_n\|^2 + \|\mathcal{Q}_n\|^2) \\ &\quad + \mathcal{C}k\sum_{n=0}^{\mathcal{M}}(\|\mathcal{P}_n\|^2 + \|\mathcal{Q}_n\|^2) + k\sum_{n=0}^{\mathcal{M}}(\|\mathcal{T}_{n+1}\|^2 + \|\mathcal{R}_{n+1}\|^2).\end{aligned}$$

Now, considering that the k is tiny enough such that $(1 - k\mathcal{C}) > 0$ or $k < \frac{1}{\mathcal{C}}$, then above inequality implies

$$\|\mathcal{P}_{\mathcal{M}+1}\|^2 + \|\mathcal{Q}_{\mathcal{M}+1}\|^2 \quad \leq \quad C(\|\mathcal{P}_0\|^2 + \|\mathcal{Q}_0\|^2 + k\sum_{n=1}^{\mathcal{M}}(\|\mathcal{P}_n\|^2 + \|\mathcal{Q}_n\|^2) + k\sum_{n=0}^{\mathcal{M}}(\|\mathcal{T}_{n+1}\|^2 + \|\mathcal{R}_{n+1}\|^2)).$$

We know that $\mathcal{M}k \leq T$, thus, we have

$$\|\mathcal{P}_{\mathcal{M}+1}\|^2 + \|\mathcal{Q}_{\mathcal{M}+1}\|^2 \leq C(\|\mathcal{P}_0\|^2 + \|\mathcal{Q}_0\|^2 + k\sum_{n=1}^{\mathcal{M}-1}(\|\mathcal{P}_{n+1}\|^2 + \|\mathcal{Q}_{n+1}\|^2) + \max_{0\leq n\leq \mathcal{M}} k(\|\mathcal{T}_{n+1}\|^2 + \|\mathcal{R}_{n+1}\|^2)),$$

where C is a generic constant that is unaffected by the extent of the grid. The discrete Gronwall's inequality (for more details, see Lemma 3.1 in [82]) is finally applied, and we obtain

$$\|\mathcal{P}_{\mathcal{M}+1}\|^2 + \|\mathcal{Q}_{\mathcal{M}+1}\|^2 \leq C(\|\mathcal{P}_0\|^2 + \|\mathcal{Q}_0\|^2 + \max_{0\leq n\leq \mathcal{M}}(\|\mathcal{T}_{n+1}\|^2 + \|\mathcal{R}_{n+1}\|^2)). \tag{5.3.37}$$

From (5.3.37), we can get,

$$\|\mathcal{P}_{\mathcal{M}+1}\|^2 + \|\mathcal{Q}_{\mathcal{M}+1}\|^2 \quad \leq \quad Ck^2. \tag{5.3.38}$$

If $k \leq (\frac{1}{\sqrt{C}})$, we have

$$\|\mathcal{P}_{\mathcal{M}+1}\| \leq 1 \qquad \text{and} \qquad \|\mathcal{Q}_{\mathcal{M}+1}\| \leq 1. \tag{5.3.39}$$

This completes the proof. □

Theorem 5.3.2 (BDF1)**.** *Suppose that the exact solution (u, v) of equation* (5.3.1) *possesses sufficient regularity with respect to norm (5.3.17). Let (u_{n+1}, v_{n+1}), be the numerical solution of the IMEX scheme* (5.3.6)*. Then for $k \to 0$, we have the following convergence results*

$$\|u - u_{n+1}\| + \|v - v_{n+1}\| \leq Ck.$$

Remark 1: We must first determine u_1 and v_1 (which may be done using the first-order backward Euler method) to begin implementing the second-order scheme (5.3.8).

Lemma 5.3.3. *Let the exact solution be sufficiently smooth (at least second-order differentiable in time and second-order differentiable in space) and there exists a constant $\mathcal{C}$. Then the following results hold for $k \leq \mathcal{C}$.*

$$\|\mathcal{P}_n\| \leq 1 \qquad \|\mathcal{Q}_n\| \leq 1 \qquad n = 1, 2, \cdots, N = \frac{T}{k}. \tag{5.3.40}$$

Proof. Considering the error equation for system (5.3.4) given as

$$\frac{3\mathcal{P}^m_{n+1}-4\mathcal{P}^m_n+\mathcal{P}^m_{n-1}}{2k}=\phi(S_m,t_{n+1})(\mathcal{P}_{S\bar{S}})^m_{n+1}+aC_ue^{\mathcal{P}^m_n-\mathcal{Q}^m_n}(\mathcal{P}^m_n-\mathcal{Q}^m_n+\mathcal{Q}^m_{n+1}-\mathcal{P}^m_{n+1})+\mathcal{T}^m_{n+1}, \quad (5.3.41)$$

$$\frac{3\mathcal{Q}^m_{n+1}-4\mathcal{Q}^m_n+\mathcal{Q}^m_{n-1}}{2k}=cC_ve^{\mathcal{Q}^m_n-\mathcal{P}^m_n}(\mathcal{Q}^m_n-\mathcal{P}^m_n+\mathcal{P}^m_{n+1}-\mathcal{Q}^m_{n+1})+\mathcal{R}^m_{n+1}, \quad (5.3.42)$$

$$\mathcal{P}^m_{n+1}(S^L)=\mathcal{P}^m_{n+1}(S^L)=0, \qquad \mathcal{Q}^m_{n+1}(S^R)=\mathcal{Q}^m_{n+1}(S^R)=0. \quad (5.3.43)$$

It is evident that $\mathcal{P}^m_0\le 1$ and $\mathcal{Q}^m_0\le 1$. We assume that at time t_n, the numerical error function has an L^2 bound, $\mathcal{P}^m_n\le 1$ and $\mathcal{Q}^m_n\le 1$ such that $e^{|\mathcal{P}^m_n-\mathcal{Q}^m_n|}\le e^{C_{uv}}$. We will then show that $\mathcal{P}^m_{n+1}\le 1$ and $\mathcal{Q}^m_{n+1}\le 1$also hold.

Multiplying (5.3.17) by $h(\mathcal{P}^m_{n+1})$ and summing up for $m=1,2,\dots,M-1$

$$\begin{aligned}\frac{\langle 3\mathcal{P}^m_{n+1}-4\mathcal{P}^m_n+\mathcal{P}^m_{n-1},h\mathcal{P}^m_{n+1}\rangle}{2k} &= h\sum_{m=1}^{M-1}\phi(S^m,t_{n+1})(\mathcal{P}^m_{n+1})_{S\bar{S}}\mathcal{P}^m_{n+1}\\ &\quad +C_1h\sum_{m=1}^{M-1}(\mathcal{P}^m_n-\mathcal{Q}^m_n+\mathcal{Q}^m_{n+1}-\mathcal{P}^m_{n+1})\mathcal{P}^m_{n+1}\\ &\quad +h\sum_{m=1}^{M-1}\mathcal{T}^m_{n+1}\mathcal{P}^m_{n+1}, \end{aligned} \quad (5.3.44)$$

where $\langle\cdot\ ,\ \cdot\rangle$ define the inner product and $C_1=cC_ve^{C_{uv}}$. Using the identity $2\,(3a-4b+c,a)=a^2+(2a-b)^2-b^2-(2b-c)^2+(a-2b+c)^2$ in left side of equation (5.3.44) and simplifying the equation, we get

$$\frac{\langle 3\mathcal{P}^m_{n+1}-4\mathcal{P}^m_n+\mathcal{P}^m_{n-1},h\mathcal{P}_{n+1}\rangle}{2k}\ge\frac{1}{4k}(\|\mathcal{P}_{n+1}\|^2-\|\mathcal{P}_n\|^2+\|2\mathcal{P}_{n+1}-\mathcal{P}_n\|^2-\|2\mathcal{P}_n-\mathcal{P}_{n-1}\|^2). \quad (5.3.45)$$

We now estimate the first term of the right-hand side of equation (5.3.44) as:

$$h\sum_{m=1}^{M-1}\Phi(S^m,t_{n+1})(\mathcal{P}^m_{n+1})_{S\bar{S}}\mathcal{P}^m_{n+1}\le C_2\|\mathcal{P}_{n+1}\|^2, \quad C_2=\frac{\sigma^2}{2}. \quad (5.3.46)$$

Now, we will use the Cauchy-Schwartz inequality for the other terms as

$$h\sum_{m=1}^{M-1}U^m_{n+1}V^m_{n+1}\le\|U_{n+1}\|\|V_{n+1}\|. \quad (5.3.47)$$

Further, we estimate the second term of the right-hand side of the equation (5.3.44) as

$$h\sum_{m=1}^{M-1}(\mathcal{P}^m_n-\mathcal{Q}^m_n+\mathcal{Q}^m_{n+1}-\mathcal{P}^m_{n+1})\mathcal{P}^m_{n+1}\le\|\mathcal{P}_n-\mathcal{Q}_n+\mathcal{Q}_{n+1}-\mathcal{P}_{n+1}\|\|\mathcal{P}_{n+1}\|, \quad (5.3.48)$$

and we estimate the third term of the right-hand side of the equation (5.3.44) as

$$h\sum_{m=1}^{M-1}\mathcal{T}^m_{n+1}\mathcal{P}^m_{n+1}\le\|\mathcal{P}_{n+1}\|\|\mathcal{T}_{n+1}\|. \quad (5.3.49)$$

Combining (5.3.45), (5.3.46), (5.3.48) and (5.3.49), we obtain

$$\begin{aligned}\|\mathcal{P}_{n+1}\|^2 - \|\mathcal{P}_n\|^2 &+ \|2\mathcal{P}_{n+1} - \mathcal{P}_n\|^2 - \|2\mathcal{P}_n - \mathcal{P}_{n-1}\|^2 \\ &\leq 4kC_2\|\mathcal{P}_{n+1}\|^2 + 8kC_1(\|\mathcal{P}_n\|^2 + \|\mathcal{Q}_n\|^2 + \|\mathcal{Q}_{n+1}\|^2 + \|\mathcal{P}_{n+1}\|^2) + 2kC_1\|\mathcal{P}_{n+1}\|^2 \\ &\quad +2k\|\mathcal{P}_{n+1}\|^2 + 2k\|\mathcal{T}_{n+1}\|^2. \end{aligned} \tag{5.3.50}$$

$$\begin{aligned}\|\mathcal{P}_{n+1}\|^2 - \|\mathcal{P}_n\|^2 &+ \|2\mathcal{P}_{n+1} - \mathcal{P}_n\|^2 - \|2\mathcal{P}_n - \mathcal{P}_{n-1}\|^2 \\ &\leq 2k(2C_2 + 5C_1 + 1)\|\mathcal{P}_{n+1}\|^2 + 8kC_1\|\mathcal{Q}_{n+1}\|^2 + 8kC_1(\|\mathcal{P}_n\|^2 + \|\mathcal{Q}_n\|^2) \\ &\quad +2k\|\mathcal{T}_{n+1}\|^2. \end{aligned} \tag{5.3.51}$$

Multiplying (5.3.18) by $h(\mathcal{Q}^m_{n+1})$ and summing up for $m = 1, 2, \ldots, M-1$

$$\begin{aligned}\frac{\langle 3\mathcal{Q}^m_{n+1} - 4\mathcal{Q}^m_n + \mathcal{Q}^m_{n-1}, h\mathcal{Q}^m_{n+1}\rangle}{2k} &= C_3 h\sum_{m=1}^{M-1}(\mathcal{Q}^m_n - \mathcal{P}^m_n + \mathcal{P}^m_{n+1} - \mathcal{Q}^m_{n+1})\mathcal{Q}^m_{n+1} \\ &\quad +h\sum_{m=1}^{M-1}\mathcal{R}^m_{n+1}\mathcal{Q}^m_{n+1}, \end{aligned} \tag{5.3.52}$$

where $C_3 = cC_v e^{C_{uv}}$. Simplifying equation (5.3.24) and using Cauchy-Schwartz inequality, we obtain

$$\begin{aligned}\frac{1}{4k}(\|\mathcal{Q}_{n+1}\|^2 - \|\mathcal{Q}_n\|^2 + \|2\mathcal{Q}_{n+1} - \mathcal{Q}_n\|^2 - \|2\mathcal{Q}_n - \mathcal{Q}_{n-1}\|^2) &\leq C_3\|\mathcal{Q}_n - \mathcal{P}_n + \mathcal{P}_{n+1} - \mathcal{Q}_{n+1}\|\|\mathcal{Q}_{n+1}\| \\ &\quad +\|\mathcal{Q}_{n+1}\|\|\mathcal{R}_{n+1}\|. \end{aligned} \tag{5.3.53}$$

After simplifying the above inequality, we get

$$\begin{aligned}\|\mathcal{Q}_{n+1}\|^2 - \|\mathcal{Q}_n\|^2 &+ \|2\mathcal{Q}_{n+1} - \mathcal{Q}_n\|^2 - \|2\mathcal{Q}_n - \mathcal{Q}_{n-1}\|^2 \\ &\leq k(9C_3 + 2)\|\mathcal{Q}_{n+1}\|^2 + 8kC_3\|\mathcal{P}_{n+1}\|^2 + 8kC_3(\|\mathcal{P}_n\|^2 + \|\mathcal{Q}_n\|^2) \\ &\quad +2k\|\mathcal{R}_{n+1}\|^2. \end{aligned} \tag{5.3.54}$$

Adding up the inequalities (5.3.51) and (5.3.51), we get

$$\begin{aligned}\|\mathcal{Q}_{n+1}\|^2 - \|\mathcal{Q}_n\|^2 &+ \|2\mathcal{Q}_{n+1} - \mathcal{Q}_n\|^2 - \|2\mathcal{Q}_n - \mathcal{Q}_{n-1}\|^2 \\ &\quad +\|\mathcal{P}_{n+1}\|^2 - \|\mathcal{P}_n\|^2 + \|2\mathcal{P}_{n+1} - \mathcal{P}_n\|^2 - \|2\mathcal{P}_n - \mathcal{P}_{n-1}\|^2 \\ &\quad \leq k\mathcal{C}(\|\mathcal{P}_{n+1}\|^2 + \|\mathcal{Q}_{n+1}\|^2) + k\mathcal{C}(\|\mathcal{P}_n\|^2 + \|\mathcal{Q}_n\|^2) \\ &\quad +k(\|\mathcal{T}_{n+1}\|^2 + \|\mathcal{R}_{n+1}\|^2), \end{aligned} \tag{5.3.55}$$

where $\mathcal{C}* = \max(C_1, C_2, C_3)$ and $\mathcal{C} = 2(7\mathcal{C}*+1)$. To maintain the generality, let us suppose that $0 \leq \mathcal{M} \leq N$ is an integer. Then, after summing up the inequality (5.3.55) for $n = 0$ to $n = \mathcal{M}$, we have

$$\|\mathcal{P}_{\mathcal{M}}\|^2 - \|\mathcal{P}_0\|^2 + \|\mathcal{Q}_{\mathcal{M}+1}\|^2 - \|\mathcal{Q}_0\|^2 + \|2\mathcal{P}_{\mathcal{M}} - \mathcal{P}_{\mathcal{M}}\|^2 + \|2\mathcal{Q}_{\mathcal{M}+1} - \mathcal{Q}_{\mathcal{M}}\|^2$$

$$
\begin{aligned}
&-\|2\mathcal{P}_1-\mathcal{P}_0\|^2-\|2\mathcal{Q}_1-\mathcal{Q}_0\|^2\\
&\leq \mathcal{C}k\sum_{n=0}^{\mathcal{M}}(\|\mathcal{P}_{n+1}\|^2+\|\mathcal{Q}_{n+1}\|^2)+4kC_3\sum_{n=0}^{\mathcal{M}}(\|\mathcal{P}_n\|^2+\|\mathcal{Q}_n\|^2)+k\sum_{n=0}^{\mathcal{M}}(\|\mathcal{T}^{n+1}\|^2+\|\mathcal{R}^{n+1}\|^2),\\
&\|\mathcal{P}_{\mathcal{M}+1}\|^2-\|\mathcal{P}_0\|^2+\|\mathcal{Q}_{\mathcal{M}+1}\|^2-\|\mathcal{Q}_0\|^2+\|2\mathcal{P}_{\mathcal{M}+1}-\mathcal{P}_{\mathcal{M}}\|^2+\|2\mathcal{Q}_{\mathcal{M}+1}-\mathcal{Q}_{\mathcal{M}}\|^2\\
&-\|2\mathcal{P}_1-\mathcal{P}_0\|^2-\|2\mathcal{Q}_1-\mathcal{Q}_0\|^2\\
&\leq \mathcal{C}k(\|\mathcal{P}_{\mathcal{M}+1}\|^2+\|\mathcal{Q}_{\mathcal{M}+1}\|^2)+\mathcal{C}k\sum_{n=1}^{\mathcal{M}}(\|\mathcal{P}_n\|^2+\|\mathcal{Q}_n\|^2)+4kC_3\sum_{n=0}^{\mathcal{M}}(\|\mathcal{P}_n\|^2+\|\mathcal{Q}_n\|^2)\\
&+k\sum_{n=0}^{\mathcal{M}}(\|\mathcal{T}_{n+1}\|^2+\|\mathcal{R}_{n+1}\|^2).
\end{aligned}
$$

Now let us consider that the k is tiny enough such that $(1-k\mathcal{C})>0$ or $k<\frac{1}{\mathcal{C}}$. Then, the above inequality implies

$$
\begin{aligned}
\|\mathcal{P}_{\mathcal{M}+1}\|^2+\|\mathcal{Q}_{\mathcal{M}+1}\|^2 \quad\leq\quad & C(\|\mathcal{P}_0\|^2+\|\mathcal{Q}_0\|^2+\|2\mathcal{P}_1-\mathcal{P}_0\|^2+\|2\mathcal{Q}_1-\mathcal{Q}_0\|^2+k\sum_{n=1}^{\mathcal{M}}(\|\mathcal{P}_n\|^2+\|\mathcal{Q}_n\|^2)\\
&+k\sum_{n=0}^{\mathcal{M}}(\|\mathcal{T}_{n+1}\|^2+\|\mathcal{R}_{n+1}\|^2)). \qquad (5.3.56)
\end{aligned}
$$

We know that $\mathcal{M}k\leq T$. Thus, we have

$$
\begin{aligned}
\|\mathcal{P}_{\mathcal{M}+1}\|^2+\|\mathcal{Q}_{\mathcal{M}+1}\|^2 \quad\leq\quad & C(\|\mathcal{P}_0\|^2+\|\mathcal{Q}_0\|^2+\|2\mathcal{P}_1-\mathcal{P}_0\|^2+\|2\mathcal{Q}_1-\mathcal{Q}_0\|^2+k\sum_{n=1}^{\mathcal{M}-1}(\|\mathcal{P}_{n+1}\|^2+\|\mathcal{Q}_{n+1}\|^2)\\
&+\mathcal{M}k\max_{0\leq n\leq\mathcal{M}}(\|\mathcal{T}_{n+1}\|^2+\|\mathcal{R}_{n+1}\|^2)), \qquad (5.3.57)
\end{aligned}
$$

where C is a generic constant that is unaffected by the extent of the grid. The discrete Gronwall's inequality (for more details, see Lemma 3.1 in [82]) is applied to obtain

$$
\begin{aligned}
\|\mathcal{P}_{\mathcal{M}+1}\|^2+\|\mathcal{Q}_{\mathcal{M}+1}\|^2 \quad\leq\quad & C(\|\mathcal{P}_0\|^2+\|\mathcal{Q}_0\|^2+\|2\mathcal{P}_1-\mathcal{P}_0\|^2+\|2\mathcal{Q}_1-\mathcal{Q}_0\|^2\\
&+\max_{0\leq n\leq\mathcal{M}}(\|\mathcal{T}_{n+1}\|^2+\|\mathcal{R}_{n+1}\|^2)). \qquad (5.3.58)
\end{aligned}
$$

From (5.3.58), we can get

$$
\|\mathcal{P}_{\mathcal{M}+1}\|^2+\|\mathcal{Q}_{\mathcal{M}+1}\|^2 \quad\leq\quad Ck^4. \qquad (5.3.59)
$$

If $k\leq\left(\frac{1}{C^{\frac{1}{4}}}\right)$, we have

$$
\|\mathcal{P}_{\mathcal{M}+1}\|\leq 1 \qquad \text{and} \qquad \|\mathcal{Q}_{\mathcal{M}+1}\|\leq 1. \qquad (5.3.60)
$$

This completes the proof. □

Theorem 5.3.4 (BDF2)**.** *Let us suppose that there is sufficient regularity (with respect to the norm (5.3.17)) for the exact solution (u,v) of equation* (5.3.1)*. Let (u_{n+1},v_{n+1}) be the numerical solution of the IMEX scheme* (5.3.8)*. Then for $k\to 0$, we have the following convergence results*

$$
\|u-u_{n+1}\|+\|v-v_{n+1}\|\leq Ck^2.
$$

5.4 American Option

By employing the operator splitting approach [78], the IMEX-BDF procedures described in the previous section can be extended to solve the LCP (5.2.11) for American option pricing problems. An equation derivable with the aid of an extra variable ψ, such that $\psi = u_t - \mathcal{L}u$, is the main rationale for introducing the operator splitting approach. Using this formulation, equation (5.2.11) can be reformulated as:

$$\begin{cases} \frac{\partial u}{\partial t} - \mathcal{L}u &= \psi, \\ \frac{\partial v}{\partial t} - \mathcal{L}^* u &= \psi^*, \\ (u(S,t) - \Phi(S)) \cdot \psi &= 0, \\ (v(S,t) - \Phi(S)) \cdot \psi^* &= 0, \\ u(S,t) - \Phi(S) &\geq 0, \\ v(S,t) - \Phi(S) &\geq 0, \\ \psi, \psi^* &\geq 0, \end{cases} \tag{5.4.1}$$

in the region $\Omega \times J$.

5.4.1 BDF1-OS Method

Let us split the governing equation $u_t - \mathcal{D}u = \psi$ at the $(n+1)^{th}$ time level into two discrete equations as

$$\left(\frac{\tilde{u}_{n+1} - u_n}{k}\right) - \mathcal{L}\tilde{u}_{n+1} = \psi_n, \tag{5.4.2}$$

$$\left(\frac{u_{n+1} - u_n}{k}\right) - \mathcal{L}\tilde{u}_{n+1} = \psi_{n+1}. \tag{5.4.3}$$

$$\left(\frac{\tilde{v}_{n+1} - v_n}{k}\right) - \mathcal{L}^*\tilde{v}_{n+1} = \psi^*_n, \tag{5.4.4}$$

$$\left(\frac{v_{n+1} - v_n}{k}\right) - \mathcal{L}^*\tilde{v}_{n+1} = \psi^*_{n+1}. \tag{5.4.5}$$

Now, the discrete problem for NLCP (5.2.11) is to search for the pairs (u_{n+1}, ψ_{n+1}) and $(u^*_{n+1}, \psi^*_{n+1})$ which satisfies both the discrete systems (5.4.2) – (5.4.4) and (5.4.3) – (5.4.5) as well as the constraints

$$\begin{cases} u_{n+1} &\geq \Phi, \\ \psi_{n+1} &\geq 0, \\ \psi_{n+1}(u_{n+1} - \Phi) &= 0. \\ v_{n+1} &\geq \Phi, \\ \psi^*_{n+1} &\geq 0, \\ \psi^*_{n+1}(v_{n+1} - \Phi) &= 0. \end{cases} \tag{5.4.6}$$

The first step is to find out the intermediate approximations $\tilde{u}_{n+1}$ and $\tilde{v}_{n+1}$ by solving the system (5.4.2–5.4.4) with known auxiliary terms ψ_n and ψ_n^* under boundary conditions

$$\tilde{u}_{n+1}(S^L) = K, \qquad \tilde{u}_{n+1}(S^R) = 0, \qquad \tilde{v}_{n+1}(S^L) = K, \qquad \tilde{v}_{n+1}(S^R) = 0.$$

The second step of the operator splitting method is to establish a connection between the terms $u_{n+1},\ v_{n+1}$ and $\psi_{n+1},\ \psi^*_{n+1}$ of the system (5.4.3 – 5.4.5) under the constraint (5.4.6). To achieve this, we need to re-express the system (5.4.3) – (5.4.5) using system (5.4.2) – (5.4.4) along with the constraints in (5.4.6), as a problem to determine the pair (u_{n+1}, ψ_{n+1}) such that

$$\begin{cases} \frac{u_{n+1}-\tilde{u}_{n+1}}{k} &= \psi_{n+1} - \psi_n, \\ \frac{v_{n+1}-\tilde{v}_{n+1}}{k} &= \psi^*_{n+1} - \psi^*_n, \\ \psi_{n+1}(u_{n+1} - \Phi) &= 0, \\ \psi_{n+1}(v_{n+1} - \Phi) &= 0, \end{cases} \tag{5.4.7}$$

with the constraints

$$u_{n+1} \geq \Phi \qquad v_{n+1} \geq \Phi \qquad \psi_{n+1} \geq 0 \qquad \psi^*_{n+1} \geq 0. \tag{5.4.8}$$

Again, by solving the problems (5.4.7)-(5.4.8) in (u_{n+1}, ψ_{n+1}) and (v_{n+1}, ψ^*_{n+1}) planes, we get

$$(u_{n+1}, \psi_{n+1}) = \begin{cases} (\Phi, \psi_n + \frac{\Phi - \tilde{u}_{n+1}}{k}) & \text{if } \tilde{u}_{n+1} - k\psi_n \leq \Phi, \\ (\tilde{u}_{n+1} - k\psi_n, 0) & \text{otherwise;} \end{cases} \tag{5.4.9}$$

$$(v_{n+1}, \psi_{n+1}) = \begin{cases} (\Phi, \psi^*_n + \frac{\Phi - \tilde{v}_{n+1}}{k}) & \text{if } \tilde{v}_{n+1} - k\psi^*_n \leq \Phi, \\ (\tilde{v}_{n+1} - k\psi^*_n, 0) & \text{otherwise.} \end{cases} \tag{5.4.10}$$

The pairs (u_0, ψ_0) and (v_0, ψ_0^*) at zeroth time level can be obtained using the given initial condition, followed by setting $\psi_0, \psi_0^* = 0$.

5.4.2 BDF2-OS Method

We assume that $\{u_n, \psi_n\}$, $\{u_{n-1}, \psi_{n-1}\}$ and $\{v_n, \psi^*_n\}$, $\{v_{n-1}, \psi^*_{n-1}\}$ are known in advance at the points t_n and t_{n-1}. At the discrete point t_{n+1}, we now execute two sub-steps. In the first step, we use the following BVP to calculate intermediate values $\tilde{u}_{n+1}$ and $\tilde{v}_{n+1}$.

$$\begin{cases} \frac{1}{k}\left(\frac{3}{2}\tilde{u}_{n+1} - 2u_n + \frac{1}{2}u_{n-1}\right) - \mathcal{L}\tilde{u}_{n+1} &= \psi_n, \\ \frac{1}{k}\left(\frac{3}{2}\tilde{v}_{n+1} - 2v_n + \frac{1}{2}v_{n-1}\right) - \mathcal{L}^*\tilde{v}_{n+1} &= \psi^*_n, \\ \tilde{u}_{n+1}(S^L) = K, \qquad \tilde{u}_{n+1}(S^R) = 0, \\ \tilde{v}_{n+1}(S^L) = K, \qquad \tilde{v}_{n+1}(S^R) = 0. \end{cases} \tag{5.4.11}$$

In the second step of the operator splitting method, $(\tilde{u}_{n+1}, \tilde{v}_{n+1})$is projected on the constraint space to obtain (u_{n+1}, v_{n+1}) with following correction terms:

$$\begin{cases} \frac{3}{2}\frac{u_{n+1}-\tilde{u}_{n+1}}{k} &= \psi_{n+1} - \psi_n, \\ \frac{3}{2}\frac{v_{n+1}-\tilde{v}_{n+1}}{k} &= \psi^*_{n+1} - \psi^*_n, \\ u_{n+1} &\geq \Phi, \\ v_{n+1} &\geq \Phi, \\ \psi_{n+1} &\geq 0, \\ \psi^*_{n+1} &\geq 0, \\ \psi_{n+1}(u_{n+1} - \Phi) &= 0, \\ \psi^*_{n+1}(v_{n+1} - \Phi) &= 0. \end{cases} \tag{5.4.12}$$

By solving the problems (5.4.12) in (u_{n+1}, ψ_{n+1}) and (v_{n+1}, ψ^*_{n+1}) planes, we get

$$(u_{n+1}, \psi_{n+1}) = \begin{cases} (\Phi, \psi_n + \frac{3}{2}\frac{\Phi - \tilde{u}_{n+1}}{k}) & \text{if } \tilde{u}_{n+1} - \frac{2k}{3}\psi_n \leq \Phi, \\ (\tilde{u}_{n+1} - \frac{2k}{3}\psi_n, 0) & \text{otherwise.} \end{cases} \tag{5.4.13}$$

$$(v_{n+1}, \psi^*_{n+1}) = \begin{cases} (\Phi, \psi^*_n + \frac{3}{2}\frac{\Phi - \tilde{v}_{n+1}}{k}) & \text{if } \tilde{v}_{n+1} - \frac{2k}{3}\psi^*_n \leq \Phi, \\ (\tilde{v}_{n+1} - \frac{2k}{3}\psi^*_n, 0) & \text{otherwise.} \end{cases} \tag{5.4.14}$$

To carry out the first stage, one may solve a discrete system of equations (5.4.11)–(5.4.12), and for the second step, the updated formula (5.4.13)–(5.4.14) can be used. For the three-level implicit approach to work, the values from the first two levels of time must be known. Using the initial condition and assigning the values $\psi_0 = 0$ and $\psi^*_0 = 0$, the pairs (u_0, ψ_0) and (v_0, ψ^*_0) at the initial time level can be obtained. Using the BDF1-OS approach, the pairs (u_1, ψ_1) and (v_1, ψ^*_1) at the first time level can then be computed.

5.5 Numerical Discussion

To demonstrate the accuracy and efficiency of the proposed numerical techniques, we carried out several computational experiments to calculate the value of American and European call options under liquidity shocks. The spatial operator was discretized using the second-order central finite difference approach

$$u_{xx}(x_i) \approx \frac{u_{i+1} - 2u_i + u_{i-1}}{h^2},$$

throughout the computational domain Ω, with a uniform spatial mesh length h. Using varying asset values, the computational error produced by the numerical approaches was determined using the double mesh concept. The simulations were performed in MATLAB R2022b on a PC with Processor Intel(R) Core(TM) i5-10500 CPU @ 3.10GHz, 3096 Mhz, 6 Core(s), 12 Logical Processor(s) and 16.00GB RAM.

We then computed the option values and the computational errors for all three scenarios, when the option holder is in the money, at the money, and out of the money, for a strike price of K. With

the following formula, we were able to calculate the errors by taking the difference between each set of numerical solutions:

$$\text{Error} = \left| u(k,h) - u(\frac{k}{2}, \frac{h}{2}) \right|,$$

and the rate of convergence was computed by the formula:

$$\text{Rate} = \log_2 \frac{\left| u(k,h) - u(\frac{k}{2}, \frac{h}{2}) \right|}{\left| u(\frac{k}{2}, \frac{h}{2}) - u(\frac{k}{4}, \frac{h}{4}) \right|},$$

in which the calculated option price with mesh lengths k for time and h for space is denoted by $u(k,h)$. We used piecewise cubic Hermite interpolation to estimate the option price at non-grid positions of the stock price and cubic splines were applied to with respect to spatial variable to ensure accuracy. Throughout all of the tests, the errors were calculated at different stock prices $S = 1.5,\ 2,\ 2.5$, with M spatial discretisation points in the spatial computational domain $\Omega^* := [0, 5]$, and N temporal discretisation points. For the schemes BDF1 and BDF2, we listed the option values, errors, and temporal convergence order in the liquid and illiquid stages using the following parameters: $\mu = 0.06, \sigma = 0.3, \nu_{01} = 1, \nu_{10} = 12, K = 2, T = 1, S_{max} = 5$, and $\gamma = 1$.

5.5.1 European Option

The first numerical simulation provided the errors, option values, and temporal convergence rates of the BDF1 approaches for various asset prices using the liquidity switching model to price European options. The corresponding data are listed in Table 5.1. We provided the results for both the liquid (R^0) and illiquid (R^1) states. In all states, we found that the temporal convergence rate of BDF1 attained an asymptotic order of one when the temporal mesh was sufficiently small. The plots of option values for BDF1 are shown in Figure 5.1. The graphs indicate a lack of significant fluctuation in option values around the strike price.

Additionally, we performed the same simulation using the BDF2 technique to determine the price of the European option using the liquidity switching model. The results are shown in Table 5.2. In all states, we found that the temporal convergence rate of BDF2 attained its asymptotic order of two when the temporal mesh was sufficiently small. The option values for BDF2 are plotted in Figure 5.3. The graphs again indicate a lack of significant fluctuations in option values around the strike price. We assessed the convergence rate of the BDF1 and BDF2 approaches for the European option by plotting the error in Figure 5.2. By referring to Figure 5.2, it is evident that the error slopes for BDF1 and BDF2 are approximately one and two, respectively.

Similarly we performed simulations for the European put option, and the corresponding results are shown in Table 5.3, where a second order convegence rate for the IMEX-BDF2 method can be observed. Furthermore, we performed simulations using Tavella-Randal's [156] non-uniform spatial mesh at $S = K$. The European call option values, successive errors, and temporal convergence orders of the BDF2 technique

Table 5.1: European option values for the liquid (upper) and illiquid state (below) for BDF1 at $M = 1000$.

	S=1.5			S=2			S=2.5		
N	Value	Error	Order	Value	Error	Order	Value	Error	Order
25	0.019770	-	-	0.168495	-	-	0.538758	-	-
50	0.019652	1.178973e-04	-	0.168892	3.970697e-04	-	0.538711	4.751057e-05	
100	0.019592	5.945299e-05	0.9877	0.169091	1.990627e-04	0.9961	0.538687	2.309818e-05	1.0404
200	0.019562	2.984385e-05	0.9943	0.169190	9.967456e-05	0.9979	0.538676	1.137017e-05	1.0225
400	0.019547	1.494993e-05	0.9972	0.169240	4.987524e-05	0.9989	0.538670	5.638101e-06	1.0119
800	0.019540	7.481771e-06	0.9986	0.169265	2.494750e-05	0.9994	0.538668	2.806953e-06	1.0062
25	0.015021	-	-	0.151819	-	-	0.530047	-	-
50	0.014842	1.788588e-04	-	0.152410	5.903113e-04	-	0.529897	1.498789e-04	-
100	0.014751	9.110646e-05	9.7319	0.152705	2.953554e-04	9.9902	0.529822	7.462257e-05	1.0061
200	0.014705	4.596749e-05	9.8693	0.152853	1.476719e-04	1.0000	0.529785	3.718255e-05	1.0049
400	0.014682	2.308621e-05	9.9358	0.152926	7.382813e-05	1.0001	0.529766	1.855202e-05	1.0030
800	0.014670	1.156853e-05	9.9682	0.152963	3.691148e-05	1.0001	0.529757	9.265217e-06	1.0016

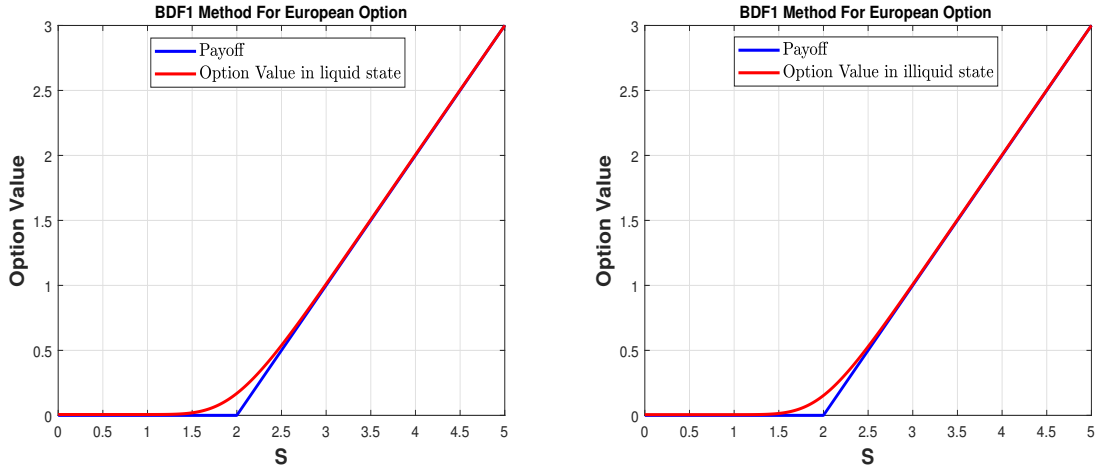

Figure 5.1: European option value for BDF1 under the liquidity switching market.

in the spatial domain $[0, 20]$ are shown in Table 5.4. These results indicate that the BDF2 approach achieves second-order temporal accuracy for governing systems. For the validation of our results, the option values and point-wise errors at $S = K$ with various discretization points are shown in Table 5.5 and Table 5.6, using the parameters provided in [118]. Our numerical results are compared to those in Tables 1 and 3 of Mudzimbabwe [118], where the authors employed two distinct schemes (Scheme 1 and Scheme 2) for the European option under liquidity switching market. We can observe that the proposed method's errors are decreasing more rapidly than those reported in [118].

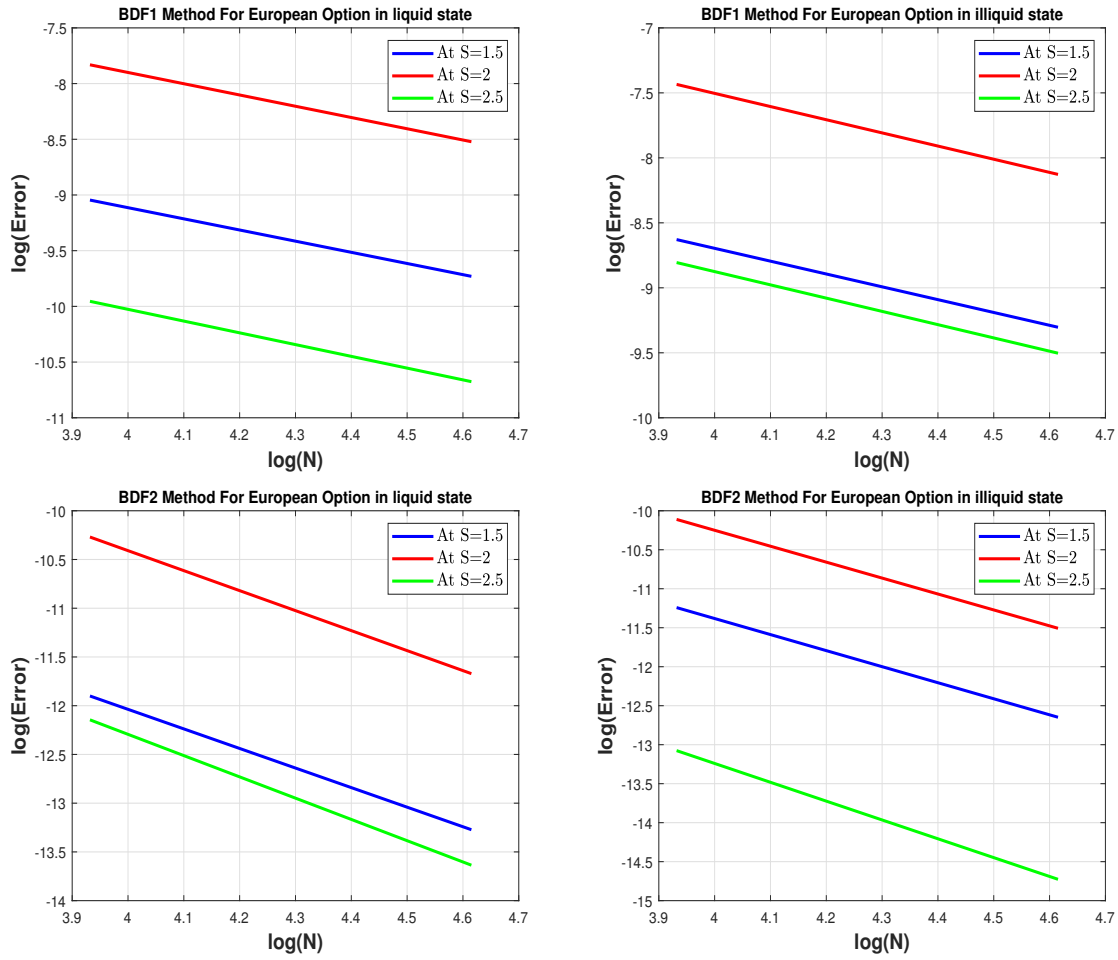

Figure 5.2: Convergence order of BDF1 and BDF2 in temporal direction for pricing European option at fixed $M = 1024$.

Furthermore conducted the sensitivity analysis of the European options. We considered three maturity times ($T = 1, 2,$ and 3) to demonstrate that the option value increases as the maturity time increases. Table 5.7 shows that while the order of convergence of BDF2 is maintained, the option value increases with increasing maturity time. The European option value for the various maturity times ($T = 1, 2, 3$) and the volatilities ($\sigma = 0.3, 0.5, 0.7, 0.9$) are shown in Figure 5.4. Figure 5.4 shows that as the volatility or maturity time increases, the option value also increases.

5.5.2 American Option

This numerical simulation demonstrates the errors, option values, and temporal convergence rates of the BDF1 approaches for pricing American call options under the liquidity switching model. The simulation

Table 5.2: European option values for the liquid (upper) and illiquid state (below) for BDF2 at $M = 1000$.

	S=1.5			S=2			S=2.5		
N	Value	Error	Order	Value	Error	Order	Value	Error	Order
25	0.019542	-	-	0.169244	-	-	0.538658	-	-
50	0.019535	6.788039e-06	-	0.169279	3.467573e-05	-	0.538663	5.314921e-06	-
100	0.019533	1.721656e-06	1.9791	0.169287	8.537609e-06	2.0220	0.538664	1.196427e-06	2.1513
200	0.019533	4.385892e-07	1.9728	0.169289	2.108965e-06	2.0172	0.538665	2.750843e-07	2.1207
400	0.019533	1.112810e-07	1.9786	0.169290	5.224311e-07	2.0132	0.538665	6.470497e-08	2.0879
800	0.019533	2.811407e-08	1.9848	0.169290	1.297212e-07	2.0098	0.538665	1.549929e-08	2.0616
25	0.014676	-	-	0.152946	-	-	0.529745	-	-
50	0.014663	1.311419e-05	-	0.152987	4.062634e-05	-	0.529747	2.094790e-06	-
100	0.014659	3.213764e-06	2.0287	0.152997	1.005790e-05	2.0140	0.529748	4.021876e-07	2.3808
200	0.014659	8.028527e-07	2.0010	0.152999	2.489735e-06	2.0142	0.529748	7.558820e-08	2.4116
400	0.014658	2.013179e-07	1.9956	0.153000	6.166180e-07	2.0135	0.529748	1.465443e-08	2.3668
800	0.014658	5.049012e-08	1.9954	0.153000	1.528752e-07	2.0120	0.529748	2.969693e-09	2.3029

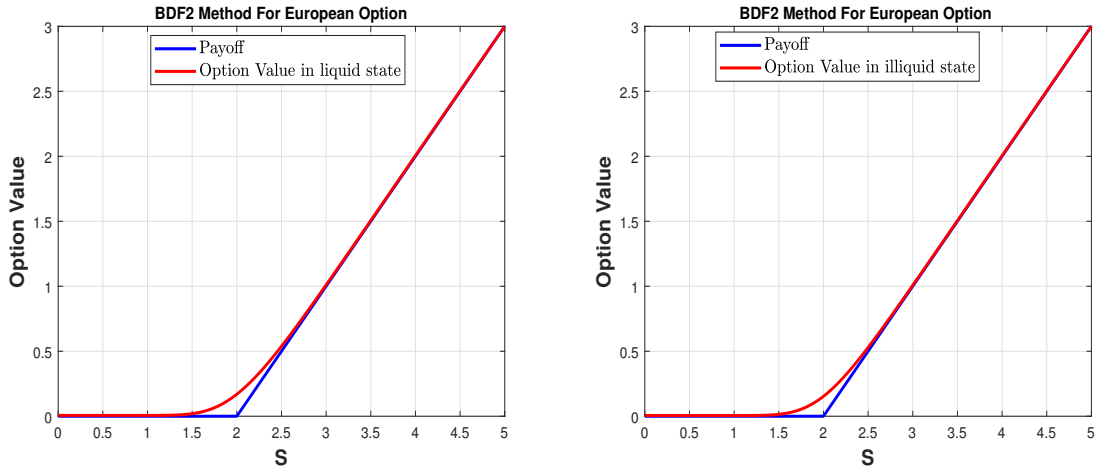

Figure 5.3: European option value for BDF2 under the liquidity switching market.

was performed at various asset values, and the results are shown in Table 5.8. We provide the results for both the liquid (R^0) and illiquid (R^1) conditions. In all states, we found that the temporal convergence rate of BDF1 attained an asymptotic order of one when the temporal mesh was sufficiently small. The option values for BDF1 are shown in Figure 5.5. The graphs indicate a lack of significant fluctuation in option values around the strike price.

Subsequently, we performed the same simulation using the BDF2 technique to determine the price of the American option under the liquidity switching model. The resulting data are shown in Table 5.9. In

Table 5.3: European put option values for the liquid (upper) and illiquid state (below) for BDF2 at $M = 1000$.

	S=1.5			S=2			S=2.5		
N	Value	Error	Order	Value	Error	Order	Value	Error	Order
25	0.519542	-	-	0.169245	-	-	0.038659	-	-
50	0.519535	6.787771e-06	-	0.169280	3.467578e-05	-	0.038664	5.315154e-06	-
100	0.519533	1.721566e-06	1.9792	0.169288	8.537696e-06	2.0220	0.038665	1.196532e-06	2.1512
200	0.519533	4.385582e-07	1.9728	0.169290	2.109016e-06	2.0172	0.038665	2.751273e-07	2.1206
400	0.519533	1.112702e-07	1.9787	0.169291	5.224544e-07	2.0131	0.038665	6.472169e-08	2.0877
800	0.519533	2.811027e-08	1.9848	0.169291	1.297308e-07	2.0097	0.038665	1.550559e-08	2.0614
25	0.514676	-	-	0.152948	-	-	0.029746	-	-
50	0.514663	1.311371e-05	-	0.152989	4.067378e-05	-	0.029748	2.095208e-06	-
100	0.514660	3.213629e-06	2.0288	0.152999	1.006845e-05	2.0142	0.029748	4.023310e-07	2.3806
200	0.514659	8.028122e-07	2.0010	0.153002	2.492377e-06	2.0142	0.029749	7.563919e-08	2.4111
400	0.514659	2.013052e-07	1.9956	0.153002	6.173299e-07	2.0134	0.029749	1.467263e-08	2.3660
800	0.514659	5.048603e-08	1.9954	0.153002	1.530770e-07	2.0117	0.029749	2.976191e-09	2.3015

all situations, we found that the temporal convergence rate of BDF2 attained its asymptotic order of 2 when the temporal mesh size was adequately refined. The option values for BDF2 are shown in Figure 5.7. Again, the graphs indicate a lack of significant fluctuations in option values around the strike price. In Figure 5.6, we demonstrated the convergence order of the BDF1 and BDF2 approaches for the American options by plotting the error as a function of $\log(N)$. From Figure 5.6, it is evident that the slopes of the errors for BDF1 and BDF2 are approximately one and two, respectively. The results for the American put option are shown in Table 5.10, where a second order convegence rate for the proposed approach can be observed.

Furthermore, we performed simulations using Tavella-Randal's [156] non-uniform spatial mesh at $S = K$. The American call option values, successive errors, and temporal convergence orders of the BDF2 technique in the spatial domain $[0, 20]$ are shown in Table 5.11. These results indicate that the BDF2 approach has second-order temporal accuracy for the governing systems. The American option value for the various maturity times ($T = 1, 2, 3$) and the volatilities ($\sigma = 0.3, 0.5, 0.7, 0.9$) are shown in Figure 5.8. We can observe that the option value increases with increase in volatility or maturity time. Furthermore, we examine the numerical Greeks Delta and Gamma, which are computed using second-order central differences, to further demonstrate the high calibre numerical results generated by the BDF2. The Greeks

Table 5.4: European option values for the liquid (upper) and illiquid state (below) for BDF2 at a fixed M=1600.

	S=9			S=10			S=11		
N	Value	Error	Order	Value	Error	Order	Value	Error	Order
10	0.102320	-	-	0.431907	-	-	1.127341	-	-
20	0.102423	1.023932e-04	-	0.432436	5.297426e-04	-	1.127528	1.867928e-04	-
40	0.102444	2.103828e-05	2.2830	0.432561	1.249597e-04	2.0838	1.127568	4.012577e-05	2.2188
80	0.102448	4.217871e-06	2.3184	0.432591	2.968858e-05	2.0734	1.127577	8.712321e-06	2.2034
160	0.102449	8.513075e-07	2.3087	0.432598	7.107124e-06	2.0625	1.127579	1.927001e-06	2.1766
320	0.102449	1.764761e-07	2.2702	0.432600	1.717151e-06	2.0492	1.127579	4.370882e-07	2.1403
640	0.102685	3.780560e-08	2.2228	0.433023	4.184088e-07	2.0370	1.127866	1.015216e-07	2.1061
10	0.079989	-	-	0.388594	-	-	1.100473	-	-
20	0.080046	5.631242e-05	-	0.389255	6.611149e-04	-	1.100662	1.893637e-04	-
40	0.080061	1.530090e-05	1.8798	0.389403	1.478074e-04	2.1611	1.100706	4.367157e-05	2.1163
80	0.080064	2.764796e-06	2.4683	0.389438	3.507080e-05	2.0753	1.100715	9.284489e-06	2.2337
160	0.080064	4.771264e-07	2.5347	0.389446	8.362873e-06	2.0681	1.100717	2.027895e-06	2.1948
320	0.080064	8.171575e-08	2.5456	0.389448	2.005298e-06	2.0601	1.100717	4.573469e-07	2.1486
640	0.080064	1.405275e-08	2.5397	0.389449	4.836648e-07	2.0517	1.100718	1.060490e-07	2.1085

Table 5.5: Comparison of numerical results with [118] for pricing European call option in liquid state using the parameters in [118].

	Present Method		Table 1 of [118]		Table 3 of [118]	
M	Option Value	Error	Option Value	Error	Option Value	Error
30	0.245325	-	0.246669	-	0.246685	-
60	0.247338	2.012663e-03	0.247438	7.70e-04	0.247444	7.59e-04
120	0.247832	4.942749e-04	0.247749	3.11e-04	0.247752	3.08e-04
240	0.247955	1.227259e-04	0.247887	1.38e-04	0.247889	1.37e-04
480	0.247985	3.055542e-05	0.247952	6.50e-05	0.247953	6.40e-05
960	0.247993	7.616512e-06	0.247983	3.10e-05	0.247984	3.10e-05

of the numerical solution, calculated using the parameters $\mu = 0.06, \sigma = 0.3, \nu_{01} = 1, \nu_{10} = 12, K = 50, T = 1, S_{max} = 100$ and $\gamma = 1$ for the scheme IMEX-BDF2 with $M = 400$ and $N = 1600$, are shown on Figures 5.9 and 5.10. We note that there are no oscillations in either Gamma or Delta. Due to the

Table 5.6: Comparison of numerical results with [118] for pricing European call option in illiquid state using the parameters in [118].

	Present Method		Table 1 of [118]		Table 3 of [118]	
M	Option Value	Error	Option Value	Error	Option Value	Error
30	0.233655	-	0.235165	-	0.234952	-
60	0.235765	2.109420e-03	0.235917	7.52e-04	0.235812	8.60e-04
120	0.236285	5.200064e-04	0.236218	3.01e-04	0.236165	3.53e-04
240	0.236414	1.292070e-04	0.236349	1.31e-04	0.236323	1.58e-04
480	0.236446	3.218109e-05	0.236410	6.10e-05	0.236397	7.40e-05
960	0.236454	8.023330e-06	0.236439	2.90e-05	0.236433	3.60e-05

Table 5.7: Empirical study of the European option values for the liquid (upper) and illiquid state (below) for BDF2 at a fixed M=1000.

	T=1			T=2			T=3		
N	Value	Error	Order	Value	Error	Order	Value	Error	Order
25	0.247929	-	-	0.448950	-	-	0.593628	-	-
50	0.247978	4.918721e-05	-	0.449049	9.827180e-05	-	0.593789	1.605334e-04	-
100	0.247990	1.189110e-05	2.04	0.449072	2.324211e-05	2.08	0.593827	3.823187e-05	2.07
200	0.247993	2.877076e-06	2.04	0.449077	5.327631e-06	2.13	0.593836	8.754297e-06	2.13
400	0.247993	6.998395e-07	2.03	0.449079	1.198373e-06	2.15	0.593838	1.919647e-06	2.18
800	0.247993	1.713318e-07	2.04	0.449079	2.702677e-07	2.14	0.593838	4.110976e-07	2.22
25	0.236387	-	-	0.442010	-	-	0.588179	-	-
50	0.236438	5.141310e-05	-	0.442110	9.979877e-05	-	0.588341	1.619550e-04	-
100	0.236451	1.253518e-05	2.03	0.442134	2.363253e-05	2.07	0.588380	3.859615e-05	2.06
200	0.236454	3.045656e-06	2.04	0.442139	5.421366e-06	2.12	0.588389	8.840178e-06	2.12
400	0.236454	7.424871e-07	2.03	0.442140	1.220171e-06	2.15	0.588391	1.938663e-06	2.18
800	0.236454	1.819880e-07	2.02	0.442141	2.753130e-07	2.14	0.588391	4.151686e-07	2.22

absence of a diffusion component in the second equation of (5.3.1), the solution v in Figures 5.9 and 5.10 has a slight edge in the Greek Delta.

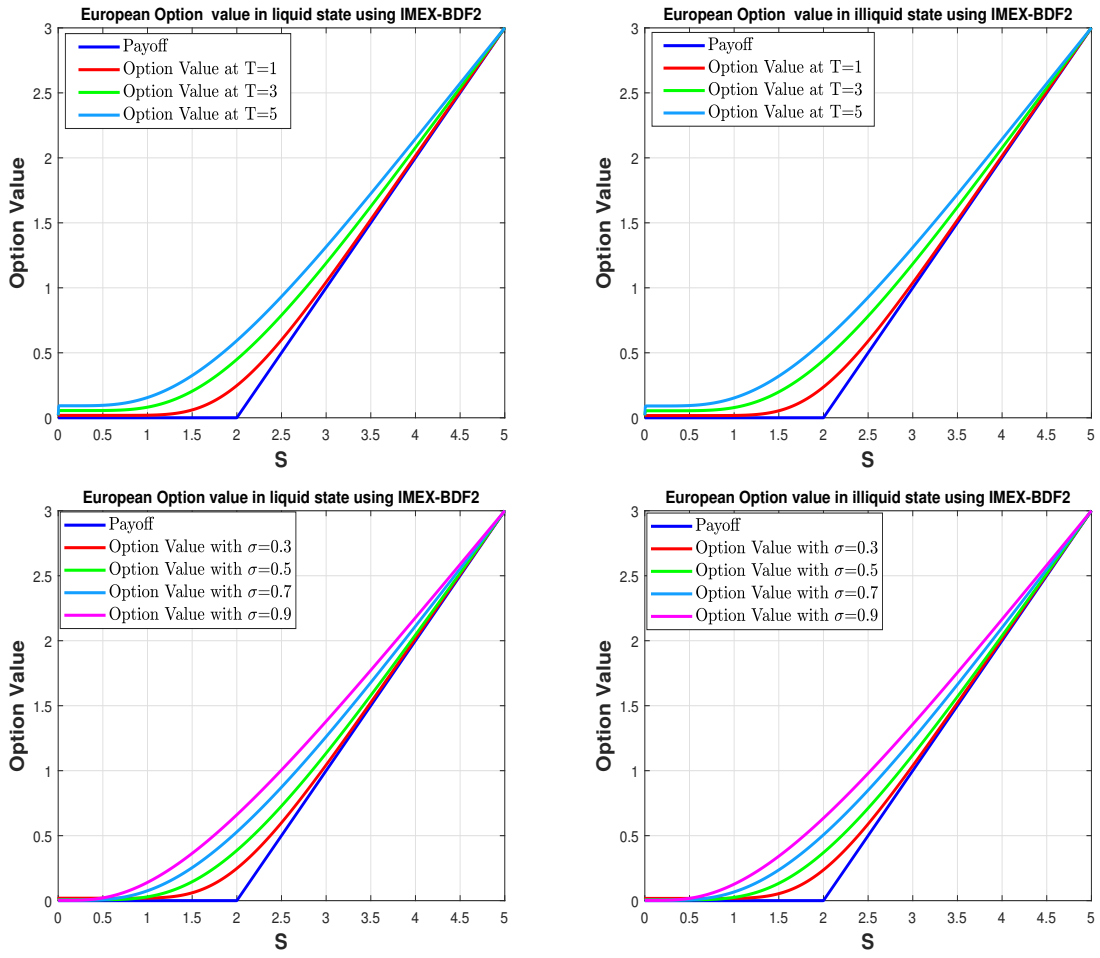

Figure 5.4: Emprical study of the European option value using IMEX-BDF2 for different values of the volatility ($\sigma = 0.3, 0.5, 0.7, 0.9$) and maturity ($T = 1, 2, 3$) under the liquidity switching market.

5.6 Conclusion

We have introduced two IMEX finite difference methods, namely BDF1 and BDF2, to solve the system of PDEs and LCPs for valuing European and American options in a market with liquidity switching behaviour. Using temporal semi-discretization, the semi-linear coupled partial differential equations for pricing European options are solved using the IMEX finite difference techniques. The inequality constraints in the system of semi-linear complementarity problems for American option pricing are handled by applying the BDF1 and BDF2 techniques in conjunction with the operator splitting method. This approach produces a linear system at each time step, which can be efficiently solved using LU decomposition without the need for fixed-point iteration. The stability of the proposed temporal semi-discrete approaches for the

Table 5.8: American option values for the liquid (upper) and illiquid state (below) for BDF1 at $M = 1000$.

	S=1.5			S=2			S=2.5		
N	Value	Error	Order	Value	Error	Order	Value	Error	Order
25	0.019770	-	-	0.168495	-	-	0.538758	-	-
50	0.019652	1.178973e-04	-	0.168892	3.970697e-04	-	0.538711	4.751057e-05	-
100	0.019592	5.945299e-05	0.9877	0.169091	1.990627e-04	0.9961	0.538687	2.309818e-05	1.0404
200	0.019562	2.984385e-05	0.9943	0.169190	9.967456e-05	0.9979	0.538676	1.137017e-05	1.0225
400	0.019547	1.494993e-05	0.9972	0.169240	4.987524e-05	0.9989	0.538670	5.638101e-06	1.0119
800	0.019540	7.481771e-06	0.9986	0.169265	2.494750e-05	0.9994	0.538668	2.806953e-06	1.0062
25	0.015021	-	-	0.151819	-	-	0.530047	-	-
50	0.014842	1.788588e-04	-	0.152410	5.903113e-04	-	0.529897	1.498789e-04	-
100	0.014751	9.110646e-05	0.9731	0.152705	2.953554e-04	0.9990	0.529822	7.462257e-05	1.0061
200	0.014705	4.596749e-05	0.9869	0.152853	1.476719e-04	1.0000	0.529785	3.718255e-05	1.0049
400	0.014682	2.308621e-05	0.9935	0.152926	7.382813e-05	1.0001	0.529766	1.855202e-05	1.0030
800	0.014670	1.156853e-05	0.9968	0.152963	3.691148e-05	1.0001	0.529757	9.265217e-06	1.0016

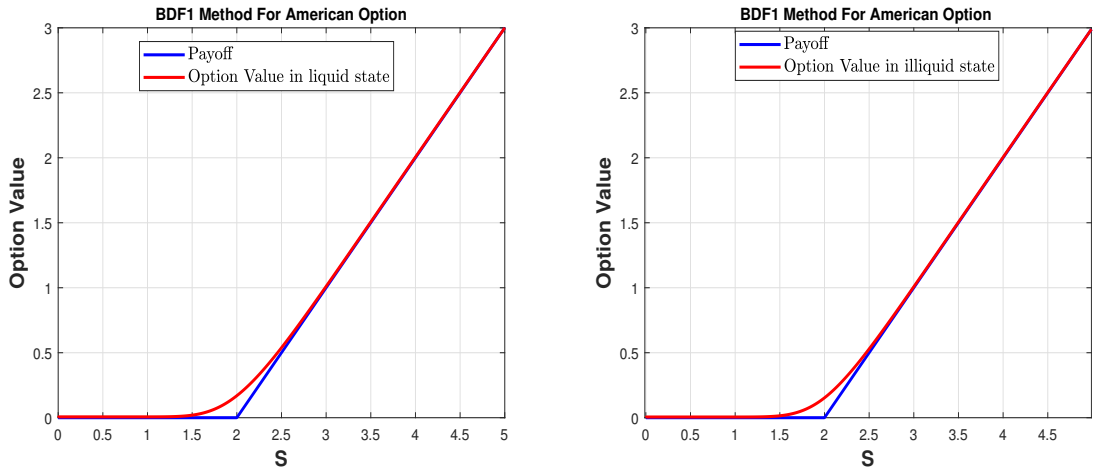

Figure 5.5: American option value for BDF1 under the liquidity switching market.

coupled PDEs are established and numerical experiments for both European and American options have shown. The numerical results demonstrate that the BDF1 and BDF2 methods are stable with first- and second-order convergence rate, rspectively. Option values, Gamma, Delta, and computational errors are also analyzed under different parameters confirming the accuracy and robustness of the proposed option pricing models.

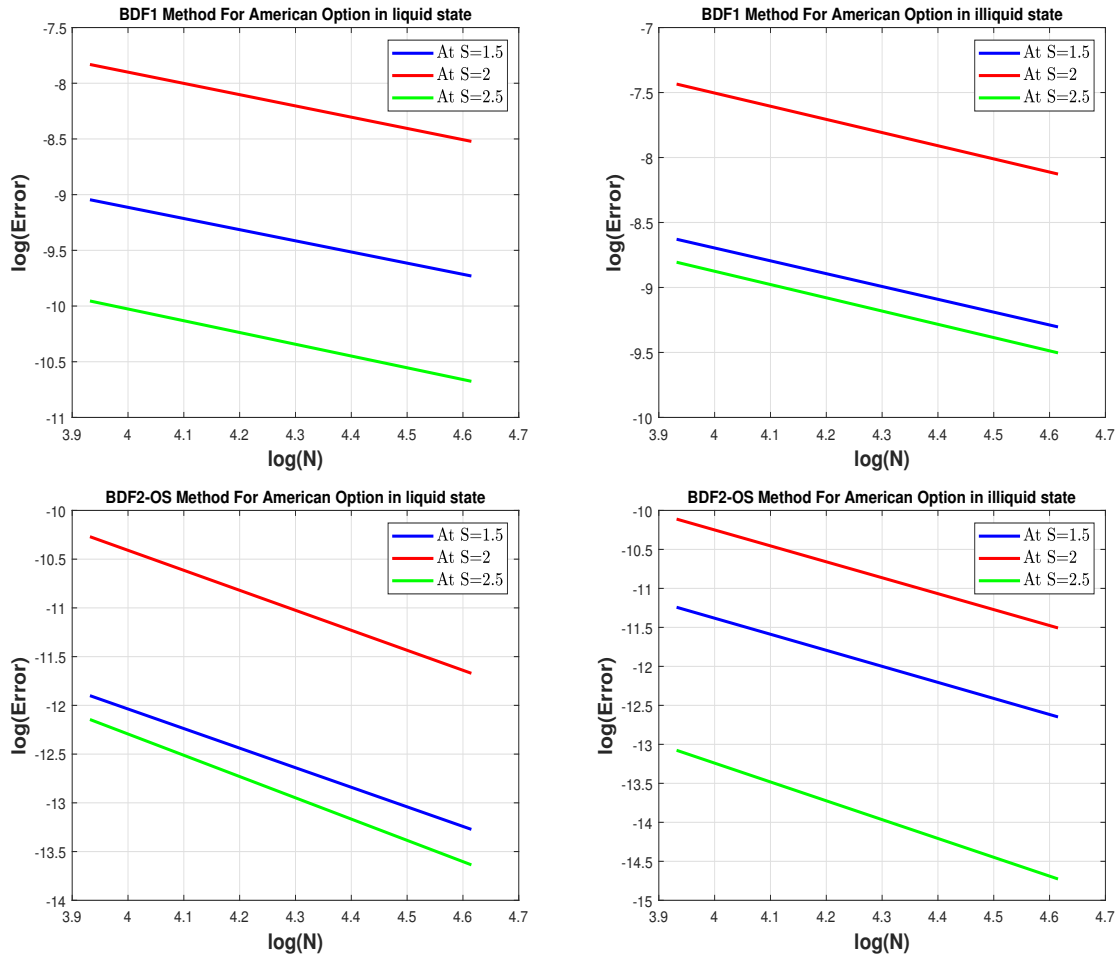

Figure 5.6: Convergence order of BDF1 and BDF2 in temporal direction for pricing American option at a fixed $M = 1024$.

Table 5.9: American option values for the liquid (upper) and illiquid state (below) for BDF2 at $M = 10^3$.

	S=1.5			S=2			S=2.5		
N	Value	Error	Order	Value	Error	Order	Value	Error	Order
25	0.019542	-	-	0.169244	-	-	0.538658	-	-
50	0.019535	6.788039e-06	-	0.169279	3.467573e-05	-	0.538663	5.314921e-06	-
100	0.019533	1.721656e-06	1.9791	0.169287	8.537609e-06	2.0220	0.538664	1.196427e-06	2.1513
200	0.019533	4.385892e-07	1.9728	0.169289	2.108965e-06	2.0172	0.538665	2.750843e-07	2.1207
400	0.019533	1.112810e-07	1.9786	0.169290	5.224311e-07	2.0132	0.538665	6.470497e-08	2.0879
800	0.019533	2.811407e-08	1.9848	0.169290	1.297212e-07	2.0098	0.538665	1.549929e-08	2.0616
25	0.014676	-	-	0.152946	-	-	0.529745	-	-
50	0.014663	1.311419e-05	-	0.152987	4.062634e-05	-	0.529747	2.094790e-06	-
100	0.014659	3.213764e-06	2.0287	0.152997	1.005790e-05	2.0140	0.529748	4.021876e-07	2.3808
200	0.014659	8.028527e-07	2.0010	0.152999	2.489735e-06	2.01426	0.529748	7.558820e-08	2.4116
400	0.014658	2.013179e-07	1.9956	0.153000	6.166180e-07	2.01354	0.529748	1.465443e-08	2.3668
800	0.014658	5.049012e-08	1.9954	0.153000	1.528752e-07	2.01202	0.529748	2.969693e-09	2.3029

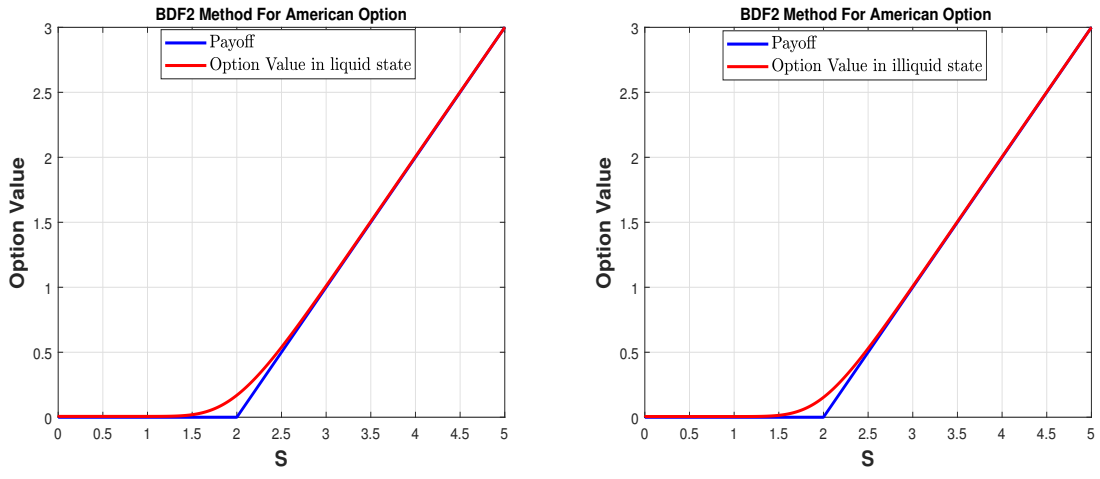

Figure 5.7: American option value for BDF2 under the liquidity switching market.

Table 5.10: American put option values for the liquid (upper) and illiquid state (below) for BDF2 at $M = 1000$.

	S=1.5			S=2			S=2.5			
N	Value	Error	Order	Value	Error	Order	Value	Error	Order	Time (Seconds)
25	0.519542	-	-	0.169245	-	-	0.038659	-	-	0.0949
50	0.519535	6.787771e-06	-	0.169280	3.467578e-05	-	0.038664	5.315154e-06	-	0.1861
100	0.519533	1.721566e-06	1.9792	0.169288	8.537696e-06	2.0220	0.038665	1.196532e-06	2.1512	0.3048
200	0.519533	4.385582e-07	1.9728	0.169290	2.109016e-06	2.0172	0.038665	2.751273e-07	2.1206	0.6008
400	0.519533	1.112702e-07	1.9787	0.169291	5.224544e-07	2.0131	0.038665	6.472169e-08	2.0877	1.1850
800	0.519533	2.811027e-08	1.9848	0.169291	1.297308e-07	2.0097	0.038665	1.550559e-08	2.0614	2.3349
25	0.514676	-	-	0.152948	-	-	0.029746	-	-	0.0920
50	0.514663	1.311371e-05	-	0.152989	4.067378e-05	-	0.029748	2.095208e-06	-	0.1808
100	0.514660	3.213629e-06	2.0288	0.152999	1.006845e-05	2.0142	0.029748	4.023310e-07	2.3806	0.3046
200	0.514659	8.028122e-07	2.0010	0.153002	2.492377e-06	2.0142	0.029749	7.563919e-08	2.4111	0.6076
400	0.514659	2.013052e-07	1.9956	0.153002	6.173299e-07	2.0134	0.029749	1.467263e-08	2.3660	1.1875
800	0.514659	5.048603e-08	1.9954	0.153002	1.530770e-07	2.0117	0.029749	2.976191e-09	2.3015	2.3294

Table 5.11: American call option values for the liquid (upper) and illiquid state (below) for BDF2 at a fixed M=1600.

	S=9			S=10			S=11			
N	Value	Error	Order	Value	Error	Order	Value	Error	Order	Time (Seconds)
10	0.377379	-	-	0.816228	-	-	1.448998	-	-	0.0888
20	0.378125	7.462047e-04	-	0.817218	9.900268e-04	-	1.449860	8.626376e-04	-	0.1596
40	0.378285	1.604125e-04	2.2177	0.817439	2.200708e-04	2.1694	1.450047	1.864721e-04	2.2097	0.3291
80	0.378320	3.446109e-05	2.2187	0.817487	4.861830e-05	2.1783	1.450087	4.026315e-05	2.2114	0.6188
160	0.378327	7.475776e-06	2.2046	0.817498	1.081680e-05	2.1682	1.450096	8.778142e-06	2.1974	1.2089
320	0.378329	1.655809e-06	2.1746	0.817500	2.448572e-06	2.1432	1.450098	1.953178e-06	2.1680	2.4096
640	0.378329	3.754877e-07	2.1406	0.817501	5.653296e-07	2.1147	1.450098	4.446689e-07	2.1350	4.8370
10	0.314912	-	-	0.735435	-	-	1.377401	-	-	0.0900
20	0.316079	1.166689e-03	-	0.736705	1.270455e-03	-	1.378763	1.362245e-03	-	0.1624
40	0.316315	2.362048e-04	2.3043	0.736966	2.605938e-04	2.2854	1.379038	2.754552e-04	2.3060	0.3294
80	0.316366	5.087654e-05	2.2149	0.737022	5.620458e-05	2.2130	1.379098	5.956101e-05	2.2093	0.6024
160	0.316377	1.129854e-05	2.1708	0.737034	1.209169e-05	2.2166	1.379111	1.327338e-05	2.1658	1.1873
320	0.316380	2.575534e-06	2.1331	0.737037	2.609534e-06	2.2121	1.379114	3.034207e-06	2.1291	2.3733
640	0.316380	6.005144e-07	2.1006	0.737037	5.664159e-07	2.2038	1.379115	7.089811e-07	2.0975	4.7404

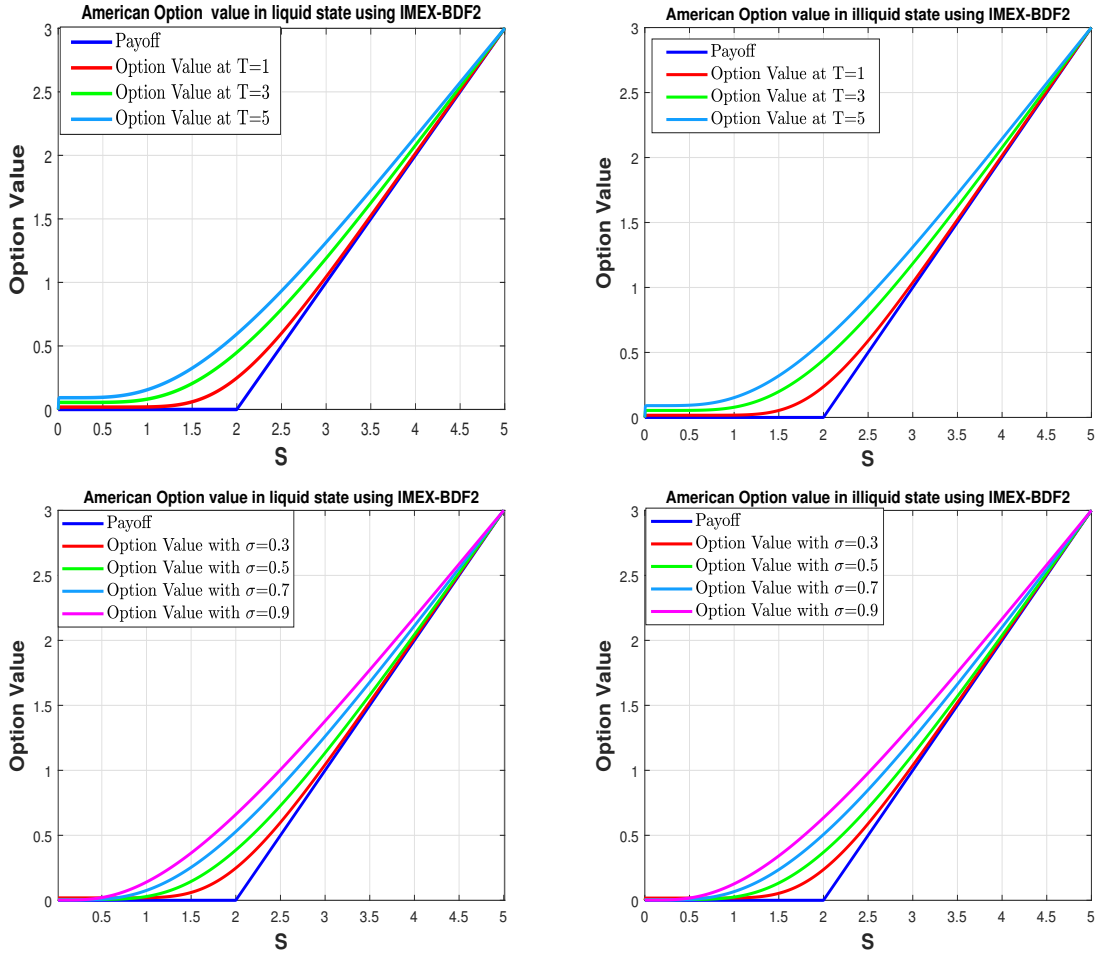

Figure 5.8: Emprical study of the American option value using IMEX-BDF2 for different values of the volatility ($\sigma = 0.3, 0.5, 0.7, 0.9$) and maturity ($T = 1, 2, 3$) under the liquidity switching market.

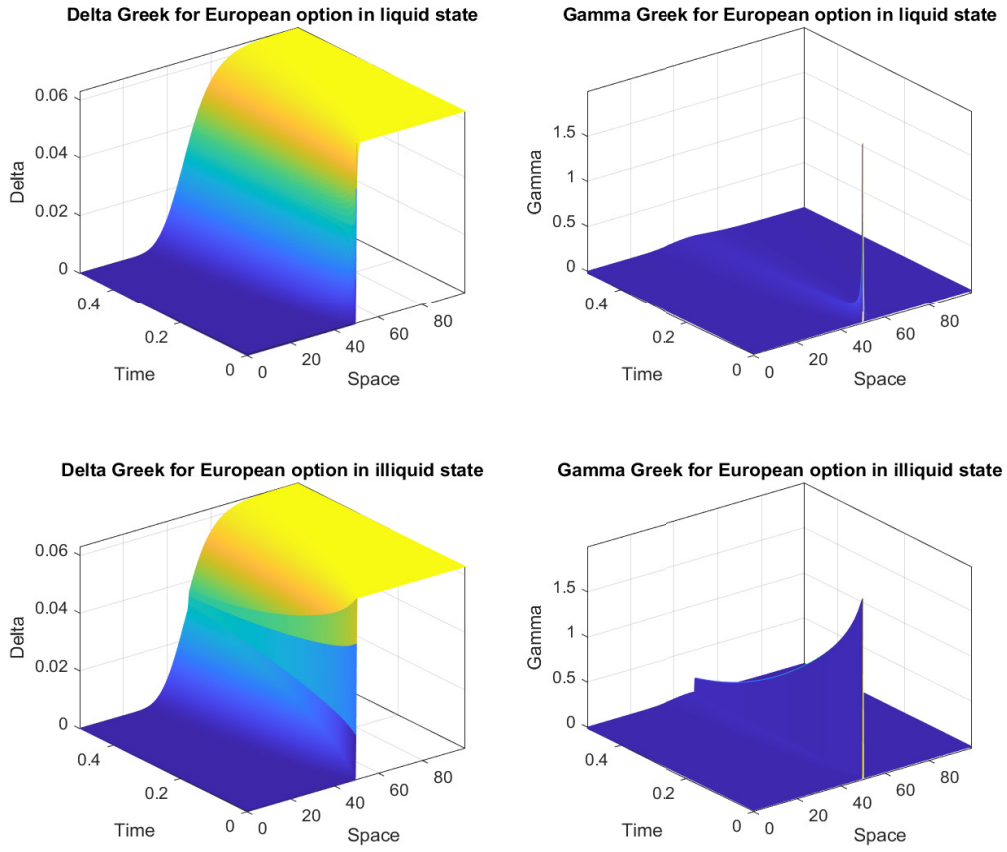

Figure 5.9: Greeks (Delta & Gamma) for pricing the European option using IMEX-BDF2-OS under liquidity switching model at N=1600 and M=400.

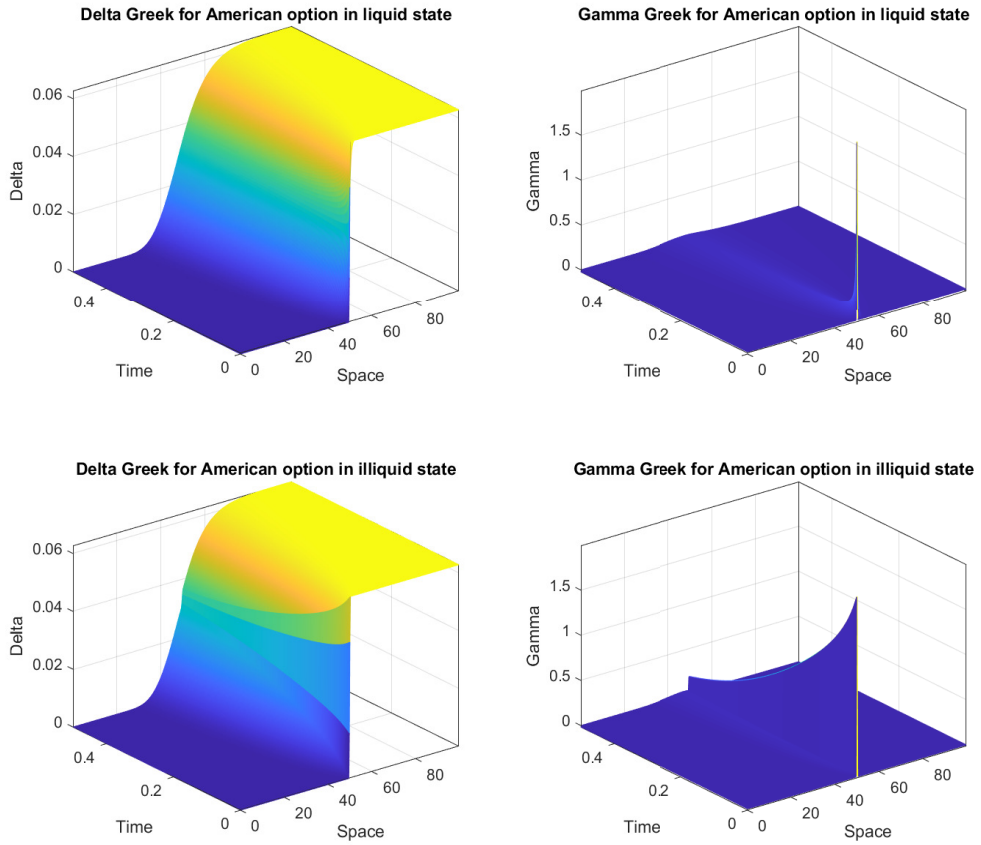

Figure 5.10: Greeks (Delta & Gamma) for pricing the American option using IMEX-BDF2-OS under liquidity switching model at N=1600 and M=400.

CHAPTER 6

Conclusion and Scope for Future Research

In this Chapter we conclude the findings of the research work accomplished throughout the thesis with an emphasis on significant points and novel contributions. During the present investigation, several ideas were originated which have the potential to extend the study further. We also highlight the scope for additional study which can be undertaken based on the findings of this work.

6.1 Summary of the Reported Work

The operator splitting approach takes advantage of the auxiliary variable to increase the accuracy and reduce the computational cost as compared to other methods. Despite these advantages of the operator splitting method, in literature, there is a lack of stability and error estimates of the operator splitting method for American option pricing problems. The first novel contribution in this direction was made by Feng Chen and Jie Shen [24]. They established the stability results for the first-order backward difference operator splitting method (BDF1-OS) and second-order backward difference operator splitting method (BDF2-OS) along with error analysis of the first-order backward difference method. We have made efforts to provide stability and error analysis of the operator splitting method for pricing the American option while avoiding the use of the derivative of the payoff function. The objective of this work was to present the BDF1-OS and BDF2-OS time semidiscretization methods for pricing American options in a Black-

Scholes framework and to provide stability and error estimates for these schemes. The BDF2-OS method exhibits an accuracy between 1.5 and 2, while the fully discrete technique corresponding to BDF1-OS is asymptotically first-order accurate. The proposed approaches effortlessly approximate the option value as well as some of its significant "Greeks" (Delta & Gamma). By condensing mesh close to the singularity, these techniques effectively handle the singularity of the non-smooth pay-off function. Iterations are not required at each time step. Our discretization results in a tridiagonal system at each time step which can be solved quickly and directly. Since the choice of spatial discretization is unrelated to the choice of temporal discretization, one may also use alternative approaches for spatial discretization, such as meshless methods (RBFs), finite elements, spectral methods, etc. The use of a non-uniform grid in spatial discretization is also permitted.

Chapter 1 introduced financial markets, including definitions of different types of financial derivatives. We also provided the basic features of IMEX-OS methods and an overview of the computational problem related to IMEX-OS schemes.

In Chapter 2, we presented the stability and error analysis of two operator splitting methods for linear complementarity problems describing the American option under the Black-Scholes model. We provided error estimates for the BDF1 and BDF2 types of operator splitting methods and showed that the order of convergence in time for BDF1-OS and BDF2-OS methods are 1 and 1.5, respectively. To verify our theoretical error estimates, we presented the numerical results demonstrating the convergence of each operating splitting method. We presented the results for the American put option and the plots for the American option value, Gamma, Delta, and exercise region. In future work, we aim to improve the stability conditions through a refined analysis.

The extension of the proposed method to investigate the jump-diffusion model was presented in Chapter 3. In this work, we established the stability and error estimates for the operator splitting method combined with implicit-explicit backward difference techniques for American option pricing problems under jump-diffusion models. The solution of the linear complementarity problem (3.2.2) corresponds to the value of the American put option under the jump-diffusion model. We approximated the integral operator using a numerical quadrature rule, while, the differential operator was computed with the help of the finite difference operator analogous to the implicit-explicit backward difference techniques. To validate the theoretical results and demonstrate the convergence behaviors of operating splitting methods, we performed numerical computations for the American put option under both Kou's and Merton's jump-diffusion models and presented plots for American put option values. In future, we aim to refine the rigorous error analysis of the IMEX-BDF2-OS method up to the second order using the variable step-size IMEX-BDF approach suggested in [167] and to explore the rigorous analysis for other classes of problems.

In Chapter 4, we examined the error estimates and stability of the IMEX-OS approaches to solve the

LCP for pricing American put options when the underlying asset follows the RSJD model. The strategy combined the operator splitting method with backward difference approaches. We employed the composite trapezoidal rule to approximate the integral operator, and the fast Fourier transform (FFT) technique was used to compute the product of a column vector a dense matrix in the integral operator. The differential operator was calculated using FD operator analogous to the backward difference IMEX procedures. To demonstrate the convergence behaviours of the operational splitting technique and present the results for the American option, we carried out several numerical experiments for IMEX-BDF-OS methods under Merton's and Kou's RSJD models. We demonstrated the plots for American option values, Gamma, Delta, and exercise region, as well as provided the findings for the American Put option.

In Chapter 5, we proposed an IMEX finite difference methods, namely, BDF2, to solve the system of PDEs and LCPs for valuing European and American options in a market with liquidity switching behaviour. As a result of the governing system's temporal semi-discretization, the semi-linear coupled partial differential equations for pricing European options were solved using the IMEX finite difference techniques. The inequality restrictions in the system of semi-linear complementarity problems for American option pricing were handled by applying the BDF2 technique in conjunction with the operator splitting method. This approach yielded a linear system at each time step, which was solved easily by LU decomposition without the need for fixed-point iteration. The stability results of the proposed temporal semi-discrete approach for the coupled PDEs were established. Numerical experiments with European and American options demonstrated that the proposed method is stable and achieves second-order convergence. The option value, Gamma, Delta, and computational errors were plotted with different parameters to perform sensitivity analysis of the proposed option pricing model.

6.2 Future Research Directions

In this thesis, we studied the operator splitting methods for solving some American option pricing models. It also identifies a number of problems that require additional investigation. Further research can proceed from different perspectives, and particularly valuable directions for future work are as follows:

- In the theoretical analysis, the restrictions on time step are not optimized. In the future, they can be enhanced through a refined analysis.
- From theroetical results, we observe that the convergence order for the BDF2-OS method can be increased using the non-uniform meshes.
- The proposed method could be extended to investigate the mixed derivative option pricing models.
- The proposed method could be extended to investigate the carbon derivative, weather derivatives, energy derivatives, etc. option pricing models.

- Multi-dimensional option pricing problems are computationally expensive to solve using conventional techniques such as finite difference methods. For these kinds of problems, we can develop a new meshless approach based on artificial intelligence called Physics-Informed Neural Networks (PINNs). The PINN paradigm has been recently introducd in the literature on deep learning.

Bibliography

[1] Mostafa Abbaszadeh, Yasmin Kalhor, Mehdi Dehghan, and Marco Donatelli. A reduced-order model based on cubic B-spline basis function and SSP Runge–Kutta procedure to investigate option pricing under jump-diffusion models. *Engineering Analysis with Boundary Elements*, 150:154–166, 2023.

[2] Yves Achdou and Jean-Luc Guermond. Convergence analysis of a finite element projection/Lagrange–Galerkin method for the incompressible Navier–Stokes equations. *SIAM Journal on numerical analysis*, 37(3):799–826, 2000.

[3] Yves Achdou and Olivier Pironneau. *Computational methods for option pricing*. SIAM, 2005.

[4] Farid Aitsahlia, Lorens Imhof, and Tze Leung Lai. Pricing and hedging of American knock-in options. *The Journal of Derivatives*, 11(3):44–50, 2004.

[5] Rahman Akbari, Reza Mokhtari, and Mohammad Taghi Jahandideh. A combined compact difference scheme for option pricing in the exponential jump-diffusion models. *Advances in Difference Equations*, 2019(1):1–13, 2019.

[6] Peter Alaton, Boualem Djehiche, and David Stillberger. On modelling and pricing weather derivatives. *Applied mathematical finance*, 9(1):1–20, 2002.

[7] Ariel Almendral and Cornelis W Oosterlee. Numerical valuation of options with jumps in the underlying. *Applied Numerical Mathematics*, 53(1):1–18, 2005.

[8] Leif Andersen. Markov models for commodity futures: theory and practice. *Quantitative Finance*, 10(8):831–854, 2010.

[9] Jesper Andreasen. The pricing of discretely sampled Asian and lookback options: a change of numeraire approach. *Journal of computational Finance*, 2(1):5–30, 1998.

[10] Samaneh Bani Asadi and Azim Rivaz. Tau Method For Pricing American Options Under Complex Models. *Journal of Mathematics and Modeling in Finance*, 1(1):127–137, 2021.

[11] Jérôme Barraquand and Thierry Pudet. Pricing of American path-dependent contingent claims. *Mathematical Finance*, 6(1):17–51, 1996.

[12] Ali Foroush Bastani, Zaniar Ahmadi, and Davood Damircheli. A radial basis collocation method for pricing American options under regime-switching jump-diffusion models. *Applied Numerical Mathematics*, 65:79–90, 2013.

[13] Hans-Peter Bermin. A general approach to hedging options: Applications to barrier and partial barrier options. *Mathematical Finance*, 12(3):199–218, 2002.

[14] Fischer Black and Myron Scholes. The pricing of options and corporate liabilities. *Journal of political economy*, 81(3):637–654, 1973.

[15] Lynn Boen and Karel J In't Hout. Operator splitting schemes for American options under the two-asset Merton jump-diffusion model. *Applied Numerical Mathematics*, 153:114–131, 2020.

[16] Phelim P Boyle and Yisong Tian. An explicit finite difference approach to the pricing of barrier options. *Applied Mathematical Finance*, 5(1):17–43, 1998.

[17] Achi Brandt and Colin W Cryer. Multigrid algorithms for the solution of linear complementarity problems arising from free boundary problems. *SIAM journal on scientific and statistical computing*, 4(4):655–684, 1983.

[18] Michael J Brennan and Eduardo S Schwartz. The valuation of American put options. *The Journal of Finance*, 32(2):449–462, 1977.

[19] Maya Briani, Claudia La Chioma, and Roberto Natalini. Convergence of numerical schemes for viscosity solutions to integro-differential degenerate parabolic problems arising in financial theory. *Numerische Mathematik*, 98:607–646, 2004.

[20] Van Emden Henson Briggs William L. and Steve F McCormick. A multigrid tutorial (2nd ed.). *Society for Industrial and Applied Mathematics, Philadelphia, PA, USA*, 12:18–19, 2000.

[21] Mark Broadie and Jerome Detemple. American option valuation: new bounds, approximations, and a comparison of existing methods. *The Review of Financial Studies*, 9(4):1211–1250, 1996.

[22] JR Cash. Two new finite difference schemes for parabolic equations. *SIAM journal on numerical analysis*, 21(3):433–446, 1984.

[23] Yoosoon Chang, Yongok Choi, and Joon Y Park. A new approach to model regime switching. *Journal of Econometrics*, 196(1):127–143, 2017.

[24] Feng Chen and Jie Shen. Stability and Error Analysis of Operator Splitting Methods for American Options Under the Black–Scholes Model. *Journal of Scientific Computing*, 82(2):1–17, 2020.

[25] Feng Chen, Jie Shen, and Haijun Yu. A new spectral element method for pricing European options under the Black–Scholes and Merton jump diffusion models. *Journal of Scientific Computing*, 52(3):499–518, 2012.

[26] Yingzi Chen, Aiguo Xiao, and Wansheng Wang. An IMEX-BDF2 compact scheme for pricing options under regime-switching jump-diffusion models. *Mathematical Methods in the Applied Sciences*, 42(8):2646–2663, 2019.

[27] Terry HF Cheuk and Ton Vorst. Complex barrier options. *The Journal of Derivatives*, 1996.

[28] Junhyun Cho, Yejin Kim, and Sungchul Lee. An accurate and stable numerical method for option hedge parameters. *Applied Mathematics and Computation*, 430:127276, 2022.

[29] Christina C Christara and Nat Chun-Ho Leung. Option pricing in jump diffusion models with quadratic spline collocation. *Applied Mathematics and Computation*, 279:28–42, 2016.

[30] Nigel Clarke and Kevin Parrott. The multigrid solution of two-factor american put options. In *Research Report 96-16*. Oxford Computing Laboratory Oxford, 1996.

[31] Nigel Clarke and Kevin Parrott. Multigrid for American option pricing with stochastic volatility. *Applied Mathematical Finance*, 6(3):177–195, 1999.

[32] Les Clewlow and Chris Strickland. Implementing derivatives models. *Wiley & Sons, London.*, 1998.

[33] Rafael Company, Vera Egorova, Lucas Jódar, and Carlos Vázquez. Computing American option price under regime switching with rationality parameter. *Computers & Mathematics with Applications*, 72(3):741–754, 2016.

[34] Rafael Company, Vera N Egorova, and Lucas Jódar. A front-fixing ETD numerical method for solving jump–diffusion American option pricing problems. *Mathematics and Computers in Simulation*, 189:69–84, 2021.

[35] Rama Cont. *Encyclopedia of quantitative finance*. Wiley, 2010.

[36] Rama Cont and Ekaterina Voltchkova. A finite difference scheme for option pricing in jump diffusion and exponential Lévy models. *SIAM Journal on Numerical Analysis*, 43(4):1596–1626, 2005.

[37] Massimo Costabile, Arturo Leccadito, Ivar Massabó, and Emilio Russo. Option pricing under regime-switching jump–diffusion models. *Journal of Computational and Applied Mathematics*, 256:152–167, 2014.

[38] Richard W Cottle, Jong-Shi Pang, and Richard E Stone. *The linear complementarity problem*. SIAM, 2009.

[39] Areski Cousin, Stéphane Crépey, Olivier Guéant, David Hobson, Monique Jeanblanc, Jean-Michel Lasry, Jean-Paul Laurent, Pierre-Louis Lions, Peter Tankov, and Stéphane Crépey. About the pricing equations in finance. *Paris-Princeton Lectures on Mathematical Finance 2010*, pages 63–203, 2011.

[40] Colin W Cryer. The solution of a quadratic programming problem using systematic overrelaxation. *SIAM Journal on Control*, 9(3):385–392, 1971.

[41] Min Dai, Qing Zhang, and Qiji Jim Zhu. Trend following trading under a regime switching model. *SIAM Journal on Financial Mathematics*, 1(1):780–810, 2010.

[42] Griselda Deelstra, Guy Latouche, and Matthieu Simon. On barrier option pricing by Erlangization in a regime-switching model with jumps. *Journal of Computational and Applied Mathematics*, 371:112606, 2020.

[43] Mehdi Dehghan, Ali Foroush Bastani, et al. On a new family of radial basis functions: Mathematical analysis and applications to option pricing. *Journal of Computational and Applied Mathematics*, 328:75–100, 2018.

[44] María del Carmen Calvo-Garrido and Carlos Vázquez. Effects of jump-diffusion models for the house price dynamics in the pricing of fixed-rate mortgages, insurance and coinsurance. *Applied Mathematics and Computation*, 271:730–742, 2015.

[45] MAH Dempster and JP Hutton. Pricing American stock options by linear programming. *Mathematical Finance*, 9(3):229–254, 1999.

[46] Yann d'Halluin, Peter A Forsyth, and George Labahn. A semi-lagrangian approach for American Asian options under jump diffusion. *SIAM Journal on Scientific Computing*, 27(1):315–345, 2005.

[47] Jim Douglas and Henry H Rachford. On the numerical solution of heat conduction problems in two and three space variables. *Transactions of the American mathematical Society*, 82(2):421–439, 1956.

[48] Daniel J Duffy. *Financial instrument pricing using C++*. John Wiley & Sons, 2018.

[49] Bertram Düring and Alexander Pitkin. High-order compact finite difference scheme for option pricing in stochastic volatility jump models. *Journal of Computational and Applied Mathematics*, 355:201–217, 2019.

[50] Ali Ebrahimijahan, Mehdi Dehghan, and Mostafa Abbaszadeh. A reduced-order model based on integrated radial basis functions with partition of unity method for option pricing under jump–diffusion models. *Engineering Analysis with Boundary Elements*, 155:48–61, 2023.

[51] Vera N Egorova, Rafael Company, and Lucas Jódar. A new efficient numerical method for solving American option under regime switching model. *Computers & Mathematics with Applications*, 71(1):224–237, 2016.

[52] Charles M Elliott and John R Ockendon. Weak and variational methods for moving boundary problems. *Pitman Publisher*, 1982.

[53] Congyin Fan, Xian-Ming Gu, Shuhong Dong, and Hua Yuan. American option valuation under the framework of cgmy model with regime-switching process. *Computational Economics*, pages 1–25, 2024.

[54] Michael C Ferris and Jong-Shi Pang. Engineering and economic applications of complementarity problems. *SIAM Review*, 39(4):669–713, 1997.

[55] Peter A Forsyth and Kenneth R Vetzal. Quadratic convergence for valuing american options using a penalty method. *SIAM Journal on Scientific Computing*, 23(6):2095–2122, 2002.

[56] Maria Giovanna Garroni, José Luis Menaldi, et al. *Green functions for second order parabolic integro-differential problems*, volume 275. Chapman and Hall/CRC, 1992.

[57] Robert Geske and Kuldeep Shastri. Valuation by approximation: a comparison of alternative option valuation techniques. *Journal of Financial and Quantitative Analysis*, 20(1):45–71, 1985.

[58] Gene H Gloub and Charles F Van Loan. Matrix computations. *Johns Hopkins Universtiy Press, 3rd edtion*, 1996.

[59] Roland Glowinski. Finite element methods for incompressible viscous flow. *Handbook of numerical analysis*, 9:3–1176, 2003.

[60] AR Gourlay and J Li Morris. The extrapolation of first order methods for parabolic partial differential equations, II. *SIAM Journal on Numerical Analysis*, 17(5):641–655, 1980.

[61] Tihomir B Gyulov and Miglena N Koleva. Penalty method for indifference pricing of American option in a liquidity switching market. *Applied Numerical Mathematics*, 172:525–545, 2022.

[62] Tihomir B Gyulov, Miglena N Koleva, and Lubin G Vulkov. Numerical approach to optimal portfolio in a power utility regime-switching model. In *AIP Conference Proceedings*, volume 1910, page 030002. AIP Publishing LLC, 2017.

[63] Wolfgang Hackbusch. *Multi-grid methods and applications*, volume 4. Springer Science & Business Media, 2013.

[64] Majid Haghi, Reza Mollapourasl, and Michèle Vanmaele. An RBF–FD method for pricing American options under jump–diffusion models. *Computers & Mathematics with Applications*, 76(10):2434–2459, 2018.

[65] Houde Han and Xiaonan Wu. A Fast Numerical Method for the Black–Scholes Equation of American Options. *SIAM Journal on Numerical Analysis*, 41(6):2081–2095, 2003.

[66] Mary R Hardy. A regime-switching model of long-term stock returns. *North American Actuarial Journal*, 5(2):41–53, 2001.

[67] Espen Gaarder Haug. Closed form valuation of American barrier options. *International Journal of Theoretical and Applied Finance*, 4(02):355–359, 2001.

[68] Anthony D Holmes and Hongtao Yang. A front-fixing finite element method for the valuation of American options. *SIAM journal on scientific computing*, 30(4):2158–2180, 2008.

[69] Cunxin Huang, Haiming Song, Jinda Yang, and Bocheng Zhou. Error analysis of finite difference scheme for american option pricing under regime-switching with jumps. *Journal of Computational and Applied Mathematics*, 437:115484, 2024.

[70] Jacqueline Huang and Jong-Shi Pang. Option pricing and linear complementarity. Technical report, 2003.

[71] Jian Huang, Zhongdi Cen, and Anbo Le. A finite difference scheme for pricing American put options under Kou's jump-diffusion model. *Journal of Function Spaces and Applications*, 2013, 2013.

[72] Yunqing Huang, Peter A Forsyth, and George Labahn. Methods for pricing American options under regime switching. *SIAM Journal on Scientific Computing*, 33(5):2144–2168, 2011.

[73] John C Hull. Options, Futures, and Other Derivatives, 2000.

[74] John C Hull and Sankarshan Basu. *Options, futures, and other derivatives*. Pearson Education India, 2016.

[75] John C Hull and Alan D White. Efficient procedures for valuing European and American path-dependent options. *The Journal of Derivatives*, 1(1):21–31, 1993.

[76] Samuli Ikonen. *On the accuracy of finite difference discretizations for parabolic problems with applications*. University of Jyväskylä, 2002.

[77] Samuli Ikonen. Efficient numerical solution of black–scholes equation by finite difference method. *Licentiate Thesis, Department of Mathematical Information Technology, University of Jyväskylä, Jyväskylä, Finland*, 2003.

[78] Samuli Ikonen and Jari Toivanen. Operator splitting methods for American option pricing. *Applied mathematics letters*, 17(7):809–814, 2004.

[79] Samuli Ikonen and Jari Toivanen. Operator splitting methods for pricing American options under stochastic volatility. *Numerische Mathematik*, 113(2):299–324, 2009.

[80] Patrick Jaillet, Damien Lamberton, and Bernard Lapeyre. Variational inequalities and the pricing of American options. *Acta Applicandae Mathematica*, 21:263–289, 1990.

[81] Mohan K Kadalbajoo, Alpesh Kumar, and Lok Pati Tripathi. Application of the local radial basis function-based finite difference method for pricing American options. *International Journal of Computer Mathematics*, 92(8):1608–1624, 2015.

[82] Mohan K Kadalbajoo, Alpesh Kumar, and Lok Pati Tripathi. An efficient numerical method for pricing option under jump diffusion model. *International Journal of Advances in Engineering Sciences and Applied Mathematics*, 7(3):114–123, 2015.

[83] Mohan K Kadalbajoo, Alpesh Kumar, and Lok Pati Tripathi. A radial basis function based implicit–explicit method for option pricing under jump-diffusion models. *Applied Numerical Mathematics*, 110:159–173, 2016.

[84] Mohan K Kadalbajoo, Lok Pati Tripathi, and Alpesh Kumar. Second order accurate IMEX methods for option pricing under Merton and Kou jump-diffusion models. *Journal of Scientific Computing*, 65(3):979–1024, 2015.

[85] Angelos Kanas. On real interest rate dynamics and regime switching. *Journal of Banking & Finance*, 32(10):2089–2098, 2008.

[86] Kamran Kazmi. An IMEX predictor–corrector method for pricing options under regime-switching jump-diffusion models. *International Journal of Computer Mathematics*, 96(6):1137–1157, 2019.

[87] Angelien Gertruda Zinnia Kemna and Antonius Cornelis Franciscus Vorst. A pricing method for options based on average asset values. *Journal of Banking & Finance*, 14(1):113–129, 1990.

[88] Jussi Keppo. Pricing of electricity swing options. *The Journal of Derivatives*, 11(3):26–43, 2004.

[89] Abdul QM Khaliq, David A Voss, and Kamran Kazmi. Adaptive θ-methods for pricing American options. *Journal of Computational and Applied Mathematics*, 222(1):210–227, 2008.

[90] Tino Kluge. *Pricing derivatives in stochastic volatility models using the finite difference method*. PhD thesis, Diplomarbeit, Chemnitz, Technische Universität Chemnitz, 2002.

[91] Miglena N Koleva, Walter Mudzimbabwe, and Lubin G Vulkov. Fourth-order compact schemes for a parabolic-ordinary system of European option pricing liquidity shocks model. *Numerical Algorithms*, 74:59–75, 2017.

[92] Miglena N Koleva and Lubin G Vulkov. Numerical method for optimal portfolio in an exponential utility regime-switching model. *International Journal of Computer Mathematics*, 97(1-2):120–140, 2020.

[93] Steven G Kou. A jump-diffusion model for option pricing. *Management science*, 48(8):1086–1101, 2002.

[94] Pavlo Kovalov, Vadim Linetsky, and Michael Marcozzi. Pricing multi-asset American options: A finite element method-of-lines with smooth penalty. *Journal of Scientific Computing*, 33(3):209–237, 2007.

[95] Alpesh Kumar and BV Rathish Kumar. A RBF based finite difference method for option pricing under regime-switching jump-diffusion model. *International Journal for Computational Methods in Engineering Science and Mechanics*, 20(5):451–459, 2019.

[96] Devendra Kumar and Komal Deswal. Haar-wavelet based approximation for pricing American options under linear complementarity formulations. *Numerical Methods for Partial Differential Equations*, 37(2):1091–1111, 2021.

[97] YongHoon Kwon and Younhee Lee. A second-order tridiagonal method for American options under jump-diffusion models. *SIAM Journal on Scientific Computing*, 33(4):1860–1872, 2011.

[98] YongHoon Kwon and Younhee Lee. A second-order tridiagonal method for American options under jump-diffusion models. *SIAM Journal on Scientific Computing*, 33(4):1860–1872, 2011.

[99] J Douglas Lawson and J Ll Morris. The extrapolation of first order methods for parabolic partial differential equations. I. *SIAM Journal on Numerical Analysis*, 15(6):1212–1224, 1978.

[100] Sunju Lee and Younhee Lee. Real option pricing under the regime-switching model with jumps on a finite time horizon. *Journal of Computational and Applied Mathematics*, 448:115893, 2024.

[101] Younhee Lee. Financial options pricing with regime-switching jump-diffusions. *Computers & Mathematics with Applications*, 68(3):392–404, 2014.

[102] Hengguang Li, Reza Mollapourasl, and Majid Haghi. A local radial basis function method for pricing options under the regime switching model. *Journal of Scientific Computing*, 79(1):517–541, 2019.

[103] Yasaman Lotfi and Kourosh Parand. Efficient image denoising technique using the meshless method: Investigation of operator splitting RBF collocation method for two anisotropic diffusion-based pdes. *Computers & Mathematics with Applications*, 113:315–331, 2022.

[104] Michael Ludkovski and Qunying Shen. European option pricing with liquidity shocks. *International Journal of Theoretical and Applied Finance*, 16(07):1350043, 2013.

[105] Guri I Marchuk. Splitting and alternating direction methods. *Handbook of numerical analysis*, 1:197–462, 1990.

[106] Michael D Marcozzi. On the valuation of Asian options by variational methods. *SIAM Journal on Scientific Computing*, 24(4):1124–1140, 2003.

[107] Ana-Maria Matache, Tobias Von Petersdorff, and Christoph Schwab. Fast deterministic pricing of options on Lévy driven assets. *ESAIM: Mathematical Modelling and Numerical Analysis*, 38(1):37–71, 2004.

[108] Brian J McCartin and Suzanne M Labadie. Accurate and efficient pricing of vanilla stock options via the crandall–douglas scheme. *Applied Mathematics and Computation*, 143(1):39–60, 2003.

[109] S McKee and Andrew R Mitchell. Alternating direction methods for parabolic equations in two space dimensions with a mixed derivative. *The Computer Journal*, 13(1):81–86, 1970.

[110] S McKee, DP Wall, and SK Wilson. An alternating direction implicit scheme for parabolic equations with mixed derivative and convective terms. *Journal of Computational Physics*, 126(1):64–76, 1996.

[111] Robert C Merton. Option pricing when underlying stock returns are discontinuous. *Journal of financial economics*, 3(1-2):125–144, 1976.

[112] Ronald E Mickens. *Nonstandard finite difference models of differential equations*. world scientific, 1994.

[113] Slobodan Milovanović and Lina von Sydow. A high order method for pricing of financial derivatives using radial basis function generated finite differences. *Mathematics and Computers in Simulation*, 174:205–217, 2020.

[114] Andrew Ronald Mitchell and David Francis Griffiths. The finite difference method in partial differential equations. *A Wiley-Interscience Publication*, 1980.

[115] Reza Mollapourasl, Majid Haghi, and Ruihua Liu. Localized kernel-based approximation for pricing financial options under regime switching jump diffusion model. *Applied Numerical Mathematics*, 134:81–104, 2018.

[116] Keith W Morton. *Revival: Numerical solution of convection-diffusion problems (1996)*. CRC Press, 2019.

[117] KW Morton and DF Mayers. Numerical solution of partial differential equations. *Journal of Fluid Mechanics*, 363:349–349, 1998.

[118] Walter Mudzimbabwe and Lubin Vulkov. Imex schemes for a parabolic-ode system of European options with liquidity shocks. *Journal of Computational and Applied Mathematics*, 299:245–256, 2016.

[119] Bjørn Fredrik Nielsen, Ola Skavhaug, and Aslak Tveito. Penalty and front-fixing methods for the numerical solution of American option problems. *Journal of Computational Finance*, 5(4):69–98, 2002.

[120] Bjørn Fredrik Nielsen, Ola Skavhaug, and Aslak Tveito. Penalty methods for the numerical solution of American multi-asset option problems. *Journal of Computational and Applied Mathematics*, 222(1):3–16, 2008.

[121] Cornelis W Oosterlee. On multigrid for linear complementarity problems with application to American-style options. *Electronic Transactions on Numerical Analysis*, 15:165–185, 2003.

[122] CW Oosterlee, JC Frisch, and FJ Gaspar. TVD, WENO and blended BDF discretizations for Asian options. *Computing and Visualization in Science*, 6:131–138, 2004.

[123] Kuldip Singh Patel and Mani Mehra. Fourth-order compact finite difference scheme for American option pricing under regime-switching jump-diffusion models. *International Journal of Applied and Computational Mathematics*, 3(1):547–567, 2017.

[124] Kuldip Singh Patel and Mani Mehra. Fourth-order compact scheme for option pricing under the Merton's and Kou's jump-diffusion models. *International Journal of Theoretical and Applied Finance*, 21(04):1850027, 2018.

[125] Donald W Peaceman and Henry H Rachford, Jr. The numerical solution of parabolic and elliptic differential equations. *Journal of the Society for industrial and Applied Mathematics*, 3(1):28–41, 1955.

[126] E Pindza, KC Patidar, and E Ngounda. Robust spectral method for numerical valuation of European options under Merton's jump-diffusion model. *Numerical Methods for Partial Differential Equations*, 30(4):1169–1188, 2014.

[127] Olivier Pironneau and Frédéric Hecht. Mesh adaption for the black and scholes equations. *East West Journal of Numerical Mathematics*, 8(1):25–36, 2000.

[128] David M Pooley, Kenneth R Vetzal, and Peter A Forsyth. Convergence remedies for non-smooth payoffs in option pricing. *Journal of Computational Finance*, 6(4):25–40, 2003.

[129] Alfio Quarteroni and Alberto Valli. *Numerical approximation of partial differential equations*, volume 23. Springer Science & Business Media, 2008.

[130] Jamal Amani Rad and Kourosh Parand. Numerical pricing of American options under two stochastic factor models with jumps using a meshless local Petrov–Galerkin method. *Applied Numerical Mathematics*, 115:252–274, 2017.

[131] Jamal Amani Rad, Kourosh Parand, and Luca Vincenzo Ballestra. Pricing European and American options by radial basis point interpolation. *Applied Mathematics and Computation*, 251:363–377, 2015.

[132] Rolf Rannacher. Finite element solution of diffusion problems with irregular data. *Numerische Mathematik*, 43:309–327, 1984.

[133] Christoph Reisinger and Gabriel Wittum. On multigrid for anisotropic equations and variational inequalities "Pricing multi-dimensional European and American options". *Computing and Visualization in Science*, 7:189–197, 2004.

[134] RD Richtmyer. Morton kw-difference methods for initial-value problems, interscience publ. *New York*, 1967.

[135] Robert D Richtmyer and EH Dill. Difference methods for initial-value problems. *Physics Today*, 12(4):50–50, 1959.

[136] Peter H Ritchken. On pricing barrier options. *The Journal of Derivatives*, 3(2), 1995.

[137] Sheldon M Ross. *An elementary introduction to mathematical finance*. Cambridge University Press, 2011.

[138] Aslam Aly El-Faïdal Saib, Désiré Yannick Tangman, and Muddun Bhuruth. A new radial basis functions method for pricing American options under Merton's jump-diffusion model. *International Journal of Computer Mathematics*, 89(9):1164–1185, 2012.

[139] Santtu Salmi and Jari Toivanen. An iterative method for pricing American options under jump-diffusion models. *Applied Numerical Mathematics*, 61(7):821–831, 2011.

[140] Santtu Salmi and Jari Toivanen. IMEX schemes for pricing options under jump–diffusion models. *Applied numerical mathematics*, 84:33–45, 2014.

[141] Rüdiger Seydel and Rudiger Seydel. *Tools for computational finance*, volume 3. Springer, 2006.

[142] Victor Shcherbakov. Radial basis function partition of unity operator splitting method for pricing multi-asset American options. *BIT Numerical Mathematics*, 56(4):1401–1423, 2016.

[143] Xian-Jun Shi, Lei Yang, and Zheng-Hai Huang. A fixed point method for the linear complementarity problem arising from American option pricing. *Acta Mathematicae Applicatae Sinica, English Series*, 32(4):921–932, 2016.

[144] Mohammad Shirzadi, Mehdi Dehghan, and Ali Foroush Bastani. On the pricing of multi-asset options under jump-diffusion processes using meshfree moving least-squares approximation. *Communications in Nonlinear Science and Numerical Simulation*, 84:105160, 2020.

[145] Mohammad Shirzadi, Mehdi Dehghan, and Ali Foroush Bastani. Optimal uniform error estimates for moving least-squares collocation with application to option pricing under jump-diffusion processes. *Numerical Methods for Partial Differential Equations*, 37(1):98–117, 2021.

[146] Mohammad Shirzadi, Mehdi Dehghan, and Ali Foroush Bastani. Optimal uniform error estimates for moving least-squares collocation with application to option pricing under jump-diffusion processes. *Numerical Methods for Partial Differential Equations*, 37(1):98–117, 2021.

[147] Mohammad Shirzadi, Mohammadreza Rostami, Mehdi Dehghan, and Xiaolin Li. American options pricing under regime-switching jump-diffusion models with meshfree finite point method. *Chaos, Solitons & Fractals*, 166:112919, 2023.

[148] Jakob Sidenius. Double barrier options: valuation by path counting. *Journal of Computational Finance*, 1(3):63–79, 1998.

[149] Gordon D Smith. *Numerical solution of partial differential equations: finite difference methods*. Oxford university press, 1985.

[150] Fazlollah Soleymani and Andrey Itkin. Pricing foreign exchange options under stochastic volatility and interest rates using an RBF–FD method. *Journal of Computational Science*, 37:101028, 2019.

[151] WF Spotz and GF Carey. Extension of high-order compact schemes to time-dependent problems. *Numerical Methods for Partial Differential Equations: An International Journal*, 17(6):657–672, 2001.

[152] Gilbert Strang. On the construction and comparison of difference schemes. *SIAM journal on numerical analysis*, 5(3):506–517, 1968.

[153] DY Tangman, A Gopaul, and M Bhuruth. A fast high-order finite difference algorithm for pricing American options. *Journal of Computational and Applied Mathematics*, 222(1):17–29, 2008.

[154] Peter Tankov. *Financial modelling with jump processes*. Chapman and Hall/CRC, 2003.

[155] Pasi Tarvainen. Block relaxation methods for algebraic obstacle problems with m-matrices: Theory and applications. 1997.

[156] Domingo Tavella and Curt Randall. Pricing financial instruments: The finite difference method. 2000.

[157] Nawdha Thakoor, Désiré Yannick Tangman, and Muddun Bhuruth. A new fourth-order numerical scheme for option pricing under the CEV model. *Applied Mathematics Letters*, 26(1):160–164, 2013.

[158] Nawdha Thakoor, Désiré Yannick Tangman, and Muddun Bhuruth. RBF-FD schemes for option valuation under models with price-dependent and stochastic volatility. *Engineering Analysis with Boundary Elements*, 92:207–217, 2018.

[159] Geraldine Tour, Nawdha Thakoor, Jingtang Ma, and Désiré Yannick Tangman. A Spectral Element Method for Option Pricing Under Regime-Switching with Jumps. *Journal of Scientific Computing*, 83(3):1–31, 2020.

[160] Geraldine Tour, Nawdha Thakoor, Désiré Yannick Tangman, and Muddun Bhuruth. A high-order RBF-FD method for option pricing under regime-switching stochastic volatility models with jumps. *Journal of Computational Science*, 35:25–43, 2019.

[161] Ulrich Trottenberg, Cornelius W Oosterlee, and A Schüller. Multigrid academic press. *New York*, page 316, 2001.

[162] Aslak Tveito and Ragnar Winther. *Introduction to partial differential equations: a computational approach*, volume 29. Springer Science & Business Media, 2004.

[163] Stephane Villeneuve and Antonino Zanette. Parabolic adi methods for pricing American options on two stocks. *Mathematics of Operations Research*, 27(1):121–149, 2002.

[164] Mohamed Ismail Mohamed Wahab, Z Yin, and NCP Edirisinghe. Pricing swing options in the electricity markets under regime-switching uncertainty. *Quantitative Finance*, 10(9):975–994, 2010.

[165] Song Wang and Xiaoqi Yang. A power penalty method for linear complementarity problems. *Operations Research Letters*, 36(2):211–214, 2008.

[166] Song Wang, XQ Yang, and Kok Lay Teo. Power penalty method for a linear complementarity problem arising from American option valuation. *Journal of optimization theory and applications*, 129(2):227–254, 2006.

[167] Wansheng Wang, Yingzi Chen, and Hua Fang. On the variable two-step IMEX BDF method for parabolic integro-differential equations with nonsmooth initial data arising in finance. *SIAM Journal on Numerical Analysis*, 57(3):1289–1317, 2019.

[168] Wansheng Wang, Mengli Mao, and Zheng Wang. An efficient variable step-size method for options pricing under jump-diffusion models with nonsmooth payoff function. *ESAIM: Mathematical Modelling and Numerical Analysis*, 55(3):913–938, 2021.

[169] Gerhard Wanner and Ernst Hairer. *Solving ordinary differential equations II*, volume 375. Springer Berlin Heidelberg New York, 1996.

[170] Pieter Wesseling. Introduction to multigrid methods. Technical report, 1995.

[171] Paul Wilmott. *Paul Wilmott on quantitative finance*. John Wiley & Sons, 2013.

[172] Paul Wilmott, Sam Howison, and Jeff Dewynne. *The mathematics of financial derivatives: a student introduction*. Cambridge university press, 1995.

[173] Lixin Wu and Yue-Kuen Kwok. A front-fixing finite difference method for the valuation of American options. *Journal of Financial Engineering*, 6(4):83–97, 1997.

[174] Chenglong Xu, Bihao Su, and Chan Liu. A quick operator splitting method for option pricing. *Journal of Computational and Applied Mathematics*, 406:113949, 2022.

[175] Deepak Kumar Yadav, Akanksha Bhardwaj, and Alpesh Kumar. Errors in the IMEX-BDF-OS methods for pricing American style options under the jump-diffusion model. *Computational and Applied Mathematics*, 43(1):6, 2024.

[176] Deepak Kumar Yadav, Akanksha Bhardwaj, and Alpesh Kumar. Operator Splitting Method to Solve the Linear Complementarity Problem for Pricing American Option: An Approximation of Error. *Computational Economics*, pages 1–27, 2024.

[177] Rajesh Yadav, Deepak Kumar Yadav, and Alpesh Kumar. RBF based some implicit–explicit finite difference schemes for pricing option under extended jump-diffusion model. *Engineering Analysis with Boundary Elements*, 156:392–406, 2023.

[178] Rajesh Yadav, Deepak Kumar Yadav, and Alpesh Kumar. RBF-FD based some implicit-explicit methods for pricing option under regime-switching jump-diffusion model with variable coefficients. *Numerical Algorithms*, pages 1–41, 2023.

[179] Hongtao Yang. A numerical analysis of American options with regime switching. *Journal of Scientific Computing*, 44(1):69–91, 2010.

[180] Muhammad Yousuf and Abdul QM Khaliq. Partial differential integral equation model for pricing american option under multi state regime switching with jumps. *Numerical Methods for Partial Differential Equations*, 39(2):890–912, 2023.

[181] Muhammad Yousuf, AQM Khaliq, and Salah Alrabeei. Solving complex PIDE systems for pricing American option under multi-state regime switching jump–diffusion model. *Computers & Mathematics with Applications*, 75(8):2989–3001, 2018.

[182] Qi Zhang, Haiming Song, and Yongle Hao. Semi-implicit FEM for the valuation of American options under the Heston model. *Computational and Applied Mathematics*, 41(2):1–20, 2022.

[183] Qing Zhang and Xun Yu Zhou. Valuation of stock loans with regime switching. *SIAM Journal on Control and Optimization*, 48(3):1229–1250, 2009.

[184] Ran Zhang, Qi Zhang, and Haiming Song. An efficient finite element method for pricing American multi-asset put options. *Communications in Nonlinear Science and Numerical Simulation*, 29(1-3):25–36, 2015.

[185] Jichao Zhao, Matt Davison, and Robert M Corless. Compact finite difference method for American option pricing. *Journal of Computational and Applied Mathematics*, 206(1):306–321, 2007.

[186] R Zvan, Peter A Forsyth, and KR Vetzal. Negative coefficients in two-factor option pricing models. *Journal of Computational Finance*, 7(1):37–74, 2003.

[187] Robert Zvan, Peter A Forsyth, and Kenneth R Vetzal. Penalty methods for american options with stochastic volatility. *Journal of Computational and Applied Mathematics*, 91(2):199–218, 1998.

[188] Robert Zvan, Peter A Forsyth, and Kenneth Roy Vetzal. *Robust numerical methods for PDE models of Asian options*. PhD thesis, University of Waterloo, 1996.

[189] Robert Zvan, Kenneth R Vetzal, and Peter A Forsyth. Pde methods for pricing barrier options. *Journal of Economic Dynamics and Control*, 24(11-12):1563–1590, 2000.

List of Publications Related to Thesis

1. **Yadav, D.K.**, Bhardwaj, A., Kumar, A.: Operator Splitting Method to Solve the Linear Complementarity Problem for Pricing American Option: An Approximation of Error. Comput Econ 64, 3353-3379 (2024). https://doi.org/10.1007/s10614-024-10564-x.

2. **Yadav, D.K.**, Bhardwaj, A., Kumar, A.: Errors in the IMEX-BDF-OS methods for pricing American style options under the jump-diffusion model. Comp. Appl. Math. 43, 6 (2024). https://doi.org/10.1007/s40314-023-02510-8.

3. **Yadav, D.K.**, Bhardwaj, A., Rakshit, G., Kumar, A.: Implicit-explicit BDF-OS schemes for pricing American style options in Markovian regime-switching economy with jumps: An Approximation of Error (Communicated).

4. Kumar, A., Rakshit, G., **Yadav, D.K.**, Yadav, R.: Computation and analysis of an implicit-explicit backward difference operator splitting method for pricing American options under the liquidity shocks (Communicated).

List of All Publications

1. Kumar, A., Rakshit, G., **Yadav, D.K.**, Yadav, R. Radial Basis Function-Based Finite DifferenceSchemes for Pricing Asian Options Under a Regime-Switching Jump Diffusion Model. Eng. Anal. Bound. Elem. 179(B) (2025), 106400. https://doi.org/10.1016/j.enganabound.2025.106400.

2. Kumar, A., Rakshit, G., **Yadav, D.K.**, Yadav, R.: RBF-based IMEX finite difference schemes for pricing option under liquidity switching. International Journal of Computer Mathematics, 101(7), 768-788 (2024). https://doi.org/10.1080/00207160.2024.2383757.

3. **Yadav, D.K.**, Bhardwaj, A., Kumar, A.: Operator Splitting Method to Solve the Linear Complementarity Problem for Pricing American Option: An Approximation of Error. Comput Econ 64, 3353-3379 (2024). https://doi.org/10.1007/s10614-024-10564-x.

4. **Yadav, D.K.**, Bhardwaj, A., Kumar, A.: Errors in the IMEX-BDF-OS methods for pricing American style options under the jump-diffusion model. Comp. Appl. Math. 43, 6 (2024). https://doi.org/10.1007/s40314-023-02510-8.

5. Yadav, R., **Yadav, D.K.**, Kumar, A.: RBF-FD based some implicit-explicit methods for pricing option under regime-switching jump-diffusion model with variable coefficients. Numer Algor 97, 645-685 (2024). https://doi.org/10.1007/s11075-023-01719-2.

6. Yadav, R., **Yadav, D.K.**, Kumar, A.: RBF based some implicit-explicit finite difference schemes for pricing option under extended jump-diffusion model. Eng. Anal. Bound. Elem. 156, 392-406 (2023). https://doi.org/10.1016/j.enganabound.2023.08.021.

7. **Yadav, D.K.**, Bhardwaj, A., Rakshit, G., Kumar, A.: Implicit-explicit BDF-OS schemes for pricing American style options in Markovian regime-switching economy with jumps: An Approximation of Error (Communicated).

8. Kumar, A., Rakshit, G., **Yadav, D.K.**, Yadav, R.: Computation and analysis of an implicit-explicit backward difference operator splitting method for pricing American options under the liquidity shocks (Communicated).